

Appendix F7

Brinkman et al. 2010

Understanding Water Column and Pelagic Ecosystem
Processes affecting the Lagoon of South Reef, Scott Reef –
Final Report, 2008-2010

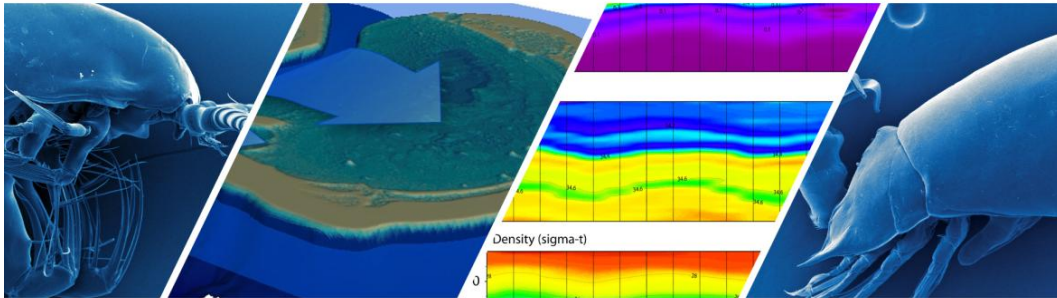


BROWSE FLNG DEVELOPMENT
Draft Environmental Impact Statement

EPBC 2013/7079
November 2014

SCOTT REEF RESEARCH PROJECT
FINAL REPORT - PROJECT 3.1 2010

Understanding water column and pelagic ecosystem processes affecting the lagoon of South Reef, Scott Reef



R Brinkman, AD McKinnon, M Furnas, N Patten

PRODUCED FOR
WOODSIDE ENERGY LTD
as operator of the
BROWSE LNG DEVELOPMENT



PERTH 2010

Australian Institute of Marine Science:

PMB No 3
Townsville MC QLD 4810

PO Box 40197
Casuarina NT 0811

The UWA Oceans Institute (M096)
35 Stirling Hwy
Crawley WA 6009

This report should be cited as:

Brinkman R, McKinnon AD, Furnas M, Patten N (2010) Understanding water column and pelagic ecosystem processes affecting the lagoon of South Reef, Scott Reef. AIMS Document SRRP-RP-RT-046. Project 3.1 2010 Final Project Report - to Woodside Energy Ltd as operator of the Browse LNG Development. Australian Institute of Marine Science, Perth, Western Australia. (199 pp.).

© Australian Institute of Marine Science & Woodside Energy Ltd 2010

All rights are reserved and no part of this document may be reproduced, stored or copied in any form or by any means whatsoever except with the prior written permission of AIMS.

ACKNOWLEDGEMENTS

The authors wish to acknowledge Simon Spagnol, Felicity McAllister, Lulu Lodder, Cary McLean, Sam Talbot, Lincoln Critchley, Matt Slivkoff, David Williams, Felipe Gusmão, Matthew Wassnig, Liza Roger, Rebecca O'Leary, Sarah Castine, Chris Davis, Greg Lambert and the crews of the RV Solander, the MV Mary V and the MV Browse Express for their contributions to this project.

DISCLAIMER

While reasonable efforts have been made to ensure that the contents of this document are factually correct, AIMS does not make any representation or give any warranty regarding the accuracy, completeness, currency or suitability for any particular purpose of the information or statements contained in this document. To the extent permitted by law AIMS shall not be liable for any loss, damage, cost or expense that may be occasioned directly or indirectly through the use of or reliance on the contents of this document.

Contents

Contents	i
Preamble	1
Project Synopsis and Key Results	3
The oceanographic context of Scott Reef.....	3
The bio-physical environment of the lagoon of South Reef.....	4
Comparisons of Scott Reef with other regions.....	5
Strongest gradients in the vertical.....	8
Is the lagoon different from the surrounding ocean?.....	8
Carbon Budget.....	9
Lagoonal water quality and the dynamics of coral reef communities.....	10
Benthic-Pelagic Coupling.....	11
Zooplankton Biodiversity.....	12
Regional Applicability.....	12
Applicability to North Reef.....	13
Executive Summary	15
Introduction	20
Materials and Methods	21
Physical Oceanography.....	21
In-situ observational instrumentation.....	21
Deployment summary.....	22
Biological Oceanography.....	25
Results	27
The physical environment of Scott Reef.....	27
Light.....	27
Oceanic conditions.....	35
Internal Waves.....	44
The physical environment of the South Reef lagoon.....	50
Nutrients in Scott Reef waters.....	68
Principal components analysis of water chemistry.....	73
Phytoplankton of Scott Reef waters.....	76
Abundance and distribution of picoplankton at Scott Reef.....	76
Abundance and distribution of nano and microplankton at Scott Reef.....	90
Primary productivity and carbon turnover in Scott Reef waters.....	92
¹⁴ C uptake Experiments.....	92
Pelagic metabolism.....	98
Bacterial Production (Thymidine uptake experiments).....	107
Correlates of Production.....	108
Historical measurements of pelagic productivity at and near Scott Reef.....	111
Sedimentation Fluxes.....	113
Zooplankton of Scott Reef waters.....	121
Zooplankton Biomass.....	122
Zooplankton abundance.....	125
Zooplankton community composition.....	126
Biodiversity of the Copepoda.....	129
Vertical distribution of trophic types.....	130
Zooplankton taxa.....	133

Indicator species	134
Secondary Production	139
Macrozooplankton of Scott Reef waters.....	139
Discussion	147
The oceanographic context of Scott Reef.....	147
Lagoon waters.....	148
Comparisons of Scott Reef with other regions	149
Strongest gradients in the vertical.....	154
Is the lagoon different from the surrounding ocean?.....	154
Origin of cool water intrusions.....	155
Carbon Budget.....	155
Lagoonal water quality and the dynamics of coral reef communities	157
Benthic-Pelagic Coupling.....	158
Zooplankton Biodiversity	158
Regional Applicability.....	159
Applicability to North Reef.....	159
References	161
Glossary	168
Appendices	172
Appendix I: Methods used on Biological Oceanography Cruises.....	172
Appendix II: Units of Measurement.....	181
Appendix III: Logger time series statistics.....	182

List of Figures

Fig. 1 Locations of biological oceanographic sampling and experimental sites, long-term water quality logger sites, mooring sites and hydrographic stations.....	23
Fig. 2 Daily input fluxes of PAR and ultraviolet radiation measured at Broome.....	27
Fig. 3 Vertical profiles of depth-averaged chlorophyll concentration and mid-day sub-surface light penetration at mid-lagoon sites on the four cruises.	29
Fig. 4 Vertical profiles of depth-averaged chlorophyll concentration and mid-day sub-surface light penetration at the Deep Channel site (CH) on the four cruises.....	30
Fig. 5 Vertical profiles of depth-averaged chlorophyll concentration and mid-day sub-surface light penetration at the NE Margin site (NE) on the four cruises.	31
Fig. 6 Vertical profiles of depth-averaged chlorophyll concentration and mid-day sub-surface light penetration at the Open Water site (SW) on the four cruises.....	32
Fig. 7 Normalised remote sensing reflectance spectra (R_{rs}) recorded at the four time series sites in and near Scott Reef and near the coastline at Broome during the November – December 2009 research voyage.	34
Fig. 8 Representative mid-day vertical profiles of water temperature ($^{\circ}\text{C}$), salinity (‰), density (σ_t), chlorophyll a (from fluorescence, $\mu\text{g L}^{-1}$) and percent surface irradiance ($\%I_0$).	37
Fig. 9 Contoured time series of water temperature ($^{\circ}\text{C}$), measured in-situ chlorophyll fluorescence ($\mu\text{g L}^{-1}$), salinity(PSU) and Density (σ_t) measured at the Open Water site (SW) on 30 June 2008.	38
Fig. 10 Contoured time series of water temperature ($^{\circ}\text{C}$), measured in-situ chlorophyll fluorescence ($\mu\text{g L}^{-1}$), salinity(PSU) and Density (σ_t) measured at the Open Water site (SW) on 4 December 2008.....	39
Fig. 11 Contoured time series of water temperature ($^{\circ}\text{C}$), measured in-situ chlorophyll fluorescence ($\mu\text{g L}^{-1}$), salinity(PSU) and Density (σ_t) measured at the Open Water site (SW) on 1 June 2009.	40
Fig. 12 Contoured time series of water temperature ($^{\circ}\text{C}$), measured in-situ chlorophyll fluorescence ($\mu\text{g L}^{-1}$), salinity(PSU) and Density (σ_t) measured at the Deep Channel site (CH) on 26 June 2008.	41
Fig. 13 Contoured time series of water temperature ($^{\circ}\text{C}$), measured in-situ chlorophyll fluorescence ($\mu\text{g L}^{-1}$), salinity(PSU) and Density (σ_t) measured at the Deep Channel site (CH) on 4 December 2008.....	42
Fig. 14 Plots of temperature-salinity (T/S) relationships in the upper 400 m for water masses at the Open Water site (SW).	43
Fig. 15 Diel temperature ranges at 100 m depth between August 1995 and January 1999.	47
Fig. 16 Estimated internal wave amplitudes during May 2009 – May 2010 at the 200m mooring site within the channel.....	48
Fig. 17 Vertical excursions of selected density surfaces due to internal wave activity over diel time frames at Scott Reef deep water sites.	49
Fig. 18 Histogram of average daily temperatures for representative sites adjacent to the channel and in the interior of the lagoon.....	50
Fig. 19 Representative temperature time series at in-situ logger site adjacent to the channel.	51
Fig. 20 Representative temperature time series at in-situ logger site within the lagoon of South Reef.....	51
Fig. 21 Time series of water depth (at Site PE16) and temperature at sites PE16, PE15 and PE14 along a North-South transect from the deep channel into the interior of the South Reef Lagoon.....	52
Fig. 22 Representative daily temperature range at in-situ logger site adjacent to the channel..	53
Fig. 23 Monthly average temperature ranges at in-situ logger sites adjacent to the channel and in the interior of the lagoon.....	54

Fig. 24 Representative vertical profiles of temperature, salinity, density, and chlorophyll within the lagoon.....	54
Fig. 25 Contoured longitudinal sections of water temperature, salinity, chlorophyll and density along the central axis of the South Reef lagoon during June 2009 and December 2009.....	55
Fig. 26 Monthly average salinity at in-situ logger sites adjacent to the channel and in the interior of the lagoon.....	56
Fig. 27 Contoured time series of water temperature, salinity, chlorophyll and density in the lagoon of South Reef during June 2008, June 2009, December 2008 and December 2009.....	58
Fig. 28 Monthly average turbidity (NTU) at observational sites PE13 and PE02.....	59
Fig. 29 Contoured mean monthly turbidity at in-situ logger sites.....	60
Fig. 30 Turbidity vs mean wave height (Hm0) at sites PE02, PE03 and PE06.....	61
Fig. 31 Turbidity vs current speed at Site PE02.....	61
Fig. 32 Sedimentation rates from in-situ sediment traps deployed at logger locations within the South Reef lagoon.....	62
Fig. 33 Monthly average maximum PAR at representative observational sites PE13 (top) and PE02 (bottom).....	63
Fig. 34 Contoured maximum PAR at logger sites.....	64
Fig. 35 Monthly average chlorophyll fluorescence at observational site PE07 adjacent to the channel and site PE13 in the interior of the lagoon.....	65
Fig. 36 Time series plots of temperature and chlorophyll at sites PE14, PE15 and PE16.....	67
Fig. 37 Profiles of temperature, chlorophyll, NO ₃ ⁻ , NO ₂ ⁻ , DON, PON, PO ₄ ³⁻ , DOP, PP, Si(OH) ₄ , dissolved organic carbon (DOC), particulate carbon (POC) in the central region of South Reef lagoon and the deep channel between North and South Reef.....	69
Fig. 38 Profiles of temperature, chlorophyll, NO ₃ ⁻ , NO ₂ ⁻ , DON, PON, PO ₄ ³⁻ , DOP, PP, Si(OH) ₄ , dissolved organic carbon (DOC), particulate carbon (POC) at deep-water sites bordering the NE margin of North Reef and at an open water site.....	70
Fig. 39 Relationships between temperature and concentrations of NO ₃ ⁻ , PO ₄ ³⁻ , Si(OH) ₄ in samples collected at the Open Water site (SW).....	71
Fig. 40 Principal Components Analysis of water chemistry data.....	74
Fig. 41 Dot plots from flow cytometric analysis of seawater samples showing groups of autotrophic (photosynthesising) picoplankton and bacterioplankton and viruses.....	77
Fig. 42 Abundances of autotrophic picoplankton (<i>Prochlorococcus</i> , <i>Synechococcus</i> and Picoeukaryotes) in June 2008, December 2008, June 2009 and November 2009.....	78
Fig. 43 Abundances of Viruses and bacterioplankton at Scott Reef in December 2008, June 2009 and November 2009.....	82
Fig. 44 Picoplankton carbon and nitrogen standing crop in the upper 100 m of the water column (50 m in lagoon).....	84
Fig. 45 Changes in virus and bacterioplankton abundances in viral production incubations.....	88
Fig. 46 Representative images of nano and microplankton taken by the FlowCAM.....	90
Fig. 47 Representative FlowCAM count data at the production sites in December 2009.....	90
Fig. 48 Vertical profiles of size fractionated primary production and chlorophyll in the South Reef lagoon in June 2008 and December 2008.....	93
Fig. 49 Vertical profiles of size fractionated primary production and chlorophyll in the South Reef lagoon in June 2009 and November 2009.....	93
Fig. 50 Vertical profiles of size fractionated primary production and chlorophyll in the Deep Channel.....	94
Fig. 51 Vertical profiles of size fractionated primary production and chlorophyll at the NE margin.....	94
Fig. 52 Vertical profiles of size fractionated primary production and chlorophyll at the Open Water reference site.....	95
Fig. 53 Size-fractionated chlorophyll standing crop, daily primary production and bacterial production in relation to primary production.....	96
Fig. 54 Oxygen flux through the water column at the Lagoon site.....	99

Fig. 55 Oxygen flux through the water column at the Channel site	100
Fig. 56 Oxygen flux through the water column at the NE margin site.....	101
Fig. 57 Oxygen flux through the water column at the Open Water site	102
Fig. 58 Community respiration and net community production at Scott Reef.....	102
Fig. 59 The relationship of P:R ratio to Gross Primary Production at Scott Reef compared to other locations where AIMS has made similar measurements.....	104
Fig. 60 Volumetric NCP vs GPP from Scott Reef.....	105
Fig. 61 Vertical profiles of daily bacterial carbon production (³ H-thymidine uptake) measured concurrently with phytoplankton primary production in the vicinity of Scott Reef during the December 2008 and June 2009 cruises.....	107
Fig. 62 Correlation matrix (heatmap) of production-related variables.	109
Fig. 63 Dendrogram originating from hierarchical cluster analysis.	110
Fig. 64 Measured sedimentation fluxes of organic carbon (OC) from the water column or euphotic zone in relation to organic carbon standing crop and concurrent daily primary production.....	114
Fig. 65 Measured sedimentation fluxes of particulate nitrogen (N) from the water column or euphotic zone in relation to the particulate nitrogen standing crop and estimated concurrent daily N demand to support measured primary production.	115
Fig. 66 A comparison between measured areal primary production rates and sedimentation fluxes of carbon and nitrogen at Scott Reef and rates measured using similar methods at the HOTS and BATS time series stations.....	121
Fig. 67 Depth distribution of >100 µm zooplankton biomass at Deep Channel site, NE margin site and Open Water site (SW) for the four cruises at Scott Reef.	124
Fig. 68 Composition of mixed layer zooplankton at Scott Reef.....	126
Fig. 69 Composition and total abundance of the zooplankton over 24 hr at the Lagoon site (LA) in June 2008.....	127
Fig. 70 Composition and total abundance of the zooplankton over 24 hr at the Lagoon site (LA) in December 2008.	127
Fig. 71 Composition of the zooplankton community at the Lagoon site (LA), contrasted with that in the 5 depth strata sampled at the Channel (CH), NE margin (NE) and Open Water (SW) sites.	128
Fig. 72 Composition of the Scott Reef copepod community by family.	129
Fig. 73 A new species of the copepod genus <i>Aetideopsis</i> from the Channel site (CH)	130
Fig. 74 The vertical distribution of copepods belonging to 3 trophic categories at deep sites around Scott Reef.....	130
Fig. 75 Redundancy analysis displaying relationships between zooplankton samples, sites and depths.....	133
Fig. 76 Depth occurrences of 64 species of Oncaeiidae across 5 depth strata at the Open Water site (SW)..	136
Fig. 77 Instrumental record of temperature from site PE06.....	138
Fig. 78 Locations at which euphausiid collections were made.....	140
Fig. 79 Histograms showing frequency of abundances of each euphausiid genus.....	141
Fig. 80 A simple conceptual model of carbon cycling and export from the mixed layer at Scott Reef.....	156

List of Tables

Table 1 Nominal positions and depths of biological oceanographic sampling stations and long-term logger sites and instrument configuration	24
Table 2 Ranges of averaged PAR attenuation coefficients for specified depth bands at the four biological oceanography sites.....	33
Table 3 Ranges of raw and low-pass filtered water temperatures within monthly periods at Scott Reef between November 1997 and January 1999 and estimated amplitudes of internal waves calculated from diel (24-hour) temperature ranges within monthly time frames.	47
Table 4 Mean surface salinities within the lagoon (LA) and at the open water (SW) sites based on time series observations.	57
Table 5 Results of T-test analysis comparing chlorophyll fluorescence between sites along the northern margin of the lagoon and within the lagoon.....	66
Table 6 Regression equations for nutrient-temperature relationships shown in Fig. 39.	72
Table 7 Depth weighted average (DWA) and integrated (Int) abundances of <i>Prochlorococcus</i> (Pro), <i>Synechococcus</i> (Syn), Picoeukaryotes (Peuk), Bacteria (Bac) and Viruses (Vir) at Lagoon (LA), Channel (CH), NE margin (NE) and Open water (SW) sites at Scott Reef during June 2008, December 2008, June 2009, December 2009.....	79
Table 8 Ranges in picoplankton and virus abundances at Scott Reef compared with other tropical ocean and reef locations.....	85
Table 9 Viral parameters in December 2008 (S 08), June 2009 (W 09) and November 2009 (S 09) in Lagoon, Channel, NE Margin and Open Water..	89
Table 10 FlowCAM summary statistics: average >5 μm cell count ($\pm\text{SD}$) and average >5 μm cell size ($\pm\text{SD}$) at each of the locations by cruise.	91
Table 11 Results of generalised linear regression model for FlowCAM data, comparing cruise and location.....	91
Table 12 Estimates of phytoplankton standing crop, daily primary production in functional group size fractions and daily bacterial production at Scott Reef production sites.	97
Table 13 Water column mean dark respiration rates ($\text{mmol O}_2 \text{ m}^{-3} \text{ d}^{-1}$) for each cruise.....	98
Table 14: Comparison of Reduced Major Axis (Model II) Regression statistics of the relationship between NCP and GPP ($\text{mmol O}_2 \text{ m}^{-3} \text{ d}^{-1}$) at Scott Reef with subtropical and tropical locations from Table I of Duarte and Regaudie-de-Gioux (2009).....	105
Table 15: Comparison of Scott Reef rates with other areas of the globe.....	106
Table 16 Estimates of bacterial biomass carbon production at Scott Reef as estimated from ^3H -thymidine uptake experiments.....	108
Table 17 A summary of historical primary production measurements (^{14}C -based) from the Great Barrier Reef, oceanic Coral Sea and outer shelf waters of NW Australia.....	112
Table 18 Average sedimentation ($\pm 1 \text{ S.D.}$) fluxes of carbon and nitrogen at the four time series sites.	116
Table 19 Measured carbon sedimentation fluxes in and around Scott Reef in relation to the organic carbon standing crop, primary production and estimated respiratory consumption of carbon by water column micro-organisms.....	117
Table 20 Measured nitrogen sedimentation fluxes in and around Scott Reef in relation to the organic nitrogen standing crop and primary production.	118
Table 21 Average of the ratios of measured sedimentation fluxes of carbon ($\pm 1 \text{ S.D.}$) relative to estimated phytoplankton biomass, water column C standing crop above the trap and daily carbon fixation at the four time series sites.	119
Table 22 Average of the ratios of measured sedimentation fluxes of nitrogen ($\pm 1 \text{ S.D.}$) relative to estimated phytoplankton biomass, water column N standing crop above the trap and daily nitrogen demand due to primary production ($\text{N/C demand} = 16/106$) fixation at the four time series sites.....	119

Table 23 Results of 2 way ANOVA on cruise, site, and zooplankton biomass (mg dry weight m ⁻³) in the top 50m of the water column, assuming no diel change in biomass.....	122
Table 24 Mean (± SD) >100µm plankton biomass (mg dry weight m ⁻³) at Scott Reef. Data represent samples taken from the Lagoon site (LA), compared to the mixed layer (<100m) and deeper water (>100m) at the Channel site (CH), NE margin site (NE) and Open Water site (SW) at 4 times during the 24 hr time series.	122
Table 25 Results of 3 way ANOVA on cruise, site, depth and zooplankton biomass from multinet samples taken at the Channel (CH), NE margin (NE) and Open Water (SW) sites, assuming no diel change in biomass.	123
Table 26 Results of 2 way ANOVA on cruise, site and total zooplankton abundance (no. m ⁻³) in the top 50 m of the water column, assuming no diel change in abundance.	125
Table 27 Mean ± SD zooplankton abundance (no. m ⁻³) in the mixed layer at each site on each cruise.	125
Table 28 Mean ± SD zooplankton abundance (no. m ⁻³) in each depth stratum sampled by the multinet.	126
Table 29 Taxonomic units identified within the Copepoda.	131
Table 30 Five most powerful indicator species for each depth stratum	135
Table 31 Five most powerful indicator species for each site.....	135
Table 32 Occurrence at the Lagoon site (LA) of indicator species characteristic of subthermocline (>100m) water. a) species of Oncaeidae found at the Lagoon site (LA)	138
Table 33 Average abundance of euphausiid genera over all sites (no. 100m ⁻³).	141
Table 34 Results of the two-stage zero-inflated generalised linear model for the genus <i>Thysanopoda</i> , indicating abundance model and presence/absence model.....	142
Table 35 Results of the two-stage zero-inflated generalized linear model for the genus <i>Thysanoëssa</i> , indicating abundance model and presence/absence model.....	142
Table 36 Results of the two-stage zero-inflated generalised linear model for the genus <i>Nematoscelis</i> , indicating abundance model and presence/absence model.....	143
Table 37 Results of the Poisson regression model for the genus <i>Euphausia</i>	144
Table 38 Results of the two-stage zero-inflated generalised linear model for the genus <i>Pseudeuphausia</i> , indicating abundance model and presence/absence model (.....)	145
Table 39 Results of the Poisson regression model for the genus <i>Stylocheiron</i>	145
Table 40 Total volume and daily input rates for sub-thermocline water and Nitrate during intrusion events.....	156

Preamble

Background and Scope of Works

The Australian Institute of Marine Science (AIMS) entered into a contract (No. 4600001754) with Woodside Energy Limited (Woodside), as operator of the Browse LNG Development, on 28 February 2008, to undertake a three year research program at Scott Reef. For the purpose of this report, this research program is known as the Scott Reef Research Project (SRRP).

The research activity within the SRRP is divided among three projects:

- Project 1: Long-term monitoring of shallow-water coral and fish communities at Scott Reef
- Project 2: Physiological performance of deep water corals at South Scott Reef
- Project 3: Understanding water column and pelagic ecosystem processes affecting the lagoon of South Reef, Scott Reef

This final project report summarises findings of Project 3: *Understanding water column and pelagic ecosystem processes affecting South Reef Lagoon* based on the research by AIMS between 2008 and 2010 under the contract with Woodside (No. 4600001754). The project builds on the significant oceanographic research undertaken by AIMS at Scott Reef since 1993. One objective of Project 3 was to provide contextual environmental information to support biological monitoring and experimental programs undertaken to better understand the status and dynamics of shallow water (Projects 1) and deep-lagoon coral communities at South Scott Reef (Projects 2).

Previous AIMS oceanographic studies at Scott Reef in the period 1993-2008 focused on:

- defining seasonal and inter-annual fluctuations in water temperature and solar radiation fluxes
- measuring and modelling the dynamics of internal waves at Scott Reef
- measuring rates of pelagic primary production in regional water masses
- elucidating the physical oceanographic mechanisms underlying the temporal and spatial variability of both coral bleaching and coral recruitment at Scott Reef

This report specifically summarises the data collected from contiguous deployments of in-situ water quality logging instrumentation spanning March 2008 – February 2010, and four inter-seasonal biological oceanography cruises in June and December 2008, and June and November 2009. The data presented in this report represent a synthesis of a multi-year observational programme designed to observe seasonal and interannual change in the pelagic environment of South Reef lagoon, Scott Reef, Western Australia.

At the project start, on-reef deployment of production infrastructure was an active option. The initial oceanographic effort was therefore focused upon South Reef lagoon dynamics and potential implications of human activities upon the lagoon environment. During the course of the project, development planning shifted to off-reef sites with reduced direct impact on the South Reef lagoon. Accordingly, scientific examination of the deep channel between North and South Reefs and its eastern approaches were given greater focus.

Scott Reef rises abruptly to the surface at the continental shelf edge in a region characterized by strong cross-shelf tidal flows, large internal tides and large internal waves. Our working hypothesis was that intensified vertical mixing would take place in the waters surrounding Scott Reef as a result of the interaction between these strong flows and the bathymetry. The enhanced mixing would support higher levels of pelagic productivity in the waters around

Scott Reef and this higher productivity would, in turn, translate into greater availability of subsurface plankton biomass and larger fluxes of sinking detritus to deep-living reef and benthic filter feeding communities. The interactions between the regional internal wave field and the bathymetry would also potentially increase the extent of intrusive upwelling of nutrient enriched waters into the South Reef lagoon.

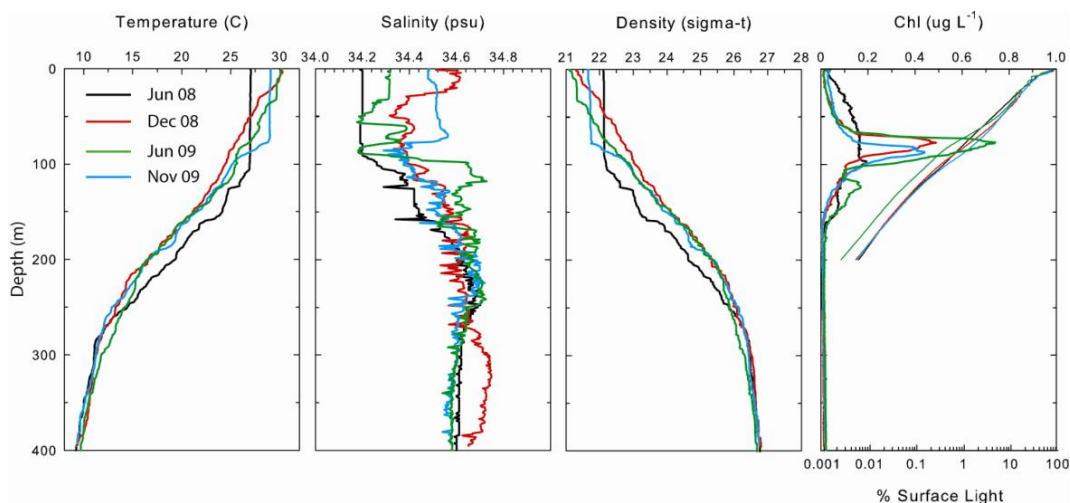
To resolve these questions, we undertook seasonal comparisons between physical and biological oceanographic processes at sites in or near Scott Reef likely to be strongly influenced by local bathymetry and a control site representative of open waters along the shelf margin.

Project Synopsis and Key Results

The oceanographic context of Scott Reef

Scott Reef is an isolated emergent reef system in the Eastern Equatorial Indian Ocean, located on the edge of the continental shelf offshore from the Kimberley coast of Western Australia. The regional oceanography is characterised by seasonally variable surface and subsurface currents that have direct impacts on both the marine ecosystems and the climate of northwest Australia and the wider region. Water masses within this region have a complicated multi-layered structure. The Indonesian Throughflow (ITF) which transports warm low salinity water into the region via a number passages through the Indonesian Archipelago, Timor Leste and northwest Australia is the dominant regional oceanographic feature. The ITF is variable on seasonal, interannual and decadal time scales. The largest and most persistent mode of ITF variation is associated with the El Niño Southern Oscillation (ENSO) phenomenon, and to a lesser degree, the Indian Ocean Dipole. Lower sea levels in the Indo-West Pacific reduce ITF transport during El Niño events. This temporal variability in water masses bathing Scott Reef was observed during the present study. Temperature/Salinity relationships from the four biological oceanographic cruises indicate a complicated and seasonally varying vertical structure of water masses around Scott Reef, with evidence for multiple interleaving layers both within the mixed layer and in the thermocline to >400 m depth.

The near-surface oceanic environment surrounding Scott Reef is typical of the Timor Sea and Eastern Equatorial Indian Ocean. It is characterised by a well mixed surface layer (~ 0–100 m water depth) of warm (27 – 30°C) highly transparent water that is deficient in nutrients. Below the surface mixed layer, water temperature declines to less than 10°C at 400 m depth. Ocean currents and the seasonal monsoonal weather cycle change the layering of the water column so that the surface mixed layer deepens during periods of persistent wind and thins during calm periods. The denser, deep water is high in nutrients but receives little light, whereas the well-lit surface layer is depleted of nutrients. Optimum phytoplankton growth occurs where there are both light and nutrients, and results in the formation of a subsurface chlorophyll maximum at the base of the euphotic zone (usually just above 100 m).



Vertical profiles of water temperature, density, chlorophyll and light penetration at an open water site in the vicinity of Scott Reef.

The stable vertical layering of the ocean supports the development of internal tides and internal waves that appear as periodic vertical excursions of the thermocline. These internal waves increase in amplitude when they encounter shoaling of the bottom or changes in the bottom topography, such as reefs and submerged banks. In such circumstances, internal waves can be an important mechanism for mixing nutrient-rich water into shallow coral reef communities.

The bio-physical environment of the lagoon of South Reef.

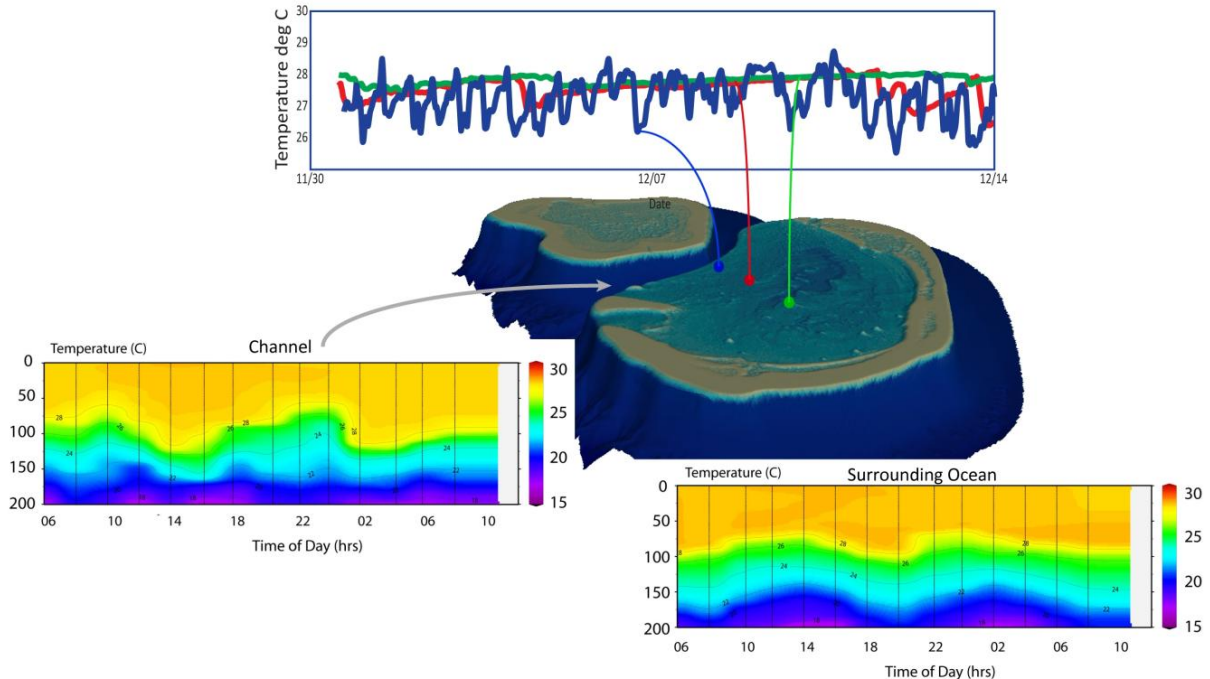
The physical environment of South Reef lagoon is largely controlled by the regional monsoonal climate, the seasonal cycle of solar radiation, seasonal characteristics of the surface layer in the surrounding ocean and tidal interaction of these waters with the topography of the reef. Like the surrounding ocean, water clarity within the lagoon is high, with no significant inter-seasonal differences in water transparency. The amount of PAR (Photosynthetically Available Radiation – visible light with wavelengths between 400 and 700 nm) reaching the lagoon benthos at the deepest in-situ observational sites (~55 m water depth) is typically >1% surface PAR and is within the range of 1% – 10% for lagoon sites at depths between 55 m and 35 m. The depth-averaged light extinction coefficient (k) of PAR in the lagoon water was of the order of 0.07 – 0.09 m⁻¹.

The lagoon environment tracks the seasonal and inter-annual variability in temperature and salinity structure exhibited by the regional oceanic waters, with additional higher frequency variability caused by local processes such as enhanced vertical mixing due to internal waves, modified horizontal advection and residence times and local evaporation. Daily averaged water temperatures within the lagoon between March 2008 and February 2010 ranged from 24.7°C – 30.4°C, with minimum and maximum temperatures of 24.4°C and 30.9°C. Lagoon water temperature varies seasonally with a maximum in April and a minimum in late August.

The primary driver for the local temporal and spatial variability of water temperature within the South Reef lagoon is the intrusion of cool water originating from the deep channel separating North and South Reef. Cool water intrusions are primarily semi-diurnal in timing, driven by the strong semi-diurnal periodicity in the prevailing internal wave and tide regime in the channel, combined with horizontal shear due to the strong tidal currents that can entrain water from below the sill depth up into the lagoon. Instrumental data suggests that the cool water intruded into the lagoon originates within the thermocline from depths shallower than 160 m. Instrumental evidence for relatively shallow origins of intruded water is supported by vertical zooplankton community structure. Particular zooplankton species are known to be associated with certain depth horizons in the water column. Zooplankton communities within the lagoon contained species associated with the 50 – 100 m stratum at deeper stations. There was no indication of the presence of deeper water (such as from the 250 – 450 m horizon) within the lagoon.

Salinity within the lagoon is, in general, horizontally and vertically uniform. However there is evidence of transient episodes of salinity stratification due to local rainfall, evaporation and vertical mixing with upper thermocline water from the deep channel. Variability in the average seasonal salinity within the lagoon reflected the variability in the regional circulation and the resulting exposure of Scott Reef to water bodies of diverse origins.

Lagoon water is persistently low in suspended matter. Total suspended sediment concentrations measured in the central lagoon were < 1 mg L⁻¹ and often close to the limits of detection for the method. Mean sedimentation fluxes determined from in-situ sediment traps within the deeper sections of the lagoon were also low (site deployment means – 0.2-0.5 mg DW cm⁻² day⁻¹).



Typical water column temperature time series around Scott Reef.

Chlorophyll concentrations within the lagoon exhibit episodic spatial variability driven by a local response to the delivery of new nutrients via intrusions of cool thermocline water. Average chlorophyll concentrations in the interior of the lagoon were consistently higher than at observational sites adjacent to the deep channel. We observed a persistent near-bottom layer of enhanced chlorophyll concentration that covered much of the central lagoon.

Dissolved nutrient concentrations in South Reef lagoon waters were consistently very low, though slightly higher than in the surface layers of the surrounding oceanic waters. Concentrations of NO_2^- , NO_3^- and PO_4^{3-} at the surface are in the range of 1's to 10's of nmoles per litre. Although intruded thermocline water was not sampled within the lagoon, slightly elevated near-bottom concentrations of NO_3^- on the order of 0.1–0.3 μM and lesser increases of PO_4^{3-} were consistently observed, indicating some (near-) continuous lateral transport of thermocline waters into the lagoon. Ratios of summed concentrations of inorganic N species to PO_4^{3-} were consistently below the canonical Redfield ratio ($\text{N}_{16}:\text{P}_1$), indicating that total phytoplankton biomass in surface waters and the lagoon is strongly constrained by nitrogen availability. Silicate concentrations were sufficiently high (1–2 μM) that it is unlikely that the relatively small assemblage of diatoms in Scott Reef waters (nominally the >10 μm size fraction of chlorophyll) are Si-limited at any time. The dominant cyanobacteria do not require Si as a nutrient.

Comparisons of Scott Reef with other regions

Phytoplankton

Phytoplankton communities at Scott Reef are typical of oligotrophic tropical oceanic waters and atoll lagoonal systems. These communities are dominated by unicellular cyanobacteria < 2 μm in size (picoplankton), chiefly *Synechococcus* and *Prochlorococcus*, and very small (pico-) eukaryotic algae. At most sampling sites, picoplankton comprised ≥ 80 percent of the

phytoplankton standing crop (as chlorophyll). With two exceptions, phytoplankton $>10 \mu\text{m}$ (most diatoms fall into this size fraction) contributed < 15 percent of the chlorophyll standing crop. The intermediate 2 – 10 m size fraction, comprised largely of small flagellates, made up approximately 10 percent of chlorophyll biomass.

Prochlorococcus and photosynthetic pico-eukaryotes were found throughout the upper 200 m of the water column while *Synechococcus* was largely restricted to the upper 100 m. *Prochlorococcus* is the most abundant phytoplankton taxon at deep (oceanic) stations, but as found in other atoll lagoon systems, *Synechococcus* is of similar or greater abundance at stations in the South Reef lagoon. The relative abundances of *Prochlorococcus* to *Synechococcus* are known to be inversely related to nutrient availability with a higher proportion of *Prochlorococcus* occurring in water with low nutrient concentration. The Pro:Syn ratio is therefore an indicator of water quality independent of the ambient nutrient concentrations. Pro:Syn ratios at deep water sites were universally >1 , while Pro:Syn ratios ≤ 1 were observed within the South Reef lagoon. Overall, the South Reef lagoon has the picoplankton community characteristics of a relatively open system with a low level of water quality modification by enclosure.

Bacteria

Abundances of bacterioplankton in Scott Reef waters ($10^5 - 10^6$ cells ml^{-1} ; including both true bacteria and Archaea) were similar to abundances in other oligotrophic pelagic systems and reef lagoons. The bacterioplankton are largely responsible for recycling organic matter in the water column by converting dissolved organic matter into biomass, which re-enters the various pelagic food webs. Bacterioplankton, in turn, are prey items for viruses, nano-flagellates and larger specialised filter feeders such as larvaceans.

Viruses

Viruses were the most abundant 'living' organisms in Scott Reef lagoon and the surrounding ocean waters ($10^6 - 10^7$ ml^{-1}). This was the first time that viral life strategies had been investigated for a coral reef system of the Indian Ocean. Vertical distributions of viruses in Scott Reef waters closely paralleled the distribution of their primary prey organisms - heterotrophic bacteria and *Prochlorococcus*. Calculated viral lysis rates indicate that viral infection and lysis are the major source of bacterioplankton mortality in Scott Reef waters. In essence, the bacterioplankton community in Scott Reef waters turns over on a daily basis.

Primary production

Pelagic primary production measured during this study ranged between 200 and 1,300 $\text{mg C m}^{-2} \text{d}^{-1}$ with winter (June – July) and summer (November – December) averages of 570 and 830 $\text{mg C m}^{-2} \text{d}^{-1}$, respectively. Primary production rates estimated concurrently from oxygen metabolism averaged 950 $\text{mg C m}^{-2} \text{d}^{-1}$. Production rates measured in this study are similar to rates measured previously at Scott Reef (averages 700 – 750 $\text{mg C m}^{-2} \text{d}^{-1}$), in the Coral Sea (~ 600 $\text{mg C m}^{-2} \text{d}^{-1}$) and Great Barrier Reef (780 $\text{mg C m}^{-2} \text{d}^{-1}$). Primary production in waters around Scott Reef is therefore within the range of modern production rates measured in oligotrophic oceanic environments. Bacterial biomass production rates within the water column ranged between 34 and 102 $\text{mg C m}^{-2} \text{d}^{-1}$, averaging 6% of concurrent primary production.

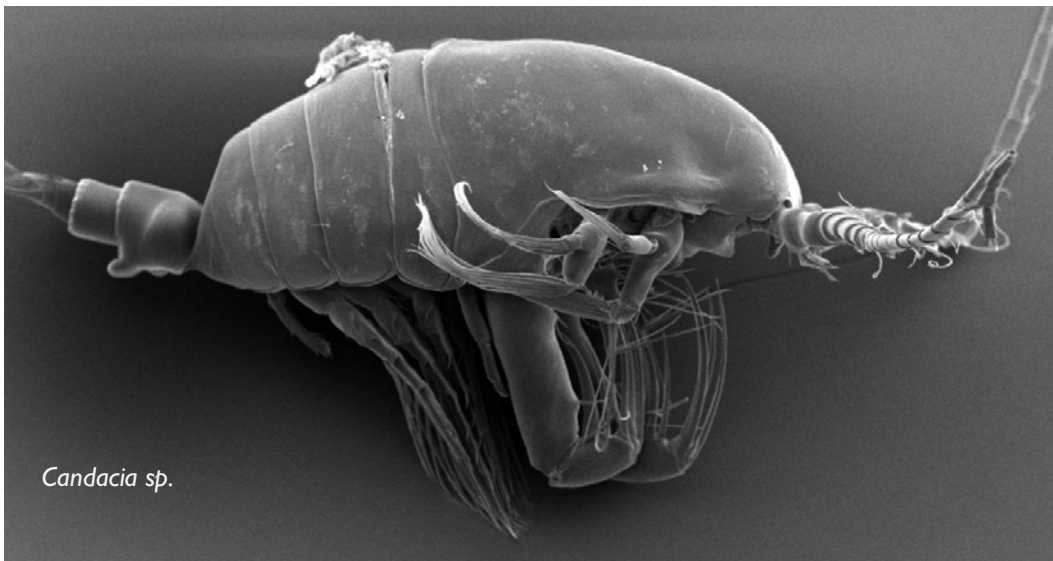
Metabolism

Water column metabolism measurements establish the balance between primary production and community respiration, determining whether the ecosystem is a net producer ('autotrophic' - consumes CO_2 , produces O_2) or consumer ('heterotrophic' - produces CO_2 , consumes O_2) of organic matter. At Scott Reef, we determined that the threshold required to achieve metabolic balance (production = respiration) is similar to oligotrophic systems such

as the subtropical Atlantic Ocean. The respiration rate of water column microbes is correlated with temperature, resulting in generally higher rates during November – December than during June. However, of 19 sets of oxygen flux measurements integrated throughout the water column at 4 sites around Scott Reef, 11 resulted in net water column heterotrophy, and of these 7 were in the summer months. Overall, the Scott Reef metabolic data are similar to other areas of the tropical or subtropical ocean such as the Banda Sea, Arabian Sea, and Equatorial Atlantic and align with the low end of data from similar experiments conducted by AIMS in the Timor Sea and the Coral Sea. The frequent occurrence of heterotrophy at Scott Reef is similar to the open ocean near Hawaii, and this may indeed be the case in many areas of the open ocean.

Zooplankton

The present study is the first to study depth-stratified zooplankton communities in Australia's Indian Ocean territory, and the first to include abundant small species (<1.0 mm in length).



Candacia sp.

Distinct zooplankton communities occurred in particular depth strata and sites of collection. The lagoon zooplankton community was a subset of the surface water community found at all study sites. The main difference from communities sampled in a similar depth range at deeper water sites in the deep channel between North and South Reef and to the North East (NE) and South West (SW) of Scott Reef was the presence of reef-associated organisms. Zooplankton from the 50 – 100 m stratum formed a distinct community associated with the deep chlorophyll maximum, and those from intermediate depths (represented by the 100 – 200 and 200 – 300 m strata) formed a third community typical of the SW site. The fourth, and most distinct zooplankton community, was a near-bottom assemblage typical of the 300 – 400 m depth stratum at the deep channel and NE sites, where the deepest samples collected coincided with the maximum water depth. These samples contained representatives of copepod families which occur elsewhere in near-bottom waters, and which are very poorly known in Australian waters.

The only directly comparable study of zooplankton community composition in the tropical Indian Ocean is an earlier (1997 – 1998) AIMS study at North West Cape, Western Australia (21° 49' S, 114° 14' E), which was restricted to coastal communities in summer. Zooplankton biomass in the lagoon of South Reef during the summer was comparable to that in Exmouth Gulf, but at the deeper stations mixed-layer biomass was half the biomass at the

shelf break at North West Cape. Similarly, the summer abundances of zooplankton at North West Cape was similar to the lagoon at Scott Reef, but 2 to 4-fold higher than in the mixed layer at the deeper water stations. As at Scott Reef, copepods overwhelmingly dominated the zooplankton. The copepod community at North West Cape was very similar to that found in the lagoon of South Reef and in the mixed layer at the deeper water stations.

Six genera of tropical krill (euphausiids) were collected at Scott Reef. We were unable to demonstrate that the deep channel was a 'hotspot' of krill abundance that might attract filter-feeding megafauna. This result should, however, be taken in the context that the methods used do not have sufficient depth resolution to detect localised aggregations of krill associated with complex bathymetry.

Strongest gradients in the vertical

Our analyses of water column properties, water chemistry and plankton community structure consistently show that the greatest changes are related to depth, with relatively little horizontal difference between samples from the same depth at different locations around Scott Reef. Within the lagoon, however, subtle differences between sites were observed. Picoplankton varied somewhat from place to place in the lagoon, but these differences were of the same order as those found vertically through the water column, with the greatest abundances found in the subsurface chlorophyll maximum.

The zooplankton community was very strongly structured according to depth, with mixed layer communities (surface and chlorophyll maximum) having both higher abundances and distinct composition differences compared to mid-water and near-bottom depth strata. Our measurements of pelagic processes also showed strong depth variation, and only slight difference between sites. On the basis of these multiple lines of evidence, we conclude that the strongest gradients of biophysical variables occur in the vertical rather than the horizontal; i.e. that depth effects outweigh the differences between sites.

Is the lagoon different from the surrounding ocean?

There are small, but consistent and significant differences between physical parameters measured in the lagoon and in surrounding surface waters, including average temperature, salinity and the underwater light climate. Lagoon waters have slightly higher concentrations of dissolved nutrients and chlorophyll, and higher abundances of autotrophic picoplankton, bacterioplankton and viruses. Relative abundances of autotrophic picoplankton are indicative of a very slightly (but naturally) eutrophied system. Zooplankton biomass is higher inside the lagoon with a community composition characterized by more reef-associated species. Persistent differences in characteristics between the lagoon and surrounding waters indicate that the water within the lagoon has a sufficient residence time for internal processes to modify its character and for distinctive planktonic biological communities to form and stabilise.

From an environmental management perspective, these differences mean that any wastewater or other discharges into or reaching the lagoon (whether planned or unplanned) will be retained within the lagoon for some time until flushed out and have the potential to affect biological communities within the lagoon. Current estimates of retention time are poorly constrained (but see below), and will depend on the tidal range, tidal and residual currents, wind speed and wind direction.

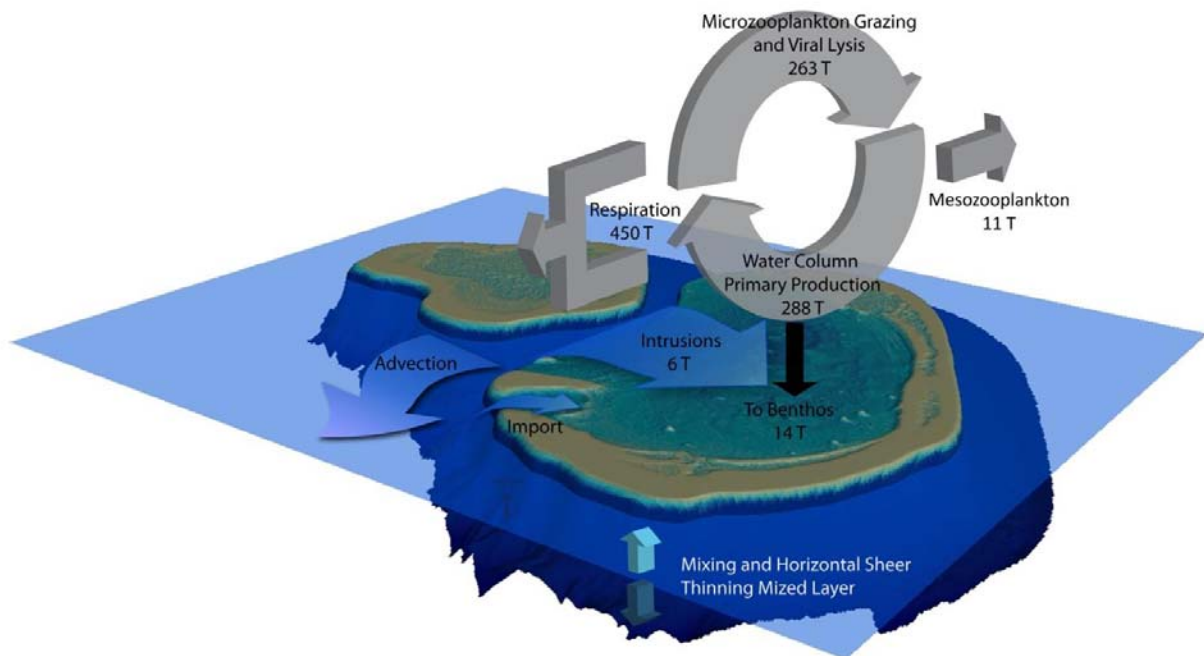
Carbon Budget

Water mass and nutrient exchange between the lagoon and the channel

The surface mixed layer around Scott Reef is characterized by extremely low nutrient levels. To determine the biological significance of nutrients in cool water intrusions, it is important to resolve the volume of the exchange of water from below the thermocline, and distinguish this input from the ongoing tidal exchanges of surface waters. Approximately 5% of the lagoon's volume is exchanged in an average tidal cycle, suggesting a first-order approximation of lagoon flushing on the order of 10 days.

The volumetric exchange of sub-thermocline water between the deep channel and lagoon is estimated to be $\sim 0.53 \text{ km}^3 \text{ d}^{-1}$, or 4% of the lagoon's volume, almost equivalent to the (semi-diurnal) tidal prism. The amount of NO_3^- introduced through the intrusions of sub-thermocline water was calculated based on the observed linear relationship between temperature and NO_3^- concentrations in the thermocline and was estimated at $0.6 \text{ Mm d}^{-1} (\text{mol} \times 10^6)$.

Based on a measured pelagic primary production of $\sim 800 \text{ mg C m}^{-2} \text{ d}^{-1}$, total carbon production in the lagoon is estimated to be $\sim 288 \text{ T C d}^{-1}$. In contrast, carbon production due to 'new' nutrients in the sub-thermocline intrusions is estimated to be of the order of 6 T C d^{-1} , and thus daily pelagic production based on nutrient recycling far exceeds (by 2 orders of magnitude) the carbon production supported by the deep water intrusions. The carbon fixed by photosynthesis within the euphotic zone (0 – 100 m) each day at Scott Reef is quickly consumed within the upper water column, and measured sedimentation fluxes of organic carbon down out of the euphotic zone (100 m) were generally $< 10\%$ of daily production rates.



A conceptual model of carbon cycling and export from the mixed layer at Scott Reef.

Biological consequences

Intense grazing by very small flagellates and ciliates and lysis by viruses means that the picoplankton community largely responsible for primary production in Scott Reef waters turns over on a daily basis. The associated pelagic bacteria are largely supported by organic matter excreted from phytoplankton cells and the cellular debris released during viral lysis. The high respiration rates of pelagic micro-organisms means that very little pelagic primary production is unconsumed and available for sedimentation from the water column. While it is known that both corals and sponges are capable of feeding on very small particles such as picoplankters, the densities of these organisms within both the lagoon and surrounding waters are too low to provide an adequate food source for rapid growth. The deep-living corals in the lagoon therefore obtain most of their energy from symbiotic photosynthesis, which is consistent with findings from SRRP Project 2.

Lagoonal water quality and the dynamics of coral reef communities

The health and resilience of reef-associated coral and fish communities are intimately linked to the physical, chemical and biological properties of the waters in which they live. The highly transparent, nutrient poor waters that bathe Scott Reef are well suited for the development of coral reefs. This is reflected in the biological diversity of the Scott Reef system which supports approximately 720 species of fish and 300 species of corals. The isolation of Scott Reef insulates the local reef communities from major terrestrial inputs and the associated stressors that affect coral reefs closer to the coast. However, a range of natural disturbances such as cyclones, increasing ocean temperatures and changing ocean chemistry still perturb coral and fish communities at Scott Reef. The factors that determine whether communities recover from perturbations, and the rate and extent to which the recovery trajectory

converges upon a healthy prior state, include the supply of new recruits (numbers and types), the rates of growth and survival of the corals and their competitors, and the prevailing physical and biological conditions at the location. This project has shown that water quality within the lagoon of South Reef is persistently high, with high clarity, low nutrients, low sedimentation rates and temperatures which are, in general, well suited to coral reef growth. If high water quality is maintained, then the dynamics of coral and fish communities at Scott Reef will be driven primarily by natural disturbance and recovery cycles, with the timescales, rates and variability of recovery as documented by SRRP Project 1.

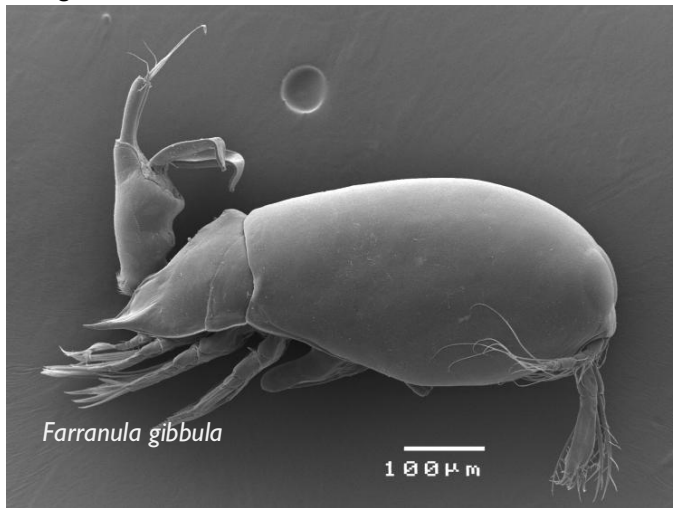
Coral bleaching is forecast to increase in frequency with increasing ocean temperatures. Recent research on the trophic response of corals to the combined effects of increased turbulence and reduced temperature associated with internal waves suggests that exposure to enhanced levels of nutrients and particulate food carried by internal waves results in higher energy reserves, which may be crucial for coral resilience to stress and survival during periods of reduced or inactive photosynthesis, as is known to occur after coral bleaching. Therefore, the coral communities most exposed to the cool water intrusion and turbulence associated with internal wave activity around the perimeter and with the deep channel of Scott Reef may show enhanced resilience to temperature-induced coral bleaching.

Benthic-Pelagic Coupling

Our starting hypotheses was that the deep-living lagoon coral communities of the South Reef lagoon would be light limited and therefore more dependent on heterotrophic nutrition. Measurements of the photosynthesis-irradiance (P vs I) characteristics of the deep-living corals (SRRP Project 2) indicate they are photoadapted to low light intensities and efficiently use the low available light. Direct measurements of inorganic and organic matter sedimentation show that organic matter fluxes to the lagoon benthos are very low. Fluxes of inorganic sediment were generally $< 5,000 \text{ mg DW m}^{-2} \text{ d}^{-1}$ ($< 0.5 \text{ mg cm}^{-2} \text{ d}^{-1}$). Organic matter fluxes in the central South Reef lagoon ranged between 25 and 61 $\text{mg C m}^{-2} \text{ d}^{-1}$. Concurrent organic nitrogen fluxes ranged between 1.7 – 6.2 $\text{mg N m}^{-2} \text{ d}^{-1}$. The deep-living corals therefore obtain most of their energy from symbiotic photosynthesis and are highly dependent on good (clear) water quality. While corals can feed on pelagic microorganisms, the densities of phytoplankton and bacteria within the lagoon are too low to provide a fully adequate food source for rapid growth.

Zooplankton Biodiversity

This project has included detailed taxonomic study of the copepod component of the zooplankton, and has identified >220 species of copepods. Most excitingly, 68 (31%) are new records for Australian waters and at least 16 are likely to be new species. The hitherto unappreciated biodiversity within one copepod family is remarkable, and appears to comprise >65 species, of which 35 are new records for Australia and 11 are undescribed, including one new genus.



By comparison, 122 species of copepods were identified during the North West Cape study, substantially fewer than found at Scott Reef. The reason for the difference is the greater representation of a distinctive deep-water community at Scott Reef. Copepod communities of the Great Barrier Reef, have a similar number of species (~200) to those of Scott Reef, but do not include the very diverse small copepods included in the present study.

Regional Applicability

There was no appreciable differences in hydrographic structure, vertical nutrient distributions, plankton biomass, community structure and productivity between the three deep-water sites around Scott Reef (Deep Channel, NE Margin, Open Water; Figure 1) despite their differing exposures to bathymetry-induced mixing. The strongest structuring factor in the pelagic environment at these sites is the vertical density gradient which is largely related to water temperature. The similarity between these sites strongly indicates that the biological and chemical oceanographic observations in the upper water column (0 – 200 m) made at these sites will be generally applicable to the broader deep water (>200 m) environment of the outer continental shelf in the Browse Basin region. This would include the waters overlying the Brecknock and Calliance gas fields. The water column conditions and processes, and pelagic ecosystem attributes observed at deep-water sites in the vicinity of Scott Reef will also likely apply to offshore oceanic waters bordering the continental shelf. The full extent of differences between plankton communities living in the vicinity of Scott Reef and other locations is not well known at present and likely reflects differences in the extent and type of sampling as much as true biological differences.

Although not examined during this study, the communities and conditions which characterize waters around Scott Reef and the outer continental shelf are likely to have a shoreward boundary in shallower waters on the continental shelf where significant interactions between deep-water internal waves or tides and the bottom begin to occur, creating enhanced vertical mixing due to bottom stress, breaking internal waves and tides. Because of this enhanced mixing, both within the thermocline and in the benthic boundary layer, generalizations about pelagic conditions derived in the current study may not wholly apply to the boundary zone. The present study does not consider the potential influence of large benthic features such as submarine canyons on water column physical, chemical and biological conditions. These features elsewhere are known to harbour diverse benthic and pelagic biological communities.

Applicability to North Reef

North Reef differs from South Reef in having a much shallower and more enclosed lagoon with only two primary points of exchange with the surrounding ocean, and therefore more limited tidal exchange. North Reef is likely to exhibit higher average temperatures than the surrounding ocean as the contained water is warmed by solar radiation. Salinities will also diverge from the surrounding ocean, being higher during times when evaporation is in excess of rainfall, and visa versa. With limited flushing, tidal currents within the interior of the lagoon will be weak, and the surficial sediments are likely to contain a larger percentage of fine material which will be more susceptible to resuspension during strong wind events. As such light attenuation may be more variable than observed in South Reef lagoon.



Executive Summary

This report summarises the results of AIMS research on the bio-physical oceanographic environment of Scott Reef between 2008 and 2010 under Woodside Contract No. 4600001754. Data was collected from contiguous deployments of in-situ water quality logging instrumentation in the lagoon and deep channel between March 2008 and February 2010, and from four inter-seasonal biological oceanography cruises in June 2008, December 2008, June 2009 and November 2009. The contemporary data is placed in the context of AIMS' historical oceanographic research undertaken at Scott Reef since 1993.

The general conclusions of this report are:

- The near-surface oceanic environment surrounding Scott Reef is typical of the Timor Sea and Eastern Equatorial Indian Ocean. It is characterised by a well mixed layer of warm (27–30°C) highly transparent water (~ 0–100 m water depth) that is deficient in nutrients. Below this surface mixed layer, water temperature decreases to less than 10°C at 400 m depth. Ocean currents and the seasonal monsoonal weather cycle change the layering of the water column so that the surface mixed layer deepens during periods of persistent wind, and thins during calm periods. The denser, deeper water is higher in nutrients but receives little light, whereas the well-lit surface layer is depleted of nutrients. Enhanced phytoplankton growth occurs where there is some of each, and results in the formation of a deep chlorophyll maximum in vertical profiles (usually just above 100 m).
- The stable vertical layering of the ocean around Scott Reef supports the existence of internal tides and internal waves that appear as periodic vertical excursions of the thermocline. The regular semi-diurnal internal tide in the surrounding ocean is modified by the local bathymetry resulting in amplified vertical displacement and increase frequency of motion of the thermocline within the channel between North and South Reef, with peak internal wave amplitudes exceeding 100 m.
- The lagoon environment mirrors the seasonal and inter-annual variability in temperature and salinity structure exhibited by the regional oceanic waters, with additional higher frequency variability caused by local processes such as enhanced vertical mixing, modified horizontal advection and residence times, as well as increased local evaporation. Daily average water temperatures within the lagoon between March 2008 and February 2010 ranged from 24.7°C – 30.4°C, with minimum and maximum observed temperatures of 24.4°C and 30.9°C. Lagoonal water temperature vary seasonally with a maximum in April followed by a minimum in late August, in concert with the seasonal cycle of insolation.
- The primary driver for local temporal and spatial variability of temperature within the South Reef lagoon is the near-bottom intrusion of cool water from the channel separating North and South Reef. Near-bottom habitats close to the channel experience daily temperature ranges of up to 5°C during strong intrusion events. Cool water intrusions are primarily semi-diurnal, driven by a combination of the strong semi-diurnal periodicity in the prevailing internal wave and tide regime and the horizontal shear due to the strong tidal currents that can entrain water from below the sill depth into the lagoon.

- Salinity within the lagoon is generally horizontally and vertically uniform, however there were transient episodes of salinity stratification due to local rainfall, evaporation and enhanced vertical mixing with water from the upper thermocline within the channel.
- Chlorophyll concentration within the lagoon exhibits episodic, event-driven spatial variability, arising as a local response to the delivery of new nutrients via intrusions of cool thermocline water. Average chlorophyll concentrations in the interior of the lagoon were consistently higher than at observational sites adjacent to the deep channel. A persistent near-bottom layer of enhanced chlorophyll covered much of the central lagoon.
- Lagoon water is persistently low in suspended matter (0.04 – 1.50 NTU), with very limited spatial variability in the deeper sections of the lagoon. Total suspended sediment concentrations measured in the central lagoon were $< 1 \text{ mg L}^{-1}$ and often close to the limits of detection. Mean sedimentation fluxes determined from in-situ sediment traps within the deeper sections of the lagoon are very low ($< 0.8 \text{ mg cm}^{-2} \text{ d}^{-1}$)
- Instrumental data suggests that the origin of cool water intruded into the lagoon is from within the thermocline from depths of less than 160m. Instrumental evidence of relatively shallow origins of intruded water is supported by analysis of changes in zooplankton community structure. Particular zooplankton species are known to be associated with certain depth horizons. Zooplankton communities within the lagoon included occurrences of species corresponding to the 50 – 100 m stratum at the deeper stations. There was no indication of the presence of water from deeper strata (such as from the 250 – 450 m horizon) within the lagoon.
- There are differences between the lagoon and the surrounding surface waters, including differences in physical variables such as temperature and salinity, and characteristics of the underwater light climate. Biologically, the lagoon has slightly higher concentrations of dissolved nutrients, higher surface chlorophyll concentrations, and higher abundances of autotrophic picoplankton, bacterioplankton and viruses, with relative abundances of autotrophic picoplankton indicative of a slightly (but naturally) eutrophied system. There is also a higher zooplankton biomass inside the lagoon, with elements of the species composition indicative of a reef associated fauna.
- Surface concentrations of nitrate, phosphate and silicate in the open ocean were very low and increased steadily with depth below the mixed layer proportionally with decreasing temperature. Within the surface waters (0 -30 m) of South Reef lagoon, dissolved nitrate and phosphate concentrations were also very low, but slightly elevated nitrate concentrations were consistently measured near-bottom in the mid-lagoon.
- Over 75% of the standing crop of phytoplankton (as chlorophyll) and 80% of the primary production was measured in the $< 2 \mu\text{m}$ size fraction (picoplankton). The picoplankton were overwhelmingly dominated by unicellular cyanobacteria $< 2 \mu\text{m}$ in size (picoplankton) from the genera *Synechococcus* and *Prochlorococcus*.
- Pelagic primary production rates measured in the general vicinity of Scott Reef ranged between 200 and 1,300 $\text{mg C m}^{-2} \text{ d}^{-1}$. The carbon fixed by photosynthesis within the euphotic zone (0 – 100 m) each day at Scott Reef is quickly consumed within the

upper water column. Measured community respiration rates, whether on a volumetric or areal basis, usually equalled or exceeded carbon fixation or net oxygen production rates. Measured sedimentation fluxes of organic carbon down out of the euphotic zone (100 m) were generally < 10% of daily production rates. There is also a small downward mixing flux of dissolved organic carbon (DOC) driven by the small concentration difference between the surface mixed layer and the deeper thermocline.

- Direct measurements of inorganic and organic matter sedimentation fluxes by bottom-mounted and floating (Lagrangian) sediment traps clearly show that fluxes to the benthos are very low within the lagoon and on the deep margins of Scott Reef. Time-averaged daily collections of new and resuspended sediment by bottom-mounted sediment traps were generally less than 5,000 mg DW m⁻² d⁻¹, with all but one average value < 8,000 mg m⁻² d⁻¹. Daily organic matter fluxes measured in the central part of the South Reef lagoon ranged between 2.1 and 5.1 mmol C m⁻² (25 - 61 mg C m⁻²), or between 0.5 and 1 % of the inorganic sedimentation flux. Concurrent organic nitrogen fluxes ranged between 0.12 and 0.46 mmol C m⁻² (1.7 – 6.2 mg C m⁻²).
- Based on our estimates of pelagic primary production, respiration and grazing, a first order carbon budget for the lagoon has been constructed. Total carbon production for the lagoon is estimated at ~288 T C d⁻¹, with an additional input 6 T C d⁻¹ due to nutrients imported by the sub-thermocline intrusions. Four percent (4%) of primary production (~11 T C d⁻¹) is transferred to mesozooplankton while five percent (5%) of primary production (~14 T C d⁻¹) is transferred to the benthos. Total community metabolism is ~450T C d⁻¹.
- One of the original hypotheses of this study was that the deep-living coral communities of the South Reef lagoon (depth 30 – 60 m) would be significantly light limited (0.4–7 % I₀ based on a depth-averaged attenuation coefficient of 0.09 m⁻¹ in the lagoon) and possibly exposed to sediment resuspension, so that they would be relatively more dependent on catching plankton or harvesting sedimenting detritus from the water column to survive and grow. However, because of the almost-complete consumption of daily primary production within the euphotic zone, very little of the pelagic organic matter produced in South Reef lagoon and surrounding waters is transferred to benthic communities via sedimentation from the water column. The energy and organic matter required by the dominant structure-building members of benthic communities in the South Reef lagoon must therefore be largely produced autotrophically through primary production by benthic algae and photosynthetic symbionts (eg. zooxanthellae) in the corals and sponges. Measurements of the photosynthesis-irradiance (P vs I) characteristics of deep-living corals (SRRP Project 2) indicate that corals living on the lagoon floor are photoadapted to low light intensities and efficiently use the low available light. While it is known that many benthic organisms, including corals and sponges are capable of feeding on very small particles such as picoplankters, the densities of this particulate matter within both the lagoon and surrounding waters are too low to provide a significant portion of their energy needs. The low amounts of suspended organic matter in the lagoon strongly suggests that obligate filter feeders in benthic communities are energy-limited and likely slow growing. The deep-living corals obtain most of their energy from symbiotic photosynthesis.

- The health and resilience of reef associated coral and fish communities are intimately linked to the physical, chemical and biological properties of the waters that surround them. The highly transparent, nutrient poor waters that bathe Scott Reef are well suited for the development of coral reefs, and this is reflected in the biological diversity of the Scott Reef system which supports approximately 720 species of fish, 300 species of corals (Gilmour et al. 2010). The isolation of Scott Reef insulates the local reef communities from major terrestrial inputs and associated stressors affecting coral reefs closer to the coast, however, a range of natural disturbances such as cyclones, increasing ocean temperatures and changing ocean chemistry still perturb the dynamics of coral and fish communities at Scott Reef. The underlying drivers that determine whether communities recover, and the rate and extent to which the recovery trajectory converges towards a prior state, include the supply of new recruits (numbers and types), the rates of growth and survival of the corals and their competitors, and the prevailing physical and biological conditions at the location (Gilmour et al. 2010). This project has shown that water quality within the lagoon of Scott Reef is persistently high, with high clarity, low nutrients, low sedimentation rates and temperatures which are, in general, well suited to coral reef growth. If high water quality is maintained, then the dynamics of reef associated coral and fish communities at Scott Reef will be driven primarily by cycles of natural disturbance and recovery, with the timescales, rates and variability of recovery as documented in SRRP Project 1 (Gilmour et al. 2010).
- Our analyses of water column properties, water chemistry and plankton community structure at Scott Reef consistently show that the greatest changes are related to depth, with relatively little horizontal difference between samples from the same depth at deeper sites. The zooplankton community, in particular, was very strongly structured according to depth, with mixed layer communities (surface and chlorophyll maximum) having both higher abundances and distinct communities compared to mid-water and near-bottom depth strata. Our measurements of pelagic processes also showed strong depth structure, and only slight difference between sites. On the basis of these lines of evidence, we conclude that the strongest gradients of biophysical variables occur in the vertical rather than the horizontal; i.e. that depth-related effects outweigh the differences between sites. This result means that the general patterns observed during the study can be extrapolated regionally.
- This project has included detailed taxonomic study of the copepod component of the zooplankton, and has identified >220 species of copepods, belonging to 5 of the 9 orders. Most excitingly, 68 (31%) are new records for Australian waters and at least 16 are likely to be new species. The hitherto unappreciated biodiversity within the family Oncaeididae alone is remarkable, and appears to comprise >65 species, of which 35 are new records for Australia and 11 are undescribed. Copepod communities of the Great Barrier Reef, as compiled by McKinnon et al. (2007), have at least a similar number of species (~200) to those of Scott Reef, but do not include the very diverse small copepods included in the present study.
- The absence of appreciable differences in hydrographic structure, vertical nutrient distributions, plankton biomass, community structure and productivity between the three deep-water sites around Scott Reef (Deep Channel, NE Margin, Open Water) with differing degrees of topographic influence strongly indicates that the biological and chemical oceanographic observations made at these sites will be generally applicable to the wider deep water (>100 m) environment of the outer continental shelf overlying the Browse Basin region. This would include the waters overlying the

Brecknock and Calliance gas fields. The water column conditions and processes, and pelagic ecosystem attributes observed in the vicinity of Scott Reef will likely apply to outer shelf waters, with a shoreward boundary for the type of conditions existing at Scott Reef on the mid-shelf at depths where significant interactions between deep-water internal waves or tides and the bottom begins, creating significant bottom stress or enhanced vertical mixing due to breaking internal waves and tides.

Introduction

Large tides and strong thermal stratification in the Indian Ocean waters surrounding Scott Reef interact with regional bathymetry to form large and dynamic internal waves. Propagating internal waves episodically lift nutrient-rich sub-thermocline water into the euphotic zone and the dissipation of internal wave energy fuels vertical and horizontal mixing, which is a key determinant of the vertical distribution of physical, chemical and biological properties of the water column. Locally, bottom topography can alter the amplitude and period of these waves. The net effect is to introduce cool nutrient-rich water from the thermocline into the low-nutrient near-surface layers of the Scott Reef ecosystem (Steinberg et al., 2003; Bird et al., 2004). These added nutrients have the capacity to enhance production of organic matter in this normally oligotrophic environment. The spatial extent and temporal variability of intrusion events linked to internal wave activity and topography is poorly understood as are their physical consequences. Nutrients introduced into the near-surface layer during enhanced mixing or upwelling events are likely to support higher plankton production, resulting in increased plankton biomass and detritus that becomes available to corals and fishes dwelling on the lagoon margin and floor. To the extent that topographic upwelling is a recurrent process at Scott Reef, this added production of organic matter and food resources has the potential to influence the distribution, productivity and resilience of local benthic communities, particularly corals and other filter feeders.

This project has had two major activity components to describe and understand the physical and biological oceanography of the lagoon of South Reef, Scott Reef. The focus of the physical oceanographic component has been to characterise: 1) the temporal and spatial dynamics of upwelling into South Reef lagoon; and 2) the temporal and spatial variability of bio-physical variables near the seabed at sites throughout the lagoon of South Reef. The focus of the biological oceanographic component has been to quantify the distribution, production and cycling of organic matter and nutrients in waters around Scott Reef and in particular the role of internal wave dynamics in shaping the horizontal and vertical variability in the pelagic environment. Important goals included defining the major spatial fields of biogeochemical variables and significant ecosystem production and trophic processes that influence food availability and quality for deep-living benthic communities on Scott Reef. This component employed a range of technologies and approaches to quantify planktonic productivity and cycling of nutrients, plankton growth rates, the cycling of organic matter in the water column (e.g. respiration – direct consumption of organic material by the plankton), plankton standing stocks and the sedimentation of organic material from the water column.

This report summarises the data collected from long-term deployments of in-situ observational instrumentation (Temperature (°C), Salinity (PSU), Photosynthetically Active Radiation (PAR), Chlorophyll fluorescence, Turbidity) and during four inter-seasonal biological oceanographic research cruises. Deployments of in-situ observational instrumentation commenced in late March 2008 and ceased in May 2010. The biological oceanography cruises were undertaken from the RV Solander over both winter (June/July 2008; May/June 2009) and early-summer (November – December 2008/2009) periods.

Materials and Methods

Physical Oceanography

In-situ observational instrumentation

Self contained, multi-parameter water quality loggers were deployed on the sea-bed to collect time series data of key bio-physical parameters within the lagoon of South Reef. Records of water temperature, salinity, depth, fluorescence, turbidity and Photosynthetically Active Radiation (PAR) were collected using Seabird SBE16 loggers (www.Seabird.com) with integrated Wetlabs ECO FLNTU and ECO PAR optical sensors (www.Wetlabs.com), deployed at a total of 16 sites within and adjacent to the lagoon of South Reef (see Fig. 1 and Table 1). Observational sites for moored instrumentation were chosen to provide good spatial coverage of the lagoon of South Reef across a range of depths and habitat types, with a focus on the exchange of water between the deep channel and the lagoon. The observational strategy was also intended to complement other historic, current and proposed ecological, biological and environmental monitoring programs, and to provide sufficient local coverage in relation to a range of development options.

Initial locations of observational sites were determined with input from Woodside, and reflected observational priorities at the time of the first deployment (March 2008). The locations of three observational sites were subsequently changed following a refinement of the Browse development plans, and three new instrumental observation sites were established. In May 2009, four shallow observational sites (Sites PE01 – PE04) were removed on request from Woodside. Logger deployments at the nine remaining observational sites were removed in February.

The SBE16 systems and integrated Wetlabs sensors are internally logging and powered by self contained batteries. The Wetlabs ECO FLNTU combines optical sensors for fluorescence at an excitation wavelength of 470 nm with optical scattering measurement at 700 nm for simultaneous determination of turbidity. It is standard practice to use the concentration of material that fluoresces at this excitation wavelength as a proxy for chlorophyll concentration. The ECO PAR utilises an integrated Satlantic PAR sensor with a 400 – 700 nm bandpass. Biological fouling in the Seabird is controlled by internal chemical antifouling devices. The Wetlabs sensors employ an integrated anti-fouling bio-wiper to minimise biological growth near the sensor face and protective copper tape to prevent fouling on the instrument body.

Seabird SBE16 systems were programmed to integrate 20 samples @ 4Hz every 15 minutes for conductivity, temperature, pressure, PAR, turbidity, and chlorophyll (fluorescence).

Vertical profiles of temperature were recorded within the deep channel and at the northern edge of the lagoon of South Reef through the deployment of two moorings spanning a large portion of the water column at depths of ~200 m and ~47 m, within the channel and on the northern margin of the lagoon, respectively. The mooring in ~200 m water depth consisted of temperature loggers at 30 m, 40 m, 60 m, 80 m, 100 m, 140 m and 180 m; the mooring in ~47m consisted of temperature loggers at 20 m and 30 m, and was deployed adjacent to a seabed mounted SBE16 water quality logger. Data from the moorings span May 2009 to May 2010.

Water column current profiles and waves were recorded at a subset of observational sites (sites PE01, PE02, PE03, PE06, PE12 in Fig. 1 and Table 1) through the deployment of Nortek 600 kHz AWAC and Nortek 1MHz Aquapro Acoustic Doppler Current Profilers (ADCP)

with wave capability. The current profilers were mounted adjacent to the water quality loggers at selected sites and acoustically sampled current velocities vertically up through the water column. Nortek AWAC and Aquapro wave current meters were programmed to record a 5 minute average at 30 minute intervals. A 20 minute wave observation burst was undertaken every 4 hours.

In addition to internally logging instrumentation, fixed sediment traps were deployed alongside the water quality loggers at a number of deepwater sites, commencing in July 2008. Sediment traps were constructed from 700 mm long cylindrical lengths of PVC tubing with an internal diameter of 110 mm. An internal baffle system, designed to prevent larger organisms (e.g. fish, crustaceans and octopus) from occupying the traps and contaminating the sample was installed at the entrance of each trap, and consisted of seven 150 mm lengths of PVC tube with an internal diameter of 30 mm. The bottom of each trap was sealed with a screw type PVC cap. After recovery, the contents (sediment and water) of each trap were processed by gravimetric settling of particulate material from a known volume of water onto a pre-weighed membrane filter. Four replicate 60 ml sub-samples were measured from the trap contents and stored frozen. Mean rates of sediment accumulation ($\text{mg cm}^{-2} \text{d}^{-1}$) were derived for each trap location for each successive period of deployment.

Deployment summary

Initial deployment of in-situ sea-bottom observational instrumentation was undertaken during the period 18 to 24 March 2008. Subsequent recovery, downloading, servicing and redeployment was undertaken as follows:

- 28 May 2008 – 03 June 2008
- 20 – 30 July 2008
- 23 September – 01 October 2008
- 17 – 24 November 2008
- 07 – 18 February 2009
- 15 – 25 May 2009
- 10 – 20 November 2010
- 18 – 28 February 2010 (logger removal)
- 28 May – 02 June 2010 (mooring removal).

Observational sites PE10, PE11 and PE12 were discontinued and sites PE14, PE15 and PE16 (see Fig. 1) were established during the research cruise undertaken within the period 23 September – 01 October 2008. The new sites provided a better spatial resolution in the zone of interaction between lagoonal and deep channel waters. Observational sites PE01, PE02, PE03 and PE04 were removed in May 2009 following a request from Woodside. Sites PE01, PE02, PE03 and PE04 were adjacent to coral monitoring sites occupied as part of AIMS SRRP Project I where temperature loggers and sediment traps remain deployed as part of that Project. The remaining sites (PE05, PE06, PE07, PE08, PE09, PE13, PE14, PE15, PE16) were recovered in February 2010.

Sediment traps were deployed on selected deep frames from July 2008. Trap contents for deployments up to February 2010 have been analysed for daily sedimentation rate.

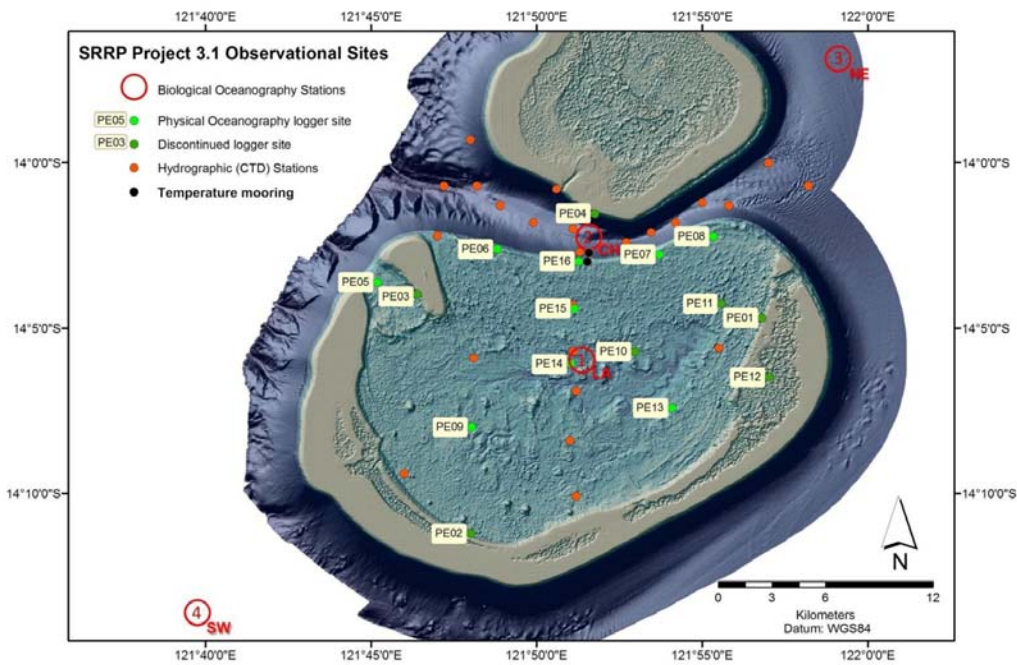


Fig. 1 Locations of biological oceanographic sampling and experimental sites, long-term water quality logger sites, mooring sites and hydrographic stations. The four regions of interest for time-series sampling and productivity measurements during the biological oceanography cruises are indicated by the red circles. During September – October 2008 observational sites PE10, PE11 and PE12 were discontinued and new sites PE14, PE15 and PE16 were established. Sites PE01, PE02, PE03 and PE04 were removed in May 2009 and all remaining loggers were removed in February 2010. Moorings were deployed in May 2009 and removed in May 2010.

Table I Nominal positions and depths of biological oceanographic sampling stations and long-term logger sites and instrument configuration (SBE16 = water quality logger, CW = current and wave meter, SBE39 = temperature logger). Horizontal Datum: WGS 84. Depth datum: Approximate depth below surface at time of deployment; not corrected to chart datum.

	Site name	Latitude (S)	Longitude (E)	Water Depth (m)	Instrument Configuration
Physical oceanographic logger sites	PE01 ⁺	14° 4.75'	121° 56.85'	24	SBE16 + CW
	PE02 ⁺	14° 11.29'	121° 48.06'	37	SBE16 + CW
	PE03 ⁺	14° 4.02'	121° 46.41'	25	SBE16 + CW
	PE04 ⁺	14° 1.48'	121° 51.60'	34	SBE16
	PE05	14° 3.60'	121° 45.18'	44	SBE16
	PE06	14° 2.65'	121° 48.80'	44	SBE16 (+ CW [#])
	PE07	14° 2.80'	121° 53.73'	44	SBE16
	PE08	14° 2.29'	121° 55.34'	43	SBE16
	PE09	14° 8.02'	121° 48.11'	49	SBE16
	PE10 [*]	14° 5.71'	121° 52.98'	45	SBE16
	PE11 [*]	14° 4.27'	121° 55.58'	47	SBE16
	PE12 [*]	14° 6.48'	121° 57.02'	18	SBE16 + CW
	PE13	14° 7.40'	121° 54.08'	48	SBE16
	PE14 [#]	14° 6.09'	121° 51.04'	54	SBE16
	PE15 [#]	14° 4.41'	121° 51.15'	50	SBE16
		PE16 [#]	14° 2.98'	121° 51.27'	46
Biological oceanographic sampling and experimental stations	200m mooring	14° 2.80'	121° 51.21'	200	SBE39
	47m mooring	14° 2.95'	121° 51.47'	47	SBE39
	Site 1: Lagoon (LA)	14° 3.60'	121° 43.80'	53	
	Site 2: Deep Channel (CH)	14° 2.20'	121° 51.70'	456	
	Site 3: NE margin (NE)	14° 6.30'	121° 51.00'	450	
	Site 4: Open water reference site (SW)	13° 52.10'	121° 52.50'	784	

* Discontinued since September 2008

Established in September 2008

+ Discontinued since May 2009

Biological Oceanography

The biological oceanography component of the project was based around four cruises to Scott Reef and surrounding waters over a 2-year period, with the rationale that two of the cruises were undertaken during the winter [dry] season: May – July in 2008 and 2009 and two in the summer [pre-wet] season November – December in 2008 and 2009. This was in order to capture the broad seasonal differences in regional pelagic community structure and productivity related to wind forcing, insolation and temperature. The initial cruise (June 2008) followed a period of strong winds and likely enhanced mixing of surface waters at Scott Reef. The remaining three cruises (December 2008, June 2008 and November 2009) took place during calm weather and largely clear skies with high insolation and local heating of surface waters.

The biological and chemical oceanographic sampling was primarily structured around activities at four sites (see Fig. 1 and Table 1) which were deemed representative of the Scott Reef region:

- 1) A lagoon site in the central part of the lagoon of South Reef (Lagoon, LA – Site 1).
- 2) A site in the channel between North Reef and South Reef (Deep Channel, CH – Site 2).
- 3) A reef-flank site (> 150 m depth) on an open, eastern margin of North Scott Reef away from the deep channel, but likely to be influenced by interactions between internal wave activity and the topography of Scott Reef (NE Margin, NE – Site 3).
- 4) A far-field site >10 km from Scott Reef which was likely to be representative of the general outer shelf pelagic environment (Open Water, OW or SW – Site 4).

Additional sampling on all four cruises was undertaken in the Deep Channel between North and South Reef to investigate potential accumulations of macrozooplankton associated with local current fields and topography.

On the initial cruise (June 2008), a grid of hydrographic and optical sampling stations was occupied in and around the deep channel (CH) and lagoon (LA) of South Reef to define the general field of oceanographic and optical characteristics of water masses in the lagoon. Beginning with the December 2008 cruise, the grid was replaced by hydrographic sampling transects down the central axis of the South Reef Lagoon and east-west along the deep channel between North Reef and South Reef. These transects were sampled at the beginning and end of the cruise to determine the extent and structure of any cool water intrusions into the lagoon.

At each of the four experimental sites on each cruise, a range of sampling and experimental activities was undertaken over a 48-hour period to resolve key ecosystem fluxes and temporal variability in the environment at these sites.

During the initial 24-hour (diel) period on-site, conductivity, temperature and depth (CTD) profiles were sampled at 2-hr intervals to quantify vertical distributions of general water column parameters (T°C, S‰, PAR, NTU, beam transmittance, chlorophyll fluorescence) in response to local internal wave/tidal activity, and to resolve day-night differences in plankton community structure and distributions. In periods between CTD casts, at least two water bottle casts were made each day (day, night) to quantify vertical distributions of dissolved nutrients, organic matter, plant pigments, suspended particulate matter and small phytoplankton in relation to the vertical temperature, salinity and density fields. Four series of depth-stratified zooplankton tows were undertaken with towed multi-net systems to quantify vertical distributions of zooplankton.

During the following 24-hour period on each time-series station, experiments or sampling was undertaken to measure:

- Phytoplankton primary production by inorganic ^{14}C uptake
- Bacterial production by ^3H -labelled thymidine uptake
- Plankton community respiration and net photosynthesis by oxygen uptake/production
- Vertical sedimentation fluxes of particulate organic matter (C, N) out of the euphotic zone by drifting sediment trap arrays
- Vertical distributions of downwelling radiance and inherent optical properties (IOP's) in the near-surface layer.
- Hyperspectral remote sensing reflectance (R_{rs}). [Jun 2009 and Nov 2009].

Instrumentation used on site consisted of:

- CTD casts – Seabird CTD (SBE19+) with chlorophyll fluorescence (Wetlabs Wetstar), PAR (Biospherical QSP-200), beam transmittance (Seastar), turbidity (OBS)
- Spectral absorbance (a) – Wetlabs AC-9+ or AC-S + DH4 data concentrator (December 2008, June 2009 and November 2009)
- Spectral backscatter (b) – Wetlabs BB9 (December 2008, June 2009 and November 2009)
- Downwelling PAR – Biospherical QSR-200 quantum sensor + data logger
- Remote sensing reflectance (R_{rs}) – DALEC 3-channel hyperspectral radiometer – AIMS/Curtin Univ – custom made with Zeiss MMS spectrometers (June 2009 and November 2009)
- Picoplankton and bacterial abundance – Becton Dickinson FACScan flow cytometer
- Zooplankton distribution – Hydro-Bios MultiNet – Laser Optical Plankton Counter [LOPC – June 2009]
- Microzooplankton distribution – FlowCAM optical plankton imager [not June 2008]

A detailed description of the experimental and analytical procedures applied during and subsequent to the Biological Oceanography cruises is given in Appendix I.

Results

The physical environment of Scott Reef

Light

The water masses in and surrounding Scott Reef are highly oligotrophic in character with very low standing stocks of phytoplankton, coloured dissolved organic matter (CDOM) and particulate matter (organic and inorganic); as a consequence, light is able to penetrate to significant depths through the water column. For example, a secchi disc disappearance depth of 43 m was observed on one occasion at the Open Water site (SW).

Scott Reef is subject to intense sunlight throughout the year. Unless noted otherwise, light measurements herein are of photosynthetically available radiation (PAR = 400 – 700 nm). Direct measurements of PAR and UV at Broome Airport (18°S) (Furnas and Steinberg, 1999) show that daily PAR energy inputs on cloudless days ranged between 7.0 and 13.0 MJ m⁻² day⁻¹ (Fig. 2). In terms of quanta, daily PAR fluxes ranged between 30 and 60 moles Q m⁻². Instantaneous mid-day quantum fluxes range from ca. 1,100 to >2,200 μmol Q m⁻² sec⁻¹ with short-lived peak values exceeding 2,500 μmol Q m⁻² sec⁻¹ due to reflection off clouds. Peak daily insolation occurs between October and April with a strong dependency on the degree of monsoonal cloud cover. The early summer cruises took place during the period of high annual insolation, while the dry season cruises were near the annual minimum.

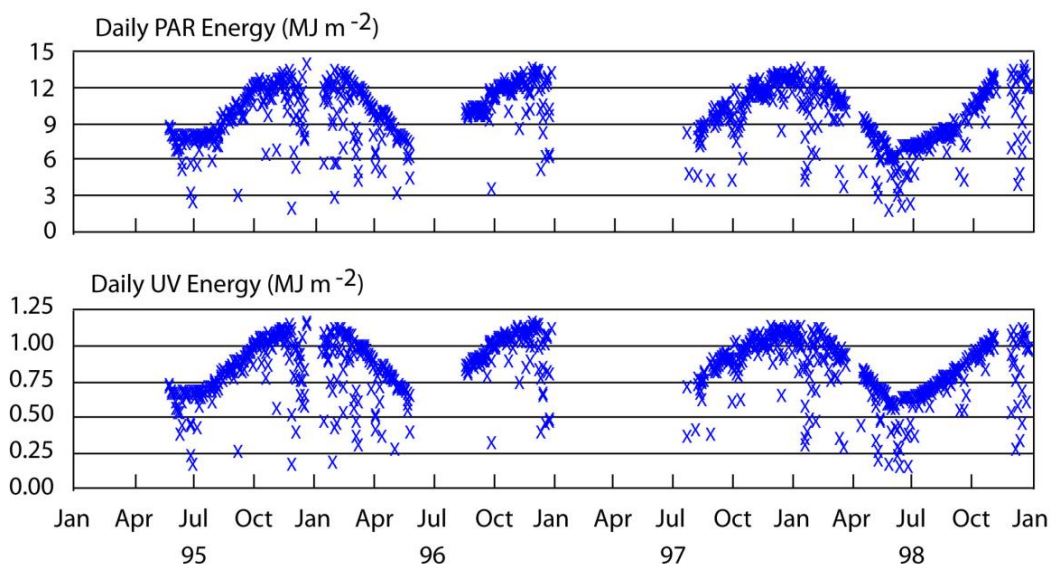


Fig. 2 Daily input fluxes of PAR and ultraviolet radiation (305 – 380 nm) measured at Broome, Western Australia, over seasonal cycles

Vertical light profiles at all four sites (Fig. 3 to Fig. 6 Vertical profiles of depth-averaged chlorophyll concentration (from in-situ fluorescence) and mid-day sub-surface light (PAR) penetration in the upper 200 m at the Open Water site (SW) on the four cruises. Line and error bar colours as in Fig. 3. Light penetration is shown as percent of surface irradiance. Horizontal error bars indicate 1 S.D. among profiles at the selected depth horizons.

) are similar in their general features. Light penetration profiles are presented as the percent of surface irradiance (%I₀) at depth where I₀ is the downwelling irradiance just below the water surface. Downwelling PAR was routinely measured on all CTD casts. Data analysis was limited to profiles selected by inspection to have been done during the middle of the day (largely 10:00 – 14:00 local

time) at a high solar angle and to be (largely) unaffected by clouds, reflectance off the ship's side or the ship's shadow underwater. Downwelling irradiance at the surface for individual profiles was estimated by extrapolating uncontaminated linear sections of log-transformed irradiance in the upper 10 m to 0 m depth.

Sub-surface downwelling irradiance at depth is related to surface irradiance through the relationship:

$$I_{\text{depth}} = I_{\text{surface}} e^{-kd} \text{ or } I = I_o e^{-kd}$$

where k is an attenuation coefficient and d is the depth. Where factors affecting light attenuation remain constant with depth, plots of $\ln(I/I_o)$ vary linearly with depth. The value of k varies spectrally, but is often dealt with as an aggregate parameter for all light within a defined waveband (e.g. PAR). In the present treatment, we refer to k for the PAR waveband (400 – 700 nm) that is measured by the underwater light sensor on our CTD package. The value of k is also influenced by suspended particulate matter in the water column, absorption by plant pigments (chiefly chlorophyll) and to a lesser extent in oligotrophic offshore waters, by chromophoric dissolved organic matter (CDOM).

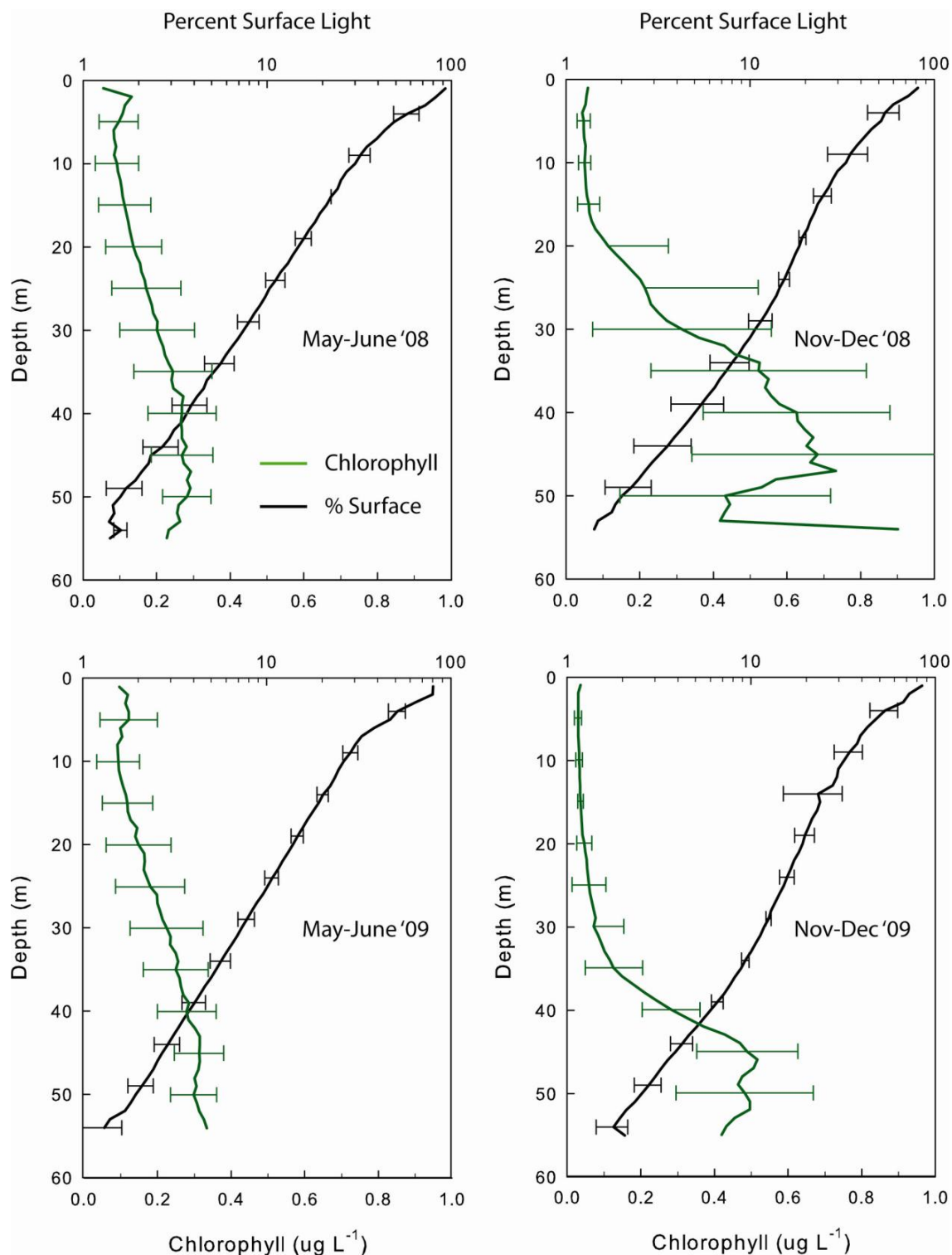


Fig. 3 Vertical profiles of depth-averaged chlorophyll concentration (from in-situ fluorescence) and mid-day sub-surface light (PAR) penetration at mid-lagoon sites on the four cruises. Light penetration is shown as percent of surface irradiance. Horizontal error bars indicate 1 S.D. among profiles at the selected depth horizons.

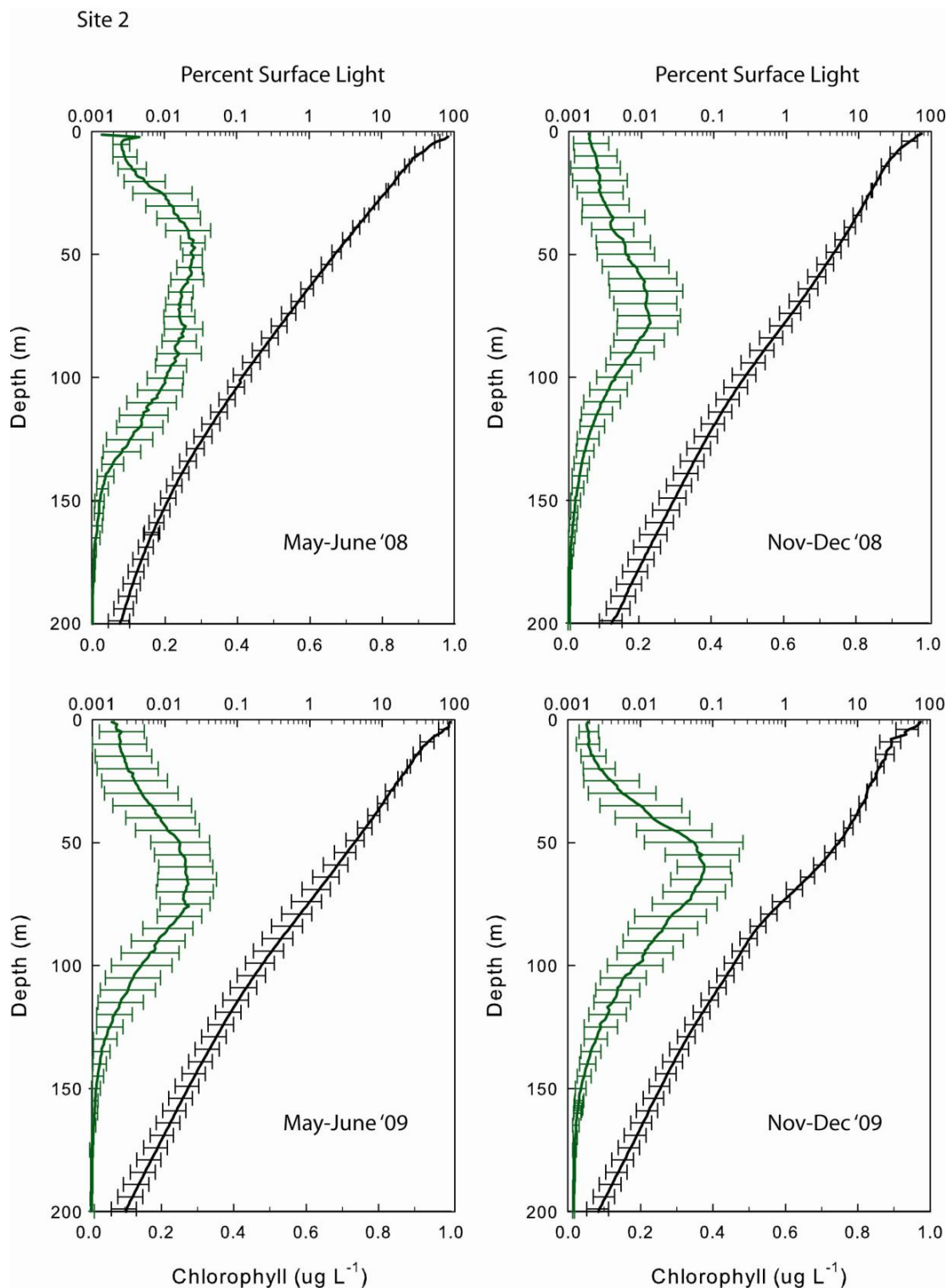


Fig. 4 Vertical profiles of depth-averaged chlorophyll concentration (from in-situ fluorescence) and mid-day sub-surface light (PAR) penetration in the upper 200 m at the Deep Channel site (CH) on the four cruises. Line and error bar colours as in Fig. 3. Light penetration is shown as percent of surface irradiance. Horizontal error bars indicate 1 S.D. among profiles at the selected depth horizons.

Site 3

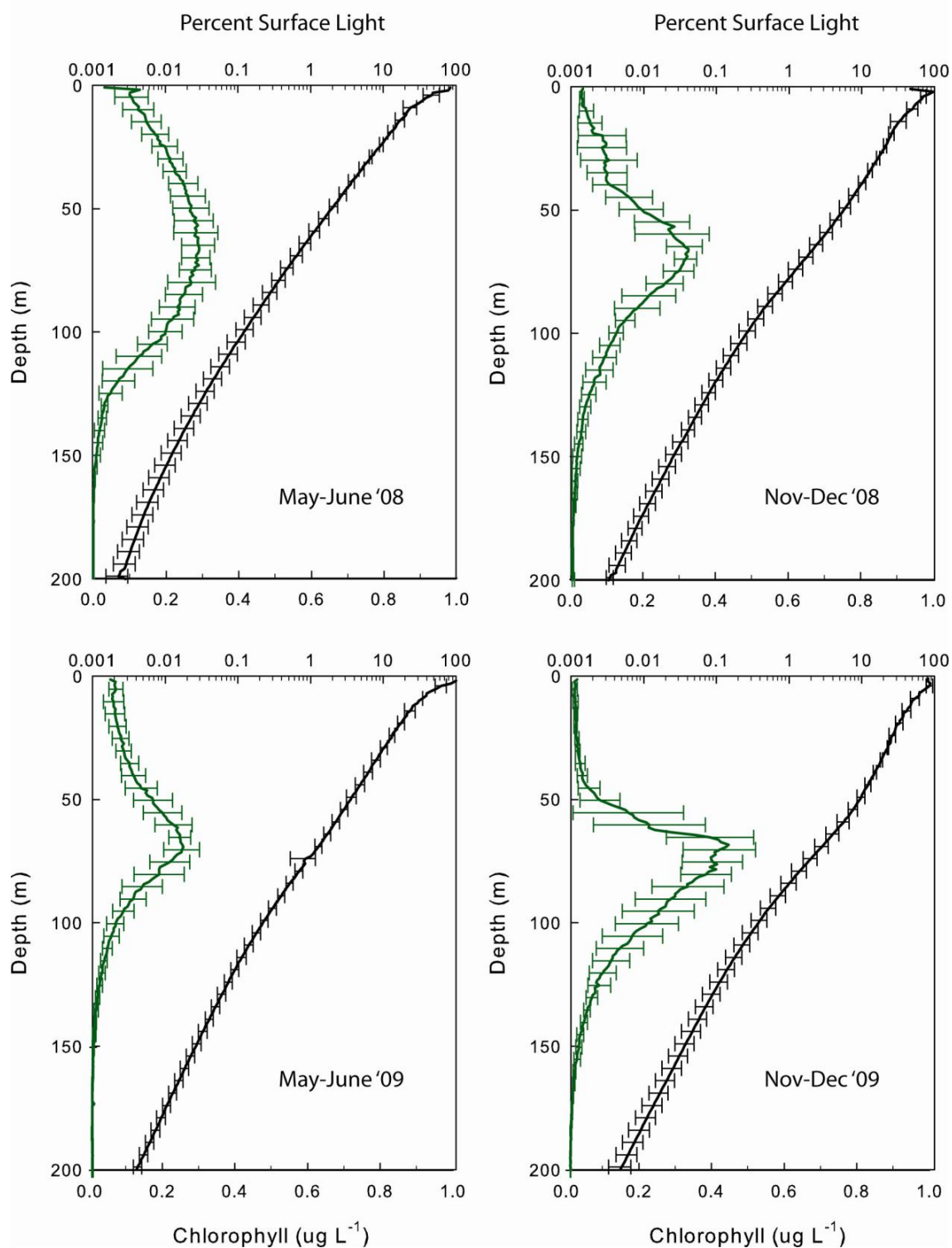


Fig. 5 Vertical profiles of depth-averaged chlorophyll concentration (from in-situ fluorescence) and mid-day sub-surface light (PAR) penetration in the upper 200 m at the NE Margin site (NE) on the four cruises. Line and error bar colours as in Fig. 3. Light penetration is shown as percent of surface irradiance. Horizontal error bars indicate 1 S.D. among profiles at the selected depth horizons.

Site 4

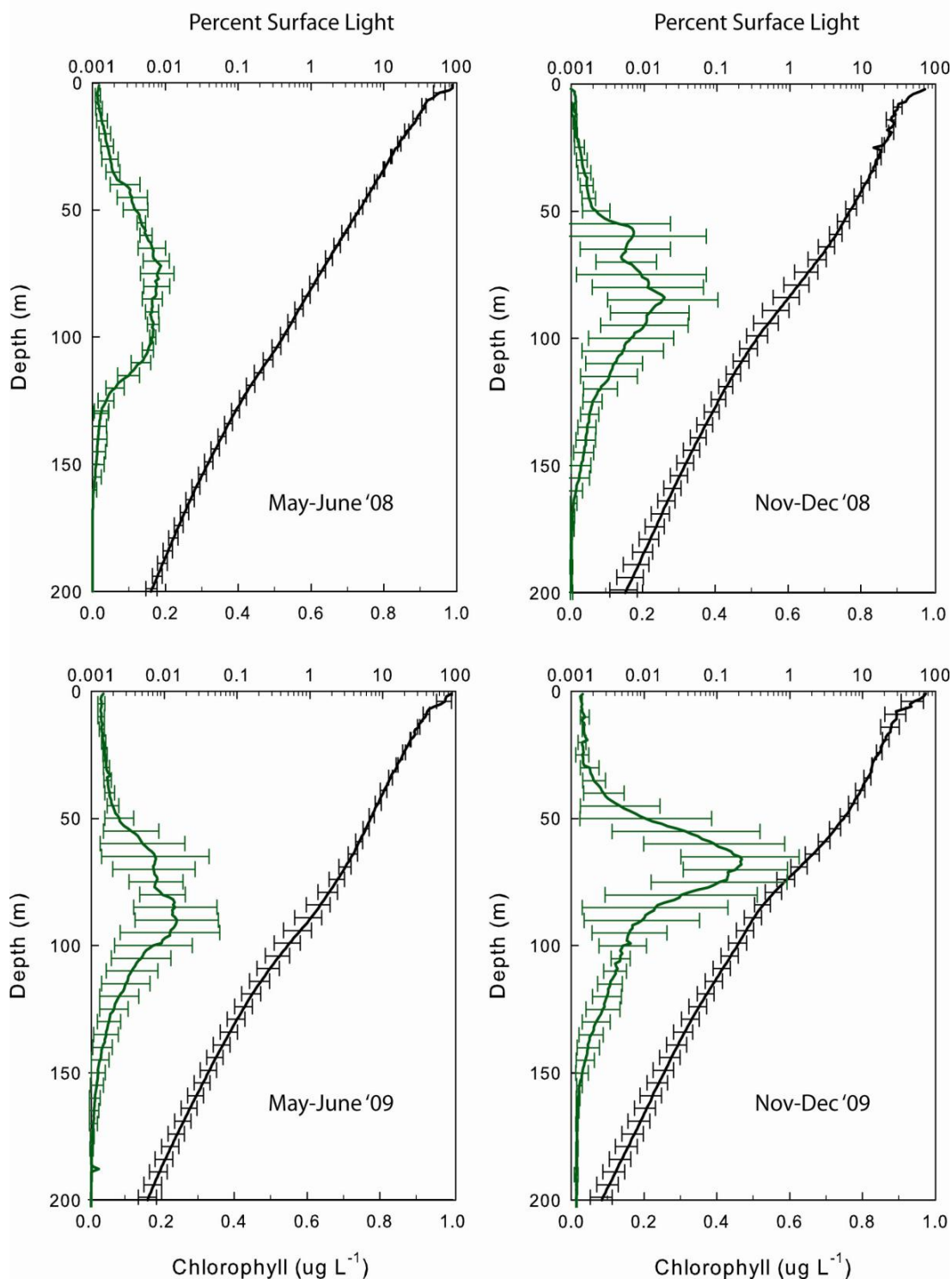


Fig. 6 Vertical profiles of depth-averaged chlorophyll concentration (from in-situ fluorescence) and mid-day sub-surface light (PAR) penetration in the upper 200 m at the Open Water site (SW) on the four cruises. Line and error bar colours as in Fig. 3. Light penetration is shown as percent of surface irradiance. Horizontal error bars indicate 1 S.D. among profiles at the selected depth horizons.

Within individual profiles there is a rapid attenuation of light in the upper 10 m ($k = 0.083 - 0.156 \text{ m}^{-1}$) as the red wavelengths ($> 550 \text{ nm}$) are absorbed by the water (Table 2). Attenuation of the remaining blue light is more gradual, with light levels between 0.01 and 0.001 percent of mid-day surface irradiance recorded at a depth of 200 m ($k = 0.030 - 0.040 \text{ m}^{-1}$ in the 150 – 200 m depth stratum). Near-bottom irradiance levels at lagoon stations range between 1 and 5 percent of surface irradiance. Attenuation coefficients in low-chlorophyll lagoon waters were of the order of $0.050 - 0.070 \text{ m}^{-1}$, increasing to $0.066 - 0.083 \text{ m}^{-1}$ in the near-bottom chlorophyll maximum layer. Attenuation coefficients in the deep chlorophyll maximum layer at the deep-water stations ranged between 0.056 and 0.082 m^{-1} . A near-bottom light level of 1% of surface irradiance at 50 m implies an average water column attenuation coefficient of 0.092 m^{-1} .

Table 2 Ranges of averaged PAR attenuation coefficients (k ; m^{-1}) for specified depth bands at the four biological oceanography sites. k is defined by the relationship: $k = -(\ln(I/I_0))/d$ for the depth ranges specified.

Depth (m)	Description	Lagoon	Channel	NE Margin	Open Water
2 – 10	Surface layer, high red attenuation	0.100–0.125	0.083–0.126	0.083–0.156	0.110–0.140
20 – 30	Above deep chl max	0.051–0.070	0.037–0.065	0.032–0.062	0.037–0.052
30 – 50	Lagoon chl max	0.066–0.083			
55 – 90	Deep chl maximum , blue light only		0.060–0.082	0.060–0.072	0.056–0.082
125 – 200	Below deep chl max, blue light only		0.034–0.040	0.033–0.042	0.038–0.040

The small observed differences between individual light profiles are related to the sampling time, local irradiance, sea state, vessel heading and solar orientation at the time of sampling, local cloudiness, in-situ chlorophyll concentrations and other turbidity sources (lagoon stations primarily). For comparison purposes, light penetration profiles were analysed as raw profiles (% I_0 vs depth) and normalised to a constant percent of surface irradiance at one depth (20 m) to minimise uncertainties in the estimation of surface irradiance (I_0) which saturated the underwater light sensor in the upper 5 m of the water column and prevented direct readings of surface light.

Differences between seasonal mean underwater light profiles at the individual sites are largely related to differing degrees of attenuation by phytoplankton and related particulate matter in the sub-surface or deep chlorophyll maximum (DCM) layer. The density and thickness of the DCM varied between cruises. Within the South Reef lagoon, the DCM was restricted to the lower 20 m of the water column. On the winter (June) cruises, the DCM at the deep stations was deeper and broader than in the summer where enhanced chlorophyll water was focused into a narrow vertical band within the more stable density structure (e.g. Fig. 8). Maximum chlorophyll concentrations in individual and averaged profiles were generally recorded around a depth of ca. 70 m in all seasons (ca. 1% I_0). The greater variability in profiled chlorophyll concentrations and sub-surface irradiance levels associated with the DCM are largely due to local vertical movements of the thermocline and the associated DCM by internal waves.

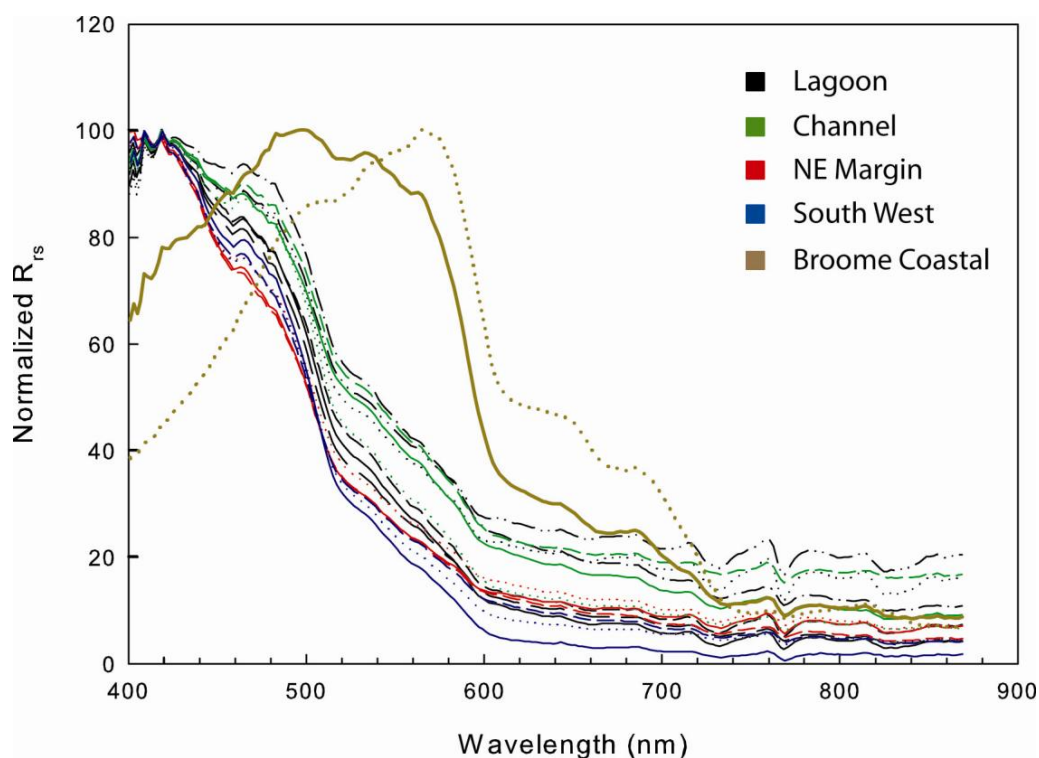


Fig. 7 Normalised remote sensing reflectance spectra (R_{rs}) recorded with a hyperspectral radiometer at the four time series sites in and near Scott Reef and near the coastline at Broome during the November – December 2009 research voyage. Spectral values on individual spectra were normalised to the highest value recorded on that spectra.

The spectral distribution of light reflected upward through the water surface (the Remote Sensing Reflectance – R_{rs}) at locations around Scott Reef illustrates the effects of suspended materials and bottom reflectance (Fig. 7). R_{rs} spectra of downwelling light (E_d), upwelling light from the water surface (L_w) and open-sky radiance for surface reflectance corrections (L_{sky}) were recorded with a 256 channel hyperspectral radiometer mounted on the ship's bow. The radiometer was oriented to avoid sun glint from the water surface and minimize open sky reflectance (Mobley, 1999). Five measured R_{rs} spectra were averaged and normalized to the highest value in a spectrum for comparison purposes.

Spectra recorded at the NE Margin (NE) and Open Water (SW) deep water sites during the November 2009 cruise are characteristic of oligotrophic oceanic regions with relatively high normalised reflectance in the blue region of the spectrum (< 450 nm) and a swift, exponential, decline to low levels at wavelengths > 480 nm. This spectral shape reflects the very low levels of phytoplankton and other suspended material in the upper 30 m of the water column and the predominance of blue light scattering by water. R_{rs} at the red end of the spectrum (> 600 nm) is very low and is typical of oligotrophic oceanic waters (Case i) in much of the tropical oceans.

At the lagoon sites and in the deep channel between North and South Reefs, the normalised R_{rs} spectrum is characterised by a shoulder of higher reflectances at wavelengths > 480 nm. This shoulder is due to reflectance in the water column by higher loads of suspended particles (phytoplankton and suspended carbonate sediments), and in the lagoon, by some small degree of bottom reflectance. The difference between R_{rs} spectra coincides with observations of differences in mean levels of other variables (e.g. salinity, chlorophyll, zooplankton) which show subtle, persistent differences between the lagoon and surrounding waters.

R_{rs} spectra recorded in coastal waters off Broome on the return voyage are characterised by a distinctly different spectral shape with high relative reflectances in the band between 500 and 700 nm. This green to red reflectance shoulder is due to considerably higher loads of suspended sediment and to a lesser degree, phytoplankton, in the water column.

Oceanic conditions

The oceanic environment surrounding Scott Reef is characterised by a stratified, oligotrophic water column exhibiting both seasonal and inter-annual variability in its temperature and salinity structure. Fig. 8 presents representative profiles of hydrographic variables at the four biological oceanography time series sites. Fig. 9 to Fig. 13 present contoured time series of hydrographic variables at the Open Water (SW) and the channel (CH) sites.

During the winter (dry season), water column hydrographic profiles at all four experimental sites are characterised by a clearly defined surface mixed layer of near uniform temperature and salinity. In June 2008, following strong winds, the mixed layer (ca. 27°C) was approximately 100 m in thickness, while in June 2009, following calm conditions, the mixed layer was considerably warmer (>28.5°C) and ca. 70m in thickness. In general, during winter the thickness of the winter mixed layer exceeds the sill depth for the South Reef lagoon.

During the November – December cruises, surface temperatures were close to or slightly greater than 30°C. As a consequence of solar heating under the relatively calm conditions of the early summer, the surface mixed layer at deep-water stations was considerably thinner than during winter (ca. 40 m during November 2009 and < 10 m thick during December 2008), with water temperatures exhibiting a steady decrease with depth (Fig. 8). Between 150 and 250 m, regardless of season, water temperatures decreased at an average rate of 0.08°C m⁻¹, though with numerous steps, indicating distinct water layering in this band; below 300 m, the rate of temperature change was lower. Winter and summer temperature profiles below 250 m were essentially similar.

Within the South Reef lagoon, the water column was well mixed during all four biological cruises with near isothermal/isohaline profiles and surface-to-bottom density differences < 1 sigma-t. No pronounced vertical stratification due to intrusive activity from the deep channel was observed during any of the time series sampling programs on the biological oceanography cruises. Although the lagoon was relatively well mixed vertically, mean salinities measured in the central lagoon (LA) were significantly different from concurrent surface layer or mixed layer salinities in waters surrounding Scott Reef (Table 4). On two of the four cruises (June 2008, November 2009), lagoonal salinities were slightly higher than those outside, while they were significantly lower on the December 2008 and June 2009 cruises. The lateral differences in salinity reflect seasonal variations in vertical salinity structure in the upper ca. 100 m. Where in-lagoon salinities were higher than outside-lagoon, salinities increased with depth. At the Open Water site, well-defined salinity minimum layers in the upper thermocline were observed in December 2008 (50 – 100 m), June 2009 (100 m) and November 2009 (150 m); the source of this lower salinity water is unknown. Weak salinity minimum and maximum layers were observed in a number of the time series. When lagoon salinities were low, there was a subsurface low-salinity layer. The lagoon's salinity differences likely reflect enhanced vertical mixing processes in the deep channel region.

Concurrent salinity profiles and temperature/salinity plots for the deep water sampling sites indicate a complicated and seasonally varying vertical structure of water masses around Scott Reef with evidence for multiple interleaving layers within the mixed layer and in the thermocline to 300 m depth. Surface salinities in December 2008 and June 2009 were distinctly higher than observed in June 2008 and November 2009 (Fig. 14), indicating a regional replacement of surface water masses. While water temperatures below 300 m are relatively uniform, the December 2008 cruise was characterised by a deep layer of distinctly higher salinities (Fig. 8) indicating a different source of water for this stratum. Salinity distributions within the upper 100 m were characterised by distinct cruise-to-cruise differences.

On the initial cruise (June 2008), which closely followed an episode of strong winds, the Open Water site (SW) was characterised by a broad sub-surface chlorophyll maximum spanning the lower portion of the mixed layer and upper thermocline (Fig. 8). Under the more stable conditions of the early summer cruises (December 2008, November 2009, Fig. 8, Fig. 10) and the second winter cruise (June 2009), the subsurface chlorophyll fluorescence maximum was concentrated within a narrow depth band at the top of the thermocline. In some cases, multiple subsurface chlorophyll peaks were observed, likely as a result of the growth of phytoplankton in distinct depth (density) horizons due to the stability of the water column. The vertical confinement of the chlorophyll maximum persisted through the tidal cycle (Fig. 10).

Over a 24-hour (diel) period, sub-surface chlorophyll fluorescence (calibrated against discrete samples) increased during the daylight hours and then fell during the night, reflecting the cell division dynamics of the dominant cyanobacteria, *Synechococcus* and *Prochlorococcus*, in these waters and also the grazing mortality over the course of the night when cyanobacteria were not growing. Both *Synechococcus* and (especially) *Prochlorococcus* have strongly diurnal-synchronised cell division cycles. Individual cells in the populations usually undergo one cycle of DNA replication and cell division during daylight hours, doubling the population (and chlorophyll). Cell division ceases at night and (about half) of the augmented population are usually consumed by grazers or killed by viral infections. The result is a relatively stable population over long (> several days) time frames with a ca. 2-fold fluctuation in cell numbers or biomass within a 24-hour period.

Vertical profiles of chlorophyll at stations close to Scott Reef (Deep Channel and NE Margin sites) were characterised by slightly higher concentrations with broader vertical distributions within the surface mixed layer. This was due to locally enhanced vertical mixing associated with the interaction of the prevailing oceanic conditions and tidal currents (surface and internal) with local topography to form large and dynamic internal waves and internal tides (Fig. 12). During summer, well defined layers of higher chlorophyll persisted in the deep channel, suggesting a reduction in vertical mixing during this period (Fig. 13).

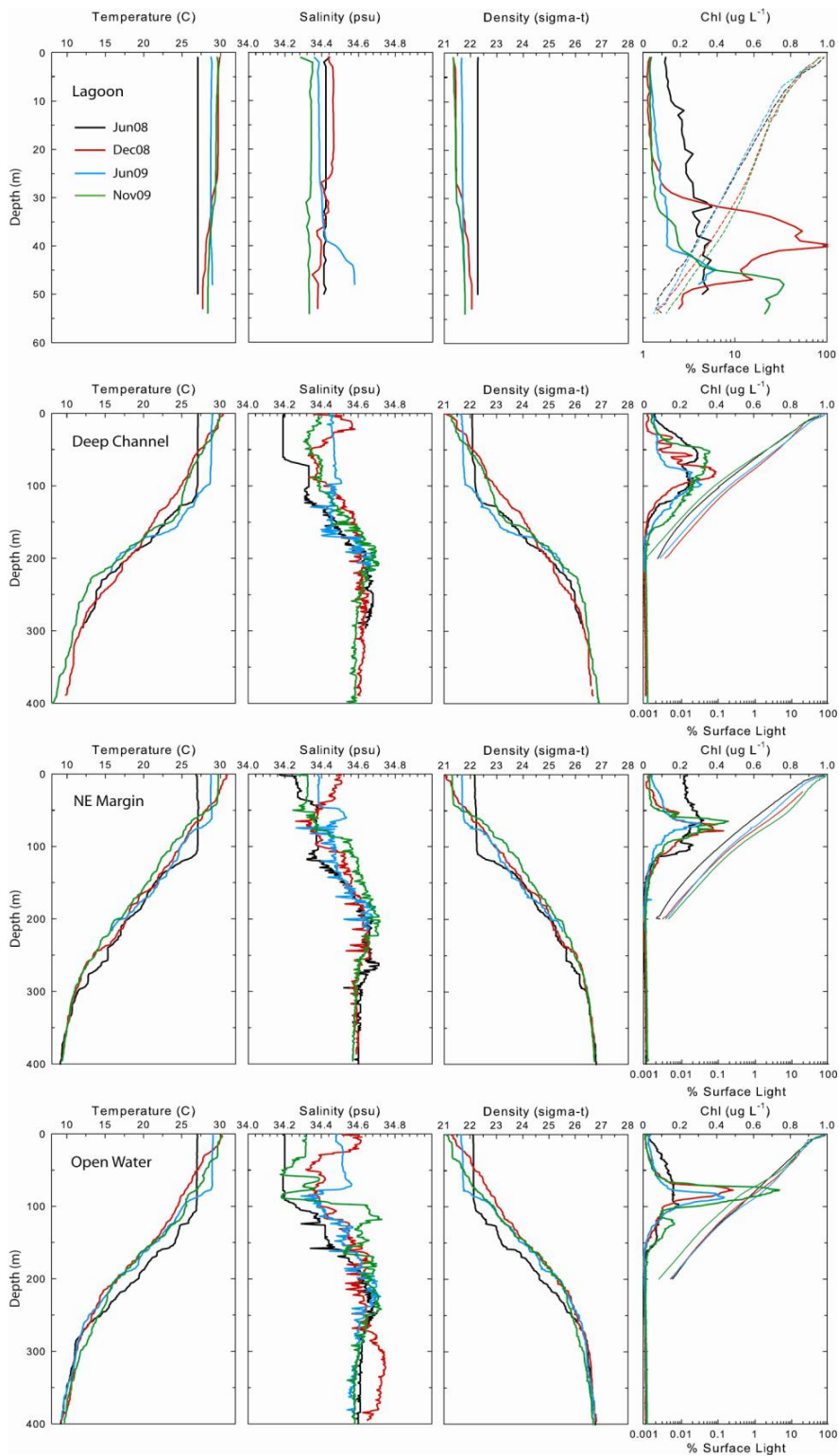


Fig. 8 Representative mid-day vertical profiles of water temperature ($^{\circ}\text{C}$), salinity (‰), density (sigma-t), chlorophyll a (from fluorescence, $\mu\text{g L}^{-1}$) and percent surface irradiance ($\%I_0$). Rows of panels from top to bottom show Lagoon (Site 1, LA), the deep channel (Site 2, CH), the NE margin of North Reef (Site 3, NE) and an open-water reference site SW of Scott Reef (Site 4, SW).

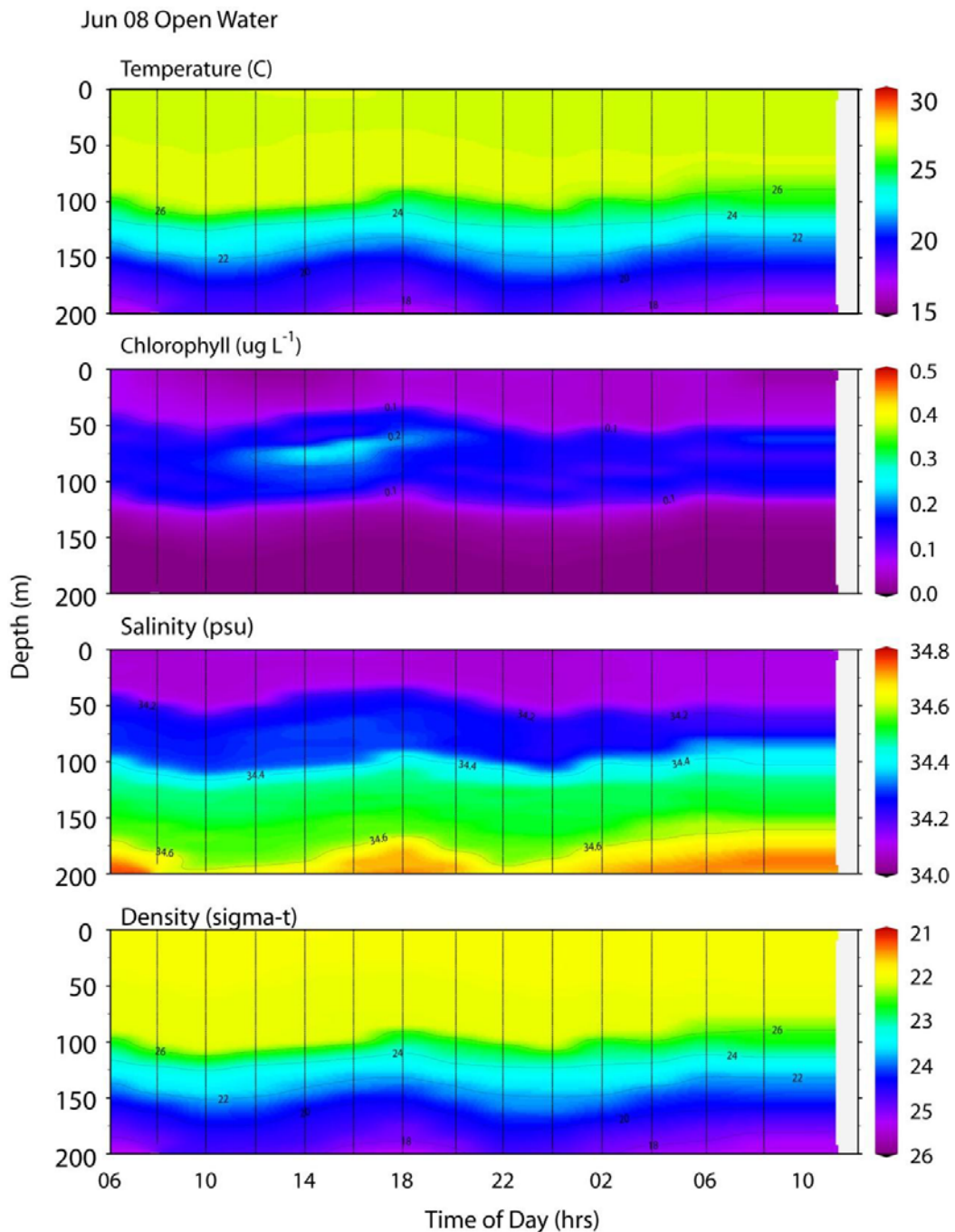


Fig. 9 Contoured time series of water temperature ($^{\circ}\text{C}$), contemporaneously measured in-situ chlorophyll fluorescence ($\mu\text{g L}^{-1}$), salinity (PSU) and Density (sigma-t) measured at the Open Water site SW of South Reef (SW) from 06:00 local time on 30 June 2008.

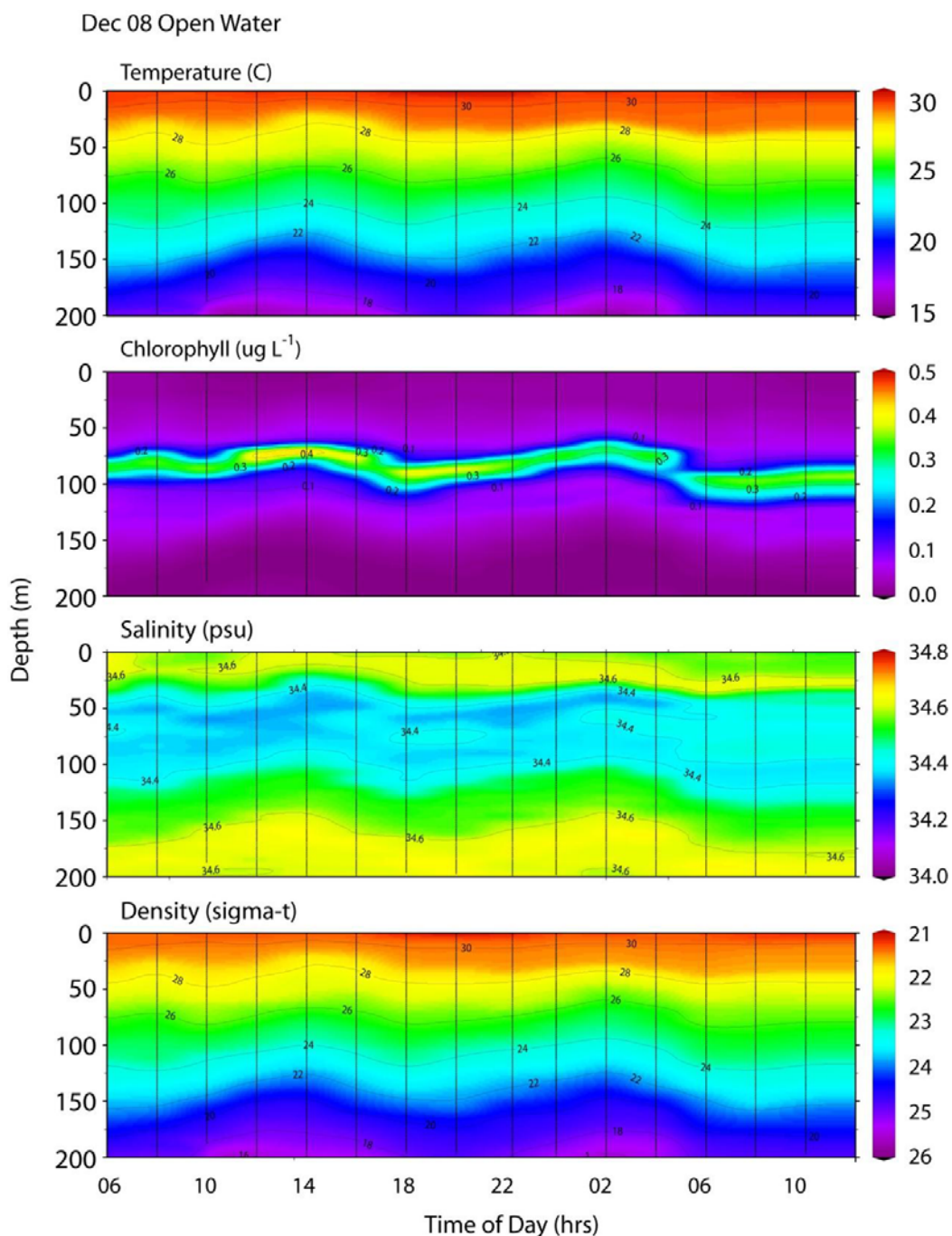


Fig. 10 Contoured time series of water temperature ($^{\circ}\text{C}$), contemporaneously measured in-situ chlorophyll fluorescence ($\mu\text{g L}^{-1}$), salinity (PSU) and Density (sigma-t) measured at the Open Water site SW of South Reef (SW) from 06:00 local time on 4 December 2008.

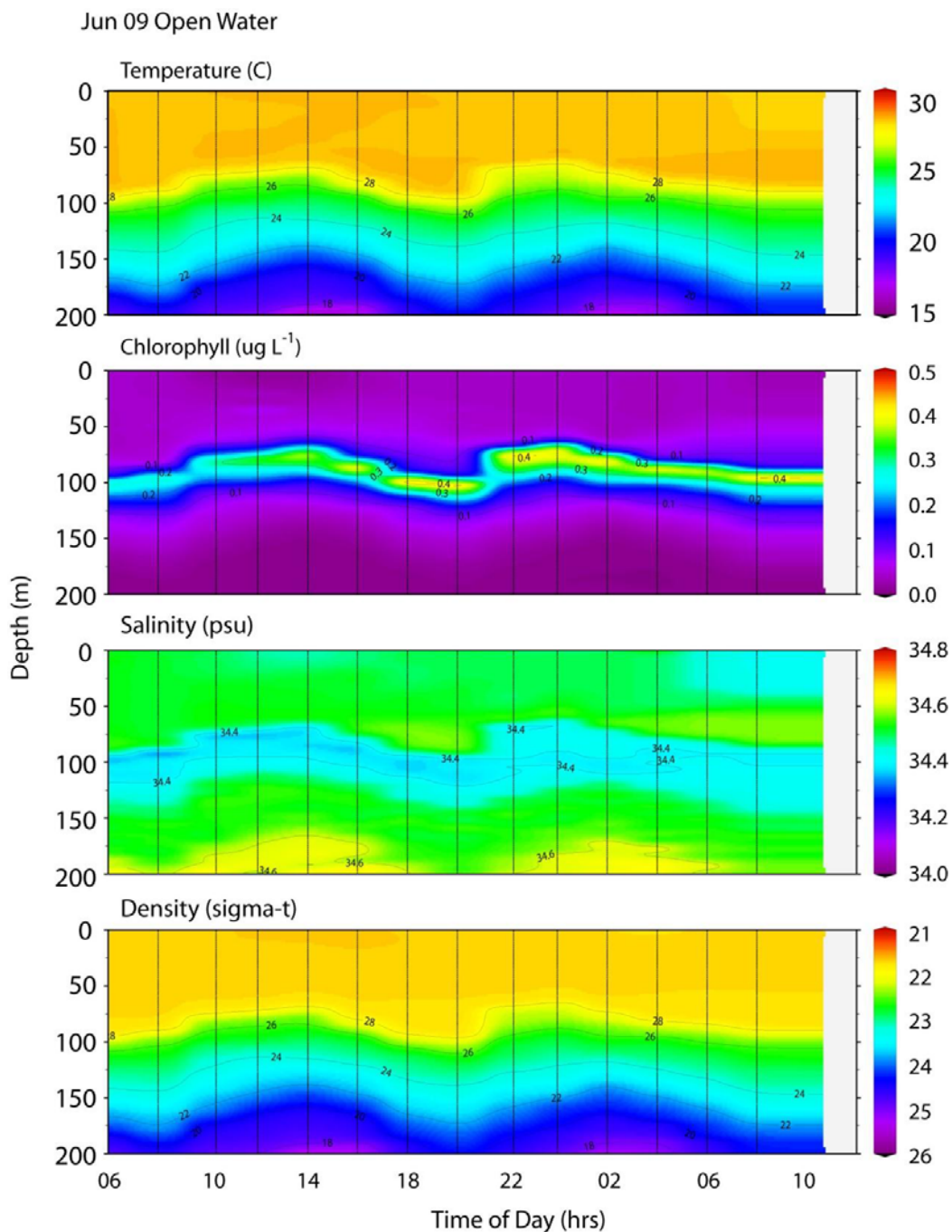


Fig. 11 Contoured time series of water temperature ($^{\circ}\text{C}$), contemporaneously measured in-situ chlorophyll fluorescence ($\mu\text{g L}^{-1}$), salinity (PSU) and Density (sigma-t) measured at the Open Water site SW of South Reef (SW) from 06:00 local time on 1 June 2009.

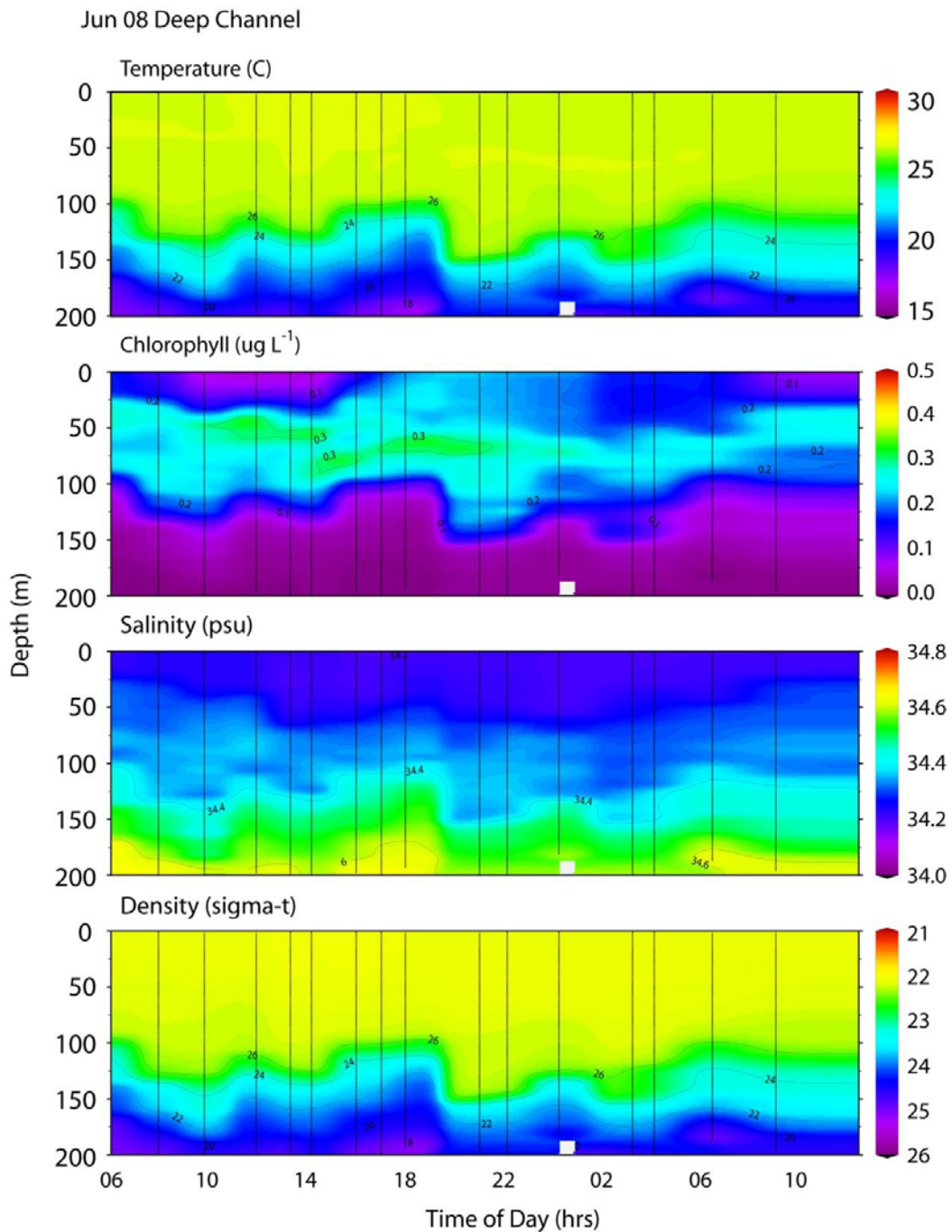


Fig. 12 Contoured time series of water temperature ($^{\circ}\text{C}$), contemporaneously measured in-situ chlorophyll fluorescence ($\mu\text{g L}^{-1}$), salinity (PSU) and Density (sigma-t) measured at the Deep Channel site between North and South Reef (CH) from 06:00 local time on 26 June 2008.

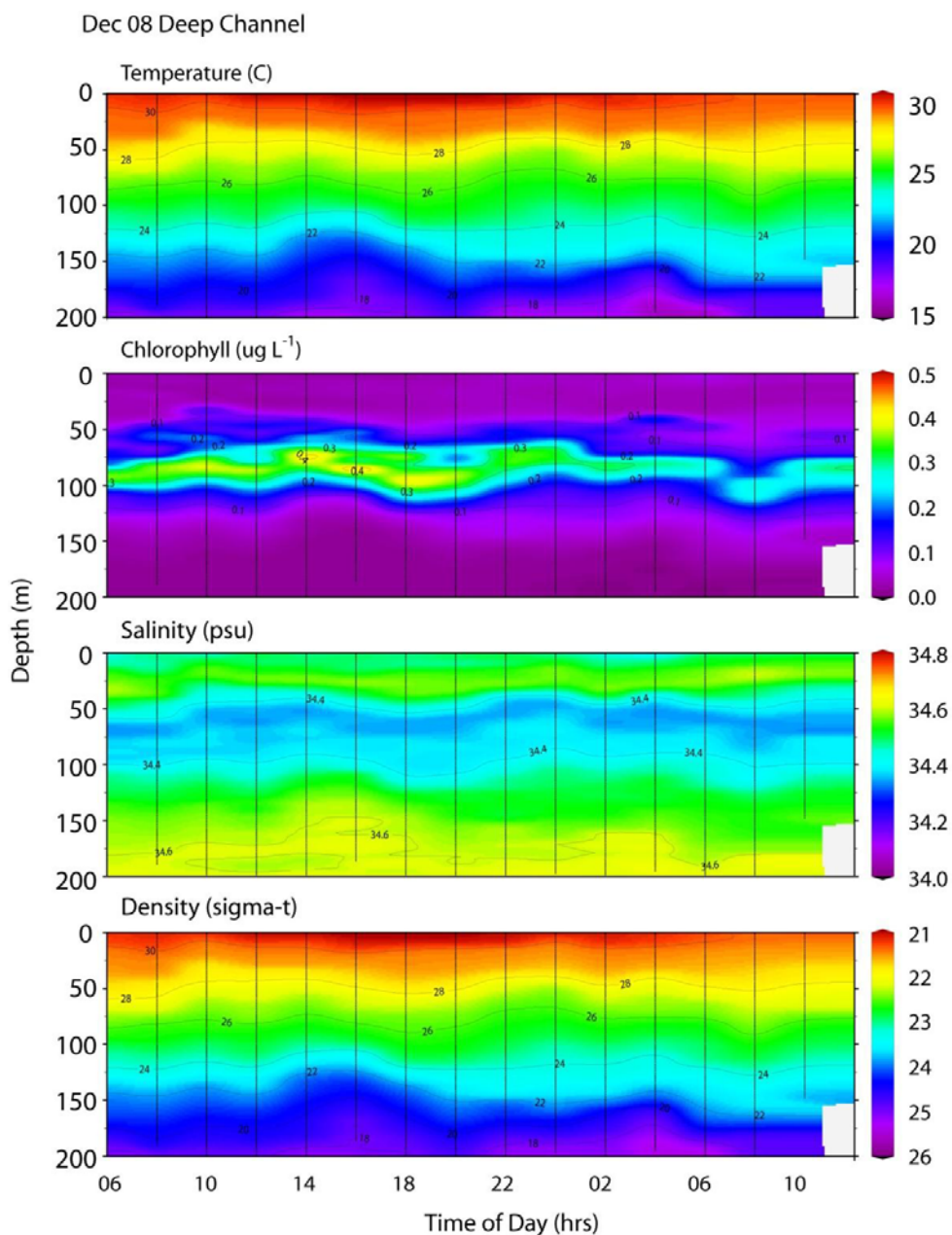


Fig. 13 Contoured time series of water temperature ($^{\circ}\text{C}$), contemporaneously measured in-situ chlorophyll fluorescence ($\mu\text{g L}^{-1}$), salinity (PSU) and Density (sigma-t) measured at the Deep Channel site between North Reef and South Reef (CH) from 06:00 local time on 4 December 2008.

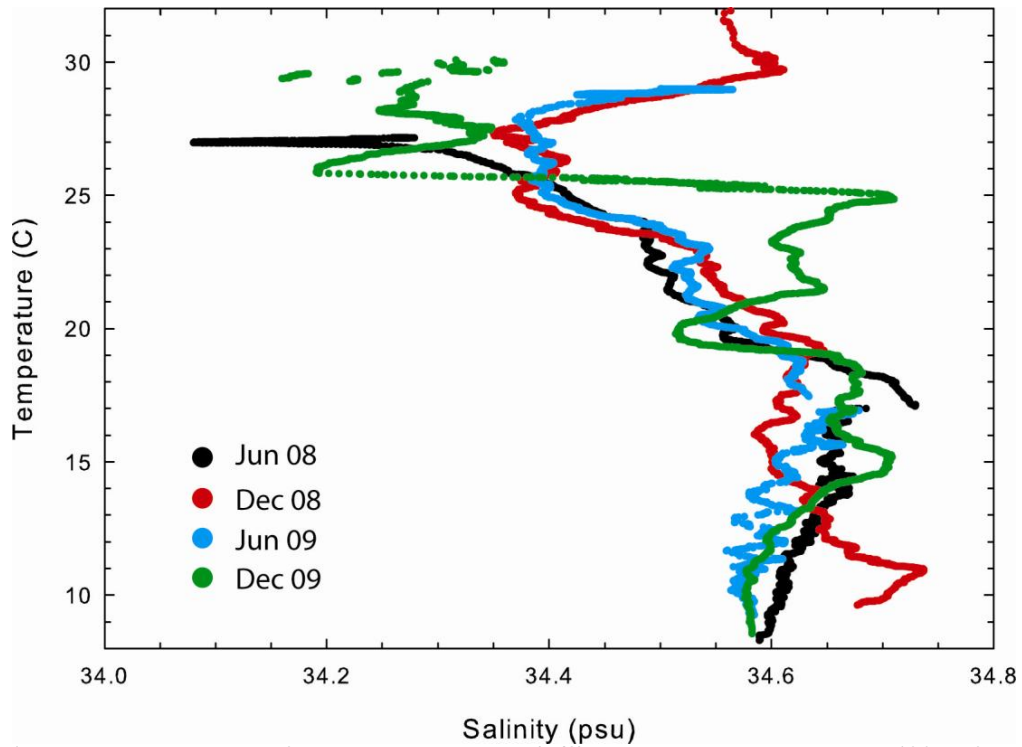


Fig. 14 Representative plots of temperature-salinity (T/S) relationships in the upper 400 m for water masses at the Open Water site SW of South Reef (SW).

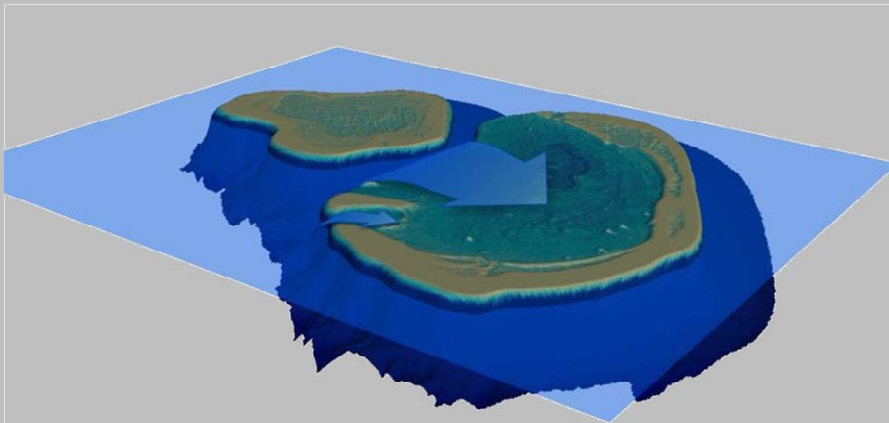
Internal waves and cool water intrusions at Scott Reef

The oceanic environment around Scott Reef is characterised by a warm surface layer of uniform density overlying water that is cooler and more dense. This vertical structure of density in the surrounding ocean supports the existence of internal waves and internal tides. Internal waves are gravity waves that propagate along the interface of density layers within the ocean interior, and appear as periodic vertical movements in the depth of the bottom of the surface mixed layer. Internal waves are produced as a response to surface tides moving water in a stratified ocean, and internal tides are internal waves at a tidal frequency. The vertical amplitude of internal waves is proportional to the density difference between the adjacent layers of fluid, and as a consequence, internal wave amplitudes are large compared to the generating surface movement.



Cartoon of internal waves at the interface of warm and cool ocean layers

At Scott Reef, the semi-diurnal internal tide in the surrounding ocean is modified by interaction with the local bathymetry (Wolanski and Deleersnijder, 1998) resulting in increased vertical displacement and frequency of motion of the thermocline within the channel between North and South Reef, compared to the adjacent open ocean. The dominant internal wave amplitude range is 30-60 m, with peak amplitudes reaching 110 m. When these large amplitude internal waves raise the top of the thermocline above the depth of the lagoon floor, nutrient-enriched water from below the surface mixed layer is able to move laterally into the deep lagoon of South Reef, providing an important mechanism for delivering nutrient rich water into shallow reef areas.



Conceptual representation of cool nutrient-enriched water from below the surface mixed layer moving laterally internal into the lagoon of South Scott Reef

Internal Waves

Internal waves are an ubiquitous feature of the world's oceans, generated by oscillating tidal flows of stratified water over steep topography. Such waves have large wavelengths (10's of kms) and amplitudes equivalent to a significant proportion of the total water depth (Holloway, 1983). Australia's North-western continental shelf is a globally significant region of internal wave generation and energy dissipation (Kunze and Llewellyn Smith, 2004), and the dynamics of the internal wave climate on the North West Shelf have been extensively studied (Holloway, 1983; Holloway, 1984; Holloway, 1996) in relation to their influence on engineering structures constructed for the offshore oil and gas industry. Relatively less is known about the internal wave dynamics at Scott Reef. Vertical mixing associated with internal wave activity is presumed to be a significant source of nutrients supporting biological productivity on the North West Shelf (Holloway et al., 1995).

The internal waves at Scott Reef are primarily semi-diurnal in periodicity, and are generated by an interaction between the local internal tide and shelf bathymetry (Wolanski and Deleersnijder, 1998). Observed internal wave activity at Scott Reef is therefore a combination of local internal tides and internal waves. Away from Scott Reef or other large bathymetric features, water motions associated with internal wave activity have a dominant cross-shelf direction (Holloway, 1984). Wave activity has a spring-neap variation in intensity, most likely modulated by the internal tide. This variation is more pronounced to the south of Scott Reef (e.g. Figure 17, Rowley Shoals, Furnas and Steinberg, 1999) than has heretofore been observed at Scott Reef.

At the far-field, Open Water site to the southwest of Scott Reef (Fig. 10, Fig. 11), the local internal waves exhibited a regular, sinusoidal character that was most pronounced at depths > 100 m. In contrast, wave dynamics observed at the Deep Channel site during winter (Fig. 12) were considerably more irregular due to interactions with the local bathymetry and again, internal wave activity was most pronounced at depths > 100 m, within the thermocline. During summer, with a much more stable water column, internal wave activity within the channel was more regular (Fig. 13) and exhibited periodicity and amplitude similar to that observed at the Open Water site during the same period.

The influence of the internal wave climate on the delivery of nutrients into the surface mixed layer is clearly evident in the representative profiles of hydrographic and biological variables at the four biological oceanography stations (Fig. 8). The well defined chlorophyll maximum that generally persists in a narrow (ca. 30 m) depth band at the base of the open ocean surface mixed layer is progressively mixed and broadened through the surface mixed layer with increasing proximity to Scott Reef. Within the channel, horizontal and vertical mixing processes are at their highest due to the interaction of the internal waves with the topography, and the enhanced mixing results in a broad chlorophyll maximum spanning a large proportion of the surface mixed layer (25 –125 m water depth).

At Scott Reef, upwelling of thermocline water and contained nutrients occurs through two mechanisms. The first is through enhanced vertical mixing of water from the upper thermocline waters into the mixed layer due to enhanced horizontal shear at the top of the thermocline. This vertical mixing process is enhanced close to Scott Reef and in the deep channel due to topographic disruptions of the waves.

The second type of upwelling occurs when the top of the thermocline is shallower than the sill depth of the South Reef lagoon. This can be due to either a regional thinning of the surface mixed layer as a consequence of regional transport of surface waters and vertical mixing processes, or the local internal wave/tidal dynamics that raise the top of the thermocline above the sill depth. The former mechanism is likely to produce a situation where the top of the thermocline is shallower than the lagoon sill depth for an extended period of time, while the latter mechanism produces a situation where the thermocline top is shallower than the sill depth on an irregular or episodic basis. In both cases, cooler, nutrient-enriched water from the thermocline is able to move laterally into the deep lagoon of South Reef. These episodic events can be seen in some of the near-bottom temperature records from temperature loggers deployed on the northern margin of the South Reef lagoon (see next section for discussion). During these intrusion events, the extent of lateral movement of thermocline waters into the lagoon depends upon both the length of time the thermocline is shallower than the sill depth and the thickness of the intruding layer (height of the thermocline top above the bottom).

The influence of the internal wave climate on the delivery of nutrients into the surface mixed layer is clearly evident in the representative profiles of hydrographic and biological variables at the four biological oceanography sites (Fig. 8). The well defined chlorophyll maximum that generally persists in a narrow (ca. 30 m) depth band at the base of the open ocean surface mixed layer is progressively mixed and broadened through the surface mixed layer with increasing proximity to Scott Reef. Within the channel, horizontal and vertical mixing processes are at their highest due to the interaction of the

internal waves with the topography, and the enhanced mixing results in a broad chlorophyll maximum spanning a large proportion of the surface mixed layer (25 – 125 m water depth).

Two studies have previously dealt with internal wave activity at Scott Reef. Firstly, Wolanski and Deleersnijder (1998) observed internal wave activity at Scott Reef using sub-surface temperature and current meter moorings on the western and north-eastern flanks of the reef system, at depths between 100 – 200 m. The observed waves were mainly semi-diurnal in nature and modulated with the spring-neap tidal cycle, with amplitudes peaking at up to 60 m during spring tides. Secondly, between 1993 and 1999, a mooring with sub-surface temperature and pressure (depth) sensors was maintained at Scott Reef by AIMS to monitor internal wave activity in the vicinity of the reef. The mooring was nominally located on the continental slope immediately to the west of South Reef (near 14 5.3'S 121 43.1'E). The mooring consisted of temperature-pressure loggers nominally deployed at 100 and 150 m in the upper thermocline. The objective of the mooring program was to record ranges of temperature variability within narrow depth strata associated with vertical movements of the thermocline in internal waves or tides.

Absolute fluctuations of temperature recorded by individual instruments at depth are related to four factors:

1. Regional-scale temperature variations associated with seasonal insolation and large-scale water movements.
2. Cross-shelf tidal oscillations of the horizontal temperature gradient past the mooring site.
3. Vertical motions of the instruments in the thermocline due to mooring lean.
4. Local vertical movements of the thermocline due to internal waves and internal tides.

Regional-scale temperature variations at Scott Reef associated with seasonal changes in insolation and large-scale water movements were found to be on the order of one to several °C per month. The largest monthly change in low-pass filtered (removing short-term variability i.e. daily, tidal) temperature between 1993 and 1999 was 3.76°C (Furnas and Steinberg, 1999). The median monthly change in low-pass filtered temperature over this period was < 1.7°C. Measured ranges of water temperature within one-month periods at ~100 and 160 m were of the order of three times the range of low-pass filtered temperatures for those periods (Table 3). In the absence of temperature changes due to the passage of frontal boundaries, daily low-pass temperature fluctuations would most likely be less than 0.1°C (Furnas and Steinberg, 1999). Cross-shelf temperature gradients in the vicinity of Scott Reef at 0, 50 and 100 m were 0.001, 0.007 and 0.049°C, respectively (Furnas and Steinberg, 1997). For a nominal cross-shelf tidal current velocity of 1 kt (1.8 km hr⁻¹), the net horizontal displacement of water during one half-tidal cycle (6 hrs) would be approximately 11 km which would lead to nominal temperature variations < 0.1°C in the upper 50 m and no greater than 0.5°C at 100m. Vertical temperature gradients in the thermocline near Scott Reef are generally between 0.04 and 0.07°C m⁻¹. Recorded vertical movements of the moored instruments at Scott Reef due to local currents were almost always < 5 m. As a result, diel temperature fluctuations due to mooring lean would be on the order of 0.2 to 0.4°C. Taken together, maximum daily temperature fluctuations at depth associated with lateral water movements past the mooring and vertical mooring motion are most likely < 1°C. The largest part of temperature variability measured at depth within a relatively short (24 hour) period is therefore associated with vertical movements of the thermocline under the influence of internal waves and tides.

Temperature fluctuations associated with internal wave or internal tide activity in a given depth band are calculated as the differences between the absolute temperature range for a monthly period and the range of low-pass filtered temperatures for that period. The maximum potential amplitude of the internal waves within monthly periods was estimated by dividing the difference between the raw and low-pass filtered temperatures by a conservative estimate of the mean temperature gradient in the thermocline (0.07°C m⁻¹). An alternative approach to estimating wave amplitude is to divide the average diel (24 hr) range of water temperatures at a particular depth by the vertical temperature

gradient. These two approaches yield similar estimates of internal wave amplitude within monthly time bands (Table 3).

Table 3 Measured ranges of raw and low-pass filtered water temperatures within monthly periods at Scott Reef between November 1997 and January 1999 and estimated amplitudes of internal waves calculated from diel (24-hour) temperature ranges within monthly time frames. From Furnas and Steinberg (1999).

	Temperature Range				Internal wave amplitude			
	Shallow (100 m)		Deep (160 m)		Shallow (100 m)		Deep (160 m)	
	Raw	Low Pass	Raw	Low Pass	Max	Mean	Max	Mean
	°C	°C	°C	°C	m	m	m	m
1997								
Nov	5.04	1.11			56	48		
Dec	6.04	2.13			56	53		
1998								
Jan	5.23	1.70			50	48		
Feb	5.93	2.13			64	52		
Mar	6.03	2.03	4.54	1.01	57	50	50	45
Apr	8.18	2.65	5.95	2.33	79	64	52	56
May	8.25	2.43	7.08	1.73	83	76	76	63
Jun	6.91	1.81	8.04	2.52	73	69	79	67
Jul	5.00	1.75	5.76	2.32	46	49	49	52
Aug	5.76	2.07	7.60	1.34	53	52	79	66
Sep	5.45	1.67	5.58	1.45	54	55	59	50
Oct	4.78	1.17	6.33	1.31	52	43	72	57
Nov	6.04	1.29	6.02	1.45	68	56	65	61
Dec	5.44	1.54	6.83	1.64	56	45	74	57
1999								
Jan	4.73	0.83	5.91	0.88	56	43	72	51
Mean	5.92	1.71	6.33	1.63	60	54	67	57

Time series of diel temperature ranges recorded at 100 m for the period between August 1995 and January 1999 (Fig. 15) exhibit fluctuations between 2 and 4°C, with peak values approaching 8°C. For a conservative temperature gradient of 0.07°C m⁻¹, this would translate to a dominant internal wave amplitude range of 30 – 60 m, with peak amplitudes reaching 110 m.

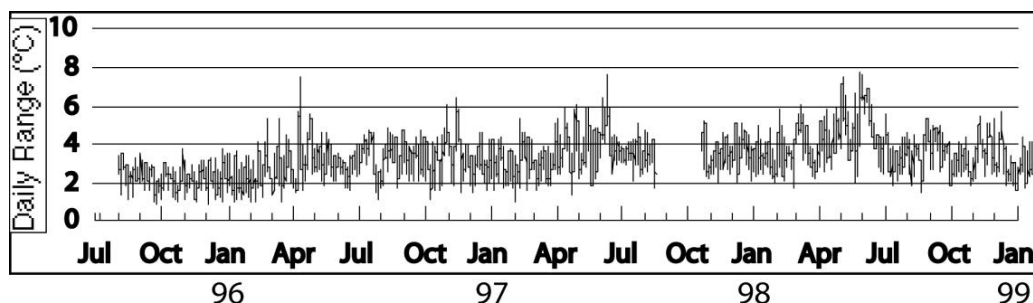


Fig. 15 Diel temperature ranges at 100 m depth between August 1995 and January 1999.

Time series data from the temperature moorings deployed in 200 m and 47 m water depths within the deep channel and at the northern edge of the lagoon of South Reef as part of the present study

display diel temperature ranges of $\sim 5^\circ\text{C}$ near the sill depth of the lagoon, and up to 10°C in the deeper water column (depths $>90\text{ m}$) in the deep channel. Using a temperature gradient of 0.08°Cm^{-1} , these ranges represent estimated internal wave amplitudes of up to 60 m near the sill depth, and $\sim 120\text{ m}$ for depths $>90\text{ m}$ (Fig. 16). These estimates would be an upper limit as there is some slight indication of contamination of the temperature data through vertical motions of the instruments in the thermocline due to mooring lean.

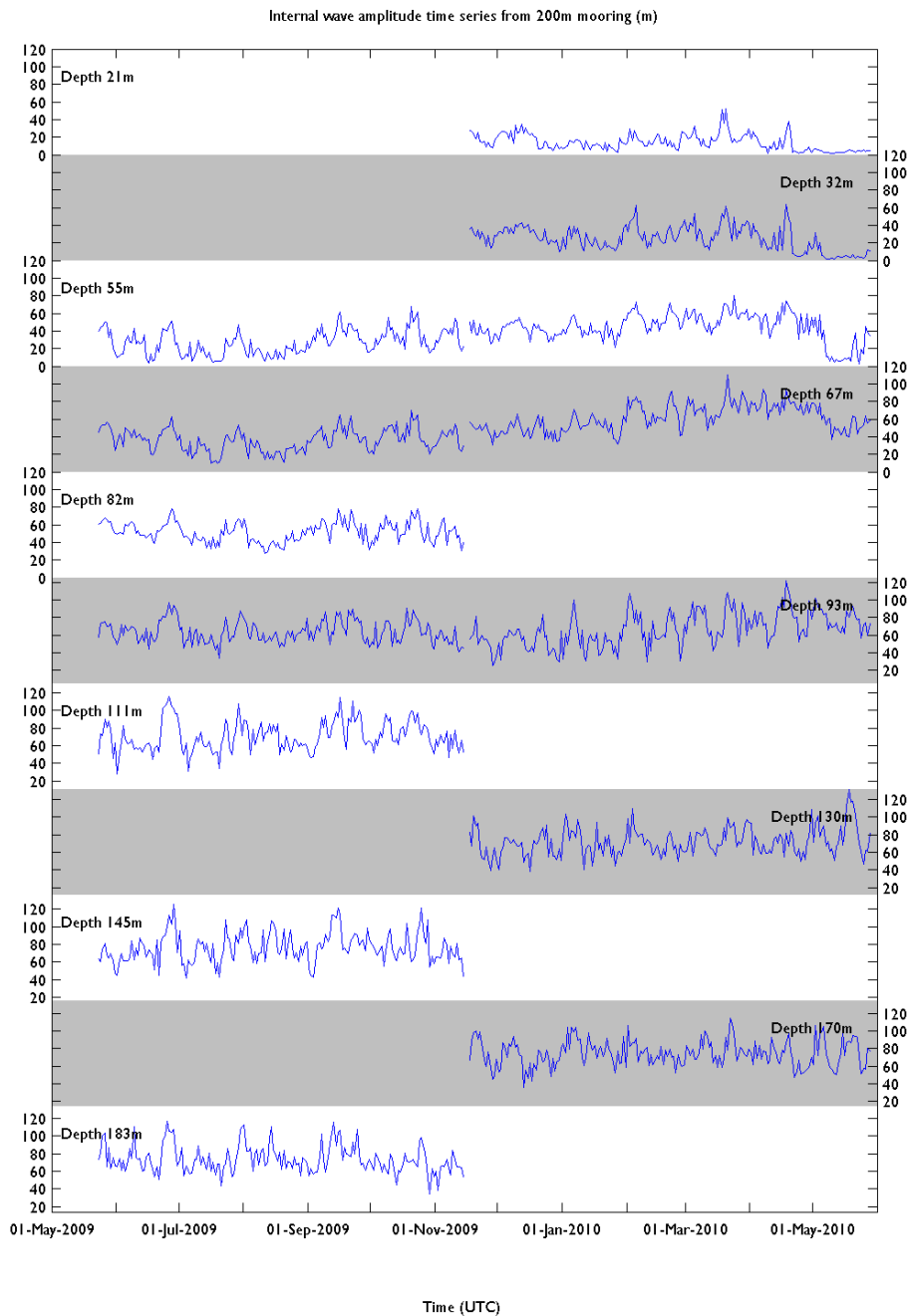


Fig. 16 Estimated internal wave amplitudes during May 2009 – May 2010 at the 200 m mooring site within the channel.

During winter in 2008 and 2009, measured vertical fluctuations of the thermocline due to internal waves over one diel period at time series sites Deep Channel, NE Margin and Open Water were ~50 – 60 m, 25 – 35 m and ~30 m, respectively (Fig. 17). During the strongly stable conditions of early summer (December 2008, November 2009), the magnitudes of the vertical fluctuations of the thermocline due to internal waves over one diel period were ~25 – 50 m at time series sites Deep Channel, NE Margin and Open Water.

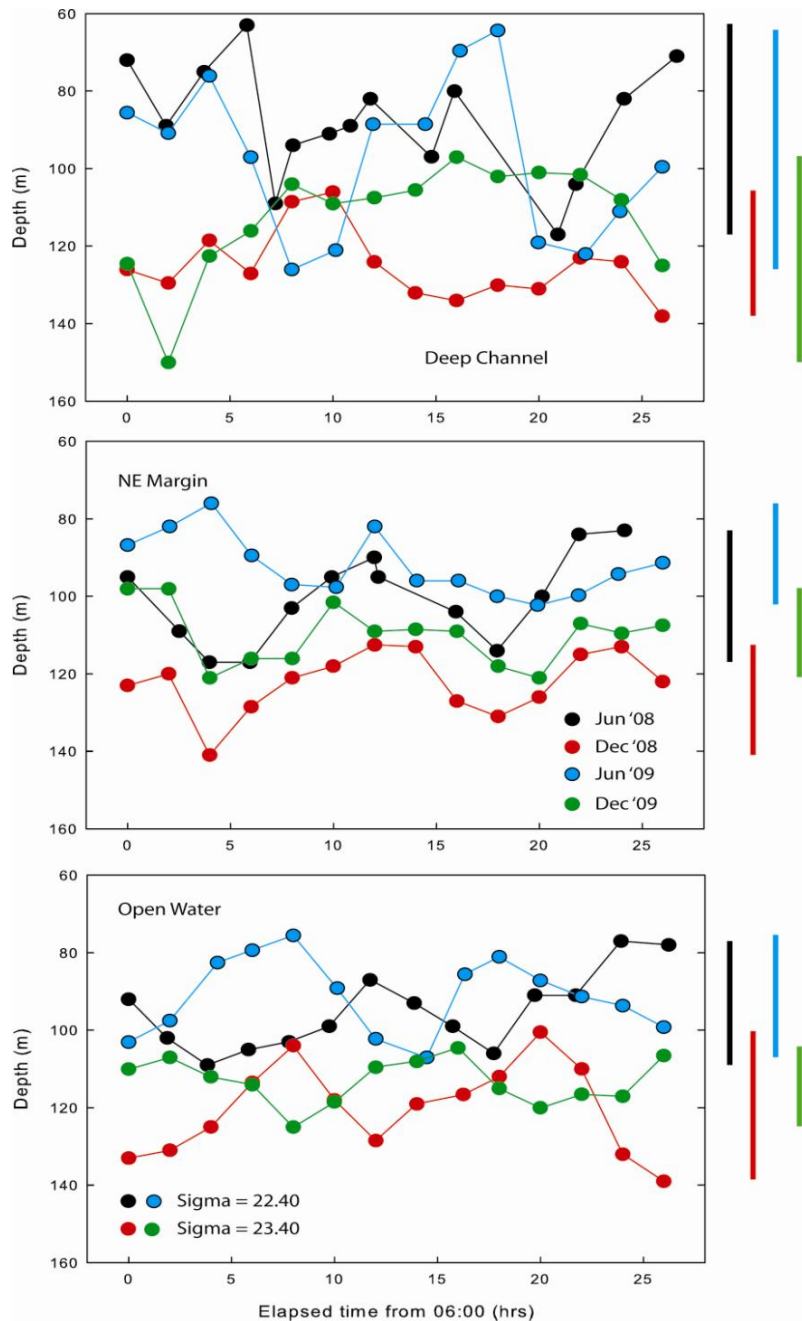


Fig. 17 Vertical excursions of selected density surfaces due to internal wave activity over diel time frames at Scott Reef deep water sites. Coloured bars on right of plot indicate amplitude of internal waves.

The physical environment of the South Reef lagoon

The physical environment of South Reef lagoon is controlled by the seasonal characteristics of the surface layer of the surrounding ocean, the tidal interaction of these waters with the topography of the reef, the regional monsoonal climate and the seasonal cycle of insolation. The lagoon environment mirrors the seasonal and inter-annual variability in the temperature and salinity structure exhibited by the regional oceanic waters, with additional higher frequency variability caused by local process such as enhanced vertical mixing, modified horizontal advection and residence times and increased local evaporation. In particular, the seasonal characteristics of the depth of the surface layer (0 – 100 m water depth) play a dominant role in controlling the exchange of water and waterborne material between the lagoon and the channel separating North Reef and South Reef. The seasonal surface temperature cycle is driven by the seasonal cycle of insolation and vertical stratification with a maximum solar energy input in November-December (ca. 26 MJ m⁻² d⁻¹) and minimum in June – July (ca. 14 MJ m⁻² d⁻¹). This energy is largely absorbed within the upper 100 m, affecting vertical stratification, mixing, and surface water temperature. Local vertical mixing processes are strongly affected by the wind stress produced by the regional monsoonal winds. Episodic cyclones produced intense mixing of waters around Scott Reef in summer.

Water Temperature

Water temperatures recorded within the lagoon of South Reef during the period March 2008 – February 2010 ranged from 23.3°C to 30.9°C. Daily average temperatures ranged from 24.7°C to 30.4°C with minimum daily average temperatures occurring in August/September and maximum daily average temperatures occurring in April (Fig. 18). This seasonality of temperature within the deep environments of the South Reef lagoon is consistent between the years of the observational period. Highest temperature were recorded by the loggers deployed at shallow sites (e.g. sites PE01, PE02, PE03, PE04, & site PE12), with the highest temperature (ca. 30.9°C) recorded within the shallow reef edge site (site PE03), presumably due to local warmed water originating from the reef top flowing past this logger site. With the exception of the shallow near-reef flat sites, daily average temperatures were higher at deep sites and consistently lower average temperatures were recorded at sites close to the channel (sites PE05, PE06, PE07, PE08, PE16) due to the persistent cooling influence of the intrusions. Daily statistics, aggregated monthly, have been calculated for all temperature time-series data and are presented in Appendix III (Table A 1).

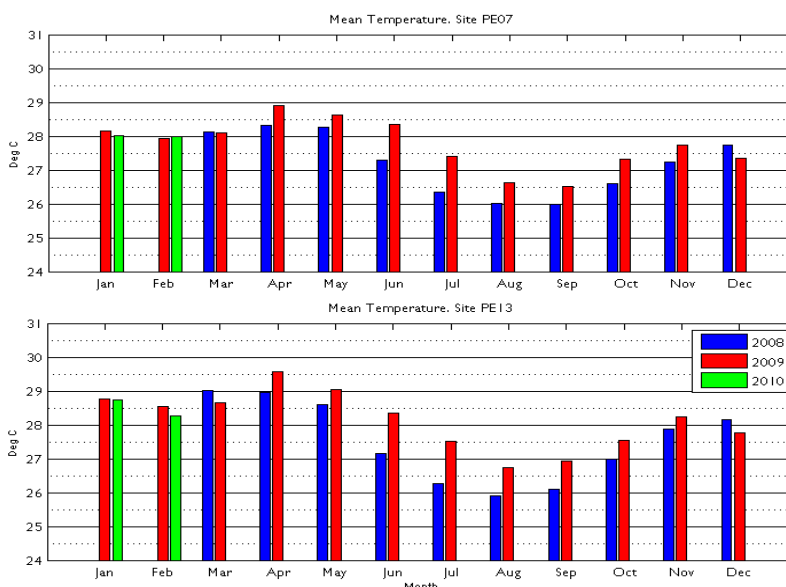


Fig. 18 Histogram of average daily temperatures for representative sites adjacent to the channel (top) and in the interior of the lagoon (bottom).

The South Reef lagoon of Scott Reef is open to exchange with the surrounding ocean primarily via the transport of water through the open northern boundary of the lagoon and the channel between North Reef and South Reef. Hydrodynamics within the channel are complex, with large amplitude internal waves resulting in large vertical heave of the thermocline and the surface mixed layer. When the depth of the surface mixed layer is equal to the sill depth of the South Reef lagoon, the internal wave dynamics episodically raise the bottom of the surface mixed layer above the sill depth, allowing cooler, nutrient-enriched water from the thermocline to intrude laterally into the lagoon. The depth of the sill between the lagoon and the channel is relatively constant (ca. 40 m depth) but shoals with proximity to East Hook and the Sandy Islet. Temperature time-series from within the lagoon reveal that intrusions of cool water are conspicuous at all sites adjacent to the channel (representative time-series shown in Fig. 19), suggesting a degree of spatial consistency in the delivery of cool water across the relatively uniform depth of the lagoon's northern margin. Fine-scale variability in the timing and location of intrusions is likely to be due to the complex internal wave dynamics within the channel (Fig. 12) and small scale non-uniformity of the local bathymetry. Recurrent tidal intrusion activity is not evident at logger sites within the interior of the lagoon (representative time-series shown in Fig. 20).

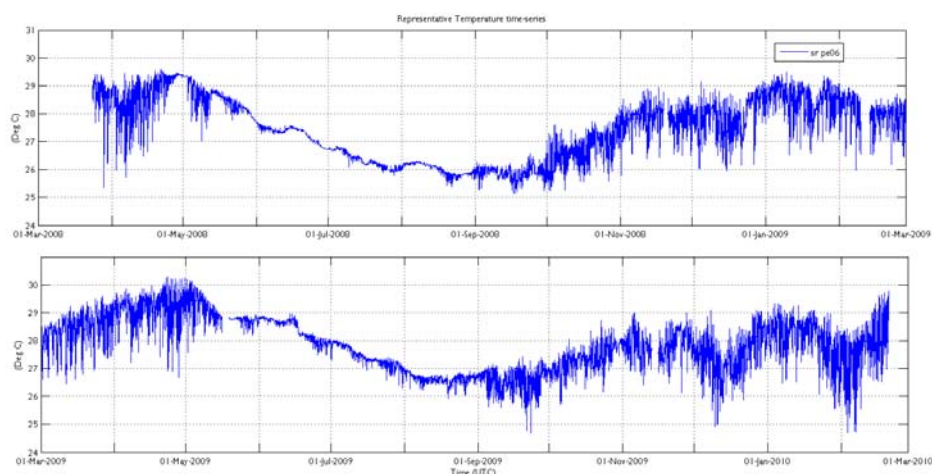


Fig. 19 Representative temperature time series (@15 minute sampling) at in-situ logger site adjacent to the channel.

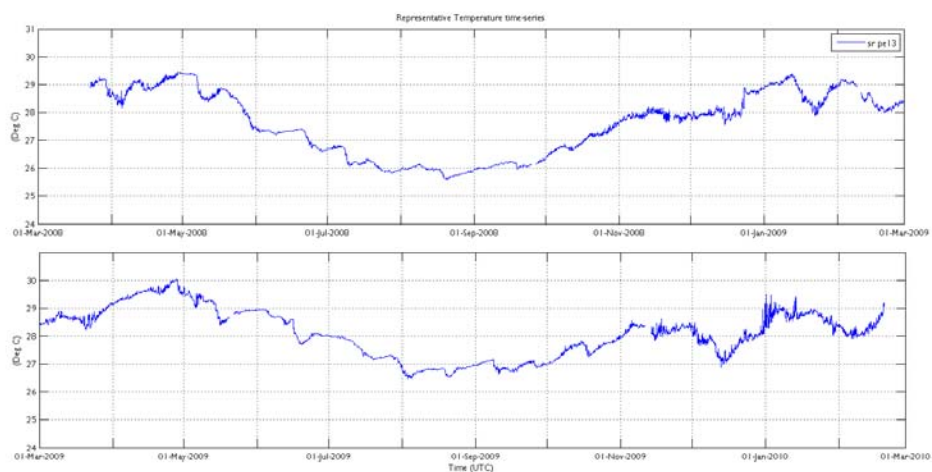


Fig. 20 Representative temperature time series (@15 minute sampling) at in-situ logger site within the lagoon of South Reef.

Cool water intrusions display strong semi-diurnal periodicity (Fig. 21) in response to a similar periodicity in both the prevailing internal wave/tide regime (see Fig. 17) and the surface tidal currents that generate horizontal shear and entrain water from below the sill depth up into the lagoon. Due to the explicit link to tidal energy, intrusion of thermocline water into the lagoon of South Reef is strongly modulated by the spring-neap tidal cycle.

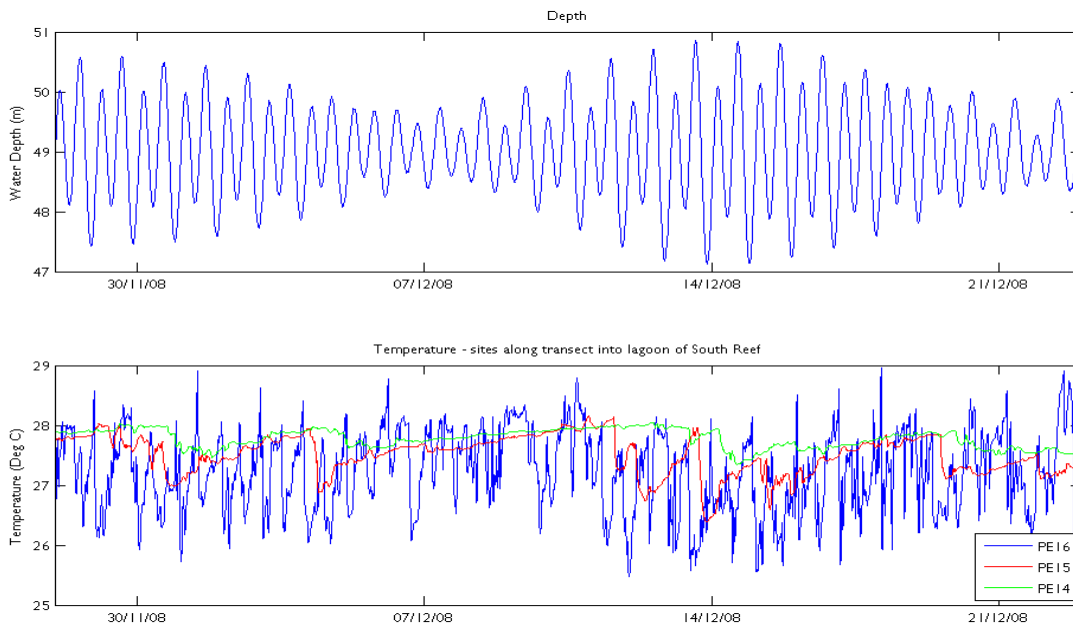


Fig. 21 Time series of water depth (at Site PE16) and temperature at sites PE16, PE15 and PE14 along a North-South transect from the deep channel into the interior of the South Reef Lagoon.

As cool water intrusions are predominantly tidally driven, they are not simply injections of cooler water into the lagoon on a flooding tide, but have both a flooding and an ebbing phase. Temperature observations along the northern margin of the lagoon suggest that a significant proportion of the volume of cool water that intrudes into the lagoon is advected out of the lagoon at the reverse of the tide, as indicated by a return to 'pre-intrusion' temperatures on the ebbing tide (Fig. 21). Mixing processes associated with horizontal current shear and bottom boundary turbulence will, however, mix a proportion of the intruded water with the lagoonal receiving waters, and remain resident in the lagoon for time scales longer than a tidal cycle (sub-tidal). The timescales of sub-tidal transport and mixing of intruded water within the interior of the lagoon can be inferred from the observed temperatures along a North-South transect from the deep channel into the interior of the South Reef lagoon (Fig. 21). At the northern margin of the lagoon (site PE16), temperature variability is of the order of 1.0 – 2.0 °C at the tidal frequency and modulated by the spring neap cycle. The magnitude and frequency of cooling events decreases with distance away from the lagoon margin, and there is an accompanying increase in the time taken for temperature to return to the 'pre-cooling' conditions. The time between rapid cooling and return to pre-cooled temperatures is indicative of the residence time and mixing of the introduced cool water; short times indicate rapid flushing and limited mixing, extended times indicate reduced flushing and extended mixing. At sites close to the northern margin, this time is approximately one tidal cycle; for sites PE15 and PE14 (Fig. 21), this time is approximately 1 – 2 days, and 2 – 5 days, respectively, suggesting that nutrient-enriched cool water delivered into the system remains resident within the interior of the lagoon for up to 5 days, before it is thoroughly mixed with the greater surrounding waters, or advected from the region.

Intrusions of cool water exhibit strong seasonal and interannual variability linked to seasonal and interannual changes in the depth of the surface mixed layer in response to atmospheric conditions, and presumably changes in large scale oceanographic circulation. Intrusions are more frequent and have an increased magnitude of cooling through summer and autumn (Fig. 19). Annual variability in intrusion activity is introduced through the interannual variability of the depth of the surface mixed layer; a deep (ca. 100 m) surface mixed layer persisted during winter 2008, while a shallow (ca. 70 m) mixed layer was observed during winter 2009. With a well mixed surface layer persisting down to a depth of approximately 100 m (as shown in Fig. 9, June 2008), vertical motions within the water column at the depth of the sill will not be accompanied by significant changes in temperature. In contrast, during late spring and early summer when the water column exhibits no clearly defined mixed layer (Fig. 12, December 2008), vertical motion of the water column will result in temperature fluctuations when observed from a fixed depth reference level.

Daily temperature range is presented as a proxy for intrusion activity as it indicates more clearly the range of temperature experienced at a particular site (Fig. 22). Temperature ranges determined from sea-bottom mounted loggers (Fig. 23) show that during the autumn period of typically increased frequency of intrusion events, the daily temperature ranges fluctuated by only 2 – 4°C, with a maximum daily temperature range of > 4.5°C, while the daily average temperatures at sites along the northern margin of the southern lagoon ranged between 28.0 and 29.0 °C. The temperature- salinity (T/S) relationship of the intruded water and temp/depth profiles of the surrounding ocean (Fig. 8) confirm the origin of intruded water from a depth of ~100 – 160 m depth within the thermocline. During October and November 2009, daily temperature ranges fluctuated by only 1.0 – 3.0 °C. During this early summer period, a reduction in temperature of this range is indicative of water originating from <100 m depth.

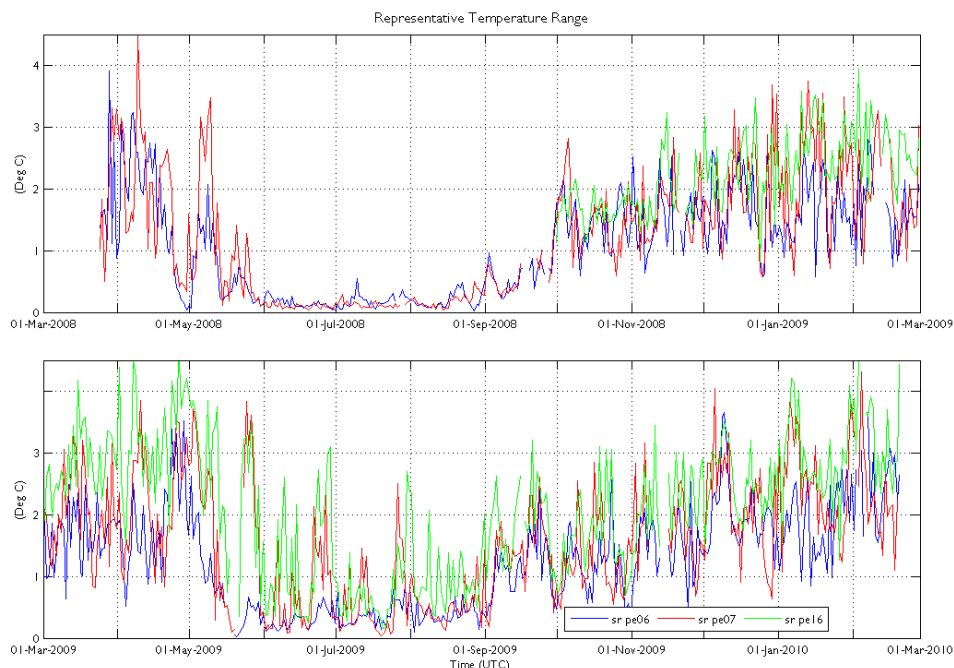


Fig. 22 Representative daily temperature range at in-situ logger sites adjacent to the channel

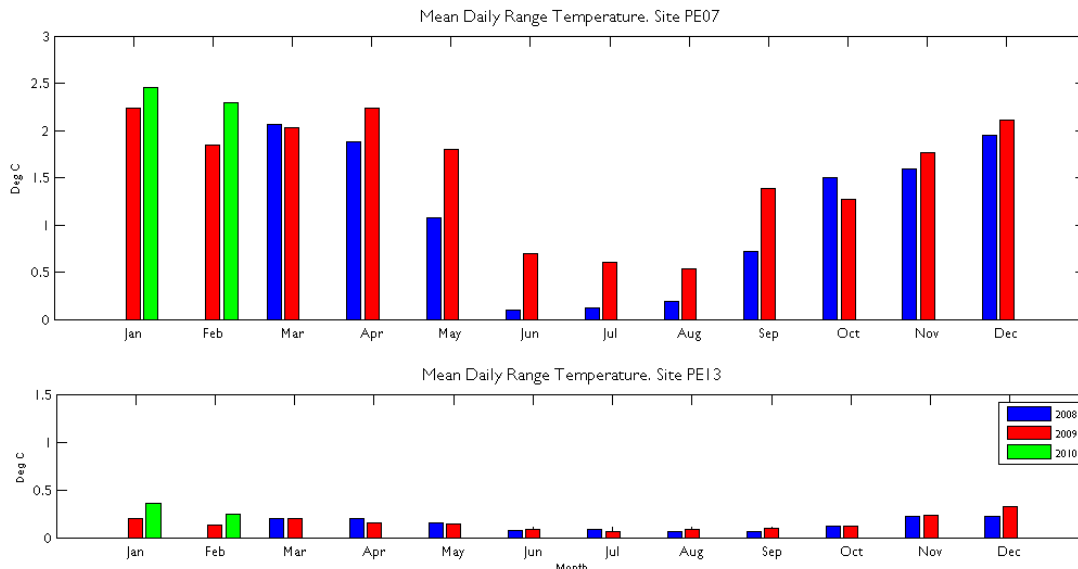


Fig. 23 Monthly average temperature ranges at in-situ logger sites adjacent to the channel (top) and in the interior of the lagoon (bottom).

Within a particular season, the waters of the South Reef lagoon show a spatially consistent vertical temperature structure and are, in general, horizontally well mixed (Fig. 24) with limited horizontal variability (Fig. 25). The degree of temperature stratification shows a strong seasonal signal, as would be expected in a relatively shallow lagoon environment, with summer stratification destroyed through autumn as the water cools to become vertically and horizontally well mixed during winter (Fig. 25).

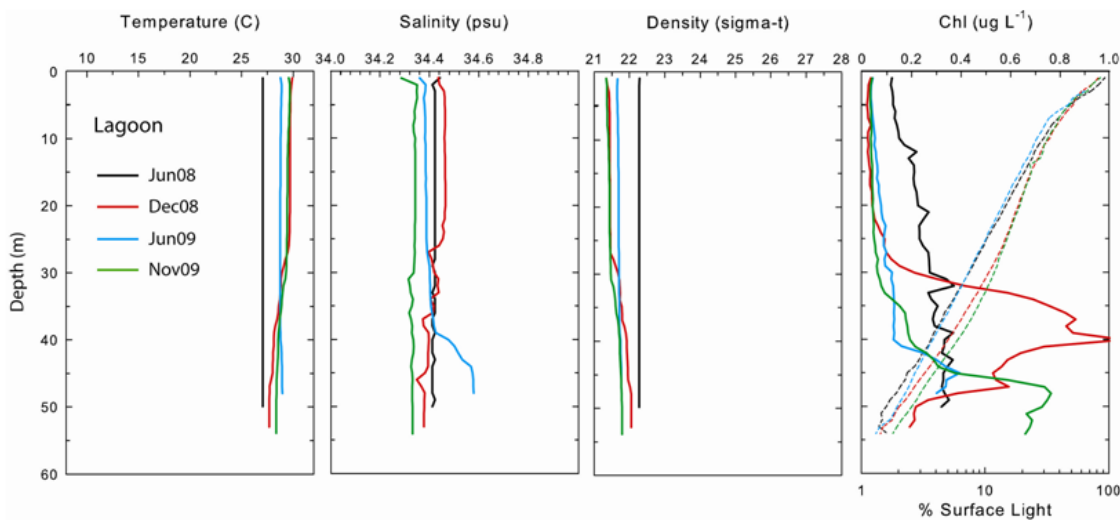


Fig. 24 Representative vertical profiles of temperature, salinity, density, and chlorophyll within the lagoon.

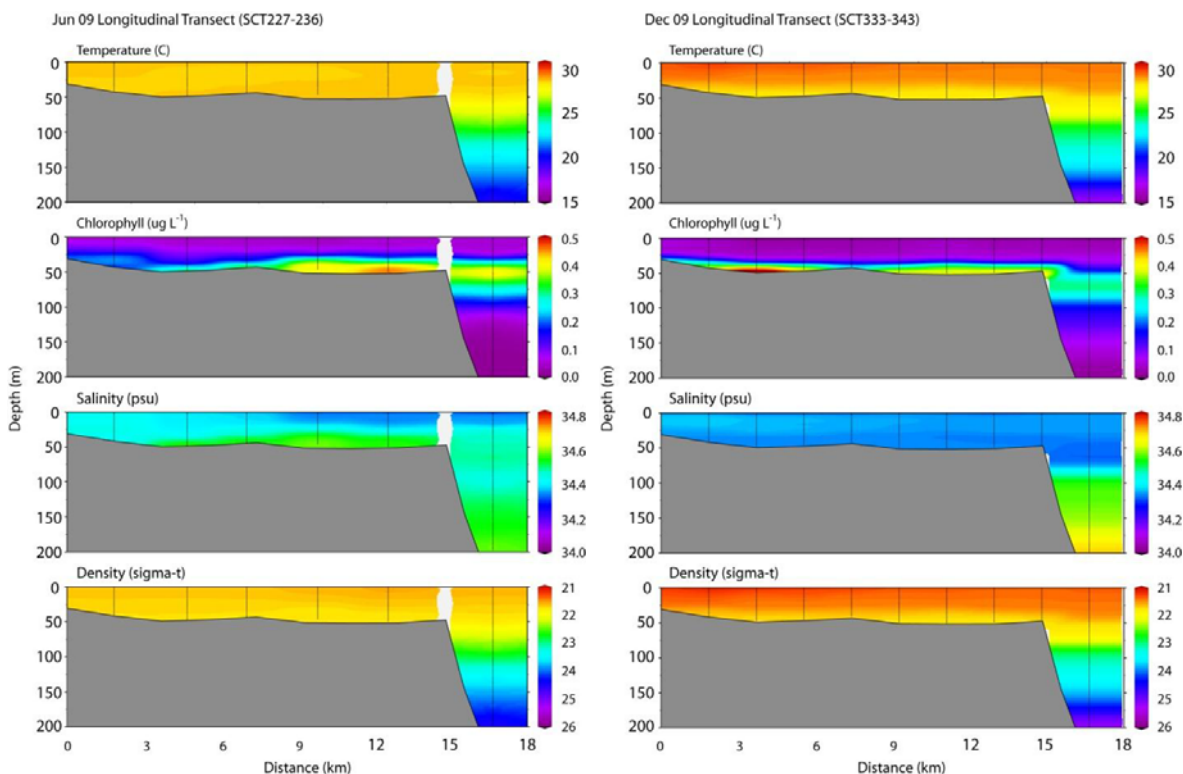


Fig. 25 Contoured longitudinal sections of water temperature, salinity, chlorophyll and density along the central axis of the South Reef lagoon during June 2009 and December 2009. Note – blank section June plot is due to interpolated data being omitted in this area of large gradients and depth change. In areas of large change the interpolation method becomes less accurate, and the unreliable data are therefore omitted.

Salinity

Daily average salinity within the lagoon ranged from 34.29 to 34.73 PSU during the observational period, and vertical profiles of salinity in the South Reef lagoon were, in general, found to be virtually isohaline (e.g. Fig. 24). Variability in the mean salinity between seasons reflects the water column characteristics of the surface mixed layer in surrounding oceanic waters, which vary noticeably between cruises (Fig. 14) in response to the variability of the regional circulation and the exposure of Scott Reef to waters originating from both the Timor Sea/Indonesian Throughflow to the north, and NW shelf water from the south (Cresswell et al, 1993). Mean monthly salinities show little consistency between years, and there appears to be no clear seasonality (Fig. 26).

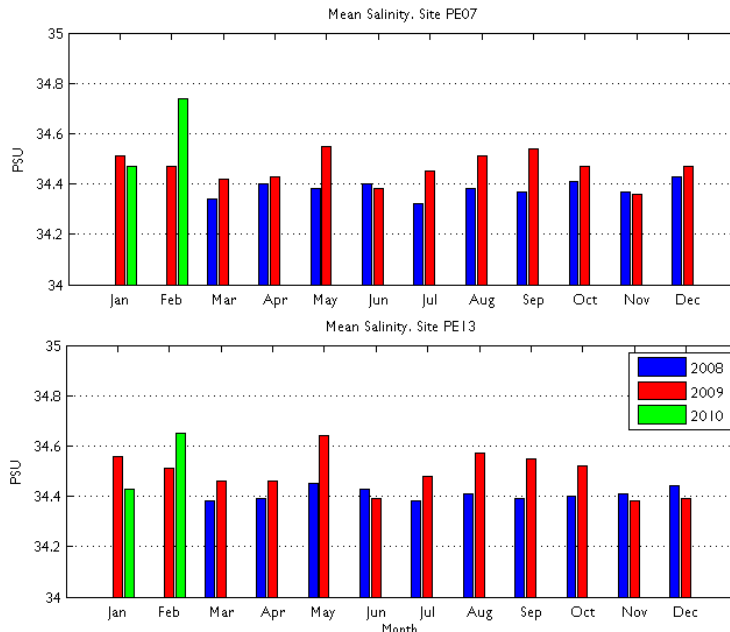


Fig. 26 Monthly average salinity at in-situ logger sites adjacent to the channel (top) and in the interior of the lagoon (bottom).

Regional scale changes in the vertical distribution of salinity also influence the vertical distribution of salinity within the lagoon of South Reef via the exchange of water associated with the near bottom intrusions. At the beginning of the May – June 2009 biological oceanography cruise (30 May 2009), a persistent near-bottom salinity maximum layer was observed (Fig. 25) that covered much of the central lagoon. This subsurface layer was embedded in a largely isothermal lagoonal water mass (Fig. 27) and was discontinuous with the sub-surface salinity maximum in the adjacent deep channel and surrounding waters. The near-bottom salinity maximum layer was not observed when the lagoon was re-sampled a few days later (9 June 2009). Conversely, during December 2008, a near-bottom salinity minimum was observed (Fig. 27). These anomalous salinities are suggestive of enhanced vertical mixing or advection of sub-sill water into the South Reef lagoon. A comparison of mean surface salinities (0 – 50 m depth) within the lagoon and at the open water sites (Table 4) suggests that lagoon salinity to some degree maps the salinity stratification present in the surface mixed layer, as would be expected in response to enhanced vertical mixing or advection of sub-surface waters into the lagoon from the deep channel driven by intrusion events.

Table 4 Mean surface (0 – 50 m depth) salinities within the lagoon (LA) and at the open water (SW) sites based on time series observations collected during the biological oceanographic cruises. 95% C.I.'s on the mean salinities are ≤ 0.01 psu.

Cruise	Mean lagoon salinity	Mean open water salinity	Vertical salinity structure at open water site
June 2008	34.38	34.10	Low salinity @ surface, increasing with depth below mixed layer
Dec 2008	34.42	34.52	Mixed layer, then mid-water salinity minimum between ca. 50-100 m
June 2009	34.43	34.50	Mixed layer, then mid-water salinity minimum between ca. 75-125 m
Nov 2009	34.34	34.30	Thin salinity maximum layer at upper side of thermocline, then increasing with depth

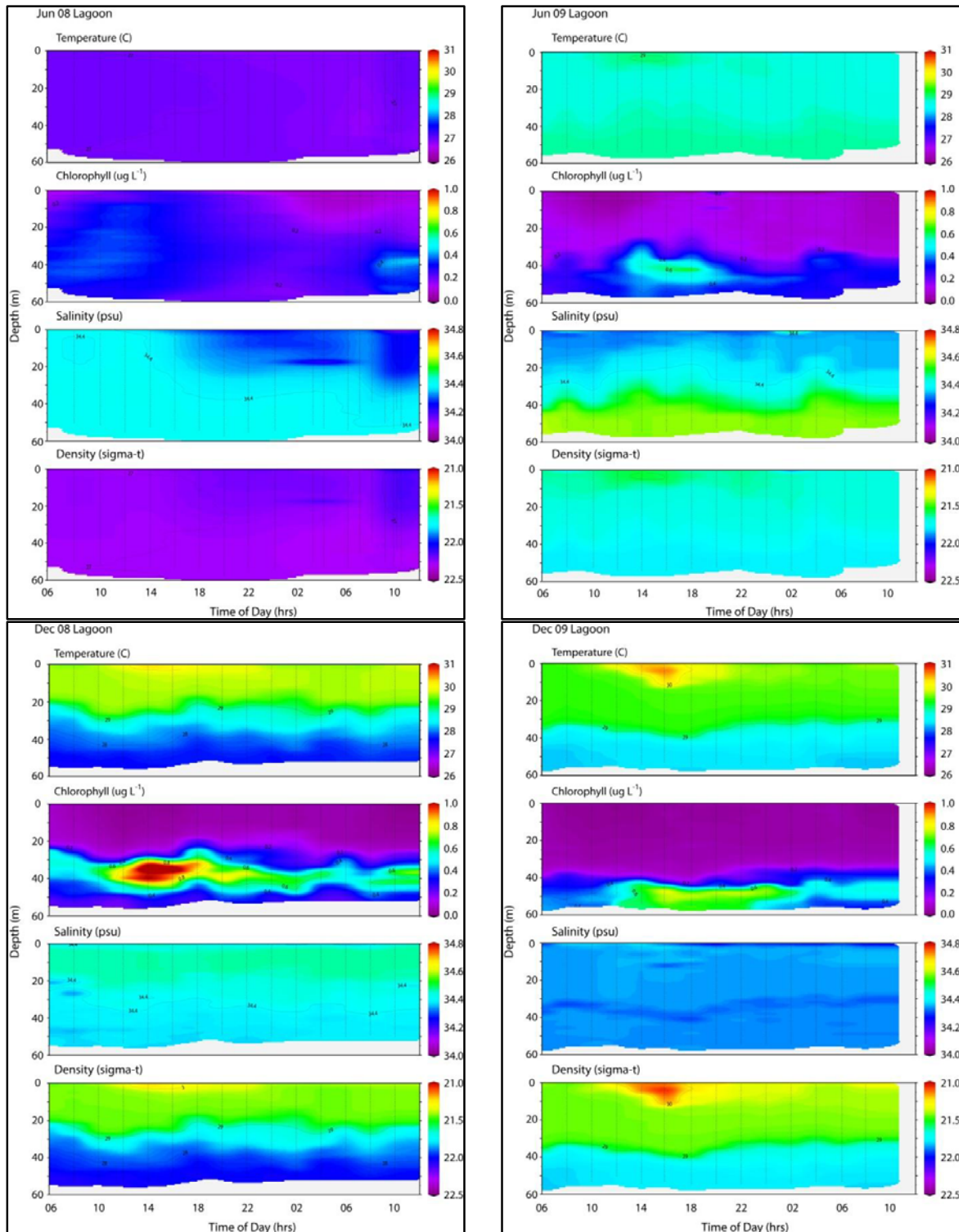


Fig. 27 Contoured time series of water temperature, chlorophyll, salinity and density in the lagoon of South Reef during June 2008 (top/left panel), June 2009 (top/right), December 2008 (bottom/left) and December 2009 (bottom/right).

Daily statistics are monthly aggregated for all logger derived salinity time-series data and are presented in Appendix III (Table A I).

Turbidity and Sedimentation rate

Turbidity within the lagoon of Scott Reef is low, with average turbidity levels of ca 0.18 NTU. Daily average turbidity across the observational sites ranged from 0.04 to 1.50 NTU. Sites located on the margins of the reef slopes (sites PE01, PE02, PE03 and PE04) and in the channel between West Hook and the Sandy Islet (PE05) show higher variability and higher average turbidity levels than that observed at the deeper lagoon sites. Site PE02, adjacent to the reef flat in the southern section of the lagoon of South Reef showed the highest average values of turbidity (Fig. 28). For sites located adjacent to shallow reef areas, this is likely a consequence of detritus and suspended material originating from the reef tops being advected from the reef flats past these sites.

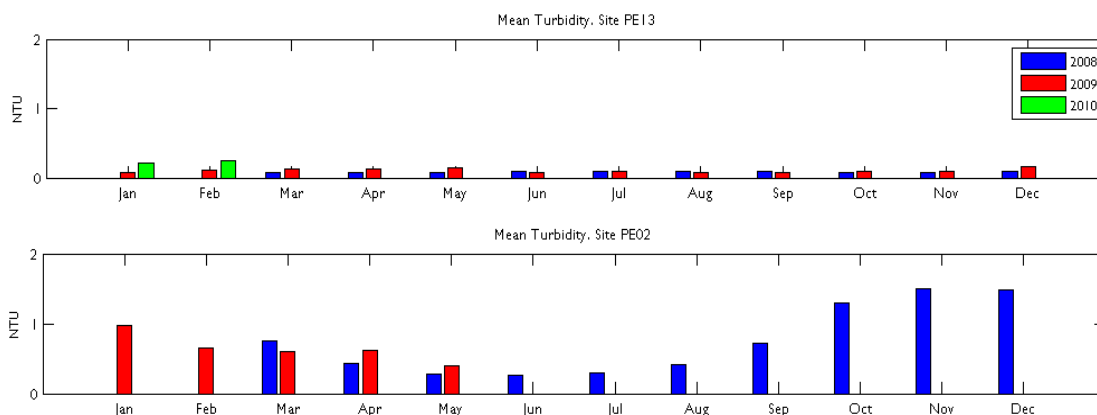


Fig. 28 Monthly average turbidity (NTU) at observational sites PE13 (top) and PE02 (bottom).

The only strong seasonality evident in the observed turbidity within the South Reef lagoon is at site PE02, with increased turbidity over the wet season presumably driven by the increase in wind and wave activity associated with storms passing through the region. At all other sites, particularly sites in the interior of the lagoon, there is little apparent seasonality and the general pattern of low turbidity persists with through time (Fig. 29).

At deeper sites in the lagoon there is little evidence of a sustained increase in turbidity near the seabed that could potentially result from resuspension of settled matter. Relationships between wave-height and turbidity (Fig. 30), and current strength and turbidity (Fig. 31) do not suggest strong correlations, indicative of environments where there is little settled matter on the sea-bed available for resuspension. The caveat to this general observation is that the data presented here do not capture any large meteorological disturbances and associated increased wave energy. Under extreme conditions, increased bed shear stresses 1) resuspend coarse material that is usually not mobile under typical conditions, and 2) produce new fine sediment through the working of existing sediments.

Monthly aggregated mean levels of turbidity, as determined from the in-situ loggers are presented in Appendix III (Table A I).

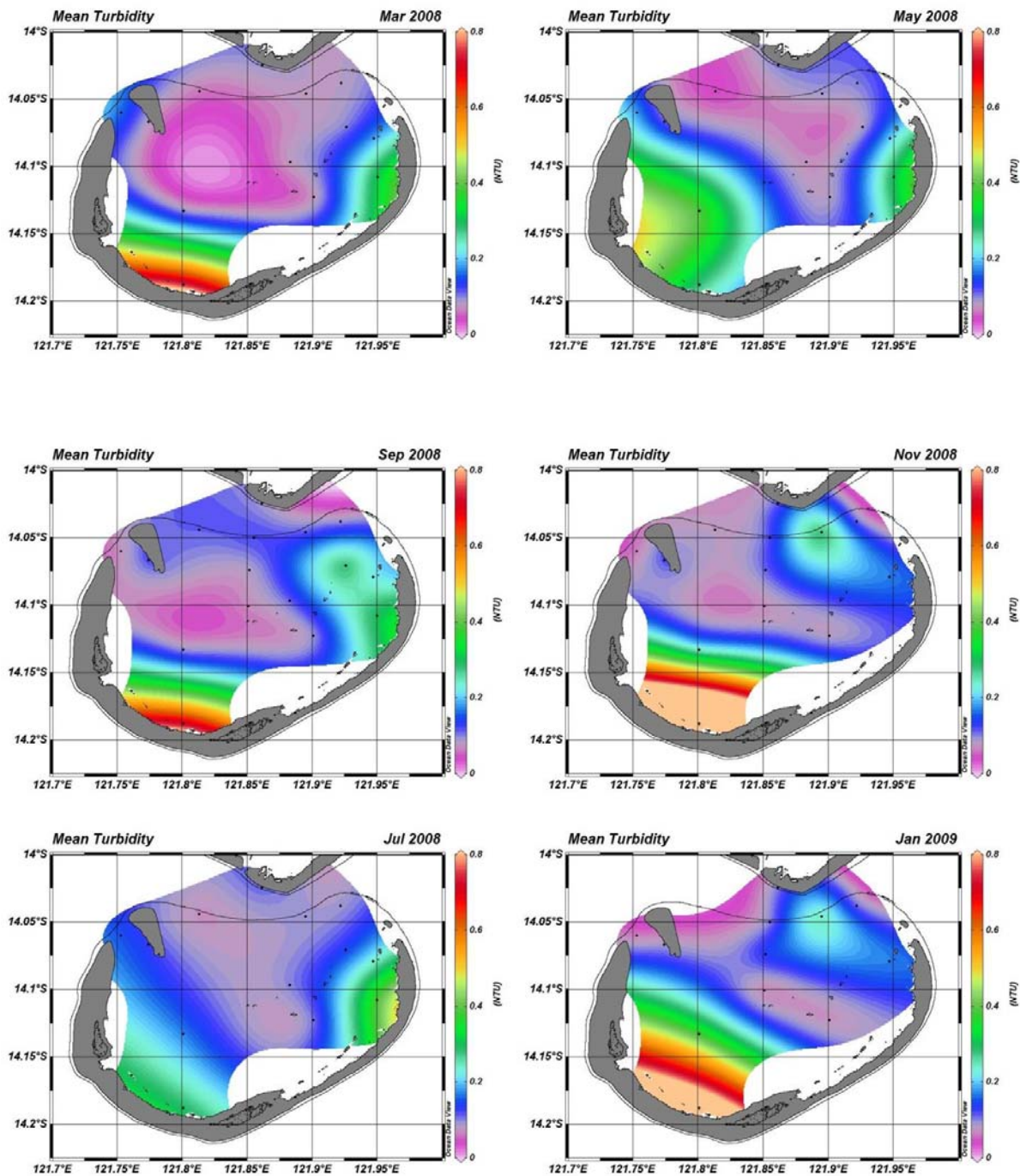


Fig. 29 Contoured mean monthly turbidity at in-situ logger sites. Only every second month (from March 2008) is shown. Colour scale shows turbidity in NTU. Dots indicate logger sites.

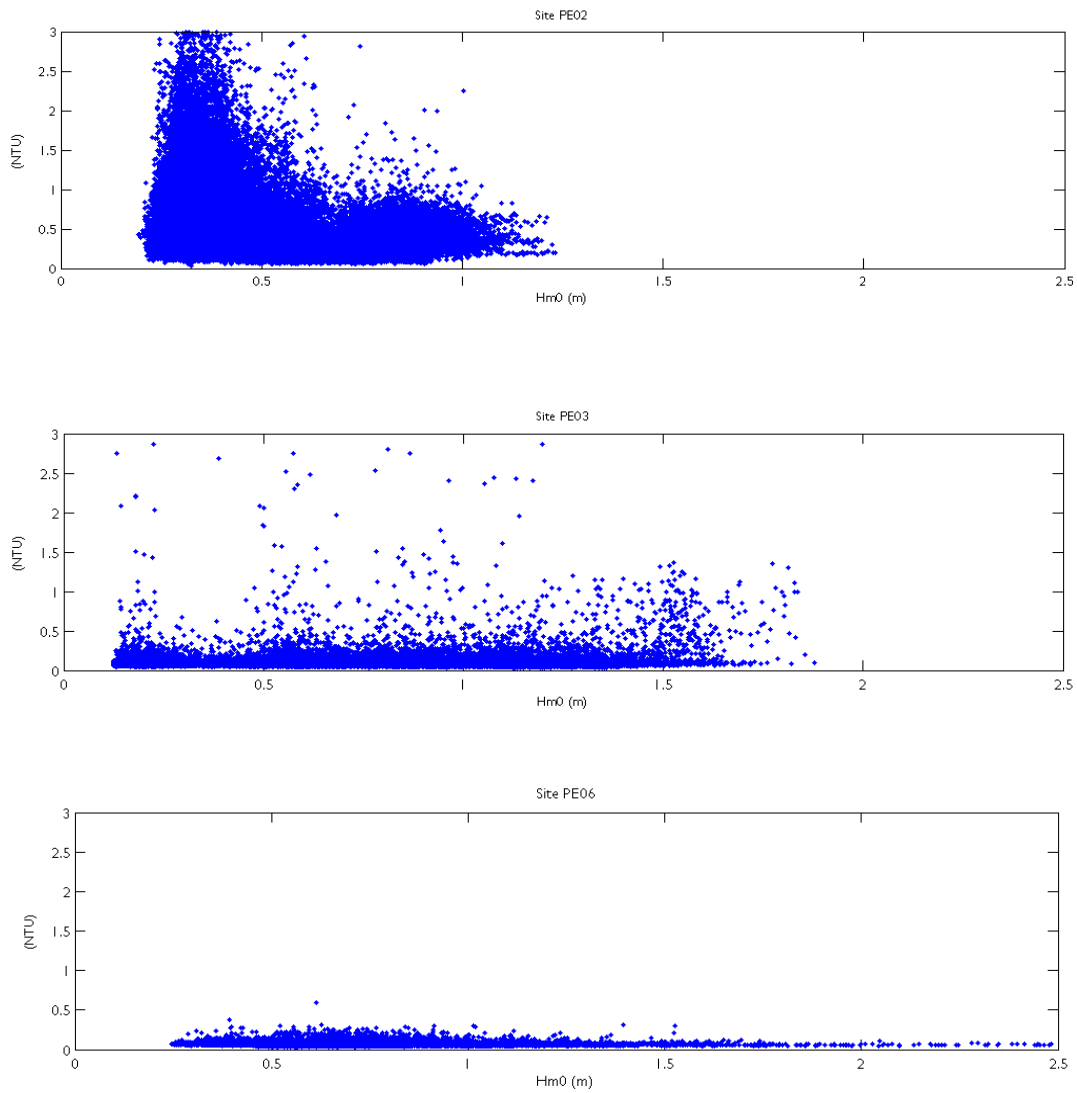


Fig. 30 Turbidity vs mean wave height (Hm0) at sites PE02, PE03 and PE06.

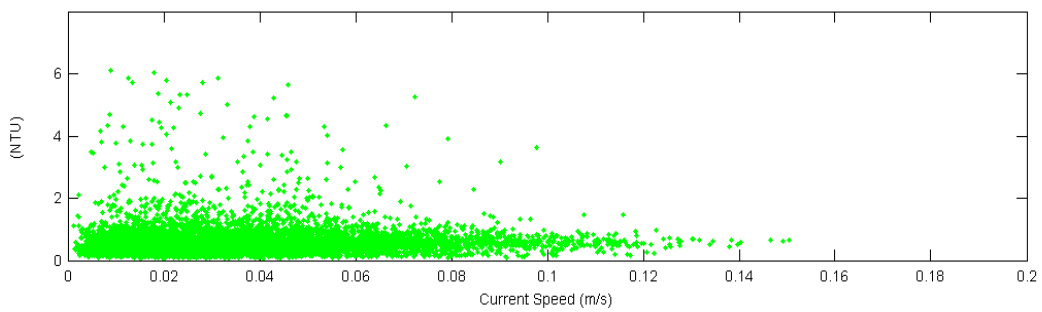


Fig. 31 Turbidity vs current speed at Site PE02.

Observed sedimentation rates reflect the general observation of high water clarity with little suspended matter. At all sites sampled with in-situ sediment traps, mean sedimentation rates were less than $0.8 \text{ mg cm}^{-2} \text{ d}^{-1}$ that is below the lower extent of the range (< 1 to $10 \text{ mg cm}^{-2} \text{ d}^{-1}$) observed at reefs not subjected to stresses from human activities (Rogers, 1990). Highest sedimentation rates for individual trap deployments and overall means were observed in the channel between West Hook and the Sandy Islet (Site PE05) and at site PE15, but this was not a temporally consistent pattern.

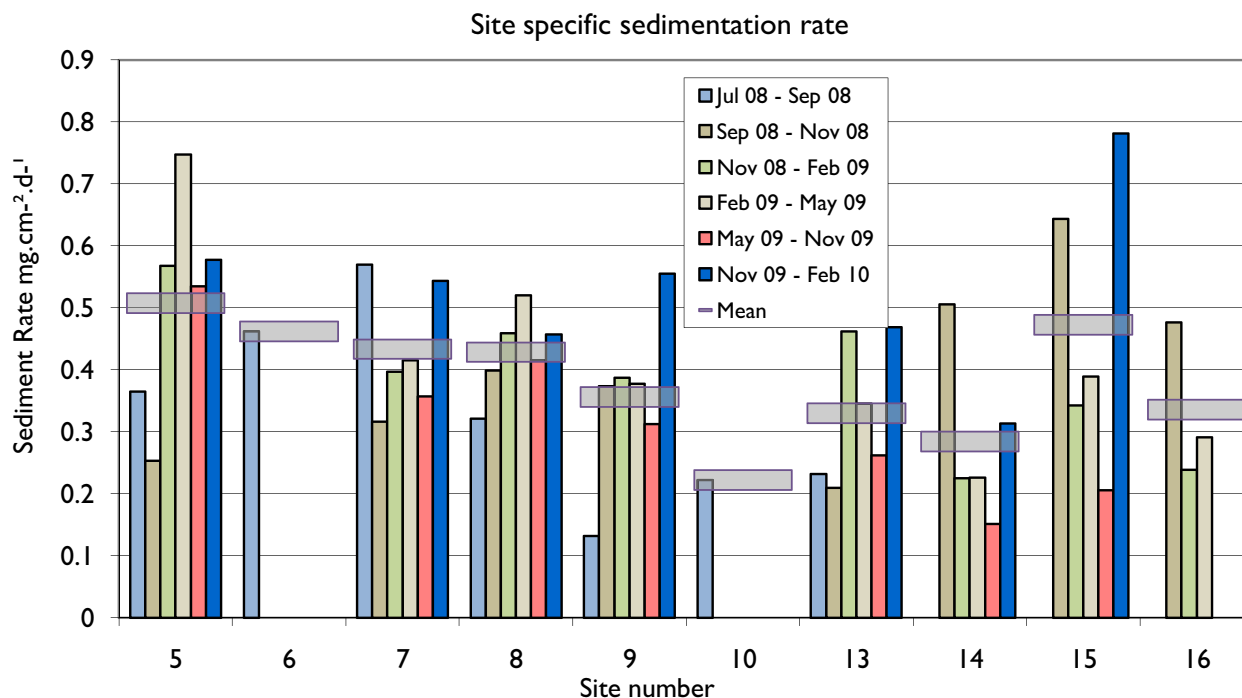


Fig. 32 Sedimentation rates from in-situ sediment traps deployed at logger locations within the South Reef lagoon.

Photosynthetically Active Radiation

Light levels within the lagoon were monitored through vertical hydrographic casts and through the accumulation of Photosynthetically Active Radiation (PAR) time series at the observation logger sites. Vertical water column profiles of PAR provide a good estimate of downwelling PAR from which we can determine the light conditions at the seabed as a percentage of incident light at the surface.

The reporting of PAR as % reaching a particular depth level can be problematic as it relies on an accurate measurement of incident PAR. This is not always straightforward. For profiling instruments, PAR sensors often saturate at the high near surface light levels, requiring some extrapolation (from deeper observations where the sensor is not saturated) to estimate near surface PAR. For in situ near bottom PAR loggers, surface incident PAR is not observed, and 'typical' values are employed to interpret the deep observations as '% of surface PAR'. With this in mind, we chose to report %PAR (particularly that recorded from our loggers) not as absolute values, but as greater than a meaningful threshold, such as $>1\%$ or less than 10% .

Downwelling PAR from hydrographic casts undertaken within the South Reef lagoon during the biological oceanographic cruises has been used to characterise the %PAR reaching the seabed. At all stations within the lagoon, %PAR reaching the seabed was $>1\%$ for the deepest sites surveyed (55m), and generally fell within the range of $>1\%$ and $\leq 10\%$, for seabed depths between 35 and 55m.

Using the relationship:

$$PAR_{depth} = PAR_{surface} e^{-kD}$$

Where PAR_{depth} is PAR at depth, PAR_{surface} is incident value PAR at the surface, D is the depth and k is the light extinction co-efficient, extinction coefficients were found to be of the order of 0.07 m⁻¹ for the entire water column above logger deployment sites.

Our data indicate that water clarity is consistently high, with significant and consistent light penetration to the benthos within the South Reef lagoon. Seasonality in the near-bottom PAR observations (Fig. 33) follow the seasonal cycle of insolation and vertical stratification with a maximum solar energy input in November-December and minimum in June – July.

Time series data of observed PAR at logger sites confirm the temporal consistency of significant light penetration (>1% surface PAR) to the benthos within the South Reef lagoon. Maximum daily PAR at observational sites (Fig. 34) was generally in excess of 100 mmol ph m⁻² s⁻¹, or equivalent to >5% surface PAR (maximum surface PAR is generally ~2000 mmol ph m⁻² s⁻¹ (Kirk, 1994)).

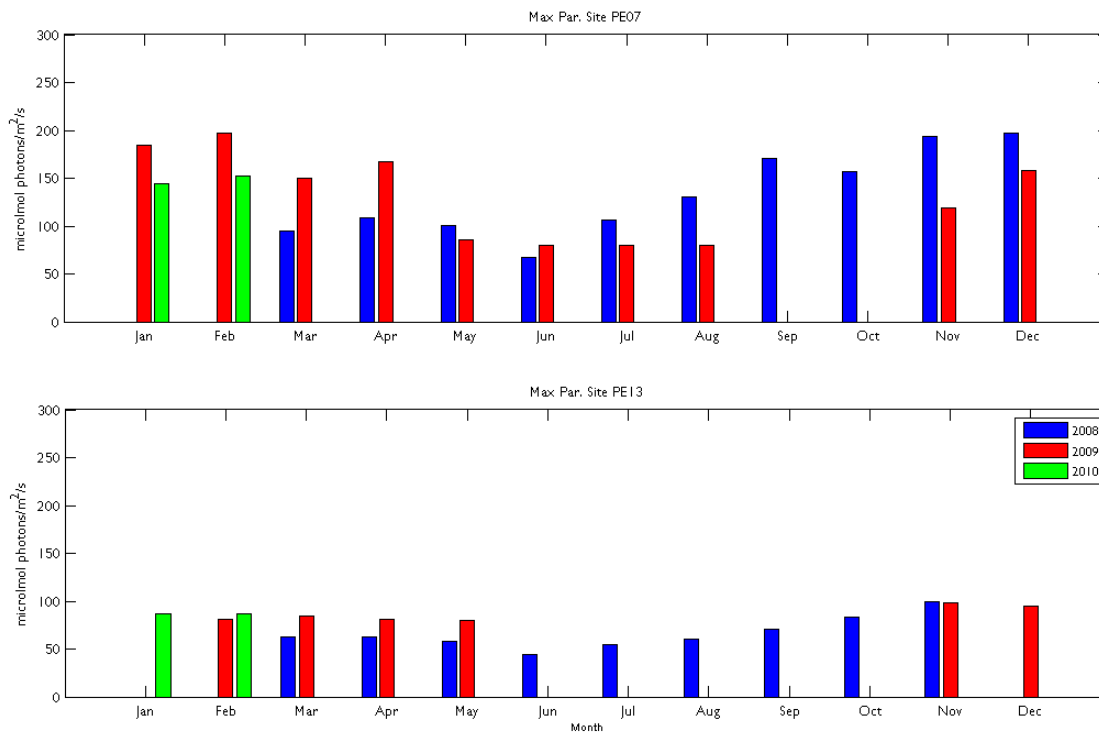


Fig. 33 Monthly average maximum PAR at representative observational sites PE13 (top) and PE02 (bottom).

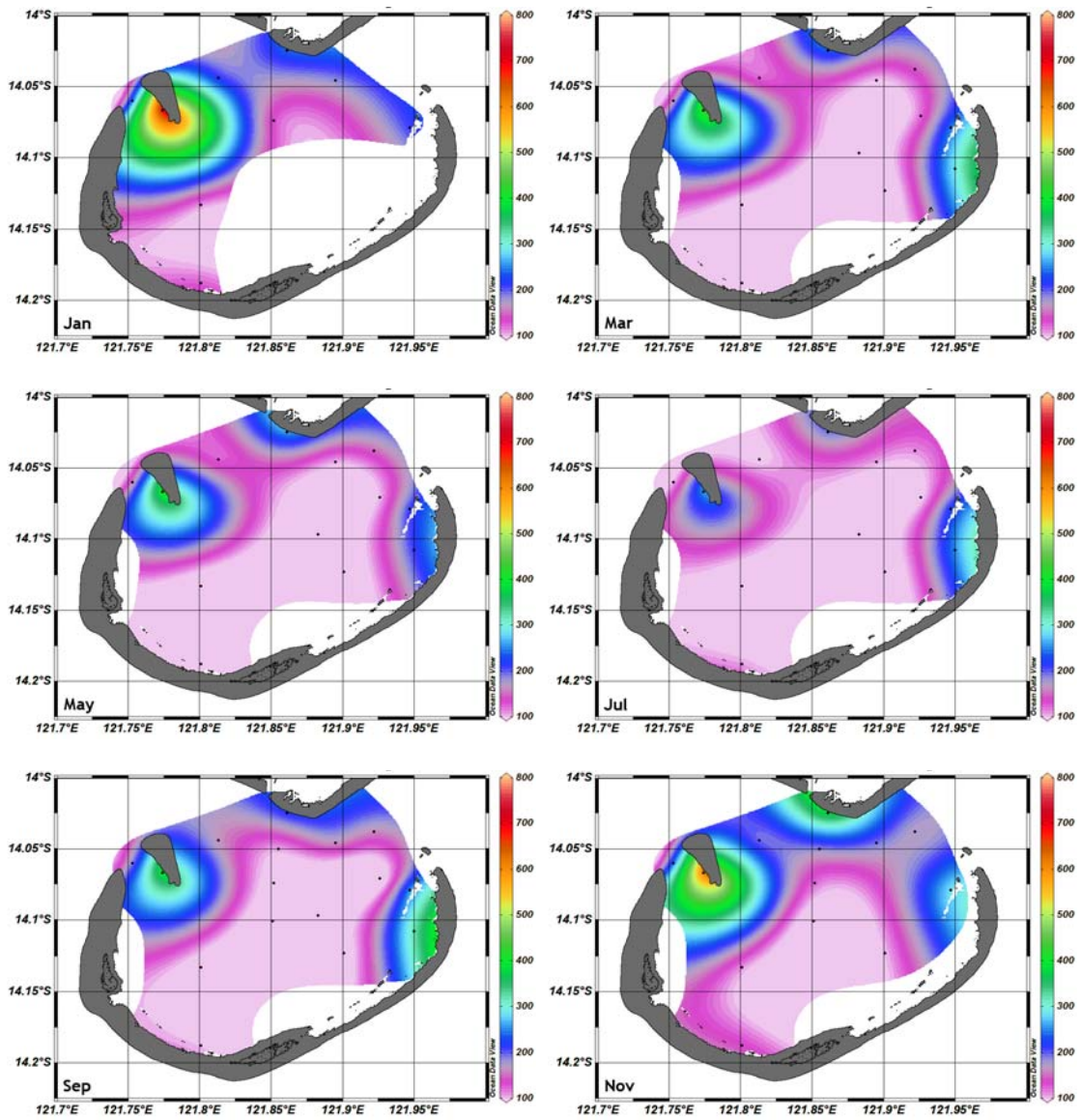


Fig. 34 Contoured maximum PAR at logger sites, shown as maximum PAR at each site within the designated month, showing only every second month from January. Depths of logger sites are given in Table I. Colour scale show PAR in units of $\text{mmol photons m}^{-2} \text{s}^{-1}$. Dots indicate logger sites.

Chlorophyll distributions

Daily average near-bottom chlorophyll fluorescence at in-situ logger sites in the interior of the lagoon ranged from 0.18 to 1.54 mg m⁻³, with slightly higher values observed at the shallow southern site (PE02). In general, chlorophyll fluorescence was higher within the interior of the lagoon compared to sites close to the channel along the northern margin of the lagoon (Fig. 35).

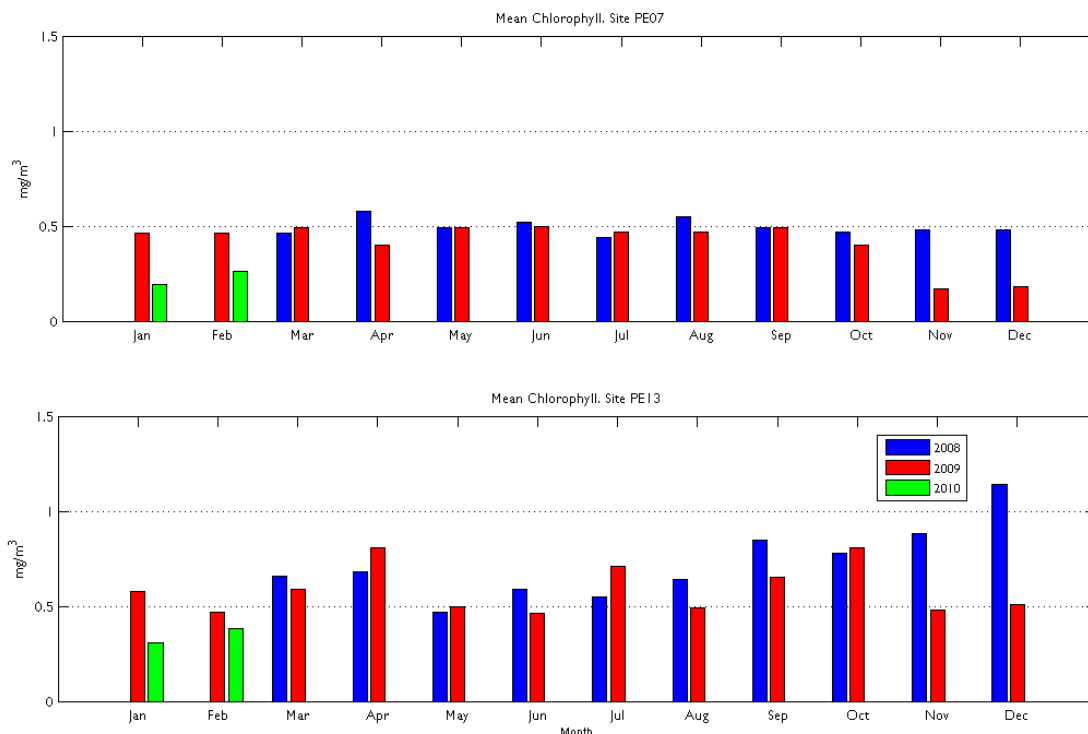


Fig. 35 Monthly average chlorophyll fluorescence at observational site PE07 adjacent to the channel (top) and site PE13 in the interior of the lagoon (bottom).

Higher chlorophyll concentrations within the interior of the lagoon, compared to locations along the northern margin of the lagoon were confirmed by a t-test analysis of chlorophyll time series along the northern margin of the lagoon, and sites within the lagoon (Table 5).

There is evidence that cool water intrusions over the sill during spring tides drive enhanced productivity at sites within the lagoon. During May – June 2009, there was a persistent near-bottom chlorophyll maximum layer observed (Fig. 25) that covered much of the central lagoon. This subsurface layer was not accompanied by cooler temperatures, indicating that the local water had been resident in the lagoon sufficiently long to mix with the surrounding water (see previous section on Temperature in the South Reef lagoon). The chlorophyll maximum within the lagoon was not continuous with a chlorophyll maximum in the adjacent deep channel (Fig. 25) suggesting that the enhanced chlorophyll was the result of local production. This observation was repeated during both biological oceanographic cruises in December 2008 and November 2009.

Concurrent time-series of temperature, chlorophyll and sea level at sites along a North-South transect into the interior of the South Reef lagoon (Fig. 36) show that following a strong intrusion event at the margin of the lagoon (site PE16), the intrusion propagates southwards and can be seen in the temperature time series at sites PE15 and PE14 within 24 hours. There is a decrease in the magnitude of cooling with distance into the lagoon and an increase in the time taken for temperature to return to the 'pre-cooling' conditions, presumably due to mixing of the intruded water. After a lag of 3 – 4 days following an intrusion observed at site PE15 (on 5 December 2008), there is an increase in the chlorophyll fluorescence at both sites PE15 and PE14. This increase in chlorophyll

fluorescence persists until a subsequent strong intrusion (ca 12 December 2008) presumably displaces the otherwise resident local water mass. We speculate that this enhanced chlorophyll fluorescence within the deeper section of the lagoon is indicative of enhanced production following the supply of new nutrients in to the lagoon. There is no obvious seasonality in chlorophyll fluorescence that is repeated between years of the observational study (Fig. 35). However, as we hypothesise that enhanced chlorophyll within the lagoon may be driven by nutrient enriched intrusions, it would follow that chlorophyll fluorescence should display a similar seasonality to the intrusion events, but this is not clearly evident in average chlorophyll fluorescence data. A discussion regarding the productivity of lagoon waters is given in the next section.

Table 5 Results of T-test analysis comparing chlorophyll fluorescence between sites along the northern margin of the lagoon and within the lagoon.

Month.Year	Mean Nth margin	Mean lagoon	p-value
Mar 2008	0.395	0.626	<2e-16
Apr 2008	0.434	0.503	<2e-16
May 2008	0.401	0.365	<2e-16
Jun 2008	0.423	0.393	<2e-16
Jul 2008	0.429	0.407	<2e-16
Aug 2008	0.460	0.449	<2e-16
Sep 2008	0.441	0.614	<2e-16
Oct 2008	0.354	0.677	<2e-16
Nov 2008	0.333	0.961	<2e-16
Dec 2008	0.275	0.904	<2e-16
Jan 2009	0.268	0.509	<2e-16
Feb 2009	0.367	0.409	<2e-16
Mar 2009	0.394	0.584	<2e-16
Apr 2009	0.352	0.623	<2e-16
May 2009	0.363	0.391	<2e-16
Jun 2009	0.386	0.312	<2e-16
Jul 2009	0.404	0.388	<2e-16
Aug 2009	0.415	0.350	<2e-16
Sep 2009	0.450	0.400	<2e-16
Oct 2009	0.351	0.537	<2e-16
Nov 2009	0.350	0.492	<2e-16
Dec 2009	0.316	0.515	<2e-16
Jan 2010	0.346	0.299	<2e-16
Feb 2010	0.364	0.302	<2e-16

Monthly aggregated daily statistics for chlorophyll fluorescence time series collected by in-situ loggers are presented in Appendix III (Table A 1). Note that these values are derived using the instrument supplied software and have not been calibrated against discrete samples.

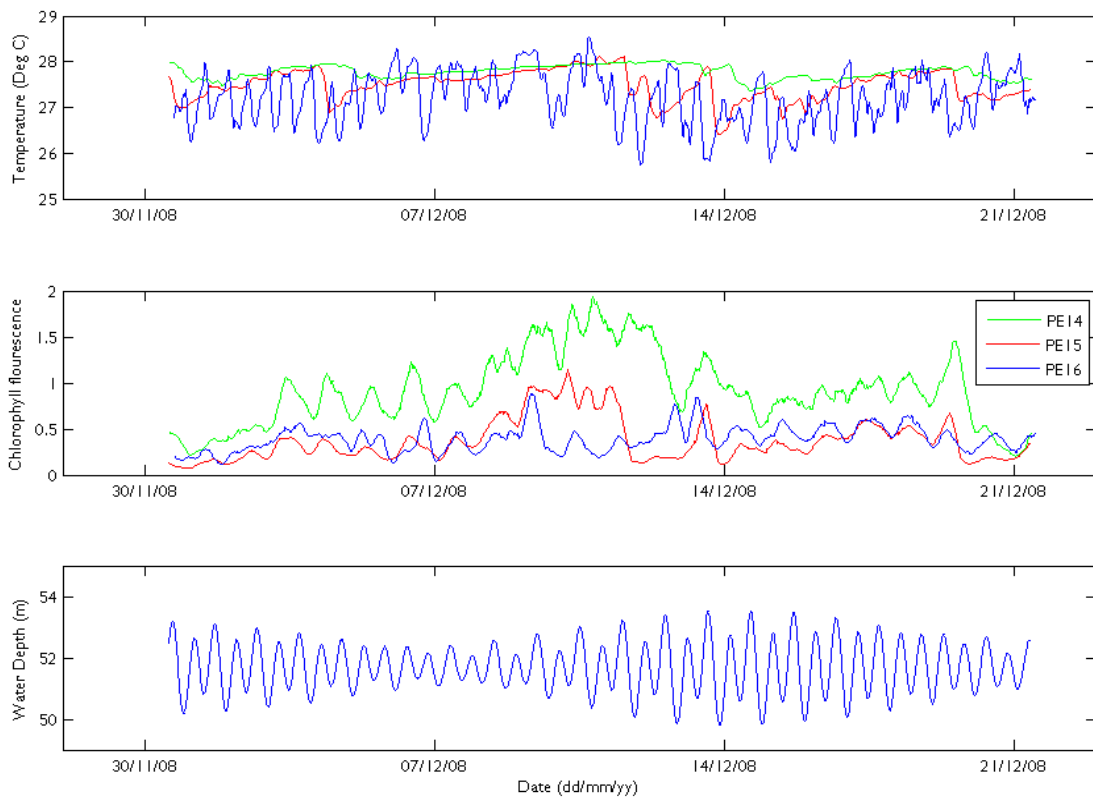


Fig. 36 Time series plots of temperature (top frame) and chlorophyll (middle frame) at sites PE14, PE15 and PE16, which lie along a North-South transect from the sill into the interior of the lagoon. Site PE14 is approximately 6 km south of site PE16. Sea level time series is shown in the bottom frame.

Water Quality

Water quality is the suitability of water for a particular purpose. In environmental or ecological studies, 'water quality' usually refers to the capacity of a water body to support a healthy, natural ecosystem or one with desirable attributes.

The dissolved nutrients which support phytoplankton and bacterial production occur in a variety of forms in seawater:

Ammonium (NH_4^+) – The preferred form of inorganic N as it is readily assimilated into amino acids and other biomolecules. Ammonium is the principal N form excreted by zooplankton. Concentrations are typically very low (10^{-8} – 10^{-9} moles L^{-1}) in surface seawater due to rapid uptake by phytoplankton and bacteria. Difficult to measure at ambient concentrations due to ready contamination of samples.

Nitrite (NO_2^-) – A transitional oxidational form between ammonium and nitrate produced by phytoplankton and bacteria. Usually only detectable at very low concentrations (10^{-8} – 10^{-9} moles L^{-1}) in a layer at the top of the thermocline.

Nitrate (NO_3^-) – The most stable and predominant form of inorganic N in deep oceanic waters. Concentrations range from 10^{-9} moles L^{-1} at the surface to 10^{-5} moles L^{-1} at depths > 1,000 m. Nitrate is energetically expensive to reduce to ammonium which can be assimilated into biomolecules.

DON: Nitrogen incorporated into dissolved organic molecules. Most DON-N is not immediately bioavailable to phytoplankton and bacteria as it is part of large and stable molecules. Some small organic molecules (urea, amino acids) can be taken up, but their concentrations are very low in tropical oceanic waters (10^{-8} – 10^{-9} moles L^{-1}).

Phosphate (PO_4^{3-}) – The predominant form of inorganic P in seawater. The most common form of P excreted by zooplankton. Concentrations typically range from 10^{-8} moles L^{-1} at the surface to 10^{-6} moles L^{-1} at depth.

DOP: Phosphorus incorporated into dissolved organic molecules. DOP-P is bioavailable to some phytoplankton and bacteria which excrete enzymes that break down the DOP to release PO_4^{3-} . Concentrations are very low in tropical oceanic waters (typically, 10^{-8} – 10^{-9} moles L^{-1}).

Silicate ($\text{Si}(\text{OH})_4$) – Silicic acid is required by diatoms to synthesise their hydrated silicate (opal) cell walls. Concentrations in tropical oceanic waters range from 10^{-6} moles L^{-1} at the surface to 10^{-4} moles L^{-1} at depths > 1,000 m.

Dissolved inorganic N and P concentrations in tropical surface waters are usually very low because nutrients assimilated by phytoplankton are gradually stripped from the surface layer through the sinking of detritus and zooplankton fecal pellets into the stable waters of the thermocline. While the biochemical composition of marine phytoplankton is influenced by a range of factors, including nutrient availability light and temperature, healthy, rapidly growing phytoplankton tend to converge on a canonical composition of C106:N16:P1 – the Redfield Ratio. Diatoms growing with sufficient nutrients typically have N:Si ratios close to 1. Dissolved inorganic N ($\text{NH}_4^+ + \text{NO}_2^- + \text{NO}_3^-$) and PO_4^{3-} concentrations in tropical oceanic surface waters typically have N:P ratios << 16. Dissolved N:Si concentrations are usually << 1, so that phytoplankton biomass is usually constrained by nitrogen availability.

Nutrients in Scott Reef waters

A variety of sampling and experimentation was carried out on each of the four biological oceanography cruises at the four time series sites. Particular emphasis was given to the South Reef lagoon and the deep channel between North and South Reefs. Upon arrival at each of the four time series sites, hydrographic casts were made every two hours for 26 hours to document diel changes in water column structure, nutrient levels and plankton biomass. During this period, four zooplankton net hauls were taken to document vertical distributions of mesozooplankton community composition and biomass. On the following day, a drifting sediment trap was deployed at the site, followed for 12 hours and retrieved at sunset. Productivity and community food-web experiments were undertaken in parallel with the trap deployment. As time permitted, hydrographic (CTD) surveys were carried out in the South Reef lagoon and deep channel to resolve spatial variability of hydrographic and optical properties of lagoon waters.

The waters around Scott Reef are extremely oligotrophic (low nutrient – low biomass) in character. The low nutrient levels in the mixed layer can support relatively small standing crops of plankton biomass. Water samples were collected through the water column to 200 m several times at all of

the experimental sites on each of the cruises. This was to define vertical distributions and variability of all major nutrient species in the biologically productive surface layers and their relationships to vertical phytoplankton biomass and hydrographic structure in the euphotic zone (in situ irradiance > 0.1 percent of surface irradiance).

Representative vertical profiles of temperature, chlorophyll (Chl) and major nutrient species: nitrite (NO_2^-), nitrate (NO_3^-), dissolved and particulate organic nitrogen (DON, PN), phosphate (PO_4^{3-}), dissolved and particulate organic phosphorus (DOP, PP), silicate ($\text{Si}(\text{OH})_4$), and dissolved and particulate organic carbon (DOC, POC) are presented in Fig. 37 and Fig. 38. Profiles of individual nutrients exhibited consistent patterns in the lagoon or upper 200 m, with small offsets between individual profiles or cruises. When normalised to a constant surface value, the similarities between mean profiles of individual nutrient species are readily seen.

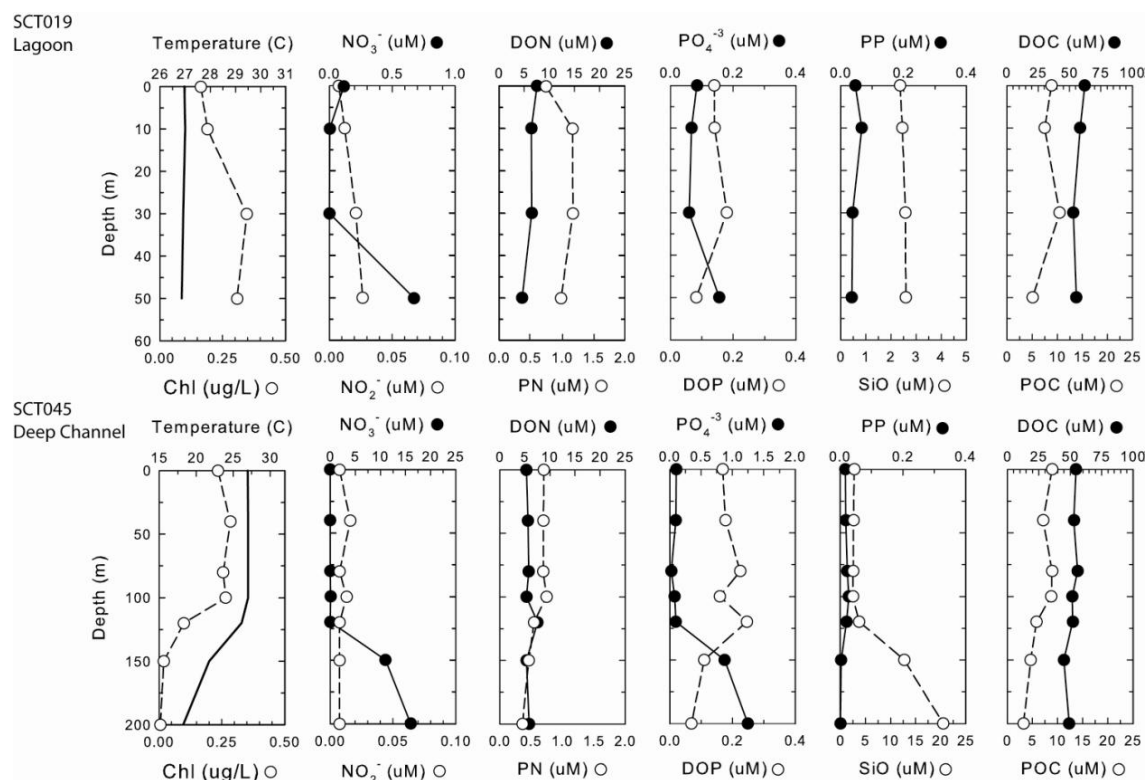


Fig. 37 Representative profiles of temperature, chlorophyll, NO_3^- , NO_2^- , DON, PN, PO_4^{3-} , DOP, PP, $\text{Si}(\text{OH})_4$, DOC, and POC in the central region of South Reef lagoon (LA, top panel) and the deep channel between North and South Reef (CH, bottom panel).

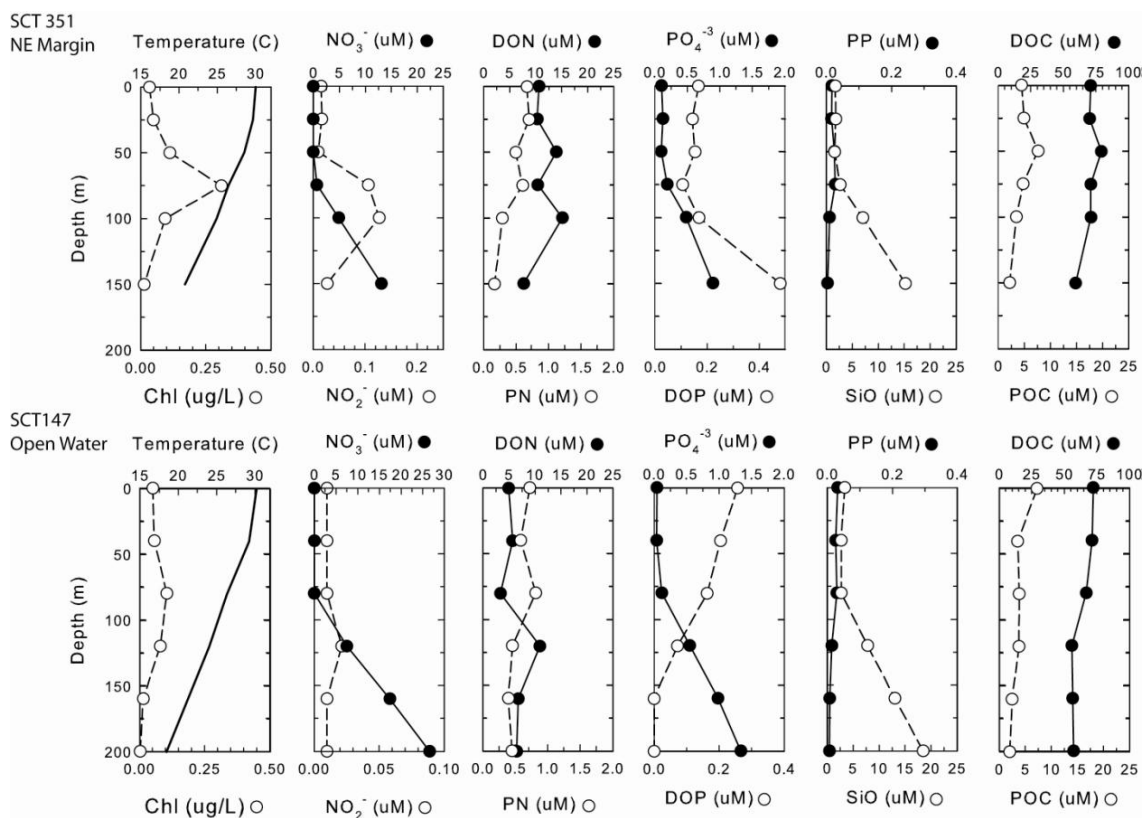


Fig. 38 Representative profiles of temperature, chlorophyll, NO_3^- , NO_2^- , DON, PON, PO_4^{3-} , DOP, PP, $\text{Si}(\text{OH})_4$, DOC, and POC at deep-water sites bordering the NE margin of North Reef (NE, top panel) and at an open water site southwest of Scott Reef (SW, bottom panel).

Mixed layer concentrations of dissolved inorganic nitrogen (NH_4^+ , NO_2^- , NO_3^-) and phosphorus (PO_4^{3-}) were very low at all three deep-water experimental sites. Within the South Reef lagoon, the upper water column (0 – 30 m) was also characterised by very low nitrate and phosphate concentrations at all times. Nitrate concentrations, in particular, were near or below detection limits ($< 0.02 \mu\text{M}$). Slightly elevated nitrite concentrations ($< 0.2 \mu\text{M}$) were consistently measured in samples collected in the upper thermocline. These mid-water nitrite maximum is a consistent feature of oceanic waters and is related to in-situ nitrification/nitrate reduction by bacteria and phytoplankton under low-light conditions in the nutricline. Ammonium concentrations have not been measured at Scott Reef with appropriate high sensitivity, low contamination methods (Holmes et al., 1999), but given the oligotrophic conditions which prevailed, it is almost certain that ambient NH_4^+ concentrations are also very low ($< 0.05 \mu\text{M}$). While very low, phosphate was consistently measurable in surface layer waters at all four sites (ca. $0.05 - 0.20 \mu\text{M}$). In contrast, near-surface silicate concentrations were generally on the order of $2 - 3 \mu\text{M}$, approximately 1 – 2 orders of magnitude more abundant than inorganic N and P. The dominant phytoplankton in Scott Reef waters, very small ($< 2 \mu\text{m}$) cyanobacteria and eukaryotes, do not require silicate as a nutrient. The observed concentration ranges and ratios of dissolved inorganic nutrients indicate that surface waters surrounding Scott Reef are most likely strongly N-limited ($\text{DIN:DIP} < 16$, $\text{DIN:Si} \ll 1$), with phytoplankton and bacterial demand for N and P being primarily met through rapid and continuous water column remineralisation of organic N and P. These conditions are typical of oligotrophic oceanic waters.

However, slightly elevated ($0.1 - 0.2 \mu\text{M}$) nitrate, and to a lesser extent, phosphate concentrations were consistently measured in near-bottom samples from the mid-lagoon site. These elevated concentrations were not associated with obvious layers of cool thermocline waters, but a variety of

evidence suggests that water from the upper thermocline in the deep channel does intrude laterally into the lagoon (e.g. temperature time series from bottom-mounted instruments, salinity differences between lagoon and surrounding waters).

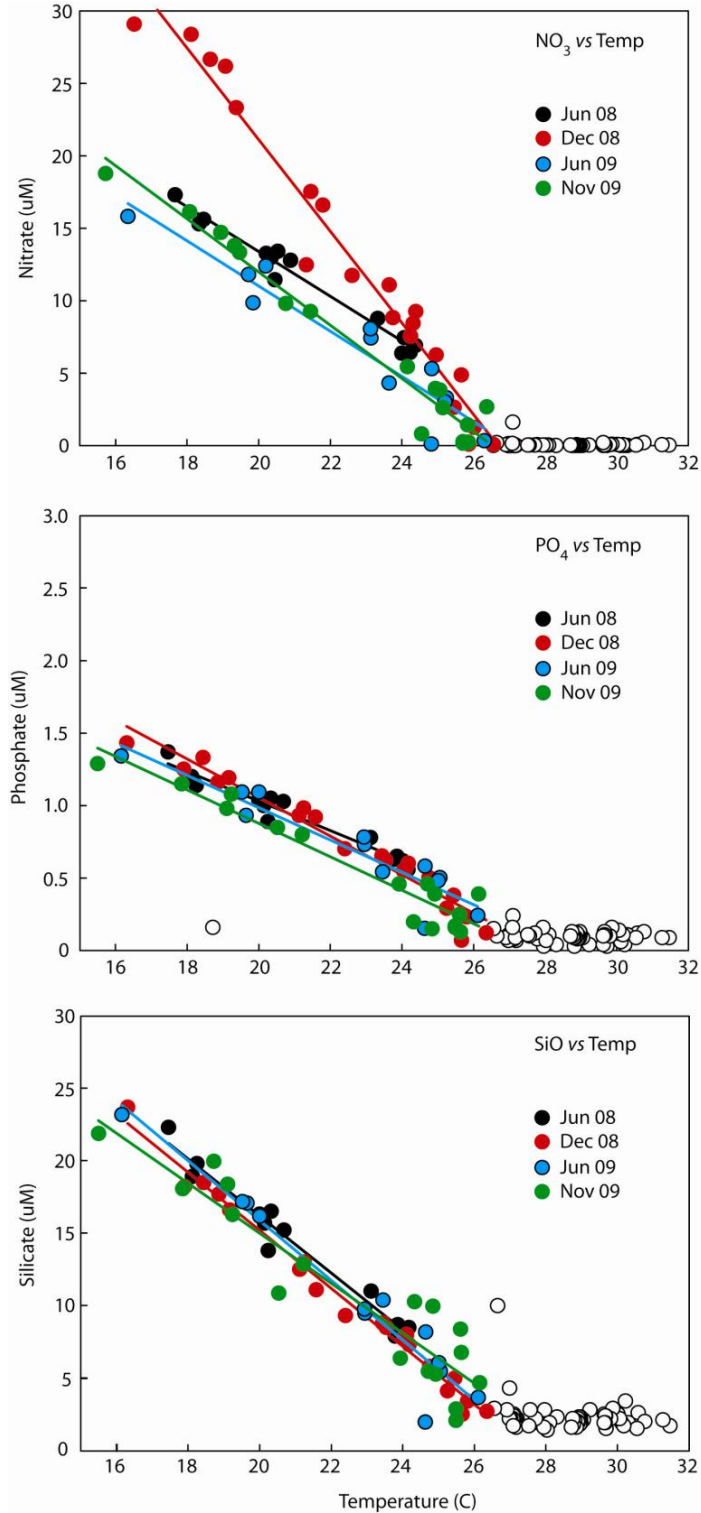


Fig. 39 Plots of relationships between temperature and concentrations of NO_3^- (top), PO_4^{3-} (middle), Si(OH)_4 (bottom) in samples collected at the Open Water site (SW). Regression lines shown are derived for data collected below the mixed layer and upper margin of the thermocline (temperature

< 26.5°C). Obvious outlier values were also excluded from the calculation. Regression coefficients are given in Table 6.

From the top of the thermocline downward, concentrations of nitrate, phosphate and silicate increased steadily with depth and decreasing temperature. Plots of nitrate, phosphate and silicate concentrations versus temperature were strongly linear for temperatures < 26.5 °C (Fig. 39), indicating that nutrient concentration gradients within the thermocline are largely determined by physical mixing between nutrient depleted surface waters and high-nutrient deep waters. Table 6 presents the equations relating nutrient concentrations to temperature in the thermocline. The strength of these relationships indicate that temperature can be used as a proxy tracer for nutrient concentration in the upper thermocline and freshly intruded water masses in the lagoon before biological uptake get strongly underway. Both phosphate and silicate exhibited little or no between-cruise variability in their concentration and temperature relationships. In contrast, the nitrate-temperature relationship for the December 2008 cruise differed significantly from the very similar relationships observed on the other three cruises. A similar degree of difference from other cruises was not observed in the T/S relationships.

Table 6 Regression equations for nutrient-temperature relationships shown in Fig. 39. Regressions are based on samples collected at the Open Water site (SW) at depth with temperatures < 26.5°C.

Cruise Dates	Regression Equations	R ²
June 2008	$[\text{NO}_3] = -1.54 (T^\circ\text{C}) + 43.8$	0.971
December 2008	$[\text{NO}_3] = -3.16 (T^\circ\text{C}) + 83.5$	0.966
June 2009	$[\text{NO}_3] = -1.56 (T^\circ\text{C}) + 41.8$	0.897
November 2009	$[\text{NO}_3] = -1.83 (T^\circ\text{C}) + 48.2$	0.962
June 2008	$[\text{PO}_4] = -0.102 (T^\circ\text{C}) + 3.07$	0.949
December 2008	$[\text{PO}_4] = -0.133 (T^\circ\text{C}) + 3.72$	0.956
June 2009	$[\text{PO}_4] = -0.111 (T^\circ\text{C}) + 3.21$	0.873
Nov-Dec'09	$[\text{PO}_4] = -0.115 (T^\circ\text{C}) + 3.18$	0.924
June 2008	$[\text{SiO}] = -1.97 (T^\circ\text{C}) + 55.6$	0.969
December 2008	$[\text{SiO}] = -2.00 (T^\circ\text{C}) + 55.2$	0.985
June 2009	$[\text{SiO}] = -2.06 (T^\circ\text{C}) + 57.2$	0.941
November 2009	$[\text{SiO}] = -1.72 (T^\circ\text{C}) + 49.5$	0.875

Dissolved organic carbon (DOC) concentrations in South Reef lagoon waters ranged between ca. 40 and 80 $\mu\text{M C}$, with no persistent vertical structure or seasonal variation. Due to sample contamination problems, no DOC data is presented from the June 2009 cruise. At deep water sites, DOC concentrations ranged from ca. 40 to ca. 120 μM , generally with higher concentrations (ca. 60 – 70 μM) at the surface, declining to 30 – 50 μM at 200 m. This persistent vertical gradient in DOC concentration indicates that DOC is continuously being produced in the surface layer through excretion by phytoplankton, phytoplankton cell lysis and sloppy feeding by grazers, and then being mixed downward from the surface layer into the thermocline to support bacterial consumption and respiration. A similar, but much less pronounced vertical gradient in particulate organic carbon (POC) concentrations was also observed, indicating production of POC near the surface and consumption at depth.

Vertical distributions of DOP, PN and PP exhibited no pronounced seasonal or depth-related distribution patterns. POC, PN and PP concentrations were poorly correlated with chlorophyll, indicating that most particulate organic matter in the water column is detrital in nature.

Principal components analysis of water chemistry

Water chemistry data from all time-series stations, as well as those occupied during the deployment and retrieval of the sediment traps, were subjected to a Principal Components Analysis (PCA) to establish the relationships between water quality, site, depth and season (i.e. cruise), at the four Biological Oceanography sites.

The PCA (Fig. 40) accounted for a total of 63% of the variance in water chemistry. The first principal component (PC1) accounted for 51% of the variance, and contrasted the effects of depth and temperature (Fig. 40a). These gradients may be seen in Fig. 37 – Fig. 39 (nutrient profile figures). Water samples were distributed according to strong gradients in nutrient concentration and temperature corresponding to the depth of their collection. Surface samples had low scores on PC1, and samples from depths >100 m the highest. The high positive scores were determined by the higher concentration of inorganic nutrients (NO_3^- , DIP, Si) from sub-thermocline waters. Conversely, negative scores were determined by proximity to the surface, where temperature, chlorophyll and concentrations of particulate nutrients (the main source of which is organic matter) were highest.

The second principal component (PC2) accounts for 11% of variance, and primarily discriminates the influence of cruise, with the June 2008 cruise having the highest scores, the November 2009 cruise the lowest, and the remaining two cruises having intermediate but similar scores (Fig. 40b). The main forcing on this component is from the combined effects of DOC, TSS and to a lesser extent, NO_2^- , all of which were lowest June 2008 and highest in November 2009. The December 2008 and June 2009 cruises were intermediate. The reasons for these patterns are unclear. Depth (Fig. 40a) and cruise (Fig. 40b) had the strongest influence on water chemistry, with location (Fig. 40c) having comparatively weak effects. The PCA indicates that there is little difference in nutrient chemistry within the mixed layer at any location, though temperature and particulate organic material (as indicated by chlorophyll, POC, PN and PP) are very slightly higher at the Lagoon site (LA).

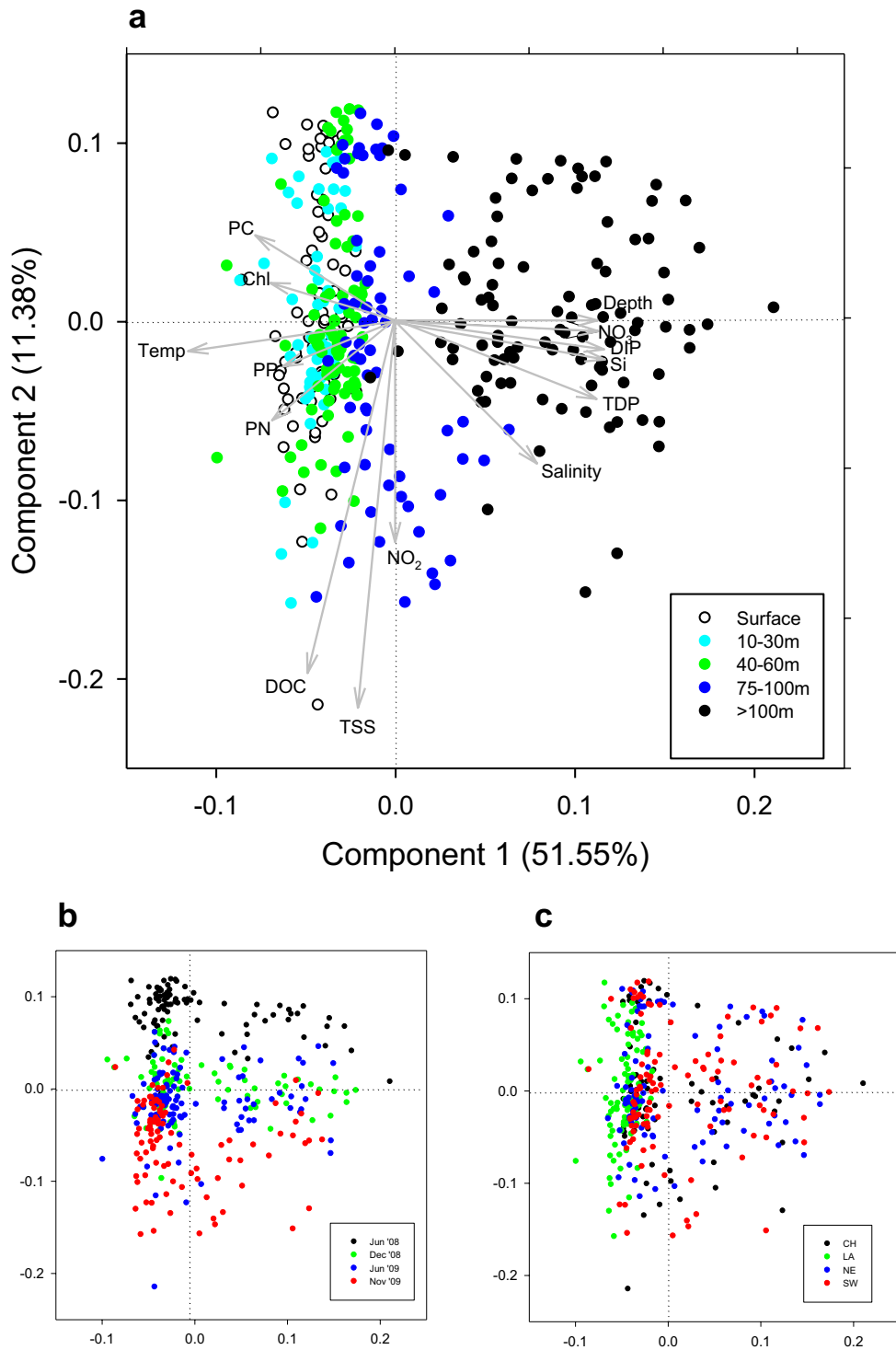


Fig. 40 Principal Components Analysis of water chemistry data. a) labelled by depth stratum, with the loading of nutrient species shown as vectors; b) labelled by cruise; c) labelled by location.

Plankton

Plankton is a generic term describing organisms that have limited locomotive ability relative to the water bodies in which they live. A wide range of organisms live in the plankton (Table below), ranging in size from viruses (femtoplankton) to large jellyfish (megazooplankton). Tropical plankton communities are highly diverse, containing organisms from almost all phyla.

The most common way to classify planktonic organisms is on the basis of size, which affects sinking, light utilisation, mobility and trophic status. Organisms with particular functional roles in the ecosystem (eg grazers and nitrogen fixers) occur in a number of size classes, though in general (viruses aside) primary producers tend to be smaller than grazers, which tend to be smaller than predators.

Phytoplankton are marine plants and photosynthetic bacteria that contribute half of global primary production, fixing an estimated 10^8 tons of carbon daily. The smallest size class of phytoplankton, the picoplankton (Table below) are the most important plants in the world in terms of the amount of carbon fixed. Each millilitre of seawater contains 10 million of these cells. Picoplankton are primarily grazed by micro-organisms only marginally larger than they are, but also suffer huge mortality from viruses. One millilitre of seawater can contain one million viruses, which infect picoplankton and cause their cell contents to be converted into viral particles, and subsequently for their cell walls to break, resulting in the loss of the cell contents to the water column.

Primary production refers to the amount of carbon fixed as a result of photosynthesis, and is expressed as a rate measurement; for phytoplankton this is usually $\text{mg Carbon m}^{-2} \text{d}^{-1}$. Regionally, primary production sets the upper bound for production at higher trophic levels and defines ecosystem carrying capacity.

Zooplankton are the animal component of the plankton. Small planktonic crustaceans, typically around 1mm in size, dominate zooplankton samples collected with plankton nets. These animals, called copepods, can be thought of as the insects of the sea and are the most abundant multicellular animals on earth. There are about 30,000 in each cubic metre of seawater. Copepods play a major role in nutrient cycling in the ocean and are the vital trophic link between the plants of the sea (phytoplankton) and larval fishes.

Size Class	Size Range	Representative Organisms	Functional Groupings
Femtoplankton	<0.2 μm	Viruses	Parasites
Picoplankton	0.2 – 2 μm	Archea, bacteria, cyanobacteria (eg <i>Synechococcus</i>), Prochlorophytes (eg <i>Prochlorococcus</i>)	Primary producers, saprophytic heterotrophs, nitrogen-fixers
Nanoplankton	2 – 20 μm	Cyanobacteria, diatoms, flagellates	Primary producers, grazers, predators, nitrogen-fixers
Microplankton	20 – 200 μm	Ciliates, coccolithophores, diatoms, dinoflagellates	Primary producers, grazers, predators
Mesoplankton	0.2 – 20 mm	Cyanobacteria (eg <i>Trichodesmium</i> colonies), pelagic tunicates (larvaceans, doliolids and salps), chaetognaths, copepods.	Primary producers, grazers, predators, nitrogen-fixers
Macroplankton	20 – 200 mm	Jellyfish, salps, pelagic molluscs, euphausiids, mysids, larval fish.	Grazers, predators
Megaplankton	> 200 mm	Jellyfish, Colonial salps	Grazers, predators, primary producers

Size classes of plankton in aquatic systems (from McKinnon et al., 2007).

Phytoplankton of Scott Reef waters

Abundance and distribution of picoplankton at Scott Reef

Plankton are classified into ecologically useful functional groups in a variety of ways in order to understand how natural communities are organised and function. Organism size is one widely used classification approach as cell or organism size influences many physical properties and ecological processes affecting plankton including: sinking rate, nutrient acquisition, light absorption, growth rate, and who is likely to eat you. The picoplankton are defined as the size class of organisms smaller than 2 μm . Primary producers within this size class include a diverse assemblage of photoautotrophic unicellular algae and bacteria which derive their energy from oxygenic photosynthesis. This assemblage is primarily composed of unicellular cyanobacteria (chiefly *Prochlorococcus* spp. $\sim 0.6 \mu\text{m}$ and *Synechococcus* spp. $\sim 1 \mu\text{m}$), with lesser numbers of very small photosynthetic eukaryotes (cells 1-2 μm in size from a number of microalgal classes with a more complicated cellular structure, also termed 'picoeukaryotes'). In oligotrophic waters such as those surrounding Scott Reef, autotrophic picoplankton overwhelmingly dominate the phytoplankton biomass ($\sim 80\%$ of total chlorophyll *a* biomass) and commonly account for $> 60\%$ of primary production.

The heterotrophic picoplankton assemblage is overwhelmingly dominated by bacteria and Archaea from a huge diversity of lineages (collectively termed 'bacterioplankton'), as well as smaller numbers of very small non-pigmented eukaryotic flagellates. Pelagic bacteria are the major consumers of organic matter (much of which is produced by the autotrophic picoplankton community via photosynthesis) in the water column and therefore play a fundamental role in the remineralisation and cycling of organic matter, nutrients and energy through marine food webs. Unlike the autotrophic picoplankton, which are restricted to the photic zone due to their dependence on light, heterotrophic bacteria live throughout the full water column.

The autotrophic picoplankton and heterotrophic bacterioplankton communities are primarily preyed upon by very small (nano-) flagellates and ciliates, most of which are $< 5 \mu\text{m}$ in size. Viruses, which are the smallest and most abundant organisms in marine waters (nominally $< 0.01 \mu\text{m}$, and referred to as the 'femtoplankton'), are pathogens of both autotrophic and heterotrophic picoplankton. Viral infection and lysis of infected cells is a major source of the dissolved and non-living organic matter which supports heterotrophic picoplankton. Most of the primary and secondary productivity of the picoplankton is consumed and recycled within a largely closed 'microbial loop' comprised of photosynthetic picoplankton, nanoflagellates and viruses. Consumption and leakage of organic matter from the microbial loop ultimately drives much of the pelagic ecosystem in oligotrophic tropical waters (i.e. the classical grazing food chain = phytoplankton to zooplankton to fish). In this way, grazing and viral infection processes not only influence the composition of microbial communities but are considered as significant drivers in biogeochemical cycles in the ocean.

The distribution of autotrophic picoplankton in Scott Reef Waters

Three groups of autotrophic picoplankton were discerned at all stations using flow cytometry: *Prochlorococcus* spp., *Synechococcus* spp. and a heterogeneous assemblage of picoeukaryotes (Fig. 41). For simplicity, the multi-strain assemblages of *Prochlorococcus* and *Synechococcus* will be treated as single entities herein. *Prochlorococcus* and picoeukaryotes were found in all samples collected through the full depth of the photic zone (depths $< 1\%$ surface light; June 2008 down to $\sim 150 \text{ m}$, December 2008/June 2009 down to $\sim 120 \text{ m}$ and November 2009 down to $\sim 150 \text{ m}$). In contrast, *Synechococcus* was limited to the upper 80 m of the water column, which corresponded with light levels of $\geq 1\%$ of surface light (Fig. 42). *Prochlorococcus* dominated autotrophic picoplankton cell abundances at all of the deep water stations, generally exceeding *Synechococcus* and picoeukaryote abundances by 1 to 3 orders of magnitude. In the South Reef lagoon, however, abundances of *Prochlorococcus* and *Synechococcus* were similar (Fig. 42). *Synechococcus* abundances further exceeded abundances of picoeukaryotes by 1 to 2 orders of magnitude and like *Synechococcus*, highest abundances of picoeukaryotes occurred in lagoon waters (Fig. 42).

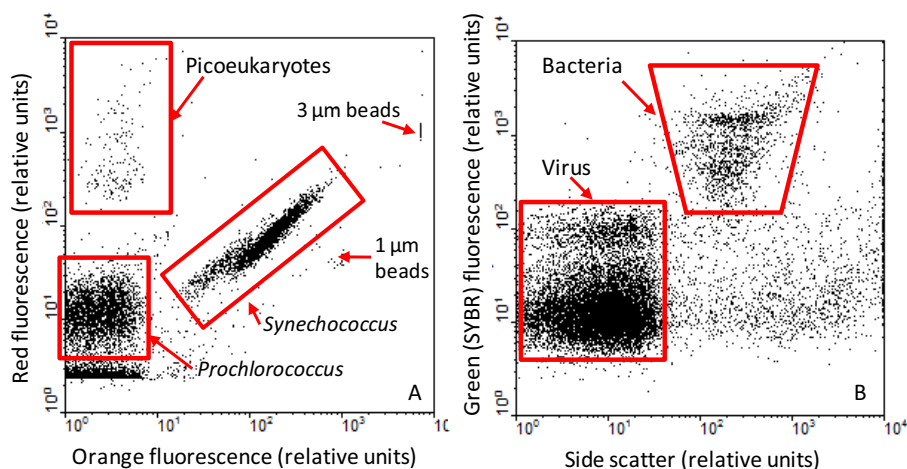


Fig. 41 Dot plots from flow cytometric analysis of seawater samples showing (A) groups of autotrophic (photosynthesising) picoplankton and (B) Bacterioplankton and viruses. (A) Auto-fluorescing autotrophic (photosynthesising) picoplankton with individual groups represented by *Prochlorococcus*, *Synechococcus* and picoeukaryotes. Vertical (y) and horizontal (x) axes (log scales) are relative levels of blue-light (488 nm) stimulated red (>640 nm) and orange (560 nm) fluorescence due to individual cellular concentrations of the pigments chlorophyll and phycoerythrin respectively. Cellular pigment levels are primarily related to cell size and degrees of physiological adaptation to in-situ light levels. Fluorescing 1 μm and 3 μm beads were added to samples as an internal reference to compare the relative fluorescence intensity and size of individual groups between samples. (B) Bacterioplankton and viruses. Vertical (y) axis (log scale) represents relative levels of blue-light (488 nm) stimulated green (500 nm) fluorescence due to the added DNA stain (SYBR Green) and the horizontal (x) axis (log scale) represents side scatter, an indicator of cell size and complexity.

Temporal and spatial variation of autotrophic picoplankton

All three groups of autotrophic picoplankton exhibited discernable differences in abundance between sampling cruises and between sampling locations around Scott Reef (Fig. 42, Table 7). Overall, the highest abundances of autotrophic picoplankton cells were measured on the first biological oceanography cruise in June 2008 (Fig. 42, Table 7). On that cruise, the depth-weighted average abundance of *Synechococcus* (100 m for deep sites, 50 m for the lagoon site) was 5 – 9 times higher, and for picoeukaryotes 3 – 6 times higher than on the following three cruises (December 2008, June 2009 or November 2009; Table 7). The same trend occurred for *Prochlorococcus* at deep water sites, with June 2008 abundances 3 – 7 times higher than in December 2008. In the lagoon, in contrast, the highest *Prochlorococcus* abundances occurred in November 2009 (Table 7). Reasons for the elevated picoplankton abundances in June 2008 are not resolved at this time. The elevated picoplankton abundances coincided with higher chlorophyll *a* biomass; particularly in the lagoon and Channel between North and South Reefs (Fig. 27). There were strong winds at Scott Reef immediately prior to the June 2008 sampling. It is likely that weather driven mixing of the water column may have led to an increase in nutrient availability to picoplankton.

There was a general inverse relationship between abundances of *Prochlorococcus* and *Synechococcus* (Table 7). The shifts between *Prochlorococcus* and *Synechococcus* can be seen in the ratio of *Prochlorococcus* to *Synechococcus* (Pro:Syn). Low Pro:Syn reflects water bodies with high nutrient status while high Pro:Syn are indicative of oligotrophic oceanic conditions. Due to comparatively low *Prochlorococcus* compared to high *Synechococcus* abundances, lowest Pro:Syn (< 1) always occurred in lagoon waters. Overall lowest Pro:Syn occurred in June 2008, further reflecting the comparatively higher abundances of *Synechococcus* at this time. Highest Pro:Syn ratios generally occurred in the Channel (Pro:Syn = 20 – 85) followed by the Open water site (Pro:Syn = 10 – 20). Similar to *Synechococcus*, highest picoeukaryote abundances occurred in June 2008 (Fig. 42, Table 7). Also

similar to *Synechococcus*, picoeukaryote abundances were always highest in the lagoon compared to any other site in a given season.

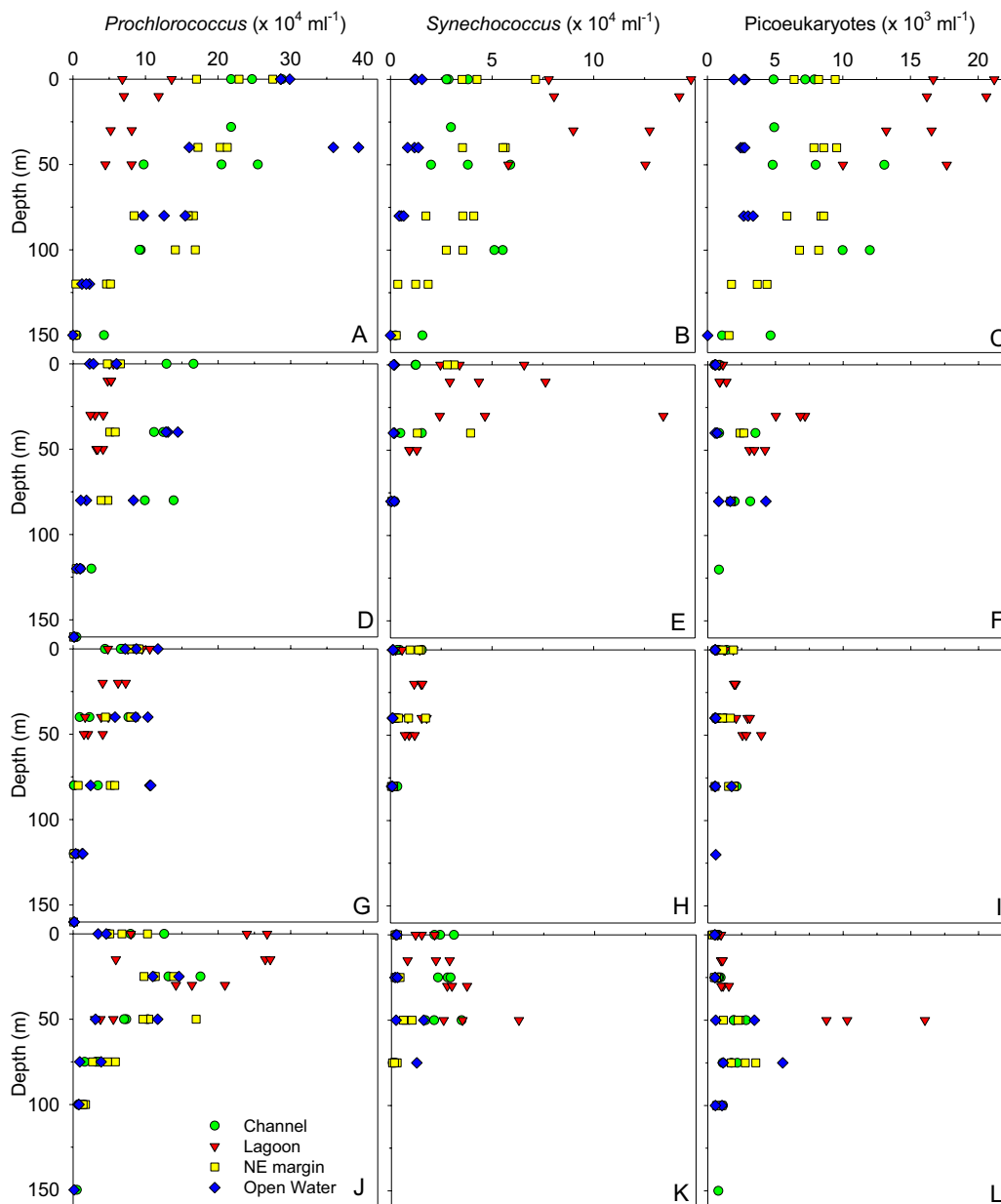


Fig. 42 Abundances of autotrophic picoplankton (*Prochlorococcus*, *Synechococcus* and Picoeukaryotes) at Scott Reef in June 2008 (A – C), December 2008 (D – F), June 2009 (G – I) and November 2009 (J – L). Data in these plots represent the combined time series data (two or three sampling periods per day, sampled at ~ 08:00, 14:00 and 20:00) for each of the four biological oceanography sites (Lagoon, Deep Channel, NE margin and Open Water). Values are means of duplicate or triplicate samples.

Table 7 Depth weighted average (DWA^a) and integrated (Int^b) abundances of *Prochlorococcus* (Pro), *Synechococcus* (Syn), Picoeukaryotes (Peuk), Bacteria (Bac) and Viruses (Vir) at Lagoon (LA), Channel (CH), NE margin (NE) and Open water (SW) sites at Scott Reef during June 2008, December 2008, June 2009, December 2009. Values are means \pm SD (1). ns indicates no samples were taken during this time for bacteria or viruses because of logistical constraints.

Season	Site	DWA Pro $\times 10^4$ cells ml ⁻¹	DWA Syn	DWA Peuk	DWA Bac	DWA Vir	Int Pro $\times 10^{10}$ cells m ²	Int Syn	Int Peuk	Int Bac	Int Vir
June 2008	LA	7.2 \pm 2.2	9.2 \pm 3.7	1.3 \pm 0.6	ns	ns	353 \pm 117	451 \pm 195	65 \pm 29	ns	ns
	CH	17.5 \pm 0.8	3.9 \pm 1.3	0.8 \pm 0.3	ns	ns	1748 \pm 447	391 \pm 126	83 \pm 32	ns	ns
	NE	19.6 \pm 2.5	4.3 \pm 0.6	0.8 \pm 0.1	ns	ns	1784 \pm 184	390 \pm 54	72 \pm 12	ns	ns
	SW	25.0 \pm 5.9	1.0 \pm 0.2	0.3 \pm 0.0	ns	ns	2030 \pm 458	84 \pm 13	22 \pm 2	ns	ns
December 2008	LA	4.0 \pm 0.8	4.1 \pm 1.9	0.3 \pm 0.1	52 \pm 8.0	482 \pm 59	202 \pm 41	204 \pm 97	15 \pm 5	2617 \pm 402	24147 \pm 2956
	CH	12.9 \pm 1.4	0.7 \pm 0.4	0.2 \pm 0.1	56 \pm 4.4	482 \pm 53	1137 \pm 251	63 \pm 25	13 \pm 8	5470 \pm 1096	45345 \pm 2615
	NE	6.5 \pm 2.2	1.7 \pm 0.9	0.2 \pm 0.0	39 \pm 15.6	344 \pm 124	582 \pm 288	146 \pm 60	15 \pm 1	3564 \pm 1758	25519 \pm 20826
	SW	8.7 \pm 0.9	0.2 \pm 0.0	0.1 \pm 0.0	61 \pm 3.1	520 \pm 77	706 \pm 151	13 \pm 1	8 \pm 4	5233 \pm 866	35944 \pm 21408
June 2009	LA	4.8 \pm 1.7	1.4 \pm 0.6	0.3 \pm 0.1	41 \pm 3.9	401 \pm 126	244 \pm 88	72 \pm 31	14 \pm 7	2105 \pm 220	20187 \pm 6177
	CH	4.9 \pm 1.1	0.6 \pm 0.4	0.1 \pm 0.0	51 \pm 5.8	409 \pm 219	420 \pm 89	53 \pm 34	9 \pm 4	4411 \pm 412	34598 \pm 16797
	NE	6.1 \pm 1.9	0.8 \pm 0.3	0.1 \pm 0.0	42 \pm 9.7	226 \pm 57	510 \pm 129	63 \pm 25	10 \pm 2	3639 \pm 904	18936 \pm 3553
	SW	9.0 \pm 2.5	0.10 \pm 0.0	0.1 \pm 0.0	46 \pm 7.4	355 \pm 143	770 \pm 268	9 \pm 1	5 \pm 1	2940 \pm 1754	30171 \pm 11706
November 2009	LA	14.4 \pm 4.5	4.3 \pm 2.2	0.3 \pm 0.1	51 \pm 7.1	351 \pm 77	721 \pm 225	215 \pm 108	16 \pm 4	2569 \pm 357	17562 \pm 3848
	CH	7.6 \pm 1.0	1.9 \pm 0.6	0.1 \pm 0.0	56 \pm 11.8	338 \pm 164	717 \pm 103	175 \pm 41	14 \pm 2	5444 \pm 1557	32640 \pm 17628
	NE	8.3 \pm 0.4	0.5 \pm 0.2	0.1 \pm 0.0	37 \pm 2.2	201 \pm 108	841 \pm 58	46 \pm 26	15 \pm 2	3812 \pm 339	30519 \pm 10389
	SW	7.5 \pm 3.0	0.6 \pm 0.2	0.1 \pm 0.0	47 \pm 2.8	263 \pm 168	700 \pm 237	55 \pm 13	14 \pm 5	4445 \pm 203	23972 \pm 13170

^a Integrated abundances (= total abundance per unit area) were calculated by trapezoidal integration of abundances at discrete depths over the depth profile

^b Depth-weighted average = the integrated abundance in a profile divided by the profile depth

Abundances of autotrophic picoplankton varied over a 24-hour diel cycle at all time series sites. The magnitude of diel cycles was generally much smaller, however, than the differences between sites or seasons (Fig. 42). In vertical profiles, the greatest changes in picoplankton abundance usually occurred in the subsurface chlorophyll a maximum layer (Fig. 42). Over a daily cycle, the highest abundances of *Prochlorococcus* and *Synechococcus* commonly occurred early in the night (20:00 local time) and usually coincided with diel peaks in chlorophyll a fluorescence (Fig. 8) suggesting cell division occurred in the late afternoon or shortly thereafter. These results are in accordance with previous studies which have shown that cell division of *Prochlorococcus* and *Synechococcus* in other oceanic locations occurs predominantly at night (Vaulot and Marie, 1999; Worden and Binder, 2003).

Bacterioplankton and viruses in Scott Reef waters

Bacterioplankton and viruses in water samples were counted by flow cytometry after staining with the DNA stain SYBR Green (Fig. 41). Bacterioplankton abundances exceeded *Prochlorococcus* abundances by approximately 1 order of magnitude (Table 7). The highest bacterioplankton abundances generally occurred in the upper 100 m of the water column, except during the November 2009 cruise, when relatively high abundances were observed to depths of 150 m (Fig. 43). In contrast to autotrophic picoplankton which were largely limited to depths less than 160 m (Fig. 42), significant numbers of bacterioplankton were found to depths of 300 m (the deepest measurement made at set sites; Fig. 43).

Viral abundances were one order of magnitude higher than bacterioplankton abundances for all investigated sites (Fig. 43, Table 7) and similar to bacterioplankton were present in high numbers down to 300 m.

Temporal and spatial variation of bacterioplankton and viruses

The variation in bacterioplankton and virus abundances between sites and seasons was smaller than the variation observed for autotrophic picoplankton (Fig. 43, Table 7). Bacterioplankton abundances at similar depths varied at most ~2-fold between sites with the highest depth-weighted average abundances generally at the Open Water or Deep Channel sites. There were no clear diel cycles evident for bacterioplankton, which varied, at most, 1.5-fold over a 24-hr period, suggesting continual growth, division and grazing mortality throughout the day and night. As observed for autotrophic picoplankton, the highest bacterial abundances and greatest temporal variability occurred close to or within the chlorophyll maximum layer at all sites.

Virus abundances closely followed distributions and abundances of bacterioplankton. Highest virus abundances, like bacteria and picoplankton, usually occurred close to or within the chlorophyll maximum at each site. Overall, when integrating abundances over the upper 100 m of the water column (or 50 m for the lagoon), highest viral abundances occurred at the Lagoon and Channel sites. However on the December 2008 cruise, the highest virus abundances occurred at the Open Water site in parallel to the highest bacterial abundances observed at any time (Table 7). As with the bacteria, there were no clear diel cycles observed for virus abundances.

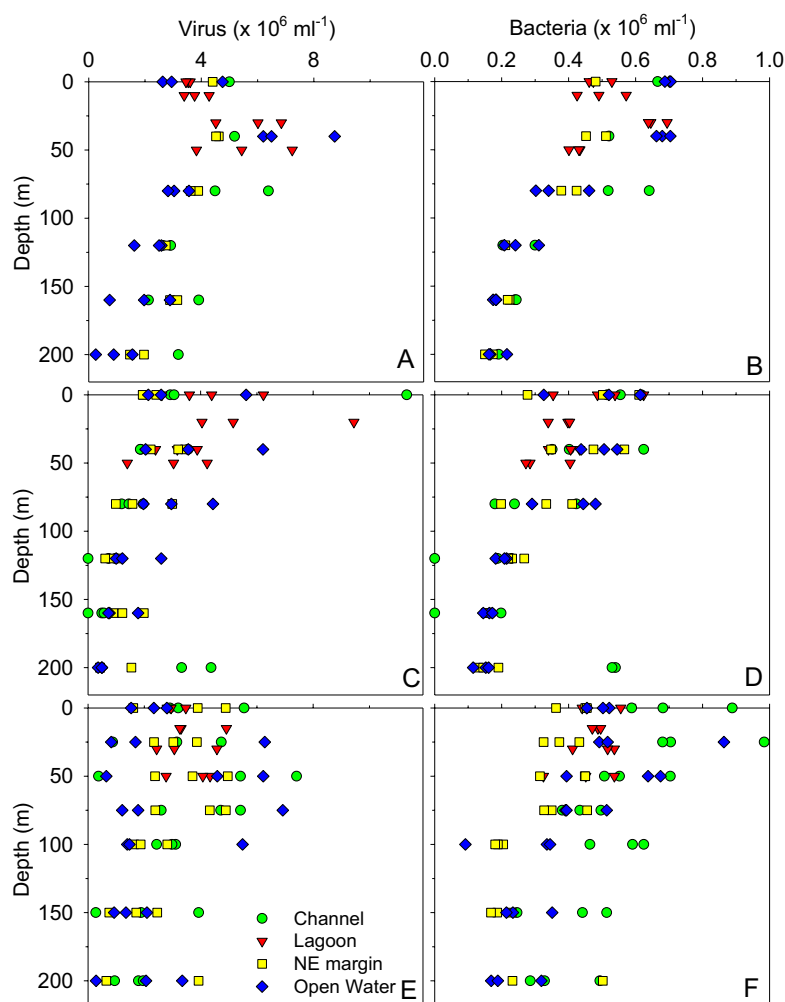


Fig. 43 Abundances of Viruses (A, C, E) and bacterioplankton (B, D, F) at Scott Reef in December 2008 (A - B), June 2009 (C - D) and November 2009 (E - F). Data in these plots represent the combined time series data (two or three sampling periods per day, sampled at approximately 08:00, 14:00 and 20:00) for each of the four biological oceanography sites (Lagoon, Deep Channel, NE margin and Open Water). Values are means of duplicate or triplicate samples.

Relationships between microbes and physico-chemical parameters

Statistical relationships between different members of the microbial loop (autotrophic picoplankton, bacteria and viruses) and physico-chemical parameters within the water column can help to elucidate which factors are potentially driving the observed picoplankton and virus distributions at Scott Reef. Within the photic zone (the upper 100 m and 50 m for the lagoon), abundances of *Synechococcus* were positively correlated with picoeukaryotes. Abundances of both *Synechococcus* and picoeukaryotes were positively correlated with total and the < 2 μm chlorophyll a fraction, implying *Synechococcus* and picoeukaryote abundances were similarly influenced by conditions in the water column. Elucidating the quantitative nature of these driving factors is difficult however, since *Prochlorococcus* and *Synechococcus* also exhibited positive linear relationships with particulate carbon, nitrogen and phosphorous, but there were no clear relationships with any of the dissolved nutrient parameters or with temperature.

Bacterioplankton abundances were positively correlated with *Prochlorococcus* and *Synechococcus* abundances indicating that the bacterioplankton community was directly utilising organic matter produced by or derived from these dominant members of the autotrophic picoplankton community.

Within the upper 100 m of the water column, virus abundances were positively correlated with *Prochlorococcus* abundance and with bacterioplankton abundances over the upper 200 – 300 m of the water column (and 50 m in the lagoon), indicating that bacterioplankton and *Prochlorococcus* were subject to viral infection. Virus abundance and bacterial production were positively correlated with temperature, suggesting higher rates of viral infection of active bacterioplankton in the warmer surface waters.

During the present study, autotrophic picoplankton comprised ca. 80% of phytoplankton (chlorophyll a) biomass at Scott Reef. Bacterioplankton are known to contribute a significant proportion of carbon (C) and nitrogen (N) biomass in other oceanic (Fuhrman et al., 1989) and coral reef environments (Ducklow, 1990). We therefore estimated the carbon and nitrogen biomass associated with autotrophic and heterotrophic picoplankton at Scott Reef. No estimate could be made for the June 2008 cruise as bacteria abundances are not available. Based on biomass conversion factors from the literature (see Fig. 44 legend) bacterioplankton made up ~ 50% of picoplankton C in all seasons except for in the lagoon during the summer, where bacterioplankton and *Synechococcus* contributed equally to C biomass (~ 40% C biomass; Fig. 44). At deep water sites, *Prochlorococcus* was the most important contributor to picoplankton C biomass (Fig. 44).

Bacterioplankton also dominated estimates of the picoplankton N standing crop, contributing on average 70% of total picoplankton N for all sites (Fig. 44). Although picoeukaryotes having a far greater per cell C and N content compared with *Prochlorococcus*, *Synechococcus* and bacteria, their contribution to the picoplankton C and N standing crop was, on average, $\leq 10\%$ due to their comparatively lower abundances (Fig. 44). While viruses were the most abundant organism at all sites around Scott Reef, their contribution to C and N biomass is negligible due to their very small size. While viruses are very small contributors to standing crop, viral infection and lysis of host cells results in the liberation of picoplankton C and N as well as other limiting nutrients to the surrounding waters as detritus, which can then stimulate microbial growth (Gobler et al., 1997).

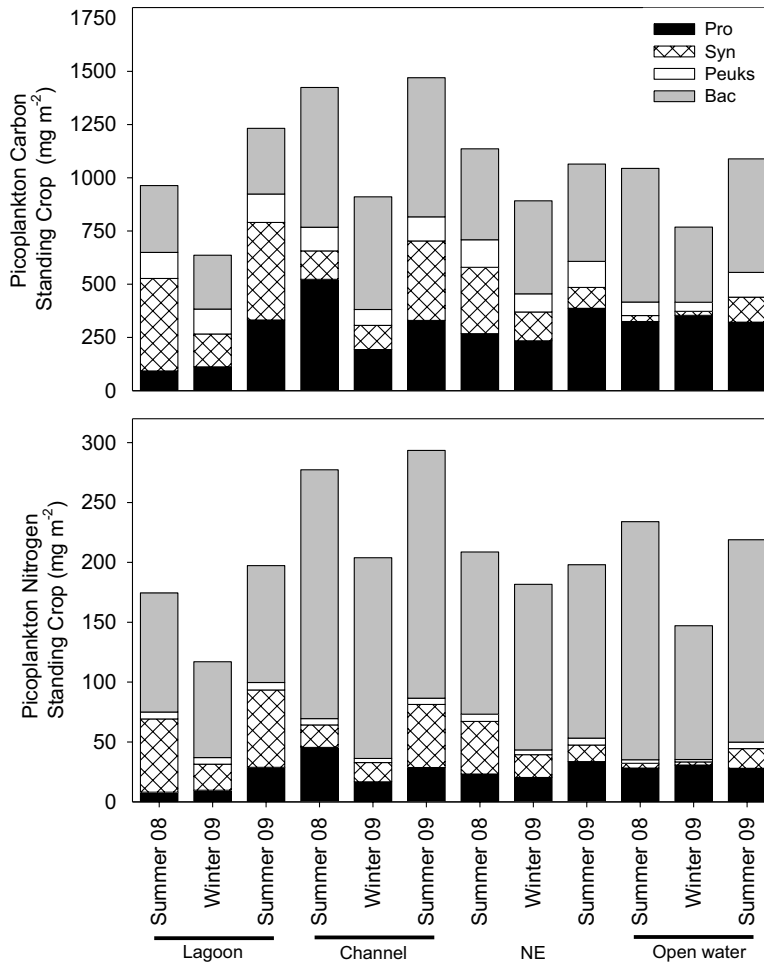


Fig. 44 Picoplankton (A) carbon and (B) nitrogen standing crop in the upper 100 m of the water column (50 m in lagoon). Pro = *Prochlorococcus*, Syn = *Synechococcus*, Peuks = picoeukaryotes and Bac = Bacteria. Data in these plots represent the combined time series data (two or three sampling periods per day, sampled at approximately 08:00, 14:00 and 20:00) plus data from the production sites (at 08:00, 24 hours following time series 8:00 sampling) for each of the four biological oceanography sites (Lagoon, Deep Channel, NE margin and Open Water) in December 2008, June 2009 and November 2009. Conversion factors from the literature were applied to convert the total abundance of each group of picoplankton to C and N biomass. Conversion factors were: *Prochlorococcus* C = 46 fg cell⁻¹, N = 4 fg cell⁻¹; *Synechococcus* C = 213 fg cell⁻¹, N = 30 fg cell⁻¹; Picoeukaryotes C = 836 fg cell⁻¹, N = 39.2 fg cell⁻¹; and bacteria C = 12 fg cell⁻¹, N = 3.8 fg cell⁻¹ (Bertilsson et al., 2003; Caron et al., 1995; Fukuda et al., 1998; Gundersen et al., 2002; Heldal et al., 2003; Verity et al., 1992).

Table 8 Ranges in picoplankton and virus abundances at Scott Reef compared with other tropical ocean and reef locations. Scott Reef data are combined from all four research cruises (June 2008, December 2008, June 2009, and November 2009). Values represent the upper 100 m of the water column (or 50 m for lagoon site). 'Absent' indicates these groups were not observed in samples at those locations. '-' indicates samples not taken to determine abundances.

Location	Prochlorococcus X 10 ⁴ cells ml ⁻¹	Synechococcus x 10 ⁴ cells ml ⁻¹	Picoeukaryotes x 10 ⁴ cells ml ⁻¹	Bacteria x 10 ⁵ cells ml ⁻¹	Virus x 10 ⁵ cells ml ⁻¹	Reference
Scott Reef						This study
Lagoon	4 - 15	1 - 10	0.1 - 2.1	4 - 7	30 - 70	
Channel	4 - 30	< 1 - 6	< 0.1 - 1.2	2 - 7	20 - 60	
NE Margin	5 - 30	< 1 - 7	< 0.1 - 1	2 - 5	10 - 50	
Open Water	5 - 40	< 1 - 4	< 0.1 - 0.4	2 - 5	40 - 50	
Great Barrier Reef (GBR)						
Lizard Island	Absent	4 - 10	-	6 - 8	10 - 20	Patten, unpublished
Heron Island	-	-	-	5 - 10	10 - 40	Patten et al., 2008
South GBR	0 - 1	7 - 17	-	-	-	Crosbie and Furnas, 2001
Central GBR	2 - 13	1 - 30	-	-	-	Crosbie and Furnas, 2001
Ningaloo	5 - 30	< 1 - 7	< 0.1 - 0.9	1 - 9	10 - 70	Patten, unpublished
Kimberley coast	Absent	2 - 13	0.1 - 0.6	2 - 5	20 - 120	Patten, unpublished
French Polynesian Atoll						
Astrolabe reef/lagoon	2	7	0.1 - 0.4	-	-	Charpy and Blanchot, 1999
Eastern Indian Ocean						
Warm core eddy	1.6	2.1	0.6	-	-	Patterson et al., 2007
Cold core eddy	6.0	0.3	0.2	-	-	Jacquet et al., 2006
New Caledonia						
Lagoon	1 - 5	5 - 12	0.3 - 2.0	-	-	
Ocean reference	18	2.5	0.2	-	-	
Line Islands Atolls (Pacific Ocean)						
	-	-	-	< 1 - 8	2 - 50	Dinsdale et al., 2008

Comparison of picoplankton and virus abundances with other oceanic and coral reef locations

To date, there have only been a handful of studies documenting autotrophic picoplankton, bacterioplankton and virus abundances in tropical Australian waters. Few studies deal with the full picoplankton community (including viruses) in tropical ocean and/or reef waters. It is important to document any changes in the picoplankton community, relative to the viral community, if we are to gain information on how organic matter is produced and cycled within pelagic food webs. Ultimately this data reveals shifts in ecosystem functioning over different temporal and spatial scales. Most studies from the late 1990s onwards have used flow cytometry to quantify autotrophic picoplankton abundances (allowing discrimination between *Prochlorococcus*, *Synechococcus* and picoeukaryotes), while both flow cytometry and epifluorescence microscopy has been employed to quantify bacterioplankton and virus abundances. A summary of picoplankton (*Prochlorococcus*, *Synechococcus*, picoeukaryote, Bacterioplankton) and virus data for Scott Reef from the four sites (Lagoon, Channel, North East Margin and Open Water) are provided and compared with other tropical ocean and reef locations around Australia and other locations (Table 8).

Prochlorococcus abundances tended towards the higher end of reported literature values for coral reef systems while *Synechococcus* and picoeukaryotes fell within the reported ranges (Table 8). Low Pro:Syn ratios measured in Scott Reef lagoon waters are an indicator of the higher nutrient status of this habitat, as is also shown by the slightly higher chlorophyll concentrations in lagoon waters. The lowest Pro:Syn ratios occurring in June 2008 in the lagoon, concomitant with generally highest chlorophyll *a* biomass at this time, may provide further evidence for weather driven mixing of lagoonal waters, leading to an increase in nutrient availability for picoplankton growth through deepening of the mixed layer. In a range of tropical ecosystems, Pro:Syn ratios are highest in oligotrophic open oceanic waters and decrease as one moves along gradients to more nutrient-enriched environments such as enclosed reef lagoons or inshore waters. Experimental studies in the Great Barrier Reef indicate *Prochlorococcus* is able to survive and grow rapidly in all these areas; however, its maximum growth rate (2 doublings day⁻¹) is less able to support high population levels in the face of enhanced grazing mortality from larger populations of microbial predators with access to higher levels of food resources from faster-growing populations of *Synechococcus* (3 doublings day⁻¹) and pico-eukaryotes. Some strains of *Prochlorococcus* are unable to reduce and assimilate NO₃, which is the primary form of 'new' nitrogen introduced in upwelled waters. Absolute and relative abundances of picoplankters can therefore provide a useful bio-indicator of ecosystem nutrient status, even when concentrations of dissolved nutrients are reduced to very low levels.

Bacterioplankton and virus abundances were in the ranges observed in the few oceanic coral reef systems where abundances have been measured. The close coupling occurring between autotrophic picoplankton and bacterioplankton abundances indicates that the bacterioplankton community were directly utilising organic matter produced by the dominant members of the photosynthesising picoplankton community. This is consistent with findings from other oceanic (Azam et al., 1994) and coral reef locations (Ferrier-Pagés and Gattuso, 1998) and supports observations that microbial loop processes dominate in oligotrophic waters such as those within and surrounding Scott Reef. The positive relationships between viruses and some autotrophic picoplankton groups suggest that viruses play important roles in the production of detritus through viral infection and lysis of host cells. Further insights into the control viruses have on bacterioplankton are detailed in subsequent sections.

Infection of bacterioplankton by viruses: Viral production experiments at Scott Reef

Viral infections of autotrophic and heterotrophic bacterioplankton are a ubiquitous feature of marine waters. Viruses infect bacteria in two major ways: 1) through lytic infections and 2) through lysogeny. During lytic infections, a virus penetrates into the host cell and hijacks the hosts' metabolism to produce progeny viruses, eventually lysing the infected cell and releasing free viruses, as well as left-over organic matter from the host cell. During lysogenic infection, the viral genome is

incorporated into the host genome where it remains dormant until the lytic cycle is induced by some internal or external factor. Whether viruses are lytic or lysogenic has important implications for the degree to which nutrients are recycled through the microbial loop.

Different environment stimuli can induce lysogenic infections to begin the lytic cycle, including UV radiation, temperature, hydrocarbons and nutrients. At Scott Reef, mixing of nutrient rich water into otherwise nutrient poor surface waters has the potential to induce lysogenic infections to lytic infections. Likewise, the Scott Reef region receives large inputs of solar UV radiation at the surface. As such, we investigated the occurrence of lytic and lysogenic infections in surface waters in the Lagoon (LA), Channel (CH), NE Margin (NE) and Open waters (SW) of Scott Reef in December 2008, June 2009 and November 2009.

Fig. 45 provides representative results obtained for viral production experiments (June 2009). Water samples were incubated with and without Mitomycin C, a chemical which induces lysogenic viruses to begin a lytic infection. An increase in virus abundances and numbers of infected cells in controls versus Mitomycin C-treated samples during the 9 – 12 hr incubations indicate a predominantly lytic infection mode (e.g. Fig. 45G). When viruses in Mitomycin C-treated samples exceed those in controls (e.g. Fig. 45E) this indicates that a large proportion of bacterioplankton contained lysogenic viruses in their genomes which were triggered into the lytic cycle by Mitomycin C.

Lytic viral production rates (VP) varied between sites within a season and between seasons at individual sites (Fig. 45, Table 9). The highest viral production rates were generally measured at the Lagoon, NE Margin and Channel sites during the June 2009 cruise and coincided with the highest fraction of infected cells (FIC) (Table 9). The greatest variability in viral production rates and FIC occurred in lagoon waters, with a 20-fold difference in VP between June and November 2009, with FIC values ranging between 6 and 68%. The fraction of lysogenic cells (FLC) was also highly variable, with 0 to 52% of cells in the bacterioplankton community in a lysogenic state. However there was no clear seasonal or spatial trend for FLC. It was estimated that between 7 and > 100% of the bacterioplankton community was lysed daily through viral infections.

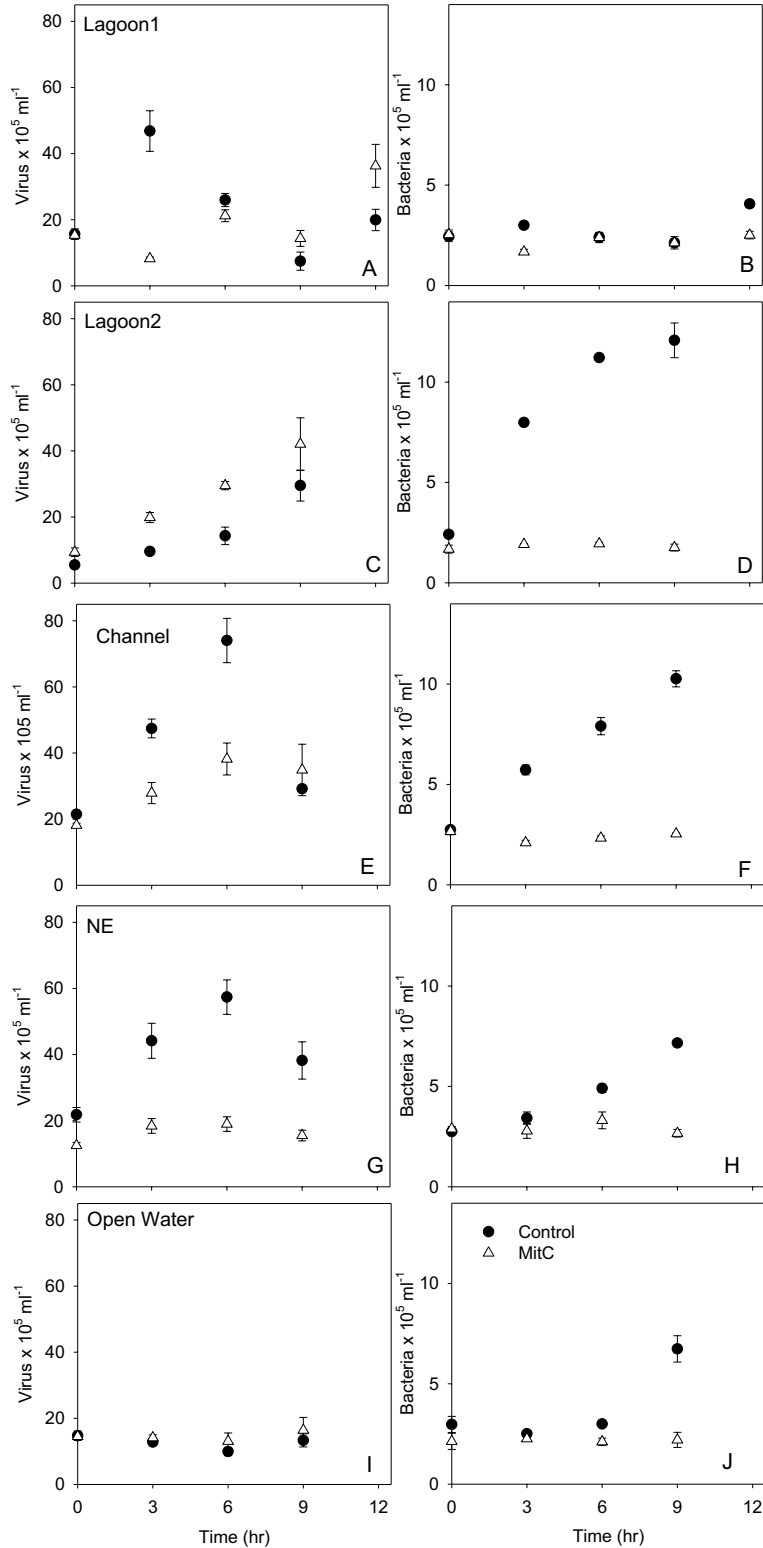


Fig. 45 Changes in virus (A, C, E, G, I) and bacterioplankton abundances (B, D, F, H, J) in viral production incubations conducted in June 2009 at Lagoon, Channel, Ne Margin and Open water sites. Lagoon1 = Viral production run at start of sampling period and Lagoon2 = Viral production run at end of sampling period in June 2009. Values are means \pm SE.

Table 9 Viral parameters in December 2008 (S 08), June 2009 (W 09) and November 2009 (S 09) in Lagoon, Channel, NE Margin and Open Water. Values are means \pm SE. (1) = Viral production experiment run at the start of the sampling period and (2) = Viral production experiment run at the end of the sampling period in the Lagoon. VP = Viral production, FIC = Fraction of infected cells, FLC = Fraction of lysogenic cells and VMM = viral mediated mortality of bacterioplankton. See methods for equations for calculating VP, FIC, FLC, and VMM.

Site	Season	Virus _{ambient} ($\times 10^9$ l ⁻¹)	Bacteria _{ambient} ($\times 10^9$ l ⁻¹)	VP ($\times 10^9$ l ⁻¹ d ⁻¹)	FIC (%)	FLC (%)	VMM (% bacteria lysed d ⁻¹)
Lagoon	S 08	4.56	0.33	6.9 \pm 6.7	8 \pm 2	51 \pm 14	106.0 \pm 103.0
	W 09 (1)	5.00	0.49	12.0 \pm 1.3	68 \pm 19	12 \pm 7	124.0 \pm 14.8
	W 09 (2)	4.61	0.31	5.0 \pm 1.0	49 \pm 8	49 \pm 14	82.0 \pm 15.37
	S 09 (1)	3.97	0.30	1.9 \pm 0.2	27 \pm 4	8 \pm 4	31.37 \pm 2.8
	S 09 (2)	3.12	0.45	0.6 \pm 0.18	6 \pm 1	2 \pm 5	7.22 \pm 2.5
Channel	S 08	4.07	0.62	5.6 \pm 1.3	25 \pm 6	0 \pm 0	45.4 \pm 11.6
	W 09	3.29	0.41	14.2 \pm 2.3	95 \pm 8	9 \pm 12	172.3 \pm 31.2
	S 09	4.62	0.43	5.6 \pm 0.1	80 \pm 17	0 \pm 0	64.2 \pm 2.1
NE Margin	S 08	5.52	0.61	4.4 \pm 1.8	22 \pm 11	18 \pm 19	36.3 \pm 15.3
	W 09	2.61	0.33	16.2 \pm 0.2	65 \pm 10	0 \pm 0	242.0 \pm 3.7
	S 09	4.45	0.31	2.4 \pm 0.4	39 \pm 6	52 \pm 8	39.2 \pm 7.6
Open water	S 08	3.87	0.64	4.5 \pm 2.2	40 \pm 24	30 \pm 16	33.8 \pm 15.7
	W 09	3.93	0.46	1.9 \pm 1.8	5 \pm 5	5 \pm 7	21.5 \pm 19.8
	S 09	2.18	0.42	4.9 \pm 2.6	10 \pm 5	2 \pm 1	56.6 \pm 29.6

Abundance and distribution of nano and microplankton at Scott Reef

Nanoplankton and microplankton are the size classes of plankton with cells 2 – 20 μm and 20 – 200 μm respectively, and comprise both autotrophic and heterotrophic cells. On all cruises but the June 2008 cruise we used a FlowCAM to enumerate cells larger than 5 μm (to complement the flow-cytometry data collected for picoplankton). The FlowCAM uses flow-cytometry principles to count cells in a larger size fraction than the flow-cytometer used for the picoplankton counts, but in addition takes photographic images of each particle to facilitate their identification.

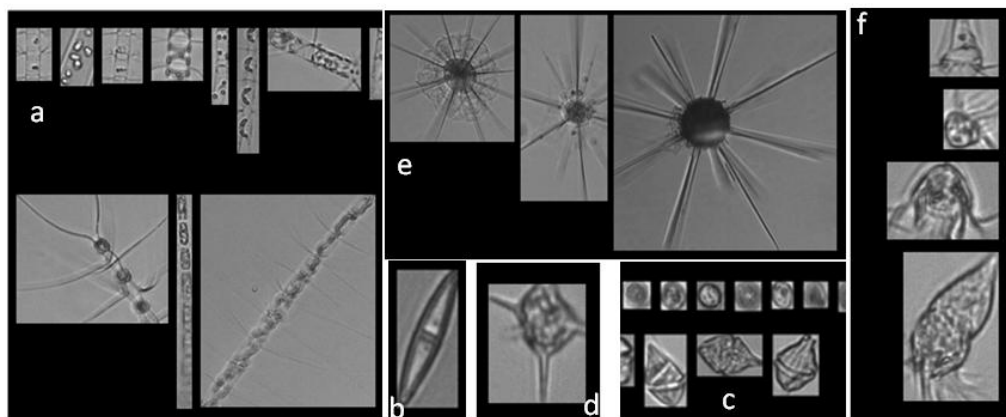


Fig. 46 Representative images of nano and microplankton taken by the FlowCAM. a) diatom chains; b) single celled pennate diatom; c) dinoflagellates; d) silicoflagellate; e) radiolarians; f) ciliates.

The taxa represented in the FlowCAM data were extremely diverse (Fig. 46). Diatom chains (Fig. 46a) were amongst the most frequently imaged plankton. These phytoplankton are probably the most important contributors to primary production in the nano and microplankton size range, and are an important trophic link to zooplankton such as copepods and euphausiids. Dinoflagellates (Fig. 46c) were common, but these cells can be autotrophic, heterotrophic or mixotrophic (both auto- and heterotrophic). Heterotrophic ciliates such as *Strombidium* and *Strobilidium* were also frequently imaged (Fig. 46f).

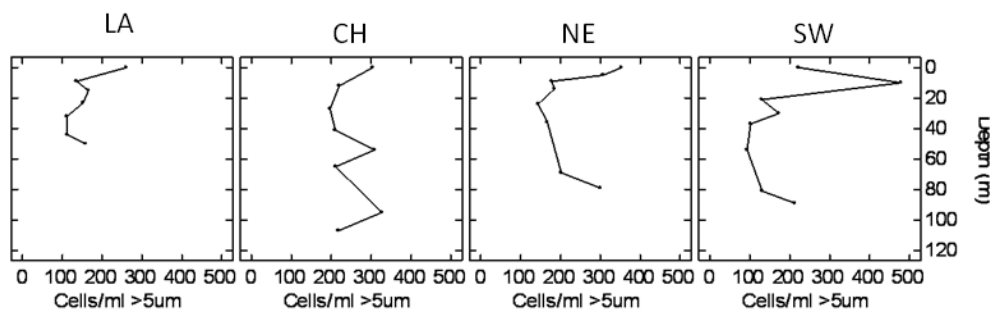


Fig.47 Representative FlowCAM count data at the production sites in December 2009. LA = Lagoon, CH = Deep Channel, NE = NE margin, SW = Open Water.

Counts of cells $>5 \mu\text{m}$ in size ranged between 106 – 313 cells ml^{-1} , and overall the average size was $12.5 \mu\text{m}$ (Table 10). There were no significant differences in cell count between day and night. Some layering of cell concentrations occurred through the water column (Fig.47), but overall the profiles cell counts were significantly higher in the surface layer ($<30\text{m}$ depth) than in deeper water: ($235 \pm 15(\text{SE})$ and 183 ± 13 cells ml^{-1} , respectively: $t\text{-value} = -2.59$, $df=157$, $p\text{-value}=0.01$). There was no difference in cell size between locations or cruises.

Table 10 FlowCAM summary statistics: average $>5 \mu\text{m}$ cell count ($\pm\text{SD}$) and average $>5 \mu\text{m}$ cell size ($\pm\text{SD}$) at each of the locations by cruise. LA = Lagoon, CH = Deep Channel, NE = NE margin, SW = Open Water.

	December 2008		June 2009		November 2009	
	Cells ml^{-1}	Cell size μm	Cells ml^{-1}	Cell size μm	Cells ml^{-1}	Cell size μm
CH	209 \pm 120	13 \pm 1	273 \pm 130	14 \pm 1	250 \pm 213	11 \pm 1
LA	310 \pm 85	12 \pm 1	313 \pm 128	14 \pm 1	149 \pm 47	11 \pm 1
NE	114 \pm 24	11 \pm 1	162 \pm 75	13 \pm 2	229 \pm 105	13 \pm 1
SW			106 \pm 78	12 \pm 1	182 \pm 88	12 \pm 1

Most FlowCAM counts were made at the production sites, in parallel with both flow cytometry counts and production experiments. We subjected the count data collected on each cruise and at each location to statistical analysis using a generalised linear regression (GLM) model to compare data between cruises and locations (Table 11). This model has the advantage of being able to handle unbalanced sample sizes, and compared patterns at one cruise/location with others. In this case, FlowCAM data were collected on 3 cruises, so the comparison was made between the December 2009 cruise and the 2 subsequent cruises. Similarly, the Channel site (CH) was arbitrarily chosen as the basis for comparison with the 3 other sites. We found a significant difference in the abundance of cells $>5 \mu\text{m}$ between locations, but not between cruises. The Open Water site (SW; 148 ± 15 (SE) cells ml^{-1}) and NE margin site (NE; 193 ± 15 cells ml^{-1}) had significantly lower cell counts than the Channel site (CH; 246 ± 24 cells ml^{-1}). Cell counts from the Channel site and the Lagoon site (LA) were not significantly different.

Table 11 Results of generalised linear regression model for FlowCAM data, comparing cruise and location. LA = Lagoon, NE = NE margin, SW = Open Water.

	Estimate	Std. Error	t value	p-value
(Intercept)	233.150	28.850	8.082	$< 2\text{e-}16$
June 2009	23.480	33.020	0.711	0.478
November 2009	13.350	32.060	0.416	0.678
LA	-23.870	26.980	-0.885	0.378
NE	-56.940	27.580	-2.065	0.041
SW	-102.700	28.760	-3.571	0.0005

Primary productivity and carbon turnover in Scott Reef waters

¹⁴C uptake Experiments

Nineteen primary production experiments based on ¹⁴C tracer methods (Steeman Nielsen, 1952) were carried out at the four experimental sites (Table 1) in and around Scott Reef. At least one productivity experiment was carried out at each site on each biological oceanography cruise. Repeat productivity experiments were carried out at the central lagoon site (LA) at the end of the December 2008, June 2009 and November 2009 cruises (see Fig. 48 – Fig. 52).

All of the primary production experiments involved the size fractionation of natural populations (Total population, > 10 µm size fraction, 2 – 10 µm size fraction, < 2 µm size fraction) to partition daily production between important functional groups within the phytoplankton community. This was done because different size classes of phytoplankton have differing physiologies and fates within pelagic food webs and may contribute differentially to potential material exports to benthic food webs.

Diatoms and dinoflagellates are the predominant phytoplankton groups of the > 10 µm size fraction, while very small unicellular photosynthetic cyanobacteria (formerly called blue-green algae) are overwhelmingly predominant in the < 2 µm size fraction (picoplankton). The intermediate 2 – 10 µm size fraction contains a diverse assemblage of small flagellates and non-motile microalgae from many algal families. While unicellular cyanobacteria < 2 µm typically dominate phytoplankton biomass and primary production in stable oligotrophic tropical oceanic waters such as those around Scott Reef, short-term phytoplankton biomass and production responses to enhanced nutrient inputs such as upwelling are commonly manifested through the preferential growth of diatom populations. These 'bloom' responses are typically short-lived until the slower-growing metazoan (e.g. copepod) grazers of these larger phytoplankters have time to reproduce and develop significant grazing biomass.

In the present study, phytoplankton populations were collected from 6 – 8 depths through the euphotic zone and incubated under light levels nominally matching the collection depths. Mid-day hourly photosynthesis rates (10:00 – 14:00 local time) were integrated to give a mid-day areal production rate (mg C m⁻² hr⁻¹) which can be converted to an estimate of daily primary production (mg C m⁻² d⁻¹). This daily production estimate is based upon the observation that approximately 50% of total daily irradiance available for photosynthesis impinges on the ocean surface between 10:00 and 14:00. Estimates of primary production based on short ¹⁴C uptake incubations are generally equivalent to (though usually less than) estimates of gross primary production calculated from community oxygen fluxes (see discussion below).

Two types of vertical chlorophyll profiles were observed in the South Reef lagoon. Most commonly, the vertical distribution of chlorophyll is characterised by a near-bottom maximum. When this was not the case, the water column was vertically well mixed. Phytoplankton collected by a 10 µm filter made noticeable contributions to community biomass on a number of occasions. As noted above, enhanced growth of larger phytoplankton is often indicative of upwelling or other nutrient input processes. Within the lagoon setting, lateral intrusion of thermocline waters from the deep channel between North and South Reefs, or from enhanced mineralisation and release of organic nutrients by benthic communities. Vertical profiles of ¹⁴C uptake rates were characterised by maxima either near the surface (high light) or bottom (higher biomass). Maximum profile productivity rates (>4 mg C m⁻³ hr⁻¹) in the shallow, high-light environment of the lagoon were consistently higher than observed at nearby deep water sites.

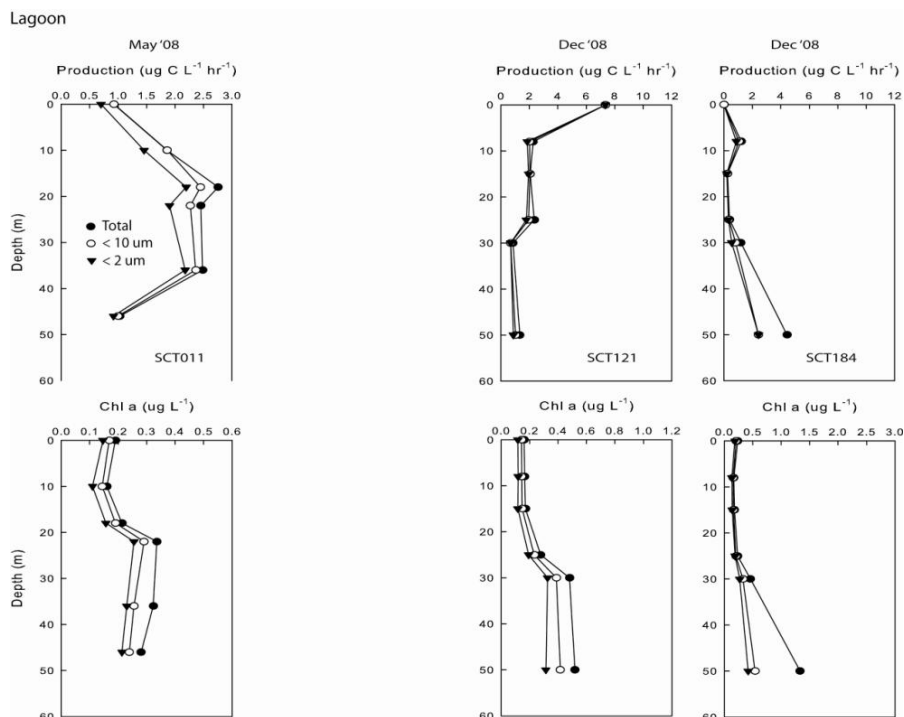


Fig. 48 Vertical profiles of size fractionated primary production (Top) and chlorophyll (Bottom) in the South Reef lagoon (LA) in June 2008 and December 2008.

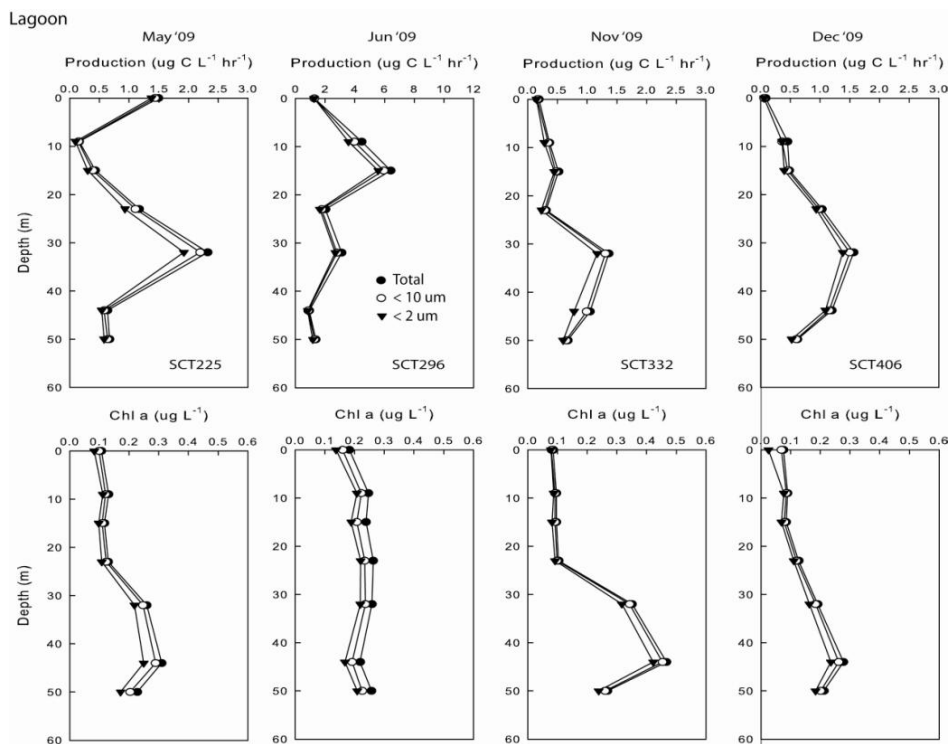


Fig. 49 Vertical profiles of size fractionated primary production (Top) and chlorophyll (Bottom) in the South Reef lagoon (LA) in June 2009 and November 2009.

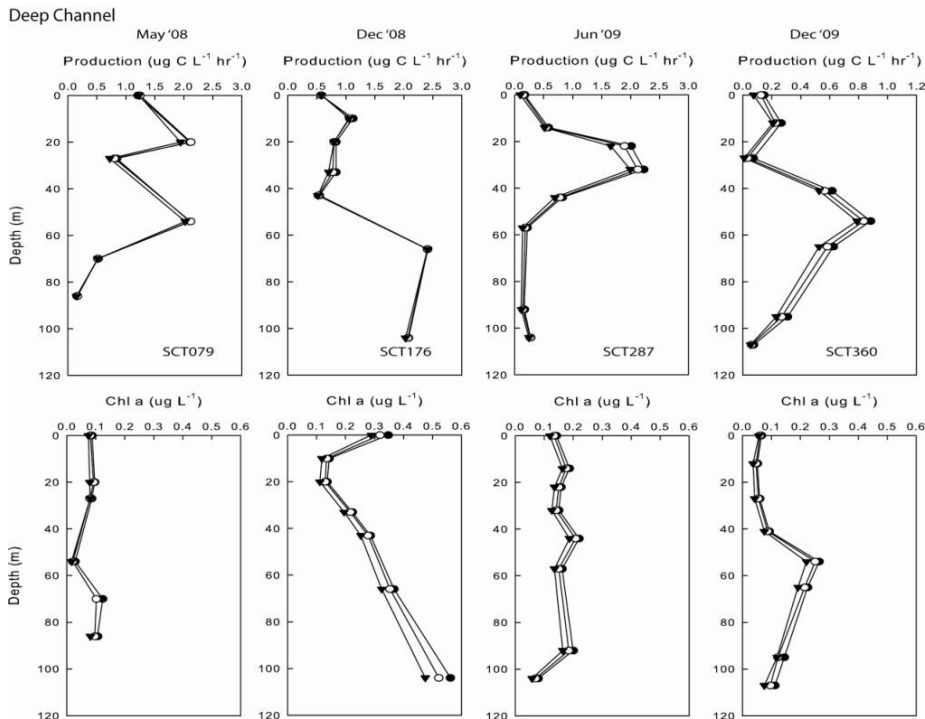


Fig. 50 Vertical profiles of size fractionated primary production (Top) and chlorophyll (Bottom) in the Deep Channel (CH) between North and South Reef.

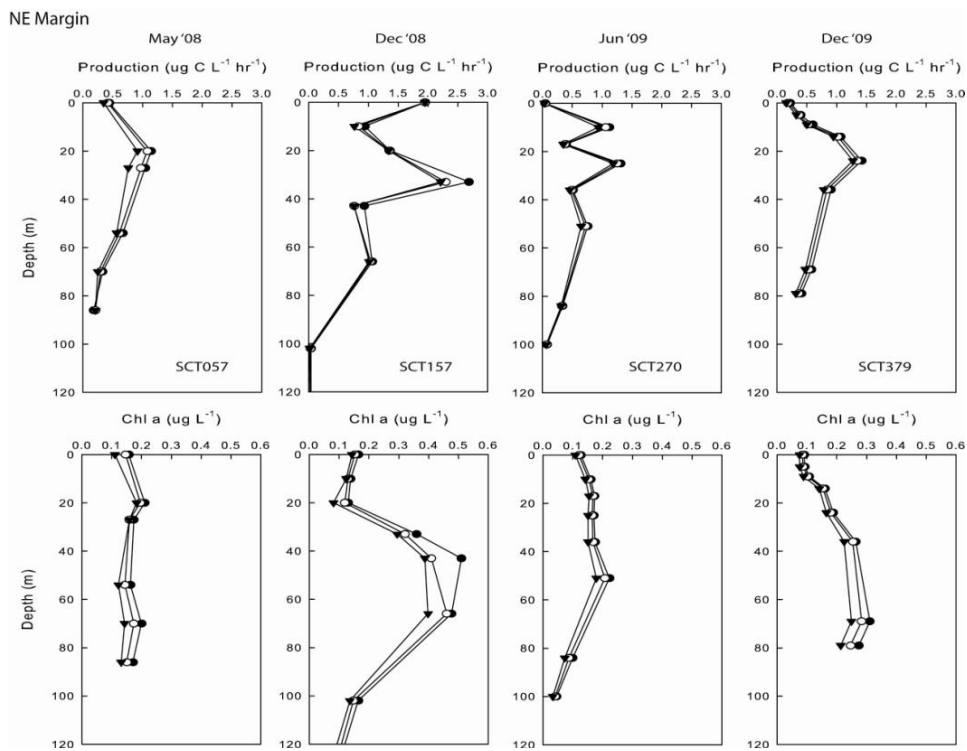


Fig. 51 Vertical profiles of size fractionated primary production (Top) and chlorophyll (Bottom) at the NE margin of North Reef (NE).

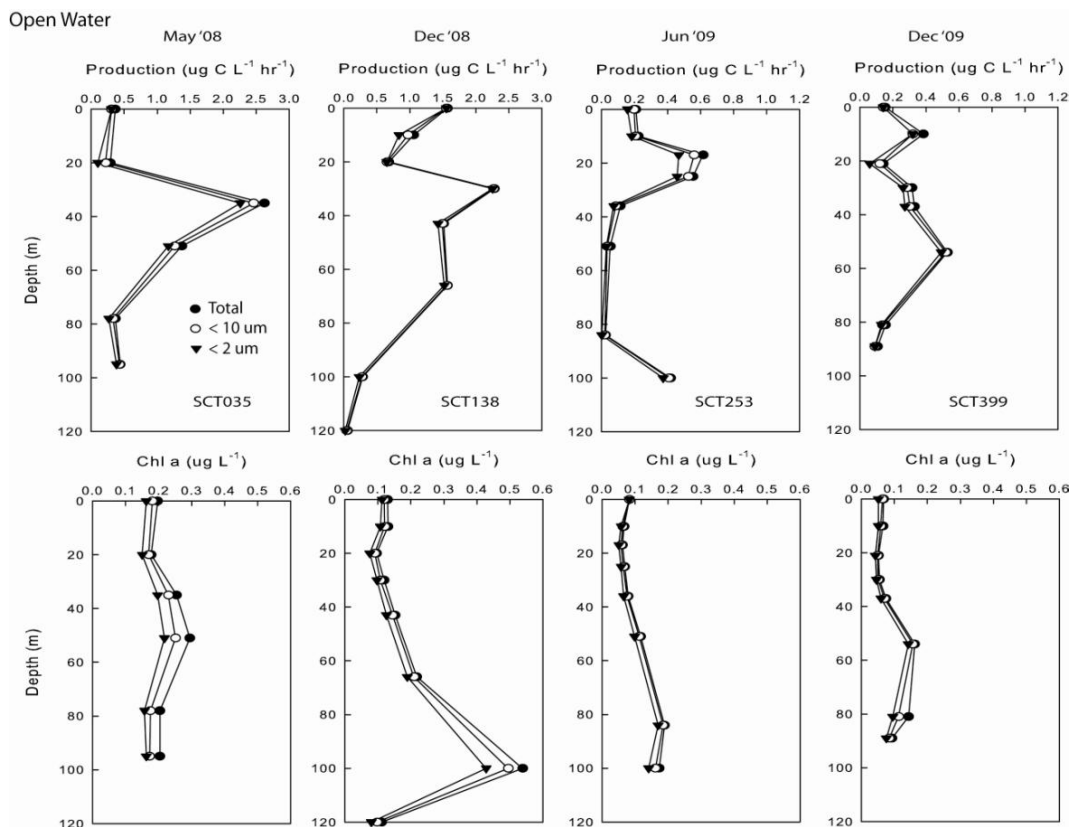


Fig. 52 Vertical profiles of size fractionated primary production (Top) and chlorophyll (Bottom) at the Open Water reference site southwest of Scott Reef (SW).

At the deep water sites (CH, NE and SW), vertical distributions of phytoplankton biomass (as chlorophyll) and primary productivity generally differed. Vertical profiles of chlorophyll were most commonly characterised by a well defined deep chlorophyll maximum (DCM) at depths ranging between 40 and 100 m (average ca. 70 m). While the highest chlorophyll concentrations (biomass) were usually found in the DCM, the highest profile primary production rates were most commonly measured in a shallower depth stratum between 20 and 40 m. This depth band is characterised by downwelling irradiance levels between approximately 20 and 5 percent of surface irradiance. Smaller secondary productivity maxima associated with the DCM layer were occasionally observed.

On all four biological oceanography cruises, phytoplankton biomass (by chlorophyll) and primary production (by ^{14}C uptake) at both lagoon and deep water sites were overwhelmingly dominated by picoplankton (< 2 μm size fraction). With one exception, picoplankton chlorophyll and primary production exceeded 75 percent of total biomass and production at the three deep sites. In 16 of 19 measurements, the picoplankton contribution exceeded 80 percent of total primary production.

Larger phytoplankton (> 10 μm size fraction) were only observed to make a significant contribution to biomass and productivity at the South Reef lagoon site (LA) and only in experiments run during the December 2008 cruise (SCT184, 10 December 2008).

The average of depth-integrated estimates of phytoplankton biomass (as chlorophyll *a*) at the dry season lagoon production sites (11.2 mg m^{-2}) were similar to standing crop values recorded at deep water sites adjacent and away from Scott Reef (dry season average 13.0 mg m^{-2}). Average

daily dry season productivity ($800 \text{ mg C m}^{-2} \text{ day}^{-1}$), however was considerably higher than measured contemporaneously at deep water sites (mean = 572 , range $204 - 1,031 \text{ mg C m}^{-2} \text{ d}^{-1}$). The average early summer chlorophyll standing crops were approximately twice those measured during the dry season (averages = 15.1 mg m^{-2} in the lagoon and 23.6 mg m^{-2} for the deep water sites). On the November – December cruises, integral daily production rates in the lagoon averaged $948 \text{ mg C m}^{-2} \text{ day}^{-1}$ compared to $831 \text{ mg C m}^{-2} \text{ d}^{-1}$ at deep-water sites (Fig. 53).

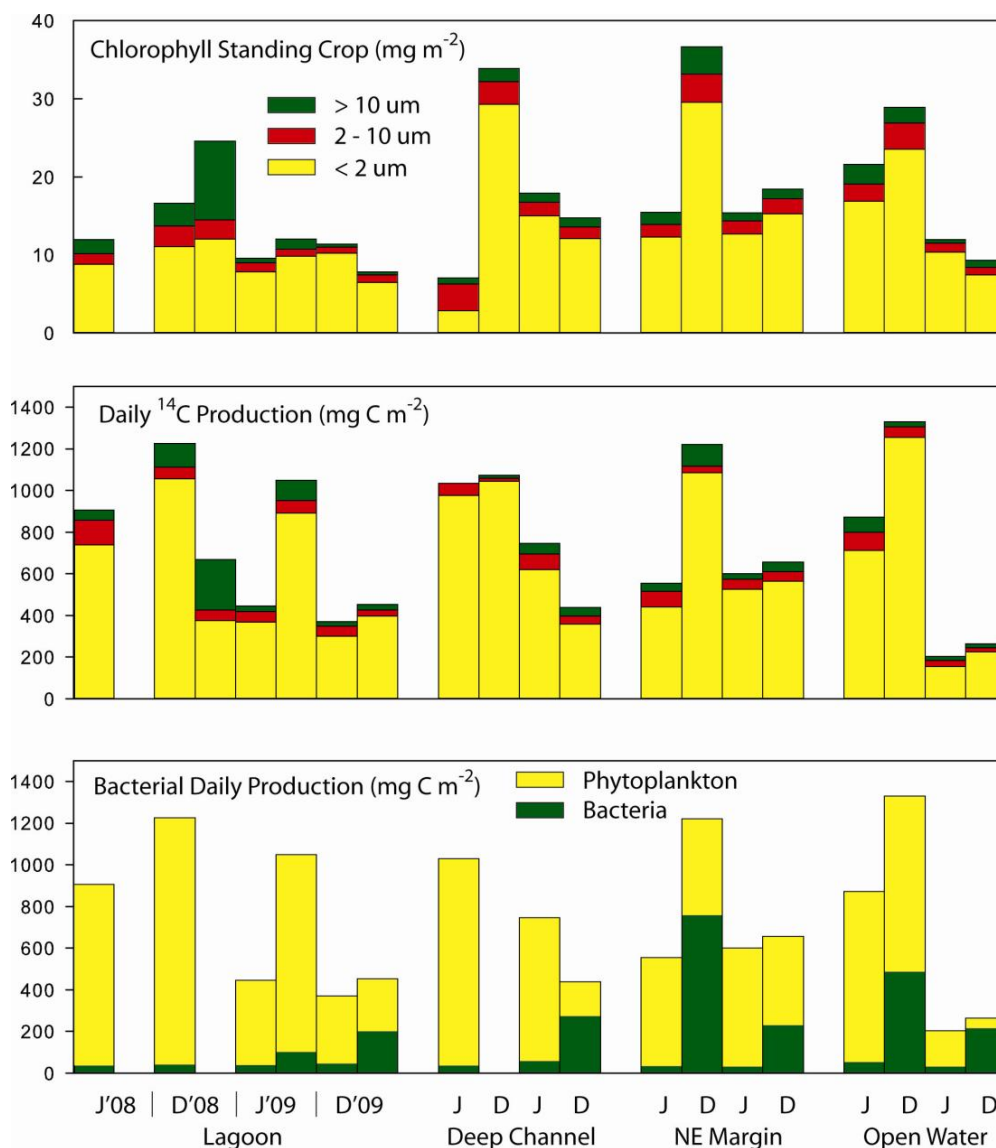


Fig. 53 Size-fractionated chlorophyll standing crop (Top), daily primary production (¹⁴C uptake: Middle) and bacterial production (³H-thymidine uptake: Bottom) in relation to primary production.

Table 12 Estimates of phytoplankton standing crop (as chlorophyll), daily primary production in functional group size fractions and daily bacterial production at Scott Reef production sites. Chlorophyll and production values in parentheses give the percent of total standing crop or daily production in experimental size fractions. Bacterial production values in brackets indicate bacterial production as a percent of concurrent primary production. ^a - All depths not sampled; ^b - contaminated samples preclude integration

Site	Date	Chlorophyll standing crop mg m ⁻²			Primary Production mg C m ⁻² d ⁻¹		Bacterial Production mg C m ⁻² d ⁻¹	
		<2 µm	<10 µm	Total	<2 µm	Total	<10 µm	Total
Lagoon	25 June 2008	8.8 (73)	10.2 (85)	12.0	740 (82)	857 (95)	905	37.6 [4]
	3 Dec 2008	11.1 (66)	13.7 (82)	16.6	1,056 (86)	1,113 (91)	1,227	42.1 [3]
	10 Dec 2008	12.0 (49)	14.5 (59)	24.6	377 (56)	428 (64)	669	^a
	31 May 2009	7.9 (82)	9.0 (94)	9.6	369 (83)	421 (94)	447	38.7 [9]
	8 June 2009	9.8 (82)	10.7 (89)	12.0	893 (85)	951 (91)	1,049	101.9 [10]
26 Nov 2009	10.2 (90)	11.0 (97)	11.4	301 (81)	350 (94)	371	46.5 [13]	
3 Dec 2009	6.5 (83)	7.4 (95)	7.8	398 (88)	426 (94)	453	200.5 [44]	
Deep Channel	1 July 2008	2.8 (40)	6.3 (89)	7.1	976 (95)	1,034 (100)	1,031	37.4 [4]
	9 Dec 2008	29.2 (86)	32.2 (95)	33.9	1,045 (97)	1,058 (97)	1,073	^a
	6 June 2009	15.0 (84)	16.7 (93)	17.9	621 (83)	695 (93)	746	57.7 [8]
	30 Nov 2009	12.1 (82)	13.6 (92)	14.7	358 (81)	397 (90)	440	273.9 [62]
NE Margin	29 June 2008	12.3 (79)	13.9 (90)	15.5	441 (79)	517 (93)	555	34.0 [6]
	7 Dec 2008	29.5 (81)	33.2 (90)	36.7	1,086 (89)	1,118 (92)	1,222	^b
	4 June 2009	12.7 (83)	14.4 (94)	15.4	526 (88)	574 (95)	601	32.1 [5]
	28 Nov 2009	15.3 (83)	17.2 (94)	18.4	565 (86)	611 (93)	657	229.5 [35]
Open Water	27 June 2008	16.9 (78)	19.1 (88)	21.6	713 (82)	800 (92)	872	52.9 [6]
	5 Dec 2008	23.6 (82)	26.9 (93)	28.9	1,255 (94)	1,306 (98)	1,330	^b
	2 June 2009	10.4 (87)	11.5 (96)	12.0	156 (76)	185 (90)	204	31.4 [15]
	2 Dec 2009	7.4 (79)	8.4 (90)	9.3	226 (85)	244 (92)	265	217.0 [82]

Pelagic metabolism

Pelagic processes in the vicinity of Scott Reef are dominated by microbes, as is typical of the oligotrophic open ocean. Microbial food chains are inefficient in transferring nutrients to higher trophic levels (ultimately producing fish), meaning that most energy is lost in respiration. The balance between net autotrophy (i.e. positive net carbon fixation) and net heterotrophy (i.e. losses of carbon due to respiration exceeding carbon fixation) is determined by hydrological events that introduce pulses of nutrients into the productive surface layers, increasing production and pushing the metabolic balance toward autotrophy. Understanding the processes that determine this balance in the unperturbed environment and the frequency and amplitude of natural production events will allow any future potential anthropogenic perturbations to be placed in context.

At each of the four sites occupied during the Biological Oceanography cruises, pelagic metabolism was measured by conducting incubations of water collected at the same sites and depths as for the ^{14}C experiments (except the Open Water site (SW) in June 2008, which was sampled one day earlier). In these experiments, one set of water samples was incubated in the dark for 24 hrs, to measure the consumption of O_2 as an index of water column respiration rate (metabolic activity by all microorganisms including bacteria, phytoplankton, and microzooplankton). In a parallel set of samples, O_2 evolution as a result of photosynthesis was measured in water samples exposed to the same light regime they would have experienced at the depth of collection. Since O_2 evolution in light bottles is proportional to carbon fixation, it is possible to use this measurement to make an additional estimate of the primary production rate by phytoplankton, though this is offset by the respiration of microorganisms in the bottle.

At all sites where surface incubations were conducted, surface production by phytoplankton was insufficient to compensate for community respiration and resulted in negative net oxygen flux (Fig. 54, 55, 56, 57) as a result of photoinhibition caused by the cells being exposed to full strength sunlight for a full day. Whether this effect occurs in the field or is a consequence of the bottle incubations is unclear, since in the field cells would be distributed through the water column by turbulence. To avoid this effect, we often omitted the surface incubation in our experiments. At depths approaching the bottom of the euphotic zone, production was light-limited and again respiration outweighed production. Production rates in the light bottle incubations usually only exceeded the compensation point (i.e. the point at which production of oxygen balances consumption) at depths of 20 – 40 m, if at all.

Water column mean dark respiration (DR) rates were consistently highest at the Lagoon site (LA; Table 13; $t=5.542$, $df=66$, $p\text{-value} < 0.0001$), and lowest at the Open Water site (SW; Table 13; $t=-4.771$, $df=52$, $p\text{-value} < 0.0001$) with the Channel site (CH) and NE margin sites (NE) intermediate. In December 2008 DR at the Lagoon site was 2 fold higher than at the other sites.

Table 13 Water column mean dark respiration rates ($\text{mmol O}_2 \text{ m}^{-3} \text{ d}^{-1}$) for each cruise. Data are mean \pm SD. LA = Lagoon, NE = NE margin, SW = Open Water.

Site	June 2008	Dec 2008	June 2009	Dec 2009
LA	1.77 \pm 0.84	2.54 \pm 0.54	1.56 \pm 0.29	1.85 \pm 0.46
CH	1.53 \pm 0.64	1.27 \pm 0.48	1.14 \pm 0.47	1.61 \pm 0.16
NE	1.25 \pm 0.18	1.57 \pm 0.63	1.23 \pm 0.34	1.62 \pm 0.56
SW	1.18 \pm 0.63	1.14 \pm 0.35	0.84 \pm 0.14	1.37 \pm 0.33
Mean	1.60 \pm 0.69	1.80 \pm 0.80	1.26 \pm 0.41	1.66 \pm 0.44

LA

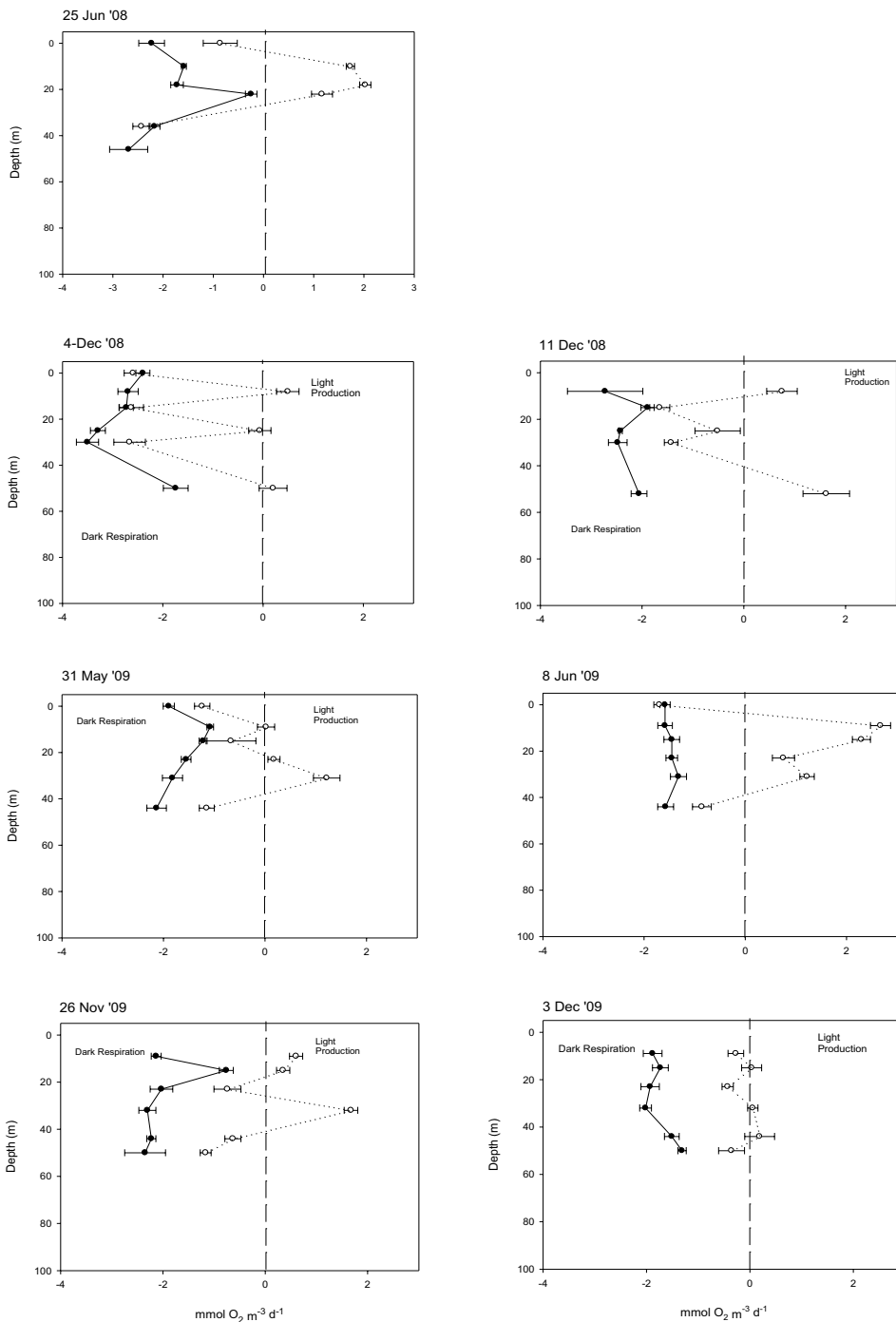


Fig. 54 Oxygen flux through the water column at the Lagoon site (LA). For all cruises except the first there were 2 site occupations (i.e. duplicate sets of measurements). Solid symbols indicate dark respiration; unfilled symbols indicate samples incubated under conditions of light corresponding to the depth of collection (light production). The compensation point, at which production = respiration (i.e. net O₂ flux is zero) is indicated by the vertical dotted line. Error bars represent SE.

LA, within the reef lagoon of South Reef, was the only site to achieve positive metabolic balance (i.e. net production of oxygen) at one or more depths for all experiments (Fig. 54). In December 2008, we observed a very strange pattern of layering of positive oxygen flux through the water column alternating with depths at which oxygen flux was negative. This pattern was observed in both experiments conducted on this cruise, and to some extent a similar, but less pronounced, phenomenon was observed in June and November 2009. It is unclear what could be causing these patterns, other than layers of microbes forming at distinct depths during the very calm weather. There is no indication of corresponding patterns in bacteria or phytoplankton abundance, but we have no measurements of micro-heterotrophs in the water column to confirm the origin of the observed patterns of oxygen flux. Surface incubations were conducted on 4 of 7 occasions, and all showed evidence of photoinhibition.

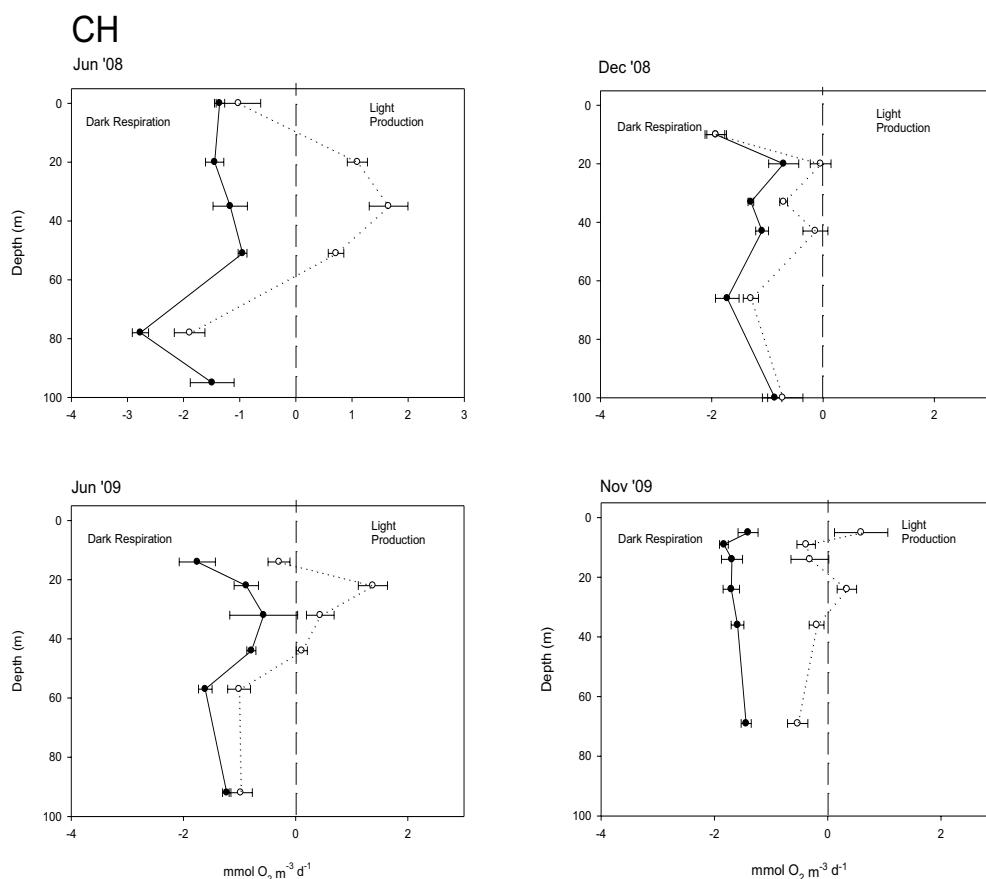


Fig. 55 Oxygen flux through the water column at the Channel site (CH), as for Fig. 54.

Metabolism experiments conducted at CH, located within the channel between North and South reefs, achieved metabolic balance at one or more depths on all cruises except that of December 2008 (Fig. 55). A surface incubation was only attempted on the first cruise, and on subsequent cruises the surface sample was omitted. The peak in oxygen production occurred between 20 and 50m. Respiration often differed through the water column, though not as markedly as at the Lagoon site.

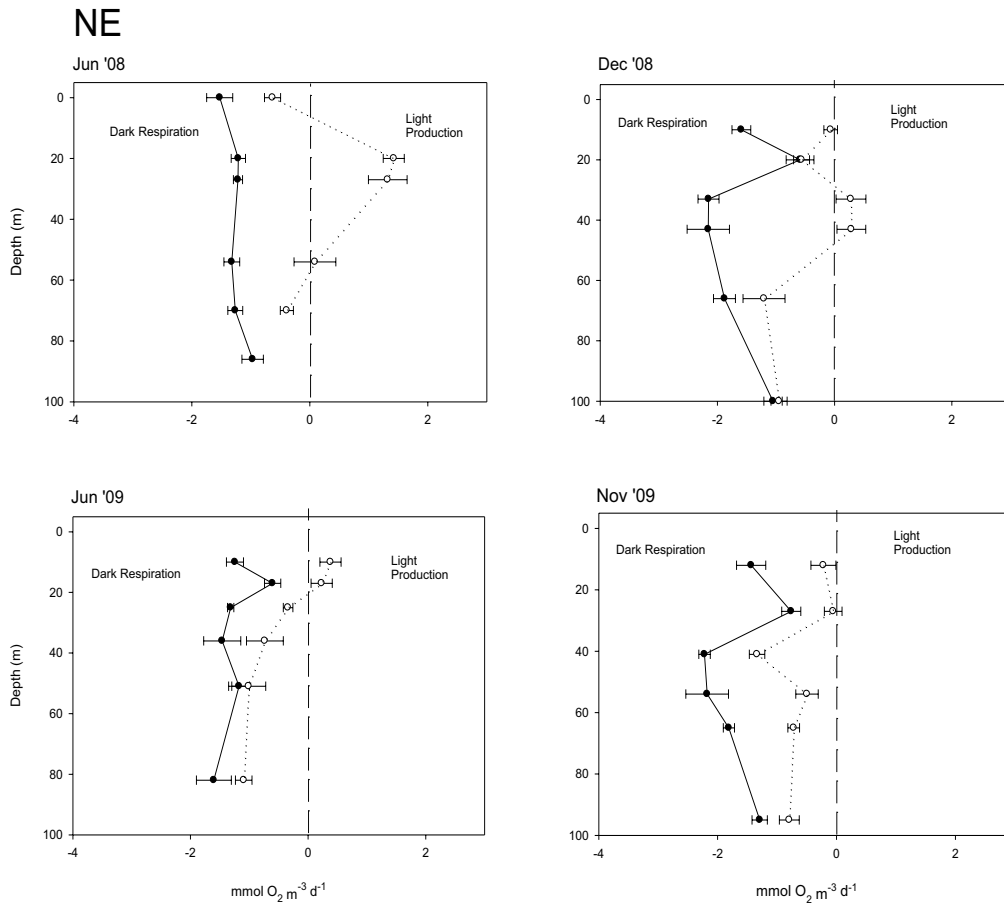


Fig. 56 Oxygen flux through the water column at the NE margin site (NE), as for Fig. 54.

Similarly, at the NE margin site (NE), metabolic balance was only achieved at some depths on the first 3 of the 4 cruises (Fig. 56). However, only on the June 2008 cruise was this substantial. At the Open Water site (SW), the trend toward lower productivity was further exacerbated (Fig. 57) and only on the June 2008 cruise was metabolic balance achieved at any depth, albeit at 4 depths. Dark respiration rates at the Open Water site (SW) were more similar through the water column than at the Lagoon (LA), Deep Channel (CH) or NE margin (NE) sites.

By integrating oxygen fluxes measured at discrete intervals through the water column down to the 1% light level, generally taken as being the bottom of the euphotic zone, it is possible to estimate area-specific rates of production and respiration (Fig. 58). This analysis reveals the waters in and around Scott Reef are usually heterotrophic (phytoplankton production insufficient to offset water column respiration rates), with only 8 of the 19 sites measured achieving a P:R ratio > 1 (i.e. autotrophic).

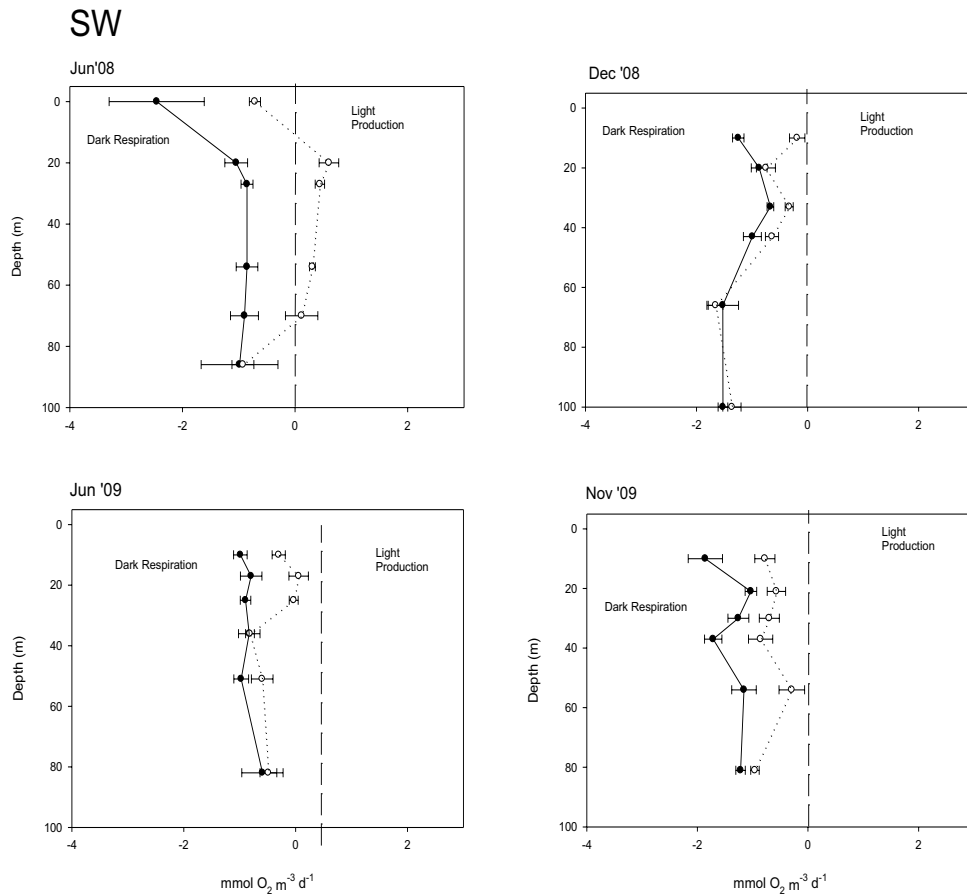


Fig. 57 Oxygen flux through the water column at the Open Water site (SW), as for Fig. 54.

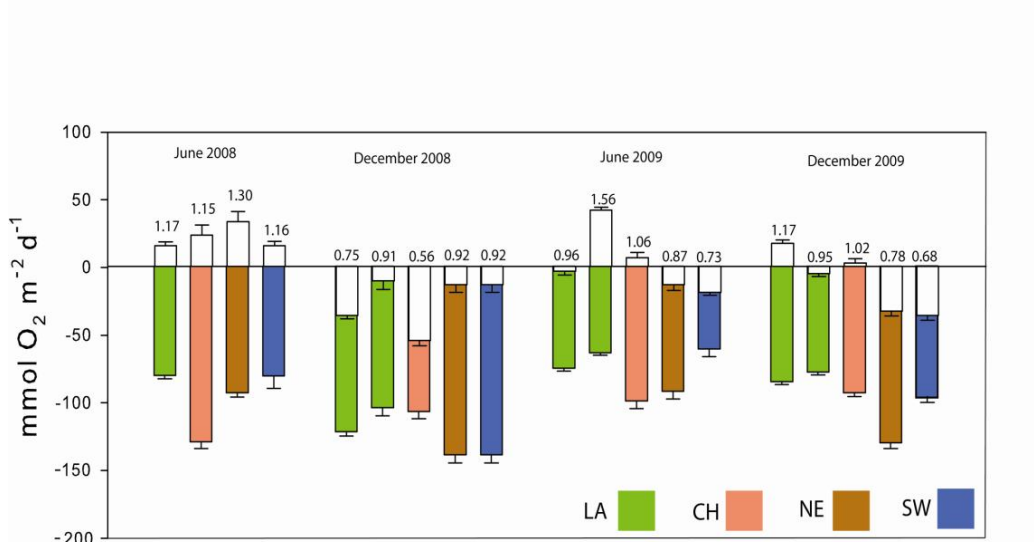


Fig. 58 Community respiration and net community production at Scott Reef. The number over each bar is the P:R ratio i.e. the ratio of Gross Production (CR+NCP) to respiration (CR). When the P:R ratio is >1 the system is autotrophic, when it is <1 the system is heterotrophic. Error bars are SE.

In June 2008, all sites were autotrophic, with a mean P:R ratio of 1.20 ± 0.07 (Fig. 58). Heterotrophy was most pronounced on the December 2008 cruise where all sites failed to achieve metabolic balance and the mean P:R ratio was 0.81 ± 0.16 . In June 2009 only the second occupation of the Lagoon site and the Channel site achieved metabolic balance. Overall, the mean P:R ratio in June 2009 was 1.04 ± 0.32 . In the 8 days between site occupations at the Lagoon site, the water column turned from being heterotrophic to strongly autotrophic, in fact having the highest NCP observed during this study. The CTD profile indicated high concentrations of chlorophyll mixed throughout the water column, suggesting that a phytoplankton bloom had occurred at the Lagoon site in the period between successive site occupations. A similar switch occurred at the Lagoon site in December 2009, with the water column going from autotrophic to heterotrophic over a period of 6 days, but here there was no indication of changes in phytoplankton abundance. In December 2009 the Channel site was just in metabolic balance, but the NE margin site and the Open Water site were both strongly heterotrophic.

The reason for the frequent occurrence of heterotrophy is not yet clear. It is important to remember that the oxygen flux measurements represent the combined respiration of all organisms, but only photosynthetic cells produce oxygen. Oligotrophic systems tend to support a higher heterotrophic biomass per unit of autotrophic biomass than more productive systems (Gasol et al., 1997), so that even though carbon flux may be positive, as indicated by the ^{14}C experiments, oxygen flux may be negative because of the higher biomass of heterotrophs. The bulk of pelagic respiration at Scott Reef is likely to be contributed by micro-heterotrophs, from bacteria to protists. Robinson and Williams (2005) have attributed 45% of respiration to bacteria, and Calbet and Landry (2004) suggest that microzooplankton contribute a similar amount.

Our data suggest that the metabolic balance of waters around Scott Reef is finely balanced. Recent oceanographic literature suggests that open ocean waters are frequently heterotrophic, and that overall metabolic balance is maintained by aperiodic net autotrophic events that can only be resolved by frequent sampling (Marañón et al., 2000, Karl et al., 2003, Williams et al., 2004). The Scott Reef data set is consistent with this hypothesis.

Comparison of the Scott Reef metabolism data to other Australian locations

We have made measurements in a number of other locations in tropical Australia using the same techniques. These results can be compared by plotting the P:R ratio against gross primary production (Fig. 59). The data from Scott Reef form a distinct cluster, characterised by very low values of gross primary production (GPP). To achieve autotrophy, our data suggest that GPP needs to exceed $113 \text{ mmol O}_2 \text{ m}^{-2} \text{ d}^{-1}$, or $2 \text{ g C m}^{-2} \text{ d}^{-1}$, assuming a photosynthetic quotient of 1.4 (Bender et al., 1999). This compares with the global average of $80 \text{ mmol O}_2 \text{ m}^{-2} \text{ d}^{-1}$, (Williams, 1998), and reflects the high respiration rates of tropical waters.

The data from Scott Reef aligns with data from the Timor Sea, though the latter is more productive, and the Coral Sea. Measurements from the Great Barrier Reef are similar in GPP, but have higher P:R ratios because of the shallower water column and consequent lower values of areal respiration. The highest production rates measured using the oxygen method has been on the shallow NW shelf en route to the Timor Sea.

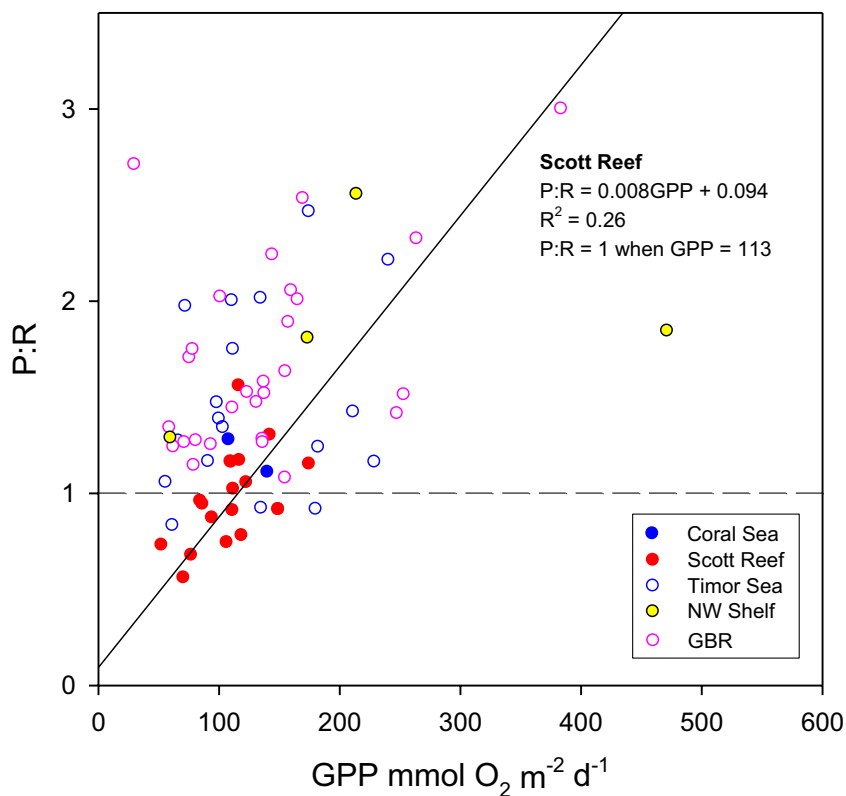


Fig. 59 The relationship of P:R ratio to Gross Primary Production at Scott Reef compared to other locations where AIMS has made similar measurements. Regression statistics use Model II regression, applied to the Scott Reef data alone.

Comparison of the Scott Reef data to other areas of the globe

Duarte and Regaudie-de-Gioux (2009) compiled all available data on the metabolic balance of marine planktonic communities, and concluded that, on average, a threshold GPP of 1 – 3 $\text{mmol O}_2 \text{ m}^{-3} \text{ d}^{-1}$ was required for open ocean planktonic communities to achieve metabolic balance (i.e. a P:R ratio of 1). The relationship between volume-based measurements of NCP and GPP at Scott Reef is highly significant (Fig. 60) and indicates that a threshold GPP of 1.50 $\text{mmol O}_2 \text{ m}^{-3} \text{ d}^{-1}$ is required to achieve metabolic balance (Table 14). Of the 35 studies listed by Duarte and Regaudie-de-Gioux (2009), only 8 significant relationships are listed for subtropical areas of the ocean. It is worthy of note that there is only one other set of measurements available from the tropical ocean (that of Robinson and Williams 1999 from the NW Indian Ocean), making the Scott Reef data particularly valuable. The data of Robinson and Williams (1999) is from the Arabian Sea, an area with both coastal and open-ocean upwelling and consequent higher rates of primary production, in contrast to the predominately oligotrophic oceanographic regime at Scott Reef.

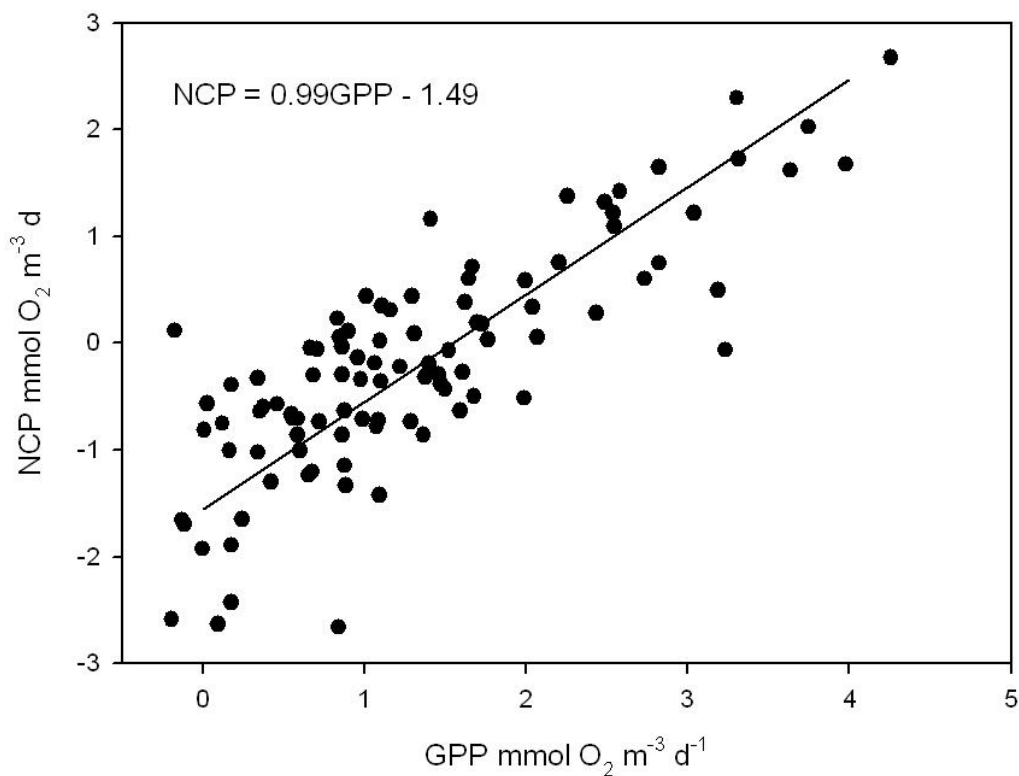


Fig. 60 Volumetric NCP vs GPP from Scott Reef. See Table 14 for regression statistics.

Table 14: Comparison of Reduced Major Axis (Model II) Regression statistics of the relationship between NCP and GPP ($\text{mmol O}_2 \text{ m}^{-3} \text{ d}^{-1}$) at Scott Reef with subtropical and tropical locations from Table 1 of Duarte and Regaudie-de-Gioux (2009).

Region	Intercept	SE	Slope	SE	R ² adj	Threshold GPP
NW Indian Ocean	-3.18	0.33	0.76	0.06	0.83	4.2
Subtropical E Atlantic	-3.34	0.45	0.94	0.04	0.94	3.56
Subtropical NE Atlantic	-1.16	0.26	0.8	0.06	0.63	1.45
Subtropical Atlantic	-3.32	0.32	2.02	0.22	0.21	1.65
Subtropical NE Atlantic	-0.63	0.04	0.99	0.01	0.99	0.63
Subtropical N Pacific	-0.56	0.05	0.66	0.08	0.23	0.84
This study	-1.49	0.10	0.99	0.07	0.66	1.50

Scott Reef is an extremely oligotrophic environment, as indicated by the comparison of locations in Table 15. The threshold GPP required to achieve metabolic balance at Scott Reef

is comparable to the subtropical Atlantic Ocean, but higher than the global average (Table 14). There are 3 possible reasons for the comparatively high threshold of GPP required for metabolic balance at Scott Reef:

1. Dissolved organic carbon release by phytoplankton is proportionally higher at low levels of primary production (Hessen and Anderson, 2008), raising the GPP threshold for metabolic balance.
2. Intense light fields may increase photorespiration, also raising the GPP threshold (Hessen and Anderson, 2008).
3. Oligotrophic planktonic communities tend to support a higher heterotrophic biomass per unit of autotrophic biomass than more productive systems (Gasol et al., 1997), raising respiration relative to GPP.

Overall, the Scott Reef metabolic data are similar to other areas of the tropical or subtropical ocean (Table 15). Areal rates of respiration and production were generally similar in the Timor Sea to those measured at Scott Reef, but there were a few episodes of very high productivity that lift the mean rates in the Timor Sea data. The Scott Reef respiration data are similar to data from other areas. There is a very wide range in the reported values of net community production (NCP), as it appears that NCP establishes the metabolic balance of the ocean (Aristegui and Harrison, 2002). The frequent occurrence of heterotrophy at Scott Reef is similar to Station ALOHA off Hawaii (Williams et al., 2004), which is consistently heterotrophic; these authors suggest that this may be the case in many areas of the open ocean.

Table 15: Comparison of Scott Reef rates with other areas of the globe. CR, average area-specific community respiration; NCP, average area-specific net community production; DR, average volume-specific dark respiration; Max P, maximum observed O₂ flux in light bottles.

Location	CR mmol O ₂ m ⁻² d ⁻¹	NCP mmol O ₂ m ⁻² d ⁻¹	DR mmol O ₂ m ⁻³ d ⁻¹	Max P mmol O ₂ m ⁻³ d ⁻¹	Reference
Scott Reef					
June 2008	112	22	1.4	2.0	This study
Dec 2008	139	-28	1.8	1.6	
June 2009	91	3	1.3	2.7	
Nov 2009	113	-11	1.7	1.7	
Sahul Shoals, Timor Sea	36 - 196	13 - 216	0.3 - 3.7	3.7	McKinnon et al., (in press)
Equatorial Atlantic	71	80	0.6-2.6	3.5	Perez et al., 2005
South Atlantic Gyre	60	20	0.2	0.5	Serret et al., 2006
Stn. ALOHA (Hawaii)	86	-24	0.5 - 1.5	1.3	Williams et al., 2004
Arabian Sea	78 - 127	2.5 - 455	1.0 - 8.0	13	Dickson et al., 2001
Banda Sea	100 - 170	108 - 1350	1.0 - 1.7		Tijssen et al., 1990
Latitudinal average	~300	~40			Robinson and Williams, 2005

Bacterial Production (Thymidine uptake experiments)

Vertical profiles of bacterial biomass production (as carbon) were also measured at the four primary production sites using radio-labelled thymidine uptake (Fig. 61). Thymidine is one of the four organic bases that make up DNA in all living organisms. Eukaryotic phytoplankton and phototrophic cyanobacteria are unable to take up and assimilate free thymidine from the environment and must synthesise their own. The bacteria production estimate is based on empirically derived estimates of thymidine/DNA ratios, the average cellular DNA content and cellular carbon contents for pelagic marine bacteria (Fuhrman and Azam, 1980; 1982).

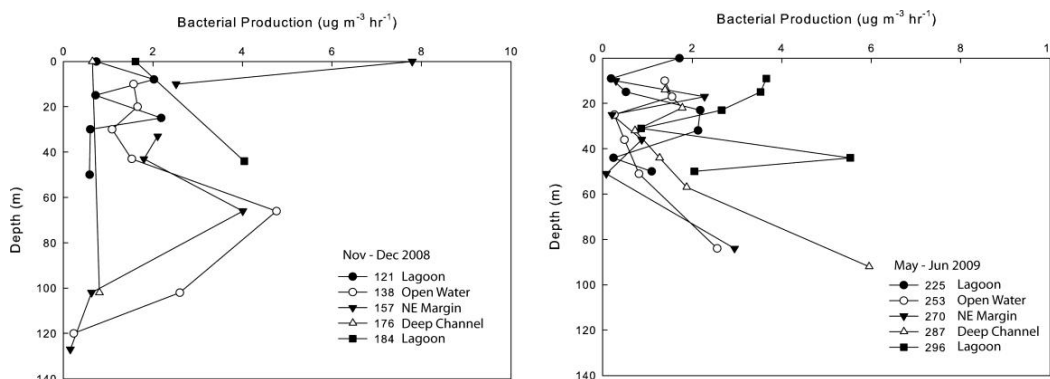


Fig. 61 Vertical profiles of daily bacterial carbon production (^3H -thymidine uptake) measured concurrently with phytoplankton primary production in the vicinity of Scott Reef during the December 2008 and June 2009 cruises.

Measured hourly bacterial production rates ranged from near nil to $8 \text{ mg C m}^{-3} \text{ hr}^{-1}$. Two extremely high rates were recorded in December 2008, but are believed to be due to contamination of the samples with excess isotope. At the other production sites, bacterial carbon production rates generally ranged between 0.3 and $4 \text{ mg C m}^{-3} \text{ hr}^{-1}$. Production maxima in individual depth profiles were variable, either coinciding with or lying somewhat below peaks in chlorophyll rather than primary production. The general coincidence between subsurface maxima in bacterial production and chlorophyll suggests that a significant portion of the organic matter supporting bacterial production may be coming from lysis of algal/cyanobacterial cells through grazing or virus attack rather than direct excretion of organic matter from photosynthesising cells in the water column. This, however, remains to be confirmed experimentally.

Estimates of daily bacterial production (assuming growth over 24 hours) at the four production sites ranged from 31 (Open Water site, June 2009) to 102 (Lagoon site, June 2009) $\text{mg C m}^{-2} \text{ d}^{-1}$ (Table 16). Estimated bacterial production rates ranged from 3.4% to 15.4% of concurrent phytoplankton production rates. This production is based upon the assimilation of low molecular weight organic compounds in the water which are derived from excretion by local phytoplankton, organic compounds released in the process of grazing on phytoplankton and lysis of bacteria and phytoplankton by viruses. Only a portion of the organic matter taken up by bacteria is converted to biomass. The remainder is metabolised and/or respired in the process of bacterial growth and metabolism. This is shown by the general correlation between primary production (^{14}C uptake) and dark-bottle respiration rates (above). The proportion of this organic matter that is converted into bacterial biomass, the Carbon Growth Efficiency (CGE) is known to be variable and is not well resolved in most ecosystems with values ranging from < 10 to 70 percent (summarised in Jones et al., 1996).

Working in a comparable pelagic environment to Scott Reef, Jones et al. (1996) measured a mean CGE for pelagic bacteria of 23%.

Table 16 Estimates of bacterial biomass carbon production at Scott Reef as estimated from ^3H -thymidine uptake experiments. LA = Lagoon, CH = Deep Channel, NE = NE margin, SW = Open Water.

Date	Site	Primary Production $\text{mg C m}^{-2} \text{d}^{-1}$	Bacterial Production $\text{mg C m}^{-2} \text{d}^{-1}$	Bacterial / Phytoplankton %
June 2008	LA	905	37.6	4.2
	CH	872	52.9	6.1
	NE	555	34.0	6.1
	SW	1,031	37.4	3.6
December 2008	LA	1,227	42.1	3.4
	SW	1,330	Contaminated	
	NE	1,222	Contaminated	
	CH	1,073		
	LA	669		
June 2009	LA	447	38.7	8.7
	SW	204	31.4	15.4
	NE	601	32.1	5.3
	CH	746	57.7	7.7
	LA	1,049	101.9	9.7
December 2009	LA	371	46.5	12.6
	CH	440	273.9	62.3
	SW	657	229.5	34.9
	NE	265	217.0	82.0
	LA	453	200.5	44.3

Correlates of Production

To better understand the factors influencing pelagic production processes, we undertook an analysis of the relationships between production-related variables. This analysis applies only to the production sites, and hence only to the euphotic zone. Data for nutrient concentrations were taken from the sediment trap deployment sites occupied approximately 1 hr before the production sites.

In order to constrain the number of variables used in the analysis, we made the following assumptions:

1. Since 92% of primary production occurred in cells $<10 \mu\text{m}$ in size we did not include total production
2. That TDN represented overall nitrogen availability – we did not include the different N species
3. That TDP represented overall phosphorus availability
4. That TDN and TDP together represent overall nutrient availability.

We included the following sets of variables in the analysis:

1. Measurements of production – $<2 \mu\text{m}$ PP ($<2 \mu\text{m}$ primary production based on ^{14}C uptake); $<10 \mu\text{m}$ PP ($<10 \mu\text{m}$ primary production based on ^{14}C uptake); NCP (net

community production, based on O₂ flux); BP (bacterial production based on ³H-thymidine uptake)

2. Measurements of biomass/abundance of key micro-organisms – <2 μmChl (<2μm chlorophyll); <10 μmChl (<10μm chlorophyll); VLP (abundance of virus-like particles); abundance of picoplankton (BACT, bacteria; VLP, virus-like particles; Syn, *Synechococcus*; Pro, *Prochlorococcus*; PEuk, picoeukaryotes)
3. Measurements of physicochemical variables – Temperature, depth, DOC (dissolved organic carbon), TDN (total dissolved nitrogen), TDP (total dissolved phosphorus).

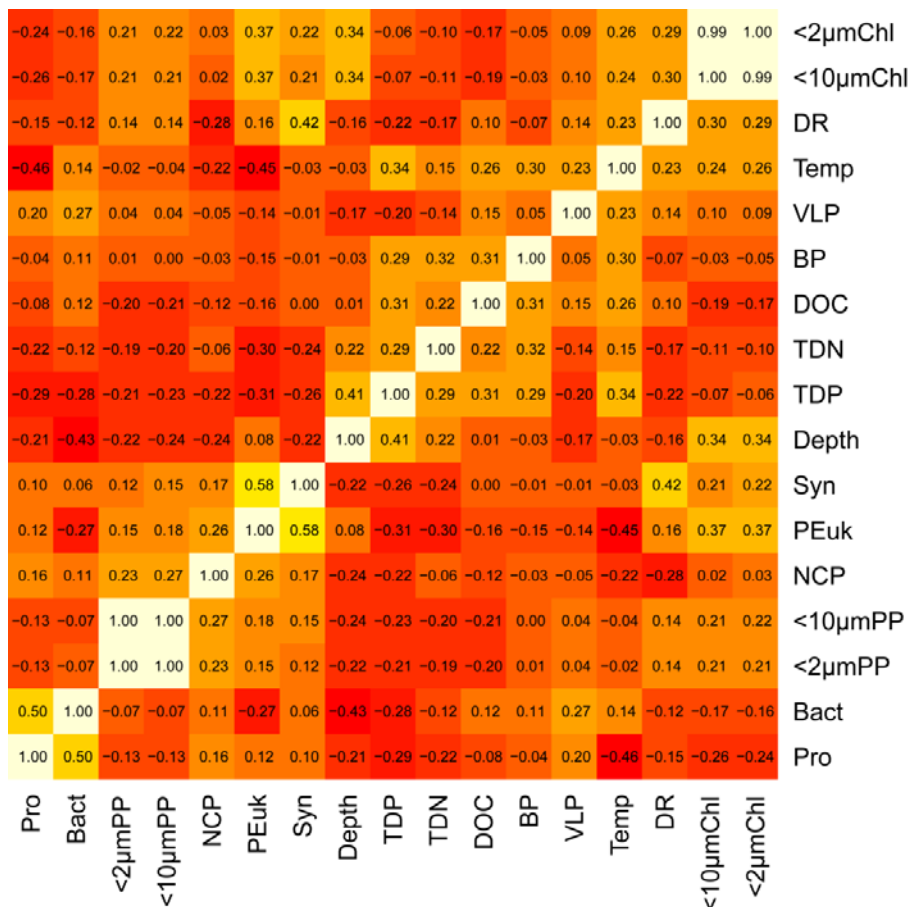


Fig. 62 Correlation matrix (heatmap) of production-related variables. The numbers are Pearson correlation coefficients, r.

Firstly, we prepared a correlation matrix to compare relationships between untransformed variables (Fig. 62). All variables were then transformed using z-scores, then analysed using hierarchical cluster analysis (Sneath and Sokal, 1973). We interpreted the resulting dendrogram (Fig. 63) as comprising 3 ecologically meaningful groups of closely related variables:

Group I – Depth-related effects. The relationship between depth and TDN and TDP originates from the higher stocks of nutrients at the bottom of the euphotic zone. Similarly, bacterial production was often highest near the thermocline, and is closely related to DOC, the primary energy source for these heterotrophic cells.

Group 2 – Production-related effects. Three measurements of production (<2 μm PP, <10 μm PP and NCP) correspond with phytoplankton biomass (both <2 μm and <10 μm) as well as the population size of picoeukaryotes.

Group 3 – Temperature-related effects, comprising 2 subgroups. Subgroup 3a highlights the positive correlation of temperature with respiration (DR) and of respiration with *Synechococcus*, possibly through the metabolic activity of their grazers. Subgroup 3b highlights the between 2 categories of picoplankton (*Prochlorococcus* and heterotrophic bacteria) and their associated viruses.

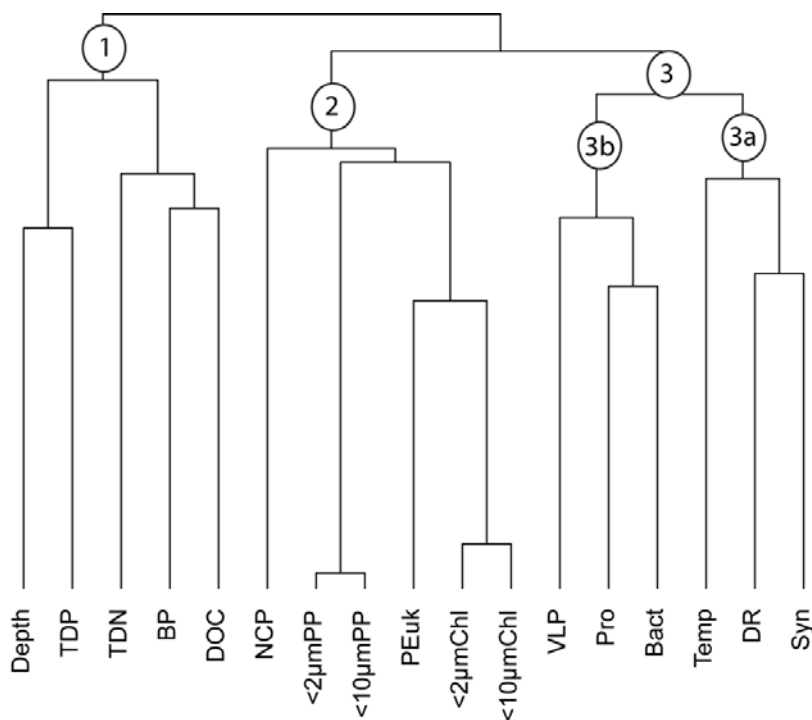


Fig. 63 Dendrogram originating from hierarchical cluster analysis. Cluster groups are discussed in the text.

We conclude from these analyses that the main forcing factors influencing the productivity of waters adjacent to Scott Reef are depth and temperature, and there is little difference between locations. Light decays with depth, and therefore influences production processes. Despite highest productivity occurring in the depth band corresponding to 5 – 20% of surface irradiance, which is normally above the chlorophyll maximum (Fig. 48 – Fig. 52), all 3 measurements of primary production (<2 μm PP, <10 μm PP and NCP) clustered with the measurements of phytoplankton biomass. There may be a small effect of temperature on the observed rates within the summer cruises when the mixed layer was less defined, but the primary temperature difference forcing change in indices of productivity is likely to be that between cruises (i.e. higher rates on the summer cruises). Temperature and the population size of picoplankton were the primary drivers of respiration rate because of the relationship between metabolic rate and temperature not only of these organisms, but that of their grazers (e.g. heterotrophic nanoflagellates, ciliates and heterotrophic dinoflagellates).

These results parallel those from the multivariate analysis of water column nutrients, where the primary effects of depth and temperature were similar.

Historical measurements of pelagic productivity at and near Scott Reef

On a global basis, the biological oceanography of the northern North West Shelf is relatively little studied; however, a significant number of primary production measurements have been made in NW Australia that can be usefully compared to those made in this project. Regional estimates of primary productivity have also been derived from ocean colour satellite estimates of near-surface chlorophyll concentrations, models of vertical phytoplankton biomass distributions and productivity-light relationships (e.g. Behrenfeld and Falkowski, 1997).

The first comprehensive set of productivity measurements in the NW Australian region were made by CSIRO oceanographers in the early 1960's (Jitts, 1969). These measurements are based upon natural populations incubated in filtered artificial light. Because of methodological differences, it is difficult to directly compare these early rate measurements with modern productivity measurements, though reported vertical distributions of productivity generally follow more recent measurements. These early results show that phytoplankton productivity in the Indian Ocean to the west of Scott Reef varied seasonally and that the euphotic zone could often be quite deep. Daily primary production in oceanic were estimated to range between 80 and 130 mg C m⁻².

The AIMS Biological Oceanography group made a number of productivity measurements at and near Scott Reef between 1993 and 1995 as part of other research activities using sites similar to those employed in this study. Measured production rates at deep-water sites near Scott Reef proper ranged between 544 and 1,109 mg C m⁻² d⁻¹ (mean = 765 ± 169 mg C m⁻² d⁻¹). This range is comparable to that measured on the June – July cruises (204 – 1,049 mg C m⁻² d⁻¹). Estimates of regional primary productivity based upon satellite ocean colour imagery are close to 670 mg C m⁻² d⁻¹ (~250 g C m⁻² year⁻¹, e.g. Behrenfeld et al., 2006).

Early measurements of oceanic primary production suggested that much of the oligotrophic tropical ocean was characterised by low rates of primary production (50 – 100 g C m⁻² year⁻¹ ~ 100 to 250 mg C m⁻² d⁻¹; e.g. Ryther, 1969). This led to the view of oligotrophic oceanic regions as 'oceanic deserts'. Gradual improvements in sampling and experimental methodologies have led to a general increase in measured production rates in these systems to levels exceeding 500 mg C m⁻² d⁻¹, even in the most oligotrophic oceanic systems (e.g. Laws et al., 1984, 1987; Jones et al., 1996). The carbon fixation rates measured in the vicinity of Scott Reef and along the continental margin of NW Australia average well above this value. Despite the apparent oligotrophy (low nutrient status) of surface waters along the seaward margin of the North West Shelf, primary production rates are reasonably high using modern techniques (Table 17). Measured primary production rates at continental margin sites bordering North West Cape and Ningaloo Reef range from 500 to 8,300 mg C m⁻² d⁻¹ (Furnas, 2007). This section of the shelf is characterised by intermittent upwelling activity due to strong wind stress from southwesterly winds, active vertical mixing due to internal wave activity and inter-annual variability in the thickness of the surface mixed layer due to changes in the strength of the Leeuwin Current. Under most conditions, oceanic primary production in the North West Cape region is dominated by picoplankton, though during the 1997 – 98 El Niño event, diatoms in the > 10 µm. Measured primary production rates at continental margin sites bordering North West Cape and Ningaloo

Measured bacterial production rates to date (31 – 102 mg C m⁻² d⁻¹) are at the low end of the range of bacterial production rates (10 – 1,100 mg C m⁻² d⁻¹ 1997/98 median = 620 mg C m⁻² d⁻¹; 1998/99 median = 110 mg C m⁻² d⁻¹) measured in continental slope waters bordering the southern North West Shelf (Furnas, 2007). Where useful profiles of bacterial production could be integrated (average = 46.6 mg C m⁻² d⁻¹) bacterial production averaged 7 percent of concurrent carbon fixation.

Table 17 A summary of historical primary production measurements (14C-based) from the Great Barrier Reef, oceanic Coral Sea and outer shelf waters of NW Australia.

Location	Range	Mean mg C m ⁻² d ⁻¹	Median	n	Source
Great Barrier Reef	32 – 5,564	784	631	186	Furnas and Mitchell, 1989, Furnas unpubl.
Coral Sea	117 – 3,033	599	356	35	Furnas and Mitchell, 1996
Continental slope (Jan–Feb, 1995)	380 – 1,904	767	644	16	Furnas, unpubl.
NW Cape (Continental slope)	356 – 8,303	1,962	999	23	Furnas, 2007
Scott Reef (1993)	544 – 841	712	725	7	Furnas, unpubl.
Scott Reef	204 – 1,330	848	872	13	This study

Sedimentation Fluxes

Vertical fluxes of organic matter (POC, PN) to the bottom of the central South Reef lagoon site (LA) and at the three deep-water time series sites (CH, NE and SW) were measured in parallel with all water column primary production experiments. The intent was to measure the proportion of water column primary production directly reaching benthic filter feeding communities in the lagoon and along the deep margins of Scott Reef, and at the deep sites, the vertical fluxes of organic matter supporting deep-living plankton communities. The downward material fluxes were measured with drifting (Lagrangian) trap arrays that drogue a particular water mass (Knauer et al., 1979). The trap arrays were suspended from a wave-compliant flotation that minimises vertical trap motion at depth due to a surface swell. The Lagrangian trap approach maximises vertical trapping efficiency by minimizing horizontal velocity shear across the mouth of the trap. This approach has been widely used in studies of vertical fluxes in pelagic systems [e.g. Bermuda Atlantic Time Series (BATS) and the Hawaiian Ocean Time Series (HOTS) stations].

At each production site, a trap array (12 traps) was deployed for 12 hours (06:00 – 18:00 local time). While longer deployments (24 hrs+) increase catches in the sub-traps, the short deployment used minimises artefacts associated with catches of vertically migrating zooplankton ('swimmers') and allowed us to avoid use of preservatives which complicate analytical protocols. Traps were deployed at 38 m in the lagoon (for a 50 m water column) to avoid trap groundings on shallow patch reefs ('bommies'). Deep water traps were deployed at 100 m near the bottom of the euphotic zone and below the mixed layer.

Measured downward carbon fluxes (Table 19) at all sites ranged between 2.1 and 7.1 mmol C m⁻² d⁻¹ (Fig. 64) with a mean of 3.9 ± 1.5 mmol C m⁻² d⁻¹. Within the South Reef lagoon, the carbon sedimentation fluxes ranged between 2.1 and 6.2 mmol C m⁻² d⁻¹ with a mean of 4.3 ± 1.5 mmol C m⁻² d⁻¹. For nitrogen, measured downward fluxes at all sites ranged between 0.06 and 0.48 mmol N m⁻² d⁻¹ (Fig. 65) with a mean of 0.26 ± 0.14 mmol C m⁻² d⁻¹. At the lagoon site, N fluxes (Table 20) varied between 0.12 and 0.46 mmol N m⁻² d⁻¹ with a mean of 0.25 ± 0.14 mmol C m⁻² d⁻¹. Mean fluxes at the four sites are given in Table 18. There were no statistical difference between mean fluxes at the four sites, or seasonally (winter vs summer), in the first case due to the small number of seasonal and site replicates. Estimates of concurrent phosphorus (P) and mass fluxes were often below the detection limits for the method, largely determined by variability in determination of blank values.

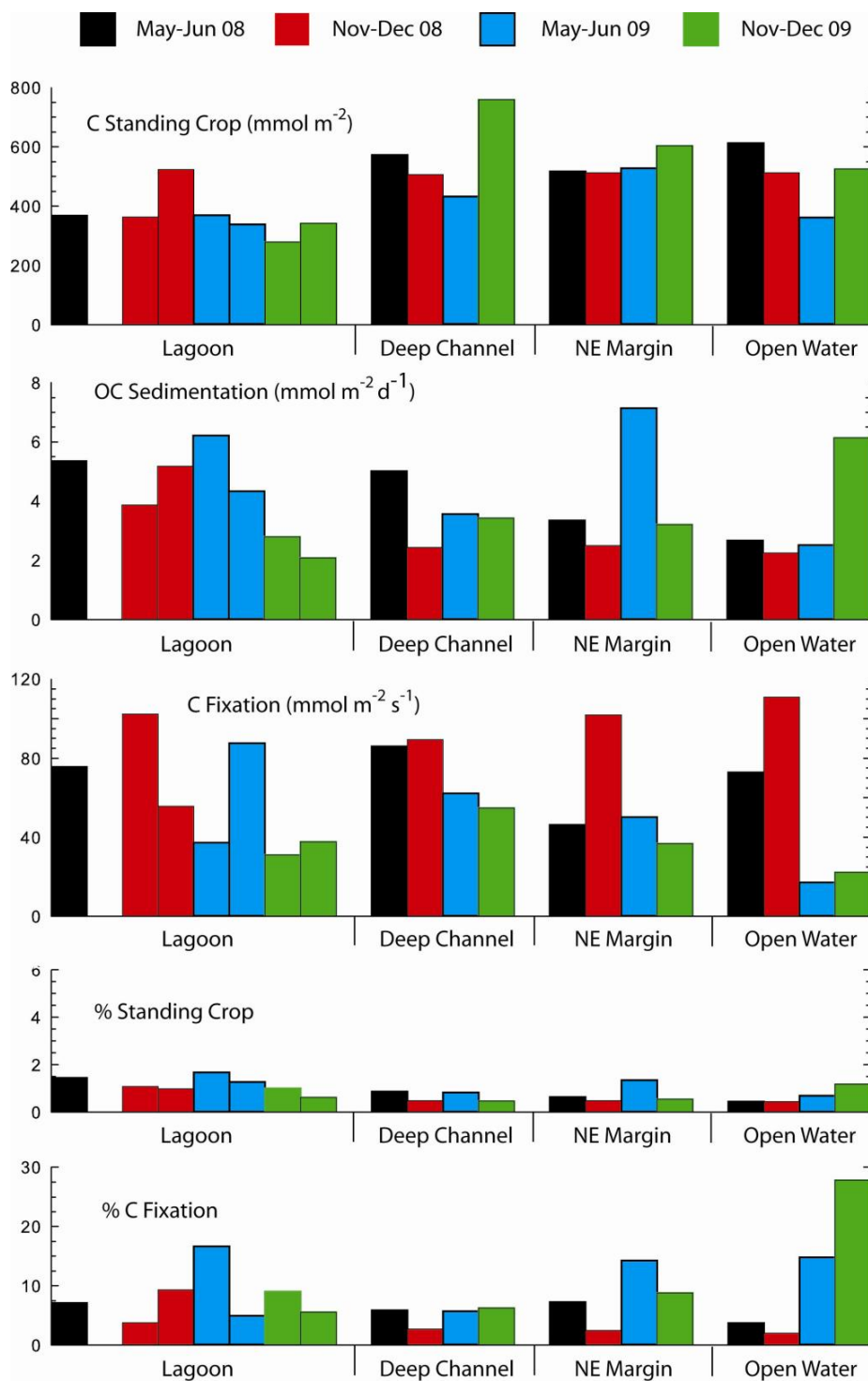


Fig. 64 Measured sedimentation fluxes of organic carbon (OC) from the water column or euphotic zone in relation to organic carbon standing crop and concurrent daily primary production (¹⁴C uptake). Lagoon fluxes and standing crop were calculated for a 50 m water column. Sedimentation fluxes and standing crop at the three deep-water sites were calculated for a 100 m euphotic zone.

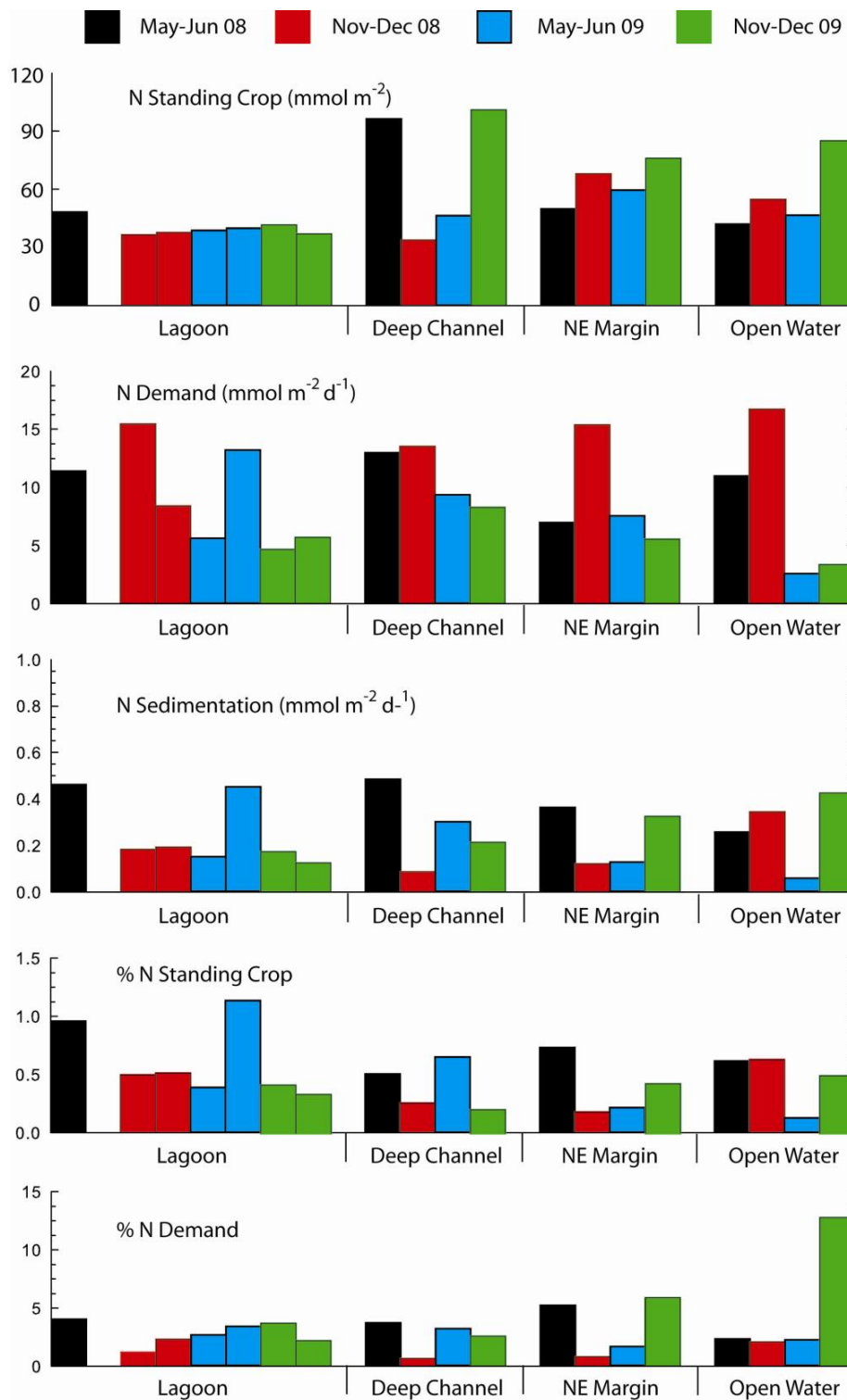


Fig. 65 Measured sedimentation fluxes of particulate nitrogen (N) from the water column or euphotic zone in relation to the particulate nitrogen standing crop and estimated concurrent daily N demand to support measured primary production (Redfield ratio from ¹⁴C uptake). Lagoon fluxes and standing crop were calculated for a 50 m water column. Sedimentation fluxes and standing crop at the three deep-water sites were calculated for a 100 m euphotic zone.

Measured carbon sedimentation fluxes at the four experimental sites ranged between 0.4 and 1.7 percent of the organic carbon standing crop in the lagoon water column (0 - 50 m) or the upper 100 m (mean = 0.9 ± 0.4 percent; Table 19), 1.6 to 15.8 percent of estimated phytoplankton biomass and 2.0 to 27.8 percent of concurrent daily primary production at that site (mean = 8.3 ± 6.3 percent; Table 19). There was no correlation between the phytoplankton biomass, C standing crop or primary production and the amount of C captured in the sediment traps.

Table 18 Average sedimentation (\pm 1 S.D.) fluxes of carbon and nitrogen at the four time series sites.

Site	C Flux ($\text{mmol m}^{-2} \text{d}^{-1}$)	N Flux ($\text{mmol m}^{-2} \text{d}^{-1}$)
Lagoon (LA)	4.3 ± 1.5	0.25 ± 0.14
Deep Channel (CH)	3.6 ± 1.1	0.27 ± 0.17
NE Margin (NE)	4.7 ± 1.8	0.25 ± 0.11
Open Water (SW)	3.4 ± 1.8	0.27 ± 0.16

Table 19 Measured carbon sedimentation fluxes in and around Scott Reef in relation to the organic carbon standing crop, primary production and estimated respiratory consumption of carbon by water column micro-organisms. Fluxes are based on 12-hr daytime trap deployments.

Site	Date	Depth (m)*	Carbon Standing Crop (mmol m ⁻²)	Primary Production** (mmol C m ⁻² d ⁻¹)	Respiratory Losses (mmol C m ⁻² d ⁻¹)	C Sedimentation Flux (mmol C m ⁻² d ⁻¹)	C Sedimented as % of Standing Crop	C Sedimented as % of Primary Production
Lagoon	June 2008	35/50+	367.3	75.4	128.3	5.34	1.5	7.1
	Dec 2008	35/50+	362.4	102.2	170.7	3.88	1.1	3.8
	June 2009	35/50+	522.7	55.7	151.6	5.18	1.0	9.3
	June 2009	35/50+	369.2	37.2	105.1	6.21	1.7	16.7
	Nov 2009	35/50+	339.1	87.4	93.0	4.34	1.3	5.0
Deep Channel	June 2008	102	572.6	86.0	177.6	5.01	0.9	5.8
	Dec 2008	102	506.0	89.4	150.2	2.44	0.5	2.7
	Nov 2009	102	758.6	54.7	131	3.43	0.5	6.3
NE Margin	June 2008	102	517.1	46.2	162.3	3.34	0.6	7.2
	Dec 2008	102	513.2	101.8	194.7	2.49	0.5	2.4
	Nov 2009	102	604.2	36.6	182.0	3.43	0.5	8.8
Open Water	June 2008	102	612.0	72.7	131.2	2.68	0.4	3.7
	Dec 2008	102	512.4	110.8	146.7	2.25	0.4	2.0
	Nov 2009	102	526.6	22.1	134.7	6.14	1.2	27.8

*Lagoon traps were set at 35 m to avoid grounding on bommies. Fluxes are corrected for the full water column depth. Deepwater traps were set at the base of the euphotic zone.

** Derived from ¹⁴C uptake experiments.

Table 20 Measured nitrogen sedimentation fluxes in and around Scott Reef in relation to the organic nitrogen standing crop and primary production. Fluxes are based on 12-hr daytime trap deployments.

Site	Date	Depth (m)*	Nitrogen Standing Crop (mmol m ⁻²)	N Demand** (mmol N m ⁻² d ⁻¹)	N Sedimentation Flux (mmol N m ⁻² d ⁻¹)	N Sedimented as % of Standing Crop	N Sedimented as % of Primary Production
Lagoon	June 2008	35/50+	48.2	11.4	0.46	1.0	4.1
	Dec 2008	35/50+	36.5	15.4	0.18	0.5	1.2
		35/50+	37.7	8.4	0.19	0.5	2.3
	Jun 2009	35/50+	38.8	5.6	0.15	0.4	2.7
		35/50+	39.9	13.2	0.45	1.1	3.4
	Nov 2009	35/50+	144.9	4.7	0.17	0.4	3.7
Deep Channel	June 2008	102	129.4	5.7	0.12	0.3	2.2
		102	96.4	13.0	0.48	0.5	3.7
	Dec 2008	102	33.6	13.5	0.09	0.3	0.6
NE Margin	Jun 2009	102	46.5	9.4	0.30	0.7	3.2
	Nov 2009	102	353.8	8.3	0.21	0.2	2.6
	June 2008	102	49.9	7.0	0.36	0.7	5.2
Open Water	Dec 2008	102	68.0	15.4	0.12	0.2	0.8
	Jun 2009	102	59.6	7.6	0.13	2.2	3.2
	Nov 2009	102	267.1	5.5	0.33	1.5	2.6
Open Water	June 2008	102	42.0	11.0	0.26	0.6	2.4
	Dec 2008	102	54.6	16.7	0.34	0.6	2.1
	Jun 2009	102	46.6	2.6	0.06	0.1	2.3
	Nov 2009	102	270.1	3.3	0.43	0.5	12.8

*Lagoon traps were set at 35 m to avoid grounding on bommies. Fluxes are corrected for the full water column depth. Deepwater traps were set at the base of the euphotic zone.

** Derived from ¹⁴C uptake experiments and assumed Redfield composition of phytoplankton

For nitrogen, measured sedimentation fluxes of organic N ranged between 0.2 and 2.2 percent of the PON standing crop in the lagoon water column (0 - 50 m) or the upper 100 m (mean = 0.49 ± 0.26 percent; Table 20). PON sedimentation fluxes ranged between 0.34 and 9.1 percent of estimated phytoplankton biomass and 0.8 to 12.8 percent (mean = 3.3 ± 2.7 percent; Table 20) of estimated daily N demand derived from concurrent primary production [C fixation $\times (16/106)$]. At the central South Reef lagoon site, measured PON sedimentation fluxes averaged 2.7 ± 2.2 percent, 0.6 ± 0.3 percent and 2.8 ± 1.0 percent of phytoplankton nitrogen biomass, PON standing crop in the water column and estimated N demand by plankton, respectively.

Table 21 Average of the ratios of measured sedimentation fluxes of carbon (± 1 S.D.) relative to estimated phytoplankton biomass, water column C standing crop above the trap and daily carbon fixation at the four time series sites.

Site	C Flux as % of C biomass	C Flux as % of C standing crop	C Flux as % of daily ¹⁴ C fixation
Lagoon (LA)	8.3 ± 3.8	1.2 ± 0.3	8.0 ± 4.3
Deep Channel (CH)	7.0 ± 6.8	0.7 ± 0.2	5.1 ± 1.6
NE Margin (NE)	6.2 ± 3.4	0.8 ± 0.4	8.8 ± 3.9
Open Water (SW)	6.4 ± 6.4	0.7 ± 0.3	12.0 ± 11.9

^a Estimated from C/Chl ratio = 50 g/g

Table 22 Average of the ratios of measured sedimentation fluxes of nitrogen (± 1 S.D.) relative to estimated phytoplankton biomass, water column N standing crop above the trap and daily nitrogen demand due to primary production (N/C demand = 16/106) fixation at the four time series sites.

Site	N Flux as % of N biomass	N Flux as % of N standing crop	N Flux as % of daily N demand
Lagoon (LA)	2.7 ± 1.7	0.6 ± 0.3	2.8 ± 1.0
Deep Channel (CH)	3.3 ± 4.0	0.4 ± 0.2	2.6 ± 1.4
NE Margin (NE)	1.9 ± 1.3	0.4 ± 0.2	3.4 ± 2.5
Open Water (SW)	2.5 ± 2.4	0.5 ± 0.2	4.9 ± 5.3

Fig. 66 shows how water column primary production and sedimentation flux measurements made at Scott Reef compare with similar measurements at two time series sites in the Pacific (HOTS) and Atlantic (BATS) Oceans. The HOTS (Hawaii Ocean Time Series) station is located north of the Hawaiian Islands and has been occupied on a quasi-monthly basis since October 1988. The BATS station (Bermuda Atlantic Time Series), located near Bermuda in the Sargasso Sea, has been occupied on a similar schedule. During most sampling events at both sites, simultaneous, or near-simultaneous measurements of sedimentation fluxes from the euphotic zone and primary production have been made. While comparable, it is important to remember that the rates are derived in slightly different manners. The Scott Reef trap fluxes are based on 12-hr trap deployments at 100 m and productivity measurements on 4-hour incubations to depths close to 100 m. In contrast, the HOTS and BATS measurements are based on 2 – 3 day trap deployments at 150 m and 12-hour production measurements over a deeper stratum of 140 m (BATS) or 150 m (HOTS).

On three of the four research cruises, measured sedimentation fluxes and areal production rates fell within the envelope of rates observed at the HOTS and BATS stations. The December 2008 cruise, where the thermocline extended to the near-surface layer, was characterised by higher productivities and low sedimentation fluxes, especially of nitrogen. Reasons for these low fluxes for the levels of productivity are as yet, unresolved. The similarity in rates clearly indicates that the outer-shelf environment surrounding Scott Reef is behaving like a typical oligotrophic oceanic environment.

Overall, the sedimentation flux measurements confirm the general findings of the water column metabolism measurements – that most of the biomass and organic matter created within the water column by primary producers is quickly consumed and recycled within the water column. Only a small portion of the fixed organic matter sediments to the bottom of the lagoon or through the thermocline into deeper water. Sedimentation fluxes of C and N averaged 0.7-1.2 percent and 0.4-0.6 percent of the water column standing crop of C and N, or 5-12 percent and 2.4-3.4 percent of daily primary production. There was no evidence of enhanced pelagic production of organic matter suitable for ready capture by benthic filter feeders and detritus feeders in the lagoon or in waters immediately surrounding Scott Reef.

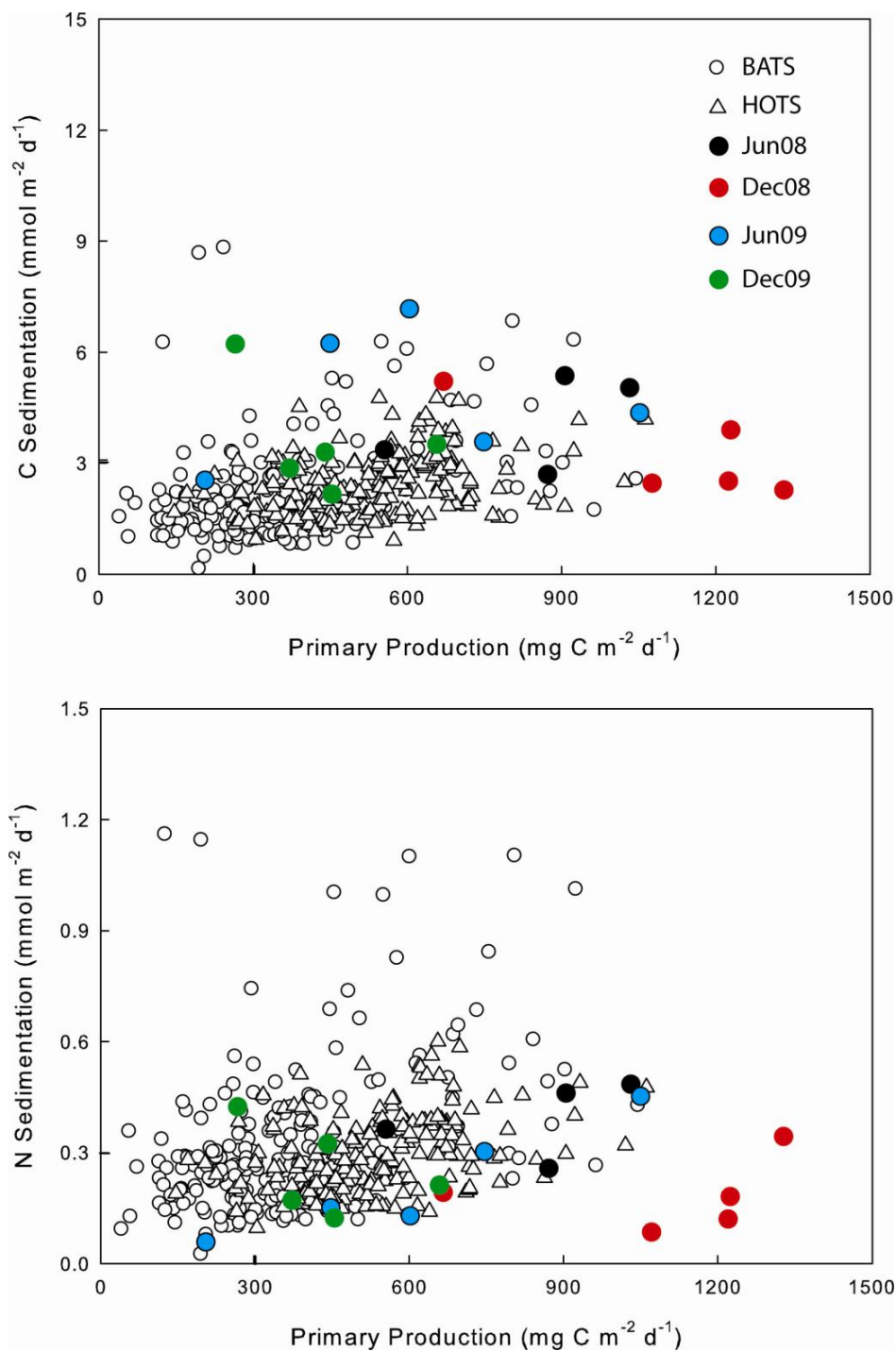


Fig. 66 A comparison between measured areal primary production rates and sedimentation fluxes of carbon and nitrogen at Scott Reef and rates measured using similar methods at the HOTS and BATS time series stations.

Zooplankton of Scott Reef waters

At each of the four time series sites (LA, CH, NE and SW; Fig. 1), single zooplankton hauls were made four times per day with plankton nets made of 100 μ m mesh. At the three deep sites (CH, NE,

SW), stratified samples were taken with a Hydrobios multinet system, which has 5 nets that can be programmed to open at different depth intervals. For this series of samples, sampling depth intervals were set to be nominally 400 – 300 m, 300 – 200 m, 200 – 100 m, 100 – 50 m (containing the chlorophyll maximum), and 50 m to the surface (surface mixed layer). Within the lagoon of South Reef the water depth was ~55 m, which was too shallow to obtain accurate stratified samples. In June 2008 we integrated the results of multinet samples from discrete depths, and on subsequent trips we used a bongo net equipped with WP-2 nets of 100 μ m mesh to sample the zooplankton in the entire water column in the shallower waters of the lagoon. All nets were equipped with flowmeters to facilitate the calculation of the volume of water filtered, and hence the volume-specific abundance or biomass of plankton. The resultant samples were split into two fractions, one of which was filtered on to a pre-weighed mesh and frozen for later measurement of biomass, as dry weight. The other fraction was preserved in formalin so that the zooplankton community composition could be determined by microscopic analysis in the laboratory.

Zooplankton Biomass

Zooplankton biomass differed significantly with both cruise and site (ANOVA; Table 23). Comparison of the F ratios from this analysis reveals that the effect of site is by far the largest, and that though the interaction of these main effects is significant, it is small in comparison to the main effects.

Table 23 Results of 2 way ANOVA on cruise, site, and zooplankton biomass (mg dry weight m^{-3}) in the top 50m of the water column, assuming no diel change in biomass i.e. treating the four samples taken at each site as replicates.

	Df	Sum Sq	Mean Sq	F value	P value
Cruise	3	6.216	2.072	14.371	<0.0001
Site	3	25.642	8.547	59.286	<0.0001
Cruise*Site	9	2.703	0.300	2.083	0.036
Residuals	126	18.166	0.144		

Biomass at the Lagoon site (LA) was 2 – 3 fold higher than in the mixed layer at the Channel site (CH), NE margin site (NE) or Open Water site (SW) in both seasons ($t=8.398$, $df=40$, p -value= <0.0001), and biomass was significantly higher in the wet season (November – December) than in the dry season (June) of both sampling years (2008 and 2009; Table 24; $t=2.085$, $df=240$, p -value= 0.038). Conditions within the lagoon allowed the development of large populations of Larvaceans (see below), and it is most likely that these animals and their discarded mucous ‘houses’ were responsible for the higher biomass observed.

Table 24 Mean (\pm SD) $>100 \mu$ m plankton biomass (mg dry weight m^{-3}) at Scott Reef. Data represent samples taken from the Lagoon site (LA), compared to the mixed layer (<100 m) and deeper water (>100 m) at the Channel site (CH), NE margin site (NE) and Open Water site (SW) at 4 times during the 24h time series.

	June 2008	December 2008	June 2009	December 2009
LA	18.2 \pm 6.2	30.8 \pm 9.2	18.5 \pm 4.6	41.5 \pm 23.3
CH,NE,SW <100 m	8.5 \pm 2.0	10.8 \pm 4.0	6.7 \pm 2.5	12.2 \pm 3.7
CH,NE,SW >100 m	1.7 \pm 0.3	2.3 \pm 1.1	1.7 \pm 1.0	2.4 \pm 1.1

way ANOVA of the biomass data from the multinet hauls comparing the main effects of cruise, site and depth stratum on biomass revealed that the strongest effect was that of depth (by comparing the magnitude of the F ratios, as above), with cruise the next strongest effect. At the three deep

water sites, though biomass in the mixed layer (~ the top 100 m) was lower than that of the lagoon, biomass in the depth strata below the mixed layer dropped to $< 3 \text{ mg m}^{-3}$ (Table 25, Fig. 67).

Table 25 Results of 3 way ANOVA on cruise, site, depth and zooplankton biomass from multinet samples taken at the Channel (CH), NE margin (NE) and Open Water (SW) sites, assuming no diel change in biomass i.e. treating the four samples taken at each site as replicates.

	Df	Sum Sq	Mean Sq	F value	P value
Cruise	3	8.197	2.732	22.775	<0.0001
Site	2	0.902	0.451	3.757	<0.0001
Depth	4	157.528	39.382	328.256	<0.0001
Cruise*Site	6	2.168	0.361	3.011	0.008
Cruise*Depth	12	2.912	0.243	2.023	0.024
Site*Depth	8	3.515	0.439	3.663	<0.0001
Cruise*Site*Depth	24	1.862	0.078	0.647	0.896
Residuals	189	22.675	0.120		

The interpretation of biomass patterns through the water column should be interpreted with caution, since any apparent differences may also be related to advection/retention of plankton. With this in mind, there is no convincing indication of biomass change between day and night as a result of diurnal vertical migration.

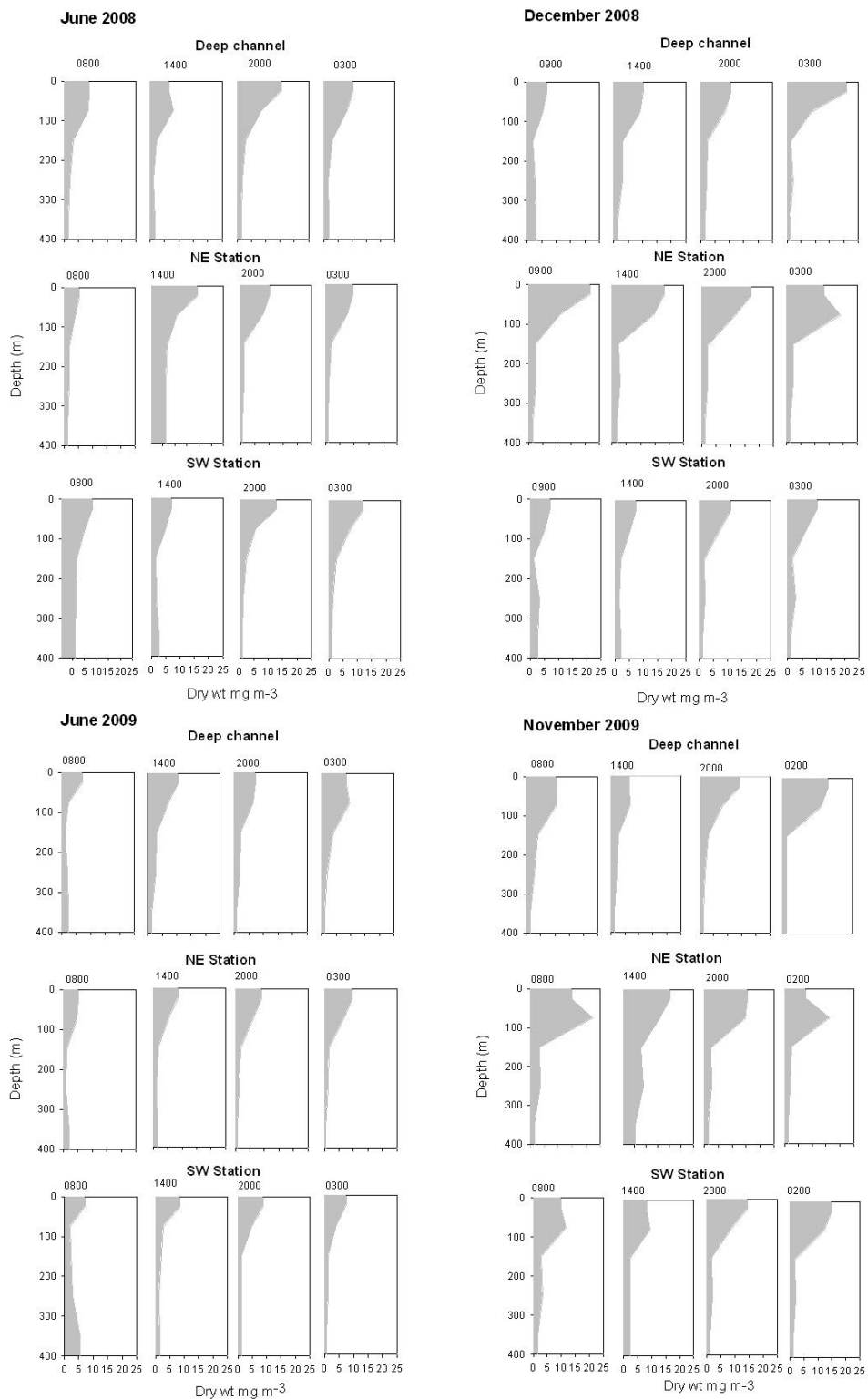


Fig. 67 Depth distribution of >100 μm zooplankton biomass at Deep Channel site, NE margin site and Open Water site (SW) for the four cruises at Scott Reef.

Zooplankton abundance

Total zooplankton abundance in the mixed layer differed significantly with site (ANOVA; Table 26), but in contrast to the biomass data there was no difference in abundance between cruises. Though the interaction of these main effects is significant, comparison of the F ratios from this analysis reveals that the effect of the interaction term is small in comparison to that of site.

Table 26 Results of 2 way ANOVA on cruise, site and total zooplankton abundance (no. m⁻³) in the top 50 m of the water column, assuming no diel change in abundance.

	Df	Sum Sq	Mean Sq	F value	P value
Cruise	3	0.506	0.169	1.298	0.283
Site	3	13.036	4.345	33.456	<0.0001
Cruise*Site	9	3.028	0.336	2.590	0.013
Residuals	62	8.053	0.130		

On all cruises but the first, the abundance of the total mixed layer (i.e. <100 m) >100 µm zooplankton at the Lagoon site (LA) was greater than the other sites ($t=6.816$, $df=12$, p value=<0.0001), whilst the abundance at the Open Water site (SW) was the lowest on all cruises (Table 27; $t=-6.8202$, $df=63$, p value=<0.0001). Abundance at the Channel (CH) and NE margin (NE) sites was similar on all cruises ($t=0.553$, $df=29$, p value=0.584). The abundance data has large variance as a result of natural plankton patchiness, combined with both sampling and subsampling error in calculation of actual field abundances. Interestingly, the samples collected in June 2008 had a very high incidence of zooplankton that were apparently dead at the time of collection. This was especially the case at the Lagoon site (LA), where 11.5% of the plankton were carcasses, double the proportion at the other sites on this cruise. On subsequent cruises, though carcasses did occur, they seldom represented a significant proportion of the sample. The occurrence of a high percentage of carcasses in zooplankton samples has been known since the 1960's (see Table I in Elliott and Tang, 2009), but the reason for their occurrence is not well understood. In the present case, it is tempting to speculate that the period of very rough weather preceding the cruise may be connected, and may also account for the lower zooplankton abundance observed at the Lagoon site (LA) on this cruise.

Table 27 Mean ± SD zooplankton abundance (no. m⁻³) in the mixed layer at each site on each cruise.

Site	June 2008	Dec 2008	Jun 2009	Nov 2009
LA	3058 ± 1030	9777 ± 2549	6208 ± 390	6138 ± 939
CH	5337 ± 3245	3333 ± 791	2885 ± 283	3379 ± 1182
NE	3660 ± 1812	4398 ± 776	2367 ± 419	3278 ± 975
SW	2145 ± 876	2110 ± 551	1976 ± 725	1843 ± 504

Summer abundances of >100 µm zooplankton in the mixed layer at Scott Reef ranged between 1843 and 9777 organisms m⁻³. By comparison, the abundance of >73 µm zooplankton in the 0 – 60 m stratum at a shelf break site near NW Cape was ~10,000 m⁻³ (McKinnon and Duggan, 2003), which is similar to that at the Lagoon site (LA), but higher than the other sites. The lower abundance at the deep water sites near Scott Reef reflects the more oceanic conditions experienced by this atoll, though the difference in mesh size of the plankton nets also affects the comparison.

As was the case with the biomass samples, zooplankton numerical abundance was significantly higher within the mixed layer than below it at the three deep sites (Table 28; $t=11.862$, $df=65$, p -value=<0.0001).

Table 28 Mean \pm SD zooplankton abundance (no. m^{-3}) in each depth stratum sampled by the multinet.

Depth stratum	Abundance
0-50m	3,234 \pm 1,470
50-100m	1,797 \pm 1,276
100-200m	553 \pm 170
200-300m	399 \pm 104
300-400m	288 \pm 261

Zooplankton community composition

Mixed layer zooplankton, as sampled by the bongo net at the Lagoon site (LA) or by the Multinet in the top 100 m of the other sites, was overwhelmingly dominated by copepods (Fig. 68). Overall, copepods comprised 91% of plankton numbers, with Larvacea the next most abundant group (4%).

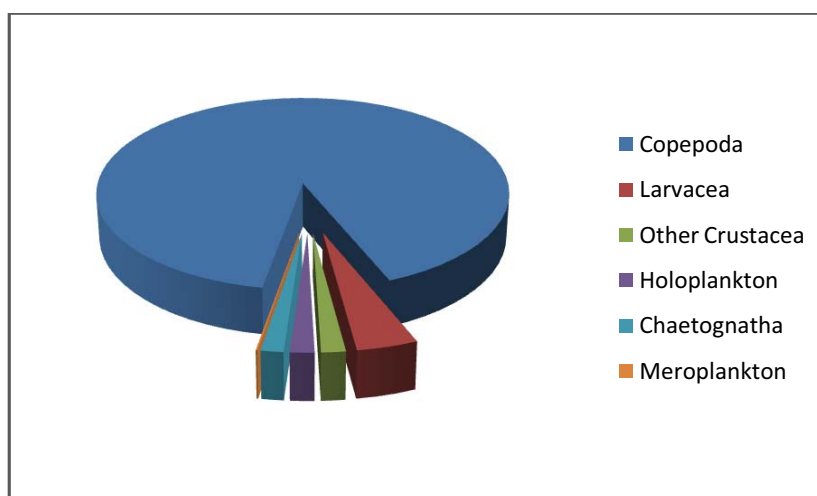


Fig. 68 Composition of mixed layer zooplankton at Scott Reef.

At the Lagoon site (LA), calanoid and cyclopoid (excluding Oncaeidae) copepods dominated the plankton in June 2008 (Fig. 69), and there was a \sim 2-fold difference in plankton abundance over the 24 hour period, which may be related to the tides. Larvaceans were the most important of the non-copepod plankton. At the Lagoon site (LA) in December of 2008 (Fig. 70), there was a bloom of larvaceans, the most common group of pelagic tunicates. The bloom appears to comprise mostly *Fritillaria* species.

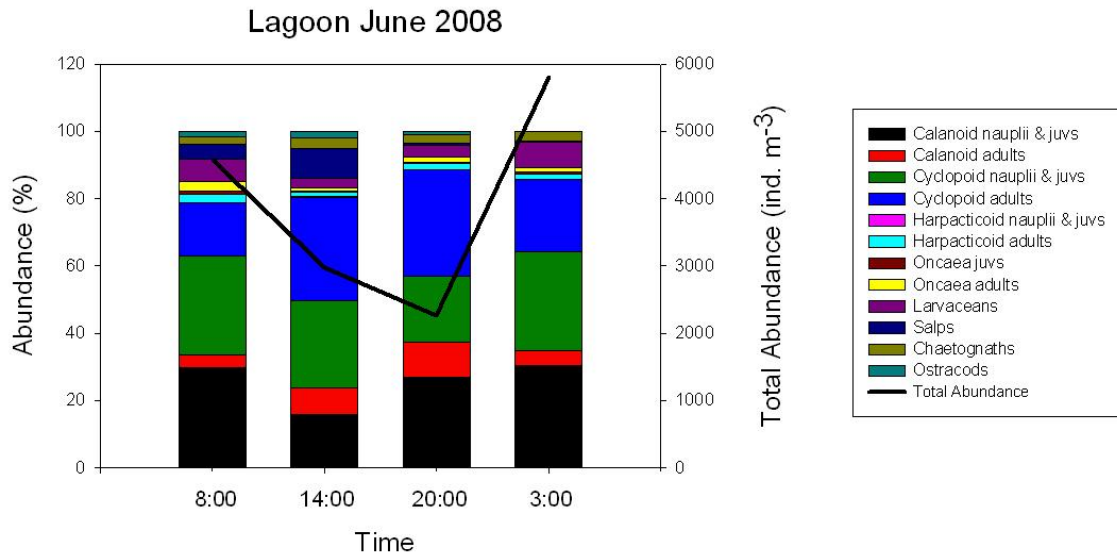


Fig. 69 Composition and total abundance of the zooplankton over 24 hr at the Lagoon site (LA) in June 2008.

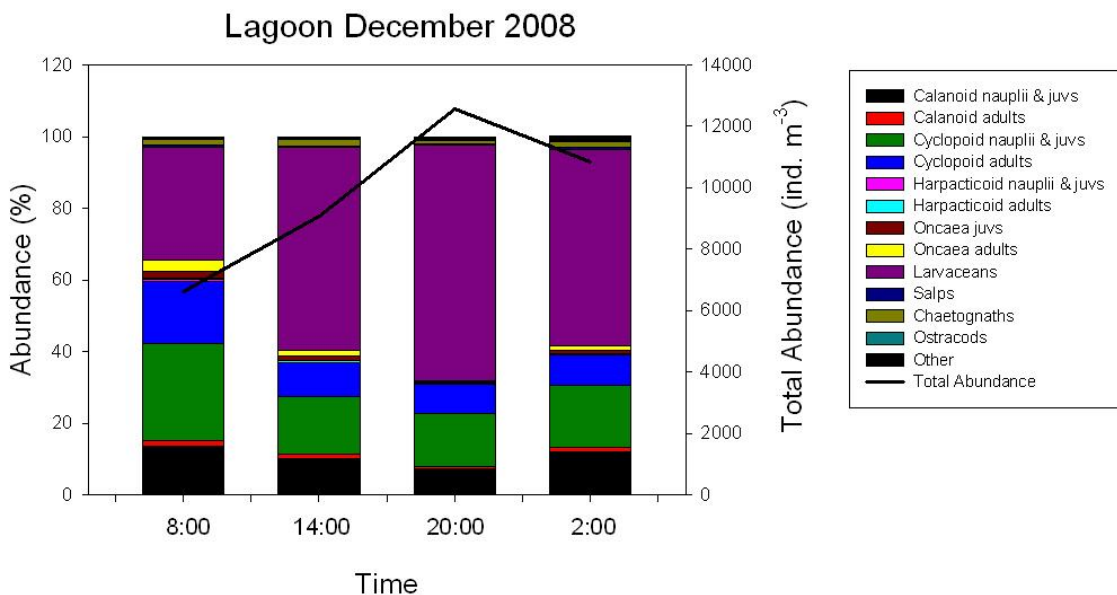


Fig. 70 Composition and total abundance of the zooplankton over 24 hr at the Lagoon site (LA) in December 2008.

Though we know that two genera of Larvacea are common at Scott Reef (*Oikopleura* and *Fritillaria*), the discrimination of species within these genera is not easy, and we have preferred to lump all larvaceans in our counts. However, these animals are of some interest, because they are mucous-net feeders and are therefore capable of grazing directly on picoplankton. Larvaceans construct a ‘house’ out of mucous, which includes intricate mesh structures that exclude large plankton and allow the animals to concentrate picoplankton on to their internal filters. Periodically the meshes become clogged, resulting in the animal abandoning the house and constructing a new one. The discarded houses become ideal substrates for microbial growth, and are one of the main sources of ‘aggregates’ of organic material, or ‘marine snow’. These large particles are likely to be responsible for the mismatches between biomass and abundance data described earlier, since they clog the biomass filters, giving a higher measurement of zooplankton biomass than would be expected from

the zooplankton abundance data. In addition, larvaceans are capable of feeding on picoplankton, and are known to have some of the highest growth rates of any metazoan. Consequently these animals may have a disproportionately high contribution in terms of total community secondary production. In a recent publication, Jaspers et al. (2009) found that larvaceans comprised a large proportion of the summer plankton in the Indian Ocean, and suggest that in terms of total production these animals will exceed the contribution of copepods. Larvaceans also 'short circuit' the microbial loop by capturing picoplankton production into their tissues and their mucous houses, both of which are then available to large predatory copepods.

Below the mixed layer, the dominance of copepods becomes even more marked than in the mixed layer (Fig. 71). We found little evidence of differences in community composition with time of day, or between locations. The community composition of the mixed layer resembled that observed in the lagoon (LA), though there was a proportionally higher contribution of larvaceans to the plankton in the surface layers, especially at the Lagoon site (LA). At the deep water sites the plankton composition changed markedly with depth, mostly because of the increasing dominance of the family Oncaeiidae with depth. Because of the fine mesh nets used (100 μm), juvenile copepods (nauplii and copepodites) were by far the largest components of the plankton. It is not possible to routinely discriminate juvenile stages of copepods below the level of order, so our knowledge of the species composition of the copepod community comes from the adult copepod fraction only.

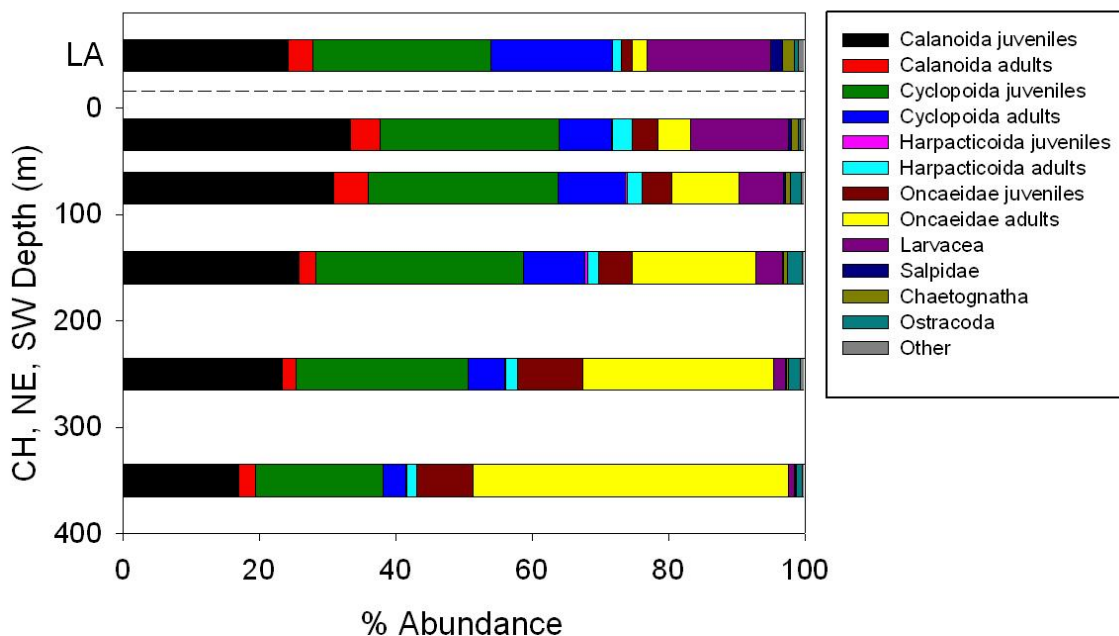


Fig. 71 Composition of the zooplankton community at the Lagoon site (LA), contrasted with that in the 5 depth strata sampled at the Channel (CH), NE margin (NE) and Open Water (SW) sites. The data are pooled over all Locations and Cruises. Calanoida, Cyclopoida and Harpacticoida are orders of copepods, and Oncaeiidae is a family of Cyclopoida. Note that this graphic presents % contribution, and there is an order of magnitude difference in abundance from the mixed layer (<100 m) to the 300 – 400m stratum (Table 28).

In designing the zooplankton sampling program, we made the decision to use 100 μm mesh nets, since tropical copepods are smaller than those in temperate ecosystems, where standard plankton sampling protocols recommend the use of 200 μm mesh nets. Our experience from previous research programs has confirmed that most of the dominant species of copepods pass through plankton nets of this size. Nevertheless, our use of fine mesh nets influenced the community composition of the plankton in our samples, and does place focus on the smaller species of the mesozooplankton. The most important family was the Oncaeidae (Fig. 72), a predominately mesopelagic family of small copepods, many of which are <400 μm long as adults. The next most important families were the harpacticoid family Ectinosomatidae, which is mainly represented in our samples by the genus *Microsetella*, which is very common in surface waters and has the ability to graze on cyanobacteria such as *Trichodesmium*, which is toxic to other grazers. The family Oithonidae is an extremely common family in the epipelagic ocean, and includes species thought to be the most abundant on the planet. The remaining copepod families all belong to the order Calanoida, the pelagic specialists of the copepod world.

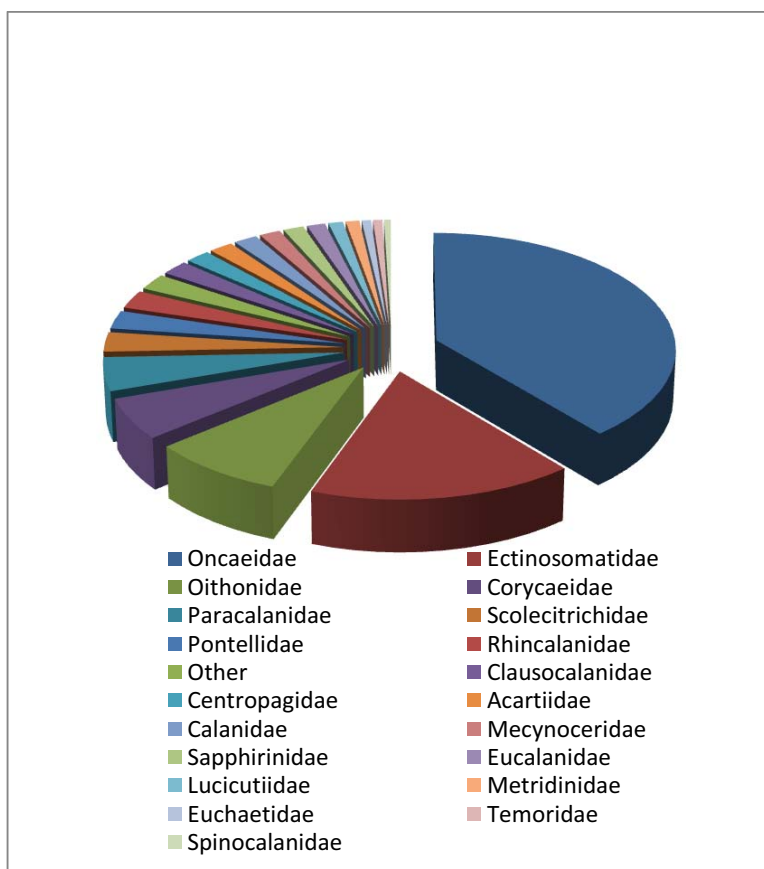


Fig. 72 Composition of the Scott Reef copepod community by family.

Biodiversity of the Copepoda

At Scott Reef, we have identified over 220 species of copepods, belonging to 5 of the 9 orders (Table 29). Other plankton have been identified to higher taxonomic units. For the copepods, some taxa are listed as species groups, since these represent closely related species that current taxonomy does not allow to be differentiated. Of the 220 species, 68 (31%) are new records for Australian waters and at least 14 are likely to be undescribed (i.e. new species). We are currently describing two new species of the calanoid family Aetideidae (Fig. 73). The family Oncaeidae has the greatest number of species of any of the copepod families recorded at Scott Reef. This hitherto unappreciated biodiversity within the family Oncaeidae alone is remarkable, and appears to comprise >65 species. We were only able to achieve this level of taxonomic resolution by collaboration with

the world expert on the group, Dr. Ruth Böttger-Schnack. However, because of this taxonomic complexity, analysis to species level was only possible for four of the deep sites, all at the Open Water site (SW), comprising day night pairs from June and December 2009 (i.e. 20 samples, taking into account the 5 depth strata) as well as all samples from the Lagoon site (LA) (i.e. 16 samples).

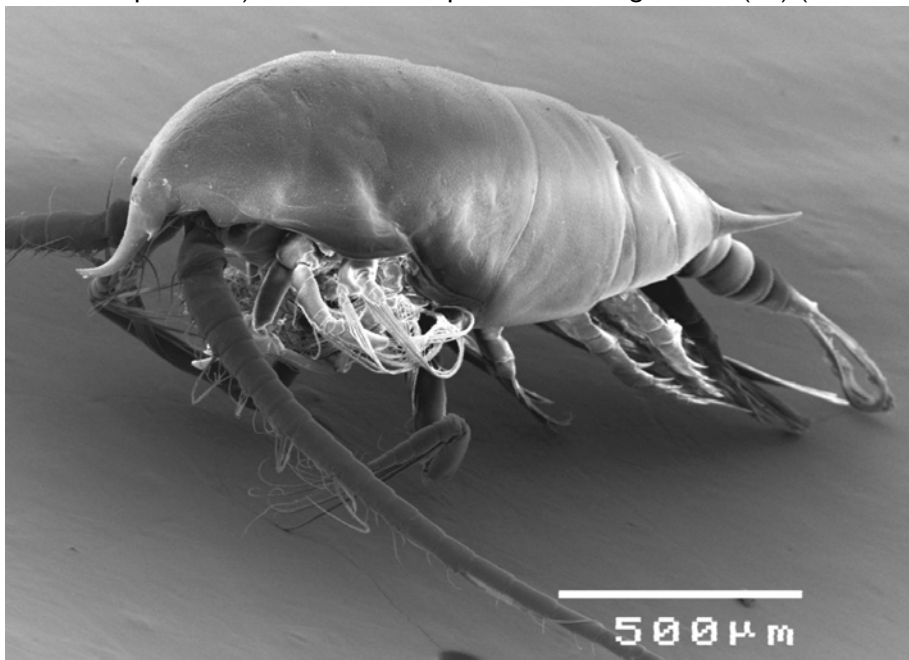


Fig. 73 A new species of the copepod genus *Aetideopsis* from the Channel site (CH).

Vertical distribution of trophic types

Copepod species were allocated to 3 trophic categories; suspension feeders, which graze on all forms of suspended particles including phytoplankton, detritus and microzooplankton; detritivores, which feed on aggregates of organic material ('marine snow'); and carnivores, which actively predate other zooplankton. The distribution of these categories was structured vertically, with suspension feeders dominating in the mixed layer and detritivores dominating in deeper waters. Carnivores were equally distributed throughout the water column. The dominance of suspension feeders in the mixed layer reflects the closer trophic coupling of the zooplankton to the primary producers in the productive surface layers. It is most likely that microzooplankton, the most important grazers of phytoplankton, form the bulk of the diet of mesozooplankton, and that phytoplankton cells represent only a minor part of the diet.

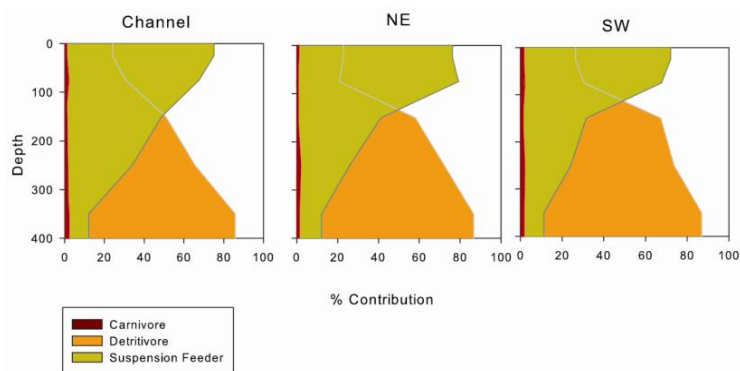


Fig. 74 The vertical distribution of copepods belonging to 3 trophic categories at deep sites around Scott Reef. Channel = Deep Channel site, NE = NE margin site, SW = Open Water site.

Table 29 Taxonomic units identified within the Copepoda.

Higher taxa are in bold, unbolded taxa are species or species groups (see text). Species listed in blue are new records for Australian waters, and those in red are putative new species.

ORDER:**CALANOIDA****Superfamily****Arietelloidea****Arietellidae***Arietellus pavoninus**Arietellus aculeatus**Metacalanus aurivilli***Augaptilidae***Augaptilus longicandatus**Euaugaptilus palumbii**Haloptilus acutifrons**Haloptilus longicornis**Haloptilus spiniceps**Haloptilus* spp*Paraugaptilus similis***Heterorhabdidae***Heterorhabdus papilliger**Heterorhabdus* spp.**Lucicutiidae***Lucicutia clausi**Lucicutia flavicornis**Lucicutia gemina**Lucicutia ovalis**Lucicutia bicornuta***Metridiidae***Metridia princeps**Pleuromamma**abdominalis**Pleuromamma**abdominalis fedentata**Pleuromamma borealis**Pleuromamma gracilis**Pleuromamma indica**Pleuromamma piseki**Pleuromamma**quadrangulata**Pleuromamma robusta**Pleuromamma* spp.*Pleuromamma xiphias***Nullosetigeridae***Nullosetigera giesbrechti**Nullosetigera helgae***Superfamily****Calanoidea****Calanidae***Calanus minor**Canthocalanus pauper**Cosmocalanus darwini**Mesocalanus tenuicornus**Nannocalanus minor**Neocalanus gracilis**Neocalanus tonsus**Undinula darwini**Undinula vulgaris***Megacalanidae***Megacalanus longicornis***Mecynoceridae***Mecynocera clausi***Paracalanidae***Acrocalanus gibber**Acrocalanus gracilis**Acrocalanus monachus**Bestiolina similis**Calocalanus gracilis* type*Calocalanus pavo**Calocalanus pavininus**Calocalanus* sp. 2*Calocalanus* sp. 3*Calocalanus plumulosus**Delibus* sp.*Paracalanus aculeatus**Paracalanus aculeatus**minor**Paracalanus indicus**Paracalanus indicus* (small morph)*Paracalanus nanus**Paracalanus* sp.*Parvocalanus crassirostris**Parvocalanus dubia***Superfamily****Clausocalanoidea****Aetideidae***Aetideus australis**Aetideus giesbrechti**Aetideopsis* sp.1*Aetideopsis* sp.2.*Chiridius poppei**Chiridius* sp.*Chirundina streetsi**Euchirella pulchra**Gaetanus purgens**Undeuchaeta plumosa***Clausocalanidae***Clausocalanus arcuicornis**Clausocalanus brevipes**Clausocalanus farrani**Clausocalanus furcatus**Clausocalanus jobei**Clausocalanus minor**Clausocalanus paululus**Clausocalanus pergens***Euchaetidae***Euchaeta indica**Euchaeta marina**Euchaeta media**Euchaeta rimana***Scolecitrichidae***Macandrewella* sp.*Scolecithricella* sp.*Scolecithrix bradyi**Scolecithrix danae**Scottocalanus helenae**Scottocalanus persecans**Scottocalanus* sp.**Stephidae***Stephos maculosus***Superfamily****Diaptomoidea****Acartiidae***Acartia danae**Acartia erythraea**Acartia fossae**Acartia negligens**Acartia pacifica***Candaciidae***Candacia aethiopica**Candacia bipinnata**Candacia bispinosa**Candacia catula**Candacia longimana**Candacia pachydactyla**Candacia simplex***Centropagidae***Centropages furcatus**Centropages gracilis**Centropages orsinii***Pontellidae***Calanopia aurivilli**Calanopia elliptica**Labidocera acuta**Labidocera laevidentata**Pontella securifer**Pontellina plumata***Pseudodiaptomidae***Pseudodiaptomus* sp**Temoridae***Temora discaudata**Temoropia minor***Superfamily****Eucalanoidea****Eucalanidae**

Eucalanus elongata
Subeucalanus crassus
Subeucalanus mucronatus
Subeucalanus pileatus
Subeucalanus subcrassus

Rhincalanidae

Rhincalanus cornutus
Rhincalanus nasutus
Rhincalanus rostrifrons

Superfamily

Spinocalanoidea

Spinocalanidae

Spinocalanidae sp. 1.
Spinocalanidae sp. 2.
Spinocalanidae sp.3.

ORDER:

CYCLOPOIDA

Corycaeidae

Agetus flaccus
Agetus limbatus
Agetus typicus
Corycaeus clausi
Corycaeus crassiusculus
Corycaeus speciosus
Ditrichocorycaeus andrewsi
Ditrichocorycaeus asiaticus
Ditrichocorycaeus dahli
Ditrichocorycaeus erythraeus
Ditrichocorycaeus subtilis
Farranula carinata
Farranula concinna
Farranula curta
Farranula gibbulus
Onychocorycaeus agilis
Onychocorycaeus catus
Onychocorycaeus latus
Onychocorycaeus ovalis
Onychocorycaeus pacificus
Onychocorycaeus pumilus
Urocorycaeus furcifer
Urocorycaeus lautus
Urocorycaeus longistylis

Oithonidae

Oithona attenuata
Oithona fallax
Oithona nana
Oithona plumifera
Oithona rigida
Oithona robusta
Oithona setigera
Oithona simplex
Oithona (Paroithona) sp. 1
Oithona similis
Oithona sp. 3
Oithona (Paroithona) sp. 4

Oithona vivida
Oithona sp. 6
Oithona tenuis

Oncaeidae

Conaea rapax
Conaea sp.
Epicalymma spp.
Oncaea atlantica grp
Oncaea brodskii
Oncaea c.f. oceanica
Oncaea clevei
Oncaea englishi
Oncaea media
Oncaea mediterranea
Oncaea notopus group
Oncaea oceanica
Oncaea ornata
Oncaea ornata group
Oncaea ovalis group
Oncaea prendeli group
Oncaea scottodicarloi
Oncaea shmelevi
Oncaea sp. A
Oncaea sp. B
Oncaea sp. C
Oncaea sp. D
Oncaea sp. E
Oncaea sp. F
Oncaea sp. G
Oncaea sp. H
Oncaea sp. I
Oncaea sp. J
Oncaea sp. K
Oncaea tenuimana
Oncaea tregoubovi group
Oncaea venusta medium
Oncaea venusta typica
Oncaea venusta venella
Oncaea waldemari
Oncaea zernovi grp
Spinoncaea c.f. tenuis
Spinoncaea humesi
Spinoncaea ivlevi
Triconia conifera
Triconia dentipes group
Triconia derivata
Triconia elongata
Triconia furcula
Triconia giesbrechti
Triconia hawii
Triconia minuta group
Triconia redacta
Triconia rufa
Triconia similis group
Triconia sp.
Triconia umerus Type 1
Triconia umerus Type 2

Lubbockiidae

Lubbockia squillimana

Sapphirinidae

Copilia mirabilis
Copilia spp
Sapphirina spp
Vettoria sp.

ORDER:

HARPACTICOIDA

Aegisthus mucronatus
Clytemnestra sp.
Euterpina acutifrons
Macrosetella gracilis
Microsetella spp

ORDER:

MORMONILLOIDA

Mormonilla phasma

ORDER: SIPHONOSTOMATOIDA

Pontoeciella abyssicola

Zooplankton taxa

Overall, we enumerated 260 taxa in 100 zooplankton samples. The count data were Hellinger-transformed and subjected to Redundancy Analysis, which allowed the relationships between samples and between taxa to be visualised (Fig. 75). Because of the large number of species included in the model, the proportion of explained variance was low, only 6.38% on axis 1 and 2.95% on axis 2. A total of 21 components would be needed to explain 50% of the variance. Irrespective of this, distinct sample groups were formed by each of the depth strata sampled, with the exception of the samples from the 100 – 200 m and 200 – 300 m depth strata, which were similar in community composition. The samples from the 0 – 50 m stratum formed a distinct but diffuse cluster, within which the samples from the Lagoon site (LA) formed a discrete sub-cluster. The LA samples were characterised by the presence of copepods commonly found in shallow coral reef systems, such as *Bestiolina similis*, *Centropages orsinii*, and *Parvocalanus dubia* as well as decapod larvae (both zoea and post larval forms). The 0 – 50 m stratum was characterised by *Oithona nana*, *O. simplex*, Larvacea, Chaetognatha, and juvenile forms of Corycaeidae and Calanoida. Samples from the 50 – 100 m stratum, which included the chlorophyll maximum, were characterised by cyclopoid copepods, including 4 species of *Oithona* as well as juvenile stages of this order. Samples from the 100 – 200 m and 200 – 300 m strata coalesced, and were most strongly associated with the Open Water site (SW) and with Ostracoda. Oncaeidae (here represented by adults of all species pooled together) exerted a very strong influence on all sample groups from depths greater than 100m, and on all the deep water sites (Channel, NE margin and Open Water). The 300 – 400 m sample cluster was very discrete, and characterised by the presence of hyperbenthic taxa such as the species of Spinocalanidae and the cyclopoid *Conaea rapax*. Interestingly, this group was more strongly associated with the Channel (CH) and NE margin (NE) sites, which were not as deep as the Open Water (SW) site, possibly reflecting that the net sampled near-bottom.

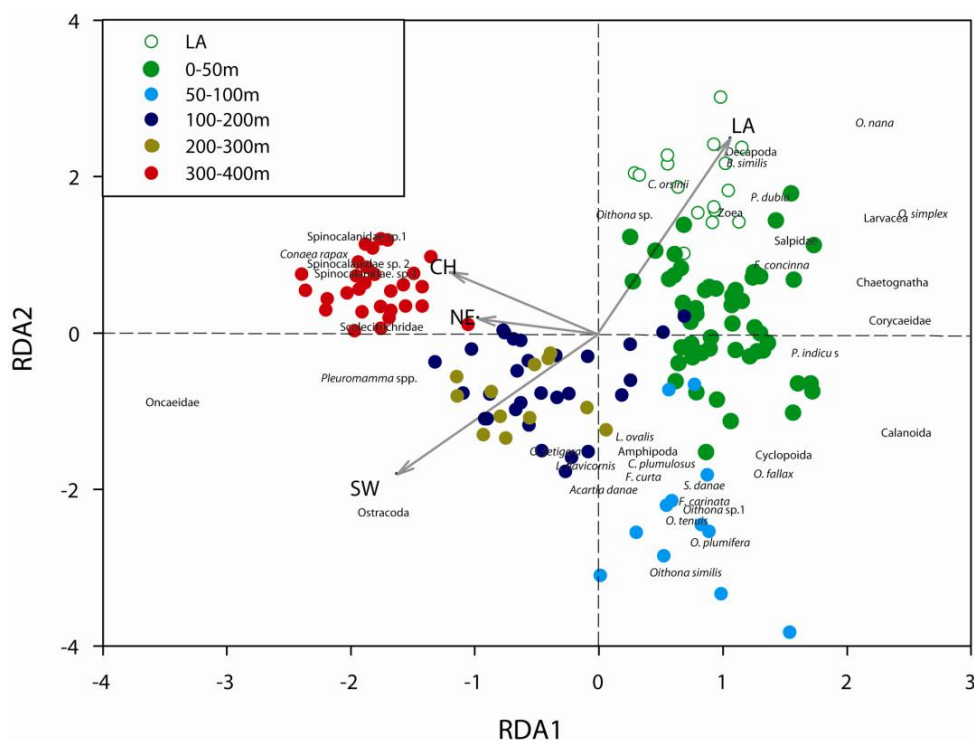


Fig. 75 Redundancy analysis displaying relationships between zooplankton samples, sites and depths.

Indicator species

One of our goals with the zooplankton work was to detect past intrusion events into the lagoon by using zooplankton indicator species. Hence, the presence in the lagoon of a species normally only found below 100 m at the open water locations would be evidence of the intrusion or upwelling of water from that depth horizon into the lagoon.

An index for indicator species, defined as the product of relative abundance and relative frequency of occurrence of the species within a group (Dufrêne and Legendre, 1997), was calculated for the five depth strata from the multinet samples and for the four locations. If there are no occurrences of the species within a group, the index takes the value of 0, increasing to 1 if the species occurs at all sites within the group, and does not occur at any other site. The index can be calculated for each species-group combination, and species with high index values for a group are indicator species for that group. The index distinguishes ubiquitous species that dominate many groups in absolute abundance from species that occur consistently within single groups but have low abundance.

The indicator species selected with the highest predictive value were consistent with those species exerting the greatest influence in the redundancy analysis (Fig. 75). The 0 – 50, 50 – 100 and 300 – 400 m depth strata had the highest indicator values (Table 30), meaning that the species selected as indicators of these strata could be used with the greatest confidence. However, the highest indicator value, 0.5975 for *Conaea rapax* at the 300 – 400 depth stratum, is still not very powerful, and most indicator values were <0.5 i.e. that these species were not completely restricted to the sample group they were indicating. Indicator values for the sampling locations (Table 31) were highest for LA, and weakest for SW. No significant indicator species were selected for CH.

The analysis of indicator values did not include Oncaeidae, since this family was not sorted to species level at all sites. Nevertheless, the pooled species of this family exerted the greatest influence of any taxon in the redundancy analysis. Species of oncaeid copepods are small, comparatively non-motile and are known to be restricted to particular depth horizons, and therefore have considerable potential as indicator species for water from subthermocline depths. However, the taxonomy of this group is extremely complex, which compromises the practicality of their use as indicator species.

Analysis of the oncaeid community to species level (or as close as possible) at SW, where topographically forced upwelling or breaking internal waves were unlikely to influence species distributions, confirmed that many species were not found above particular depth horizons (Fig 76). Eleven species were widely distributed through the water column, but were never found above 50m at this site, and a further 10 species were never found above 100 m. Therefore, the occurrence of any of these species in the shallow waters of South Reef lagoon should indicate that water has originated from that particular depth stratum off-reef.

Table 30 Five most powerful indicator species for each depth stratum (see text). All indicator values shown are significant at the $p < 0.001$ level, except where indicated by * $p < 0.05$, and ** $p < 0.01$. IV = Indicator value.

	0 – 50m	50 – 100m	IV	100 – 200m	IV	200 – 300m	IV	300 – 400m	
<i>Oithona nana</i>	0.4705	<i>Calocalanus</i> sp. 1	0.4492	<i>Clausocalanus paululus</i>	0.2933**	<i>Clausocalanus</i> spp.	0.2548**	<i>Conaea rapax</i>	0.5975
<i>Oithona simplex</i>	0.3749	<i>Oithona tenuis</i>	0.4327	Ostracoda	0.2893**	<i>Clausocalanus arcuicornis</i>	0.2491*	<i>Spinocalanidae</i> sp.1	0.5561
Larvacea	0.3666	<i>Farranula carinata</i>	0.4235	<i>Oithona</i> sp.4	0.2814*	<i>Heterorhabdus</i> spp.	0.2202**	<i>Spinocalanidae</i> sp. 2	0.5277
Decapods	0.3349	<i>Oithona fallax</i>	0.4163	Cyclopoid juveniles	0.2189**	<i>Temoropia minor</i>	0.1969**	<i>Spinocalanidae</i> sp. 3	0.4139
<i>Farranula concinna</i>	0.3148	<i>Oithona</i> sp. 2	0.4024	<i>Mesocalanus tenuicornis</i>	0.1379*	<i>Pleuromamma indica</i>	0.1867*	Oncaeiidae	0.3134

Table 31 Five most powerful indicator species for each site, as for Table 30. There were no significant indicator species for the Channel site. LA = Lagoon site, NE = NE margin site, SW = Open Water site.

	LA	IV	NE	IV	SW	IV
<i>Oithona nana</i>	0.5654	Harpacticoida	0.3166**	Ostracoda	0.33**	
<i>Bestiolina similis</i>	0.5446	<i>Oithona plumifera</i>	0.2903*	Oncaeiidae	0.3295	
<i>Parvocalanus dubius</i>	0.4949	<i>Oithona</i> sp.3	0.2429**	<i>Oithona</i> sp.2	0.2821*	
Decapod larvae	0.4485			<i>Lucicutia flavicornis</i>	0.229*	
Salpidae	0.4452			<i>Pleuromamma</i> spp.	0.2069*	

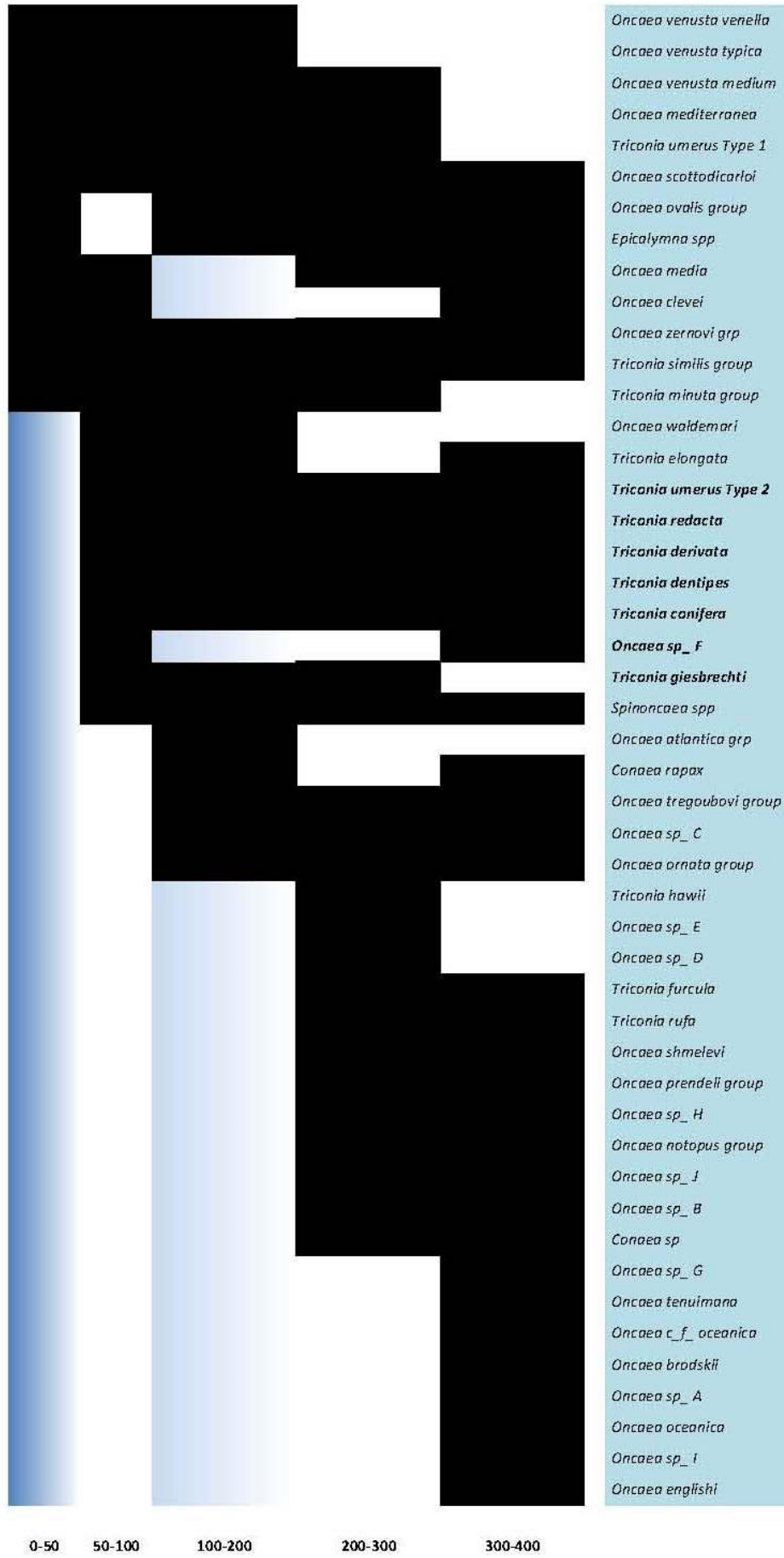




Fig. 76 Depth occurrences of 64 species of Oncaeidae (in black) across 5 depth strata at the Open Water site (SW). Species considered to be of some utility as indicators of intrusions are in bold.

A total of 14 species of Oncaidae occurred at the Lagoon site (LA; Table 32a), amongst which were 4 species that never occurred in the mixed layer of the 4 sites at SW for which all species of Oncaidae have been identified. However, 3 of these species (*Oncaea atlantica*, *O. waldemari* and *Triconia elongata*) have been recorded from the mixed layer at North West Cape by McKinnon et al. (2008), and their value as indicators of subthermocline water is therefore weak. One of these species, *O. waldemari*, is well recognised as epipelagic, but for some reason did not occur at the Open Water (SW) site in the mixed layer. Nevertheless, the occurrence of 12 species of Oncaidae at the Lagoon site (LA) in December 2008, including the four species potentially of indicator value, is suggestive that there was greater influence of subthermocline water at LA on this cruise than on the other cruises.

































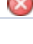
Indicator values for copepod species characteristic of the 100 – 200m depth stratum were low (<0.3), and therefore of little power (Table 30). However, 2 of the 3 species selected did occur at LA; *Clausocalanus paululus* (June 2008 only) and *Oithona* sp. 4 (all except December 2009; Table zp08b). The only indicator species of depths below this to occur at LA were *Clausocalanus* spp. and *Clausocalanus arcuicornis*, the indicator values of which are weak and both of which do occur in surface waters elsewhere, for instance at North West Cape (McKinnon et al., 2008).

Interpretation of the presence of indicator species within the lagoon necessarily requires some judgement about the longevity of these animals once transported into the lagoon. The longevity of copepods in the field is not well understood, but is likely to be in the order of one week at temperatures typical of the mixed layer at Scott Reef based on the global models of Hirst and Kiørboe (2002). Therefore, the presence of one of the indicator species within the lagoon may represent the occurrence of an intrusion up to 10 days previously.


The instrumental record from temperature recorders at PE06 (Fig. 77) confirms that the influence of intrusions was strongest in our December 2008 cruise. Intrusions occurred prior to the June 2008 and June 2009 cruises, but were not pronounced during the cruises. Strangely, there was moderate intrusion activity apparent from the December 2009 instrumental record, but no indication in the plankton of the presence of species characteristic of subthermocline waters.

Table 32 Occurrence at the Lagoon site (LA) of indicator species characteristic of subthermocline (>100m) water. a) species of Oncaeidae found at LA, with those identified as having indicator value (see Fig. 76) indicated by , and other species not identified as having indicator value by ; b) other copepod species identified as having indicator value of the 100-200 m depth stratum using the procedure of Dufrêne and Legendre, 1997 (Table 30).

a) Oncaeidae indicator species

	Jun-08	Dec-08	Jun-09	Dec-09
<i>Oncaea atlantica</i> grp				
<i>Oncaea clevei</i>				
<i>Oncaea media</i>				
<i>Oncaea mediterranea</i>				
<i>Oncaea scottodiarloi</i>				
<i>Oncaea venusta</i> medium				
<i>Oncaea venusta typica</i>				
<i>Oncaea venusta venella</i>				
<i>Oncaea waldemari</i>				
<i>Oncaea zernovi</i> grp				
<i>Triconia elongata</i>				
<i>Triconia redacta</i>				
<i>Triconia similis</i> group				
<i>Triconia umerus</i> Type 1				

b) Non-Oncaeidae indicator species.

	Jun-08	Dec-08	Jun-09	Dec-09
<i>Clausocalanus paululus</i>				
<i>Oithona</i> sp 4				

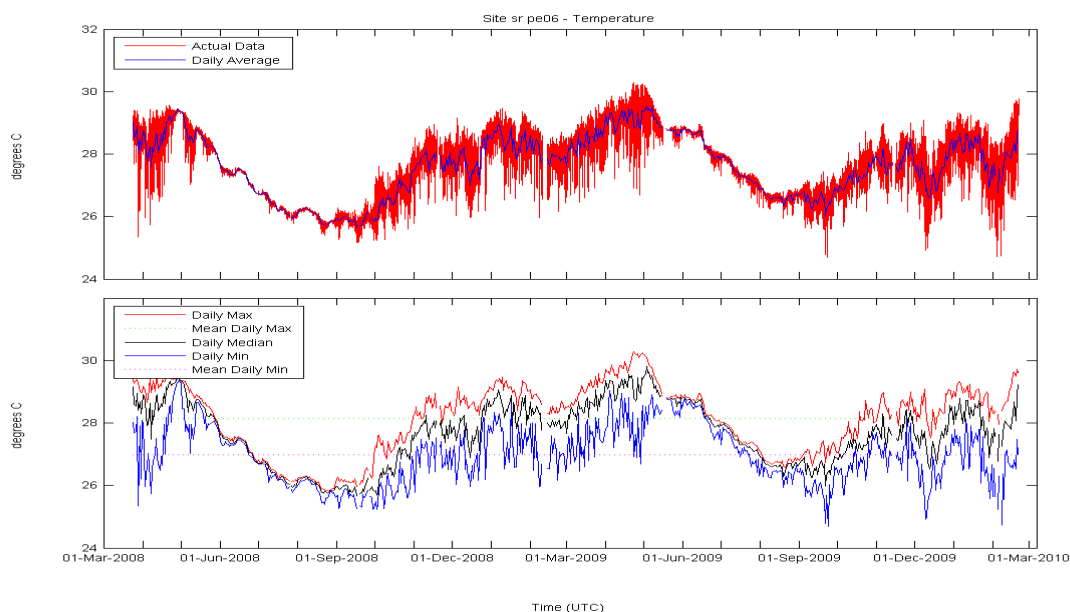


Fig. 77 Instrumental record of temperature from site PE06.

Secondary Production

On 3 cruises (December 2008, June 2008, and December 2009) zooplankton growth rates at the Lagoon site (LA) were measured experimentally, using the artificial cohort technique (Kimmerer and McKinnon, 1987). Living plankton was sampled with a gentle tow of a 100 µm net, and then an 'artificial cohort', or size fraction, was created by filtration through a 125 µm screen. Equal aliquots of the resulting 100 – 125 µm artificial cohort were then either preserved in formalin (time-zero samples) or dispensed to clean 2.4 litre polycarbonate bottles filled with water from the chlorophyll maximum depth. The experimental bottles were then incubated on-deck at ambient temperatures for 24 hrs, after which the contents were condensed and preserved in formalin.

In the laboratory, each sample was further concentrated and transferred to a Sedgewick-Rafter counting cell. The plankton was then imaged with a digital camera mounted on a microscope. The images were processed using ImageJ software and the group and stage of individual copepods were identified, and the total length (for nauplii) or the prosome length (for copepodites) were measured. The length of each individual was then converted to carbon content using length-weight regressions from the literature.

Growth rates (g) were then calculated for each copepod group as:

$$[\ln(\text{mean individual C content at T24}) - \ln(\text{mean individual C content at T0})]/(T24-T0)$$

In December 2008, June 2009 and December 2009 we were able to calculate g for the guild of cyclopoid copepods as 0.31, 0.09 and 0.15. In addition, sufficient animals were available for us to calculate g for calanoid copepods in December 2009 as 0.33. These numbers are in good agreement with previous measurements at North West Cape (McKinnon and Duggan, 2003). We then calculated secondary production with the following two assumptions: 1) that the copepod growth rates were representative of the whole plankton community; and 2) that the mean carbon content of the copepods at the commencement of the experiment (0.206 µg) was representative of the whole copepod population. Accordingly, we calculated the total copepod biomass using the abundance data (Table 24) and multiplied by the growth rate to obtain a carbon-specific estimate of secondary production (Runge and Roff, 2000). For the December 2009 cruise we used the mean of the calanoid and cyclopoid growth rate i.e. 0.24. The resulting estimation of total copepod production for the three cruises was 32, 6 and 15 mg C m⁻² d⁻¹.

Macrozooplankton of Scott Reef waters

In December 2008 WEL requested that AIMS conduct some exploratory sampling to investigate areas of high backscatter identified during other research within the deep channel. On the basis of the information provided, we speculated that these areas of high backscatterance were caused by aggregations of krill (euphausiids), a component of the zooplankton which is a potentially important resource to megafauna. Accordingly, we sampled with a bongo net fitted with 500 µm nets that would more efficiently sample the larger plankton responsible for backscatter. Though there were a few euphausiid individuals in the samples, these samples were dominated by species of large copepods.

To test the hypothesis that areas of high backscatter indeed represented higher zooplankton biomass, we took triplicate bongo hauls in areas of backscatter, and triplicate hauls in nearby areas with no backscatter. Analysis of the zooplankton biomass from these samples revealed that there was a highly significant difference in biomass (ANOVA, $p < 0.01$); the >500 µm plankton within the backscatterance area had a biomass of 4.4 ± 0.5 SD mg m⁻³, and in non-backscatter areas 3.6 ± 0.3 SD mg m⁻³.

Because euphausiids are strong swimmers and form discrete aggregations, they are very difficult to sample with plankton nets. They also undergo substantial vertical migrations from the deeper layers they inhabit during the day to surface layers during the night. To determine whether there were indeed significant numbers of euphausiids in the deep channel, we conducted tows with the bongo net to sample macroplankton down to 700 m, where because of the cooler temperatures and lack of light we would have a better chance of sampling these mobile animals. Though euphausiids comprised only a small proportion of these samples, we have identified 6 species from the area of the deep channel (Brinton et al., 2000).

Species of euphausiids collected included:

Nematoscelis tenella
Stylocheiron affine
Thysanopoda orientalis
Thysanopoda obtusifrons
Euphausia pseudogibba
Euphausia diomedea

In December 2009 we conducted more structured sampling at our three deep water sites (CH, NE and SW) as well as an additional sample to the east of CH, at the location of the sediment fan radiating out from the entrance to the deep channel (ER = east rim; Fig. 78). At each of these four sites, we conducted triplicate near-bottom to surface oblique hauls of the bongo net during the day and during the night. The hypotheses to be tested were: “Are krill more abundant in the deep channel area than at other locations near Scott Reef?” and “Are krill more abundant in the water column at night?”

Euphausiids in these sample sets were identified to genus and counted. Six genera were found in these samples (Table 33). Counts were standardised to numbers per 100m³, using the flow meter fitted to the bongo net. Note that these numbers are averaged over the whole duration of the oblique tow, and therefore represent an average volumetric measurement over the whole depth range. Densities of each species are possibly very much greater at specific depth intervals.

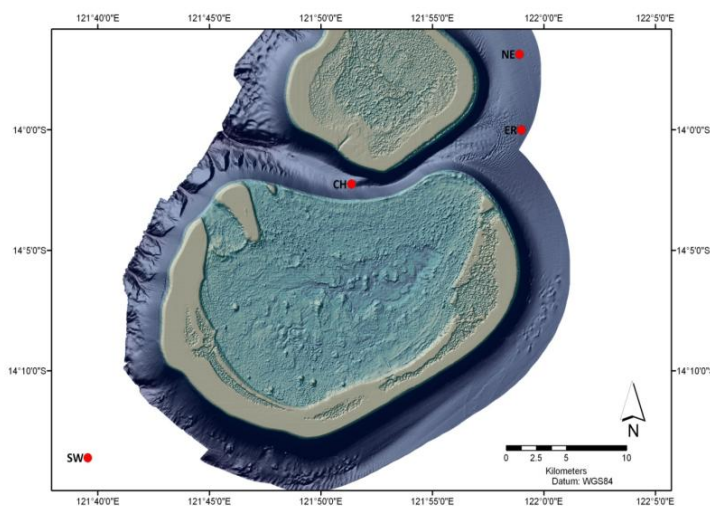


Fig. 78 Locations at which euphausiid collections were made.

Table 33 Average abundance of euphausiid genera over all sites (no. 100m⁻³).

<i>Euphausia</i>	<i>Pseudeuphausia</i>	<i>Thysanopoda</i>	<i>Stylocheiron</i>	<i>Nematoscelis</i>	<i>Thysanoëssa</i>	TOTAL
30.3	2.7	0.6	15.1	1.0	2.8	52.6

The relationship between the abundance of each of the six krill genera and the covariates (day/night and location) were tested using Poisson regression. For 5 of the genera (*Pseudeuphausia*, *Thysanopoda*, *Nematoscelis*, *Thysanoëssa*) the abundance was very low, including a large number of zeros, and the assumptions of standard statistical tests such as ANOVA and regression were violated. Consequently, the abundances of these genera were modelled using a zero-inflated generalised linear model (Martin et al., 2005; Sileshi, 2008). This model consists of two stages. Firstly, the presence and absence of the species is modelled using logistic regression. Then conditional on presence, the abundance is modelled using truncated Poisson regression. This method is the best possible approach for each of these genera because of the large proportion of absences/zero values. For example, *Pseudeuphausia* contained 20 absences of 48 observations. For these 5 genera, the results are based on only a small number of presence sites where data was present and should be interpreted with caution.

All genera but *Euphausia* and *Stylocheiron* had high frequencies of samples containing <5 individuals (Fig. 79).

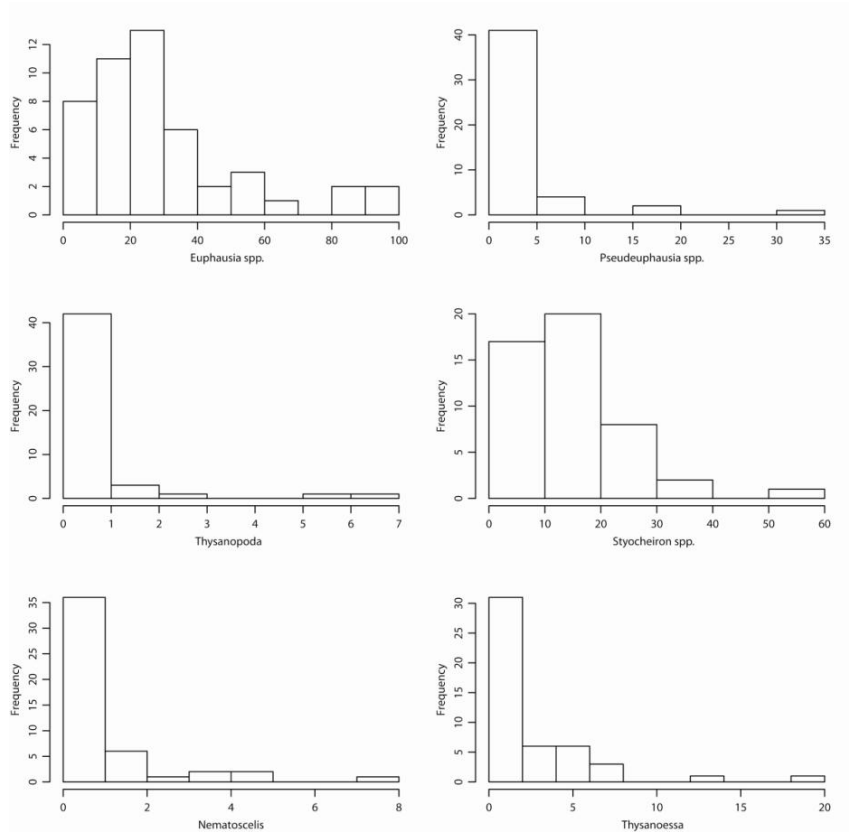


Fig. 79 Histograms showing frequency of abundances of each euphausiid genus.

Two genera did not show any significant differences in abundance (*Thysanopoda*, Table 34; and *Thysanoëssa*, Table 35). Though species have not been determined for this sample set, we know from

the 2008 sampling that *Thysanopoda obtusifrons* occurs at Scott Reef, and this species has a preference for depths >200m . These predominately deep water forms were only present in extremely low abundances (<1 per 100m³ on average, with many zero occurrences), probably not sufficient to detect differences. By contrast, *Thysanoëssa* spp. are often epipelagic, and thus may not show any vertical migration pattern and be well distributed in near surface waters by the currents. It is therefore likely that the depth preferences of these genera were responsible for the lack of detectable differences in abundance with location or time of day.

Table 34 Results of the two-stage zero-inflated generalised linear model for the genus *Thysanopoda*, indicating a) abundance model (exclude zeros; n=15), and b) presence/absence model (n=48).
abundance model (exclude zeros; n=15)

	Estimate	Std. Error	z-value	p-value
(Intercept)	0.135	0.723	0.187	0.852
Day.Night	0.563	0.475	1.185	0.236
Site ER	1.166	0.710	1.643	0.100
Site NE	-1.228	1.162	-1.057	0.291
Site SW	-1.049	0.938	-1.118	0.264

presence/absence model (n=48)

	Estimate	Std. Error	z-value	p-value
(Intercept)	-1.718	0.849	-2.023	0.043
Day.Night	0.209	0.647	0.323	0.747
Site ER	0.512	1.023	0.500	0.617
Site NE	0.918	0.988	0.929	0.353
Site SW	1.613	0.967	1.668	0.095

Table 35 Results of the two-stage zero-inflated generalized linear model for the genus *Thysanoëssa*, indicating a) abundance model (exclude zeros; n=35), and b) presence/absence model (n=48).
abundance model (exclude zeros; n=35)

	Estimate	Std. Error	z-value	p-value
(Intercept)	-0.032	0.685	-0.046	0.963
Day.Night	0.434	0.503	0.863	0.388
Site ER	0.912	0.717	1.272	0.203
Site NE	0.958	0.624	1.535	0.125
Site SW	0.913	0.626	1.459	0.145

presence/absence model (n=48)

	Estimate	Std. Error	z-value	p-value
(Intercept)	0.995	0.736	1.353	0.176
Day.Night	0.213	0.653	0.326	0.745
Site ER	-0.406	0.906	-0.448	0.654
Site NE	5.37E-12	0.944	5.69E-12	1.000
Site SW	5.37E-12	0.944	5.69E-12	1.000

There is no significant difference in *Nematoscelis* abundance between day/night and sites (Table 36). However, the probability of *Nematoscelis* presence (presence/absence model) is significantly greater at night than during the day (Table 36b). Also the probability of *Nematoscelis*

presence is significant higher in NE and SW compared to CH, indicating that *Nematoscelis* is more likely to occur at off-reef locations, and is more of an open water species.

Table 36 Results of the two-stage zero-inflated generalised linear model for the genus *Nematoscelis*, indicating a) abundance model (exclude zeros; n=20), and b) presence/absence model (n=48).
abundance model (exclude zeros; n=20)

	Estimate	Std. Error	z-value	p-value
(Intercept)	-0.382	1.026	-0.372	0.710
Day.Night	0.848	0.459	1.847	0.065
Site ER	0.887	1.030	0.861	0.389
Site NE	-0.208	1.008	-0.207	0.836
Site SW	0.771	0.945	0.816	0.415

presence/absence model (n=48)

	Estimate	Std. Error	z-value	p-value
(Intercept)	-4.678	1.564	-2.990	0.003
Day.Night	3.000	1.205	2.490	0.013
Site ER	0.883	1.372	0.644	0.520
Site NE	3.734	1.502	2.486	0.013
Site SW	5.471	1.708	3.203	0.001

The abundances of *Euphausia* spp. (Table 37) , *Pseudeuphausia* spp. (

Table 38) and *Styoecheiron* spp. (Table 39) are very significantly higher at night (mean abundance is 3.31, 1.21 and 2.69 individuals 100 m⁻³, respectively) than during the day (mean abundance is 2.88, 0.33 and 2.16 individuals 100 m⁻³ respectively). *Euphausia* spp. had significantly higher abundance outside the Scott Reef complex (i.e. at the non-channel locations). Similarly, *Styoecheiron* spp. were significantly more abundant in two of the locations (NE and SW) outside the Scott Reef complex than at CH, but significantly less abundant in ER than at CH. *Pseudeuphausia* spp. was significantly more abundant in SW but less abundant in NE than at CH. There was no significant difference in *Pseudeuphausia* spp. abundances between the CH and ER locations.

Table 37 Results of the Poisson regression model (includes zeros in the model) for the genus *Euphausia*.

	Estimate	Std. Error	z-value	p-value
(Intercept)	2.295	0.092	25.070	< 2e-16
Day.Night	0.210	0.053	3.970	7.17E-05
Site ER	1.089	0.100	10.860	< 2e-16
Site NE	1.166	0.099	11.750	< 2e-16
Site SW	1.296	0.098	13.240	< 2e-16

Table 38 Results of the two-stage zero-inflated generalised linear model for the genus *Pseudeuphausia*, indicating a) abundance model (exclude zeros; n=28), and b) presence/absence model (n=48).

abundance model (exclude zeros; n=28)

	Estimate	Std. Error	z-value	p-value
(Intercept)	-0.035	0.449	-0.078	0.938
Day.Night	1.750	0.427	4.100	4.12E-05
Site ER	-0.446	0.356	-1.252	0.210
Site NE	-1.740	0.575	-3.027	0.002
Site SW	0.747	0.221	3.386	0.001

presence/absence model (n=48)

	Estimate	Std. Error	z-value	p-value
(Intercept)	-0.526	0.704	-0.747	0.455
Day.Night	1.883	0.667	2.824	0.005
Site ER	-0.415	0.915	-0.454	0.650
Site NE	2.96E-14	0.917	3.23E-14	1.000
Site SW	0.432	0.934	0.463	0.643

Table 39 Results of the Poisson regression model (includes zeros in the model) for the genus *Stylocheiron*.

	Estimate	Std. Error	z-value	p-value
(Intercept)	2.164	0.098	21.981	< 2e-16
Day.Night	0.424	0.076	5.574	2.49E-08
Site ER	-0.394	0.137	-2.874	0.004
Site NE	0.502	0.110	4.549	5.39E-06
Site SW	0.766	0.105	7.273	3.51E-13

Based on these analyses, we are unable to support the hypothesis that the channel is a 'hotspot' of krill abundance. However, it is important to bear in mind the limitations of this study. Firstly, because the bongo net remains open throughout the tow, it samples throughout the water column and does not provide any information on the depth range at which particular species occur. Secondly, all net systems do a poor job of sampling the local aggregations characteristic of macrozooplankton and micronekton. Though it is possible that the net passed through such an aggregation, there is no indication of it once the density of plankton is calculated based on the total volume filtered. To adequately identify features such as localised aggregations of organisms that would be attractive to planktivorous megafauna it would be necessary to use acoustic techniques.

Methodological issues aside, our results do not necessarily discount the hypothesis that the deep channel is a preferred feeding area for megafauna. Genin (2004) reviewed the mechanisms responsible for the formation of zooplankton and fish aggregations over abrupt topographies. They include:

- I. Upwelling, with the caveats that upwelling of deep nutrient rich water be strong enough to reach the photic zone, and that upwelled water remain resident for long enough to elevate local phytoplankton biomass (1-2 days).

2. Topographic blockage of descending zooplankton. For vertically migrating species, topography can block the animals' pre-dawn descent, trapping them in well-lit water during daylight hours and rendering them susceptible to visual predation.
3. Counter-upwelling depth retention. Aggregations form when animals swim downward against an upwelling current to reach a preferred isolume to avoid visual predation.
4. Counter-downwelling depth retention, in which aggregations form by animals swimming upward against a downwelling current. This mechanism has been invoked to explain aggregations along fronts, but never directly demonstrated.
5. Enhanced horizontal flux – the “feed-rest” hypothesis. Amplification of near-bottom flows enhances flux of suspended particles used as food by suspension feeders.

At Scott Reef, there is no evidence of persistent upwelling or downwelling currents – the strongest currents are in the horizontal and are extremely variable in speed and direction. Mechanisms 1, 3 and 4 are unlikely to apply. Mechanism 2 could conceivably apply to those taxa showing strong diel patterns of abundance, such as *Pseudeuphausia* spp. Mechanism 5 is most likely to apply to Scott Reef, as there is good evidence of strong current flow near the bottom, and of the presence of filter feeding communities at depth. The reef structure provides shelter for aggregations of krill, as well as generating “trophic focusing”, where food particles from large volumes of water are accumulated into a relatively small area (Genin, 2004). The occurrence of aggregations of krill and other macrozooplankton/micronekton in refugia at Scott Reef could be attractive to plankton feeding megafauna. However, demonstrating this linkage requires a more targeted study than has been possible within the present project.

Discussion

Coral reefs are highly sensitive to changes in the physical, chemical and biological properties of the waters in which they grow. The near-surface oceanic environment surrounding Scott Reef is typical of the Timor Sea and Eastern Equatorial Indian Ocean. It is characterised by a well mixed layer of warm (27 – 30°C) highly transparent water (~ 0 – 100 m water depth) that is deficient in nutrients. Below the surface mixed layer, water temperature declines to less than 10°C at 400 m depth. Ocean currents and seasonal monsoonal weather cycles change the layering of the water column so that the surface mixed layer deepens during periods of persistent wind and thins during calm periods. The dense, deep water is high in nutrients but receives little light, whereas the well-lit surface layer is nutrient depleted. Optimum phytoplankton growth occurs where there is some of each, and results in the formation of a deep chlorophyll maximum (usually just above 100 m). The stable vertical layering of the ocean supports the existence of internal tides and internal waves that appear as periodic vertical excursions of the thermocline. These internal waves increase in amplitude when they encounter shoaling of the bottom or changes in the bottom topography, such as reefs and submerged banks. In such circumstances, internal waves are an important mechanism for mixing nutrient-rich water into shallow coral reef communities.

The oceanographic context of Scott Reef

The Eastern Equatorial Indian Ocean has a complex structure of surface and subsurface currents together with temperature and salinity distributions that have direct impacts on the marine ecosystems and climate of northwest Australia and the wider region. The Indonesian Throughflow (ITF) delivers warm, low salinity water into the region and is the key source and driver of regional ocean circulation. The ITF comprises a system of currents flowing through the passages between the Indonesian Archipelago, Timor Leste and northwest Australia (Wijffels et al., 2008), with the largest single component of flow occurring through the Timor Trough, between Darwin and Timor Leste (Sprintall et al., 2009). The combined flows of the ITF control global climate cycles through the transport of a significant amount of heat between the Pacific and Indian Oceans. The ITF is highly variable on seasonal, interannual and decadal time scales (Sprintall et al., 2009) with the largest and most persistent mode of variation associated with the El Niño Southern Oscillation (ENSO) phenomenon, and to a lesser degree on the Indian Ocean Dipole (IOD). Lower sea levels in the Indo-West Pacific reduce ITF current flows during El Niño events. Observations suggest that the ITF has been weakening during the past four decades (Wainwright et al., 2008), however, due to the high variability of the circulation in the region on seasonal to decadal time scales, it is unclear whether these changes are natural fluctuations of the climate system in this highly variable region, or a response to anthropogenic climate change. An important feature of the Eastern Equatorial Indian Ocean is the so called 'Barrier layer' (Sprintall and Tomczak, 1992), which forms in the top 200 m of the water column where the fresher water from the ITF flows over more dense, but warmer subsurface waters. This forms a low salinity mixed layer over a high salinity layer, which has consequences for the trapping of incoming solar radiation in the surface layer and generation of SST anomalies in the region. In addition to the ITF, the Eastern Gyral current delivers waters from the central Indian Ocean into the region, with the Browse basin lying in the confluence of water masses from a diverse range of origins (Tomczak and Large, 1989). This high degree of temporal variability in water bodies bathing Scott Reef was observed during the present study. Temperature/Salinity relationships from the four biological oceanographic cruises indicate a complicated and seasonally varying vertical structure of water masses around Scott Reef, with evidence for multiple interleaving layers within the mixed layer and in the thermocline to 300 m depth.

Lagoon waters

The physical environment of the South Reef lagoon is controlled by the seasonal characteristics of the surface layer of the surrounding ocean, the tidal interaction of these waters with the topography of the reef, the regional monsoonal climate and the seasonal cycle of insolation. Like the surrounding ocean, the water clarity within the lagoon is high, with no significant inter-seasonal difference in water transparency. Mid-day fluxes of PAR at the surface range between approximately 1,500 $\mu\text{mol Q m}^{-2} \text{sec}^{-1}$ in the winter to approximately 2,200 $\mu\text{mol Q m}^{-2} \text{sec}^{-1}$ in the summer. Red wavelengths of light ($>600 \text{ nm}$) are rapidly attenuated in the upper 10 m of the water column. Thereafter, the blue light can penetrate to significant depths. The amount of PAR reaching the lagoon benthos is typically $>1\%$ surface PAR at the deepest in-situ observational sites ($\sim 55 \text{ m}$ water depth) and was within the range of $1\% - 10\%$ for lagoon sites at depths between 55 m and 35 m. The depth-averaged light extinction coefficient (k) of the lagoonal water was of the order of $0.07 - 0.09 \text{ m}^{-1}$.

The lagoon environment mirrors the seasonal and inter-annual variability in the temperature and salinity structure exhibited by the regional oceanic waters, with additional higher frequency variability caused by local processes such as enhanced vertical mixing, modified horizontal advection and residence times, and increased local evaporation. The seasonal surface temperature cycle is driven by the seasonal cycle of insolation and vertical stratification with a maximum solar energy input in November – December and minimum in June – July. The average daily water temperature within the lagoon between March 2008 and February 2010 ranged from 24.7°C to 30.4°C , with minimum and maximum observed temperatures of 24.4°C and 30.9°C . Lagoonal water temperature shows strong seasonality with a maximum in April followed by a minimum in late August.

The primary driver for local temporal and spatial variability of temperature within the South Reef lagoon is the intrusion of cool water originating from the channel separating North and South Reef, with the near-bottom habitats close to the channel experiencing daily temperature ranges of up to 5°C during strong intrusion events; elsewhere within the interior of the lagoon daily temperature ranges were generally less than 1°C .

Salinity within the lagoon is, in general, horizontally and vertically uniform, however there is evidence of transient episodes of salinity stratification due to local rainfall, evaporation and enhanced vertical mixing with water from the upper thermocline within the channel. Episodes of salinity stratification included a near-bottom salinity maximum during May/June 2009 and a near bottom salinity minimum during Dec 2008. These subsurface layers of anomalous salinity were often discontinuous with similar salinities in the adjacent deep channel and surrounding waters, but the vertical structure of salinity within the lagoon mapped, to some degree, the salinity stratification present in the surrounding surface mixed layer. These salinity anomalies confirm that vertical exchanges of water and nutrients occur between the lagoon and deeper waters in the adjacent channel. Mean salinity within the lagoon ranged between $34.29 - 34.73 \text{ PSU}$, and this variability reflects the regional circulation and the exposure of Scott Reef to waters originating from both the Timor Sea/Indonesian Throughflow to the north, and NW shelf water from the south (Cresswell et al., 1993).

Chlorophyll concentration (as inferred from chlorophyll fluorescence) within the lagoon exhibits episodic, event-driven spatial variability, driven by a local response to the delivery of new nutrients via intrusions of cool water. Average chlorophyll concentrations in the interior of the lagoon were consistently higher than at observational sites adjacent to the deep channel and a persistent near-bottom layer of enhanced chlorophyll that covered much of the central lagoon was observed. The chlorophyll maximum within the lagoon was contiguous with a chlorophyll maximum in the adjacent deep channel. This subsurface layer was not accompanied by cooler temperatures, indicating that the local water had been resident in the lagoon sufficiently long to mix with the surrounding water and was the result of local production. Background levels of chlorophyll fluorescence within the lagoon ranged from 0.18 to 1.54 mg m^{-3} .

Lagoon water is persistently low in suspended matter, with very limited spatial variability in the deeper sections of the lagoon. Mean daily turbidity levels recorded by near-bottom loggers ranged between 0.04 – 1.50 NTU, with slightly higher levels observed in the high current region between West Hook and the Sandy Islet, and at sites adjacent to the back reefs. At deeper sites in the lagoon, there was little evidence of a sustained increase in turbidity near the seabed that could potentially result from resuspension of settled matter, suggestive of an environment where there is little settled matter on the sea-bed available for resuspension.

Total suspended sediment concentrations measured in the central lagoon were $< 1 \text{ mg L}^{-1}$ and often close to the limits of detection for the method. Mean sedimentation rates determined from in-situ sediment traps within the deeper sections of the lagoon were very low ($< 0.8 \text{ mg cm}^{-2} \text{ d}^{-1}$).

Dissolved nutrient concentrations in South Reef's lagoonal waters are consistently very low, though slightly higher than in the surface layers of the surrounding oceanic waters. Concentrations of NO_2^- , NO_3^- and PO_4^{3-} at the surface are in the range of 1's to 10's of nmoles per litre. While NH_4^+ was not measured in this study, conditions are such that ambient concentrations would also be of the order of several 10's of nM or less.

Even though intruded layers of thermocline water were not sampled within the lagoon, elevated near-bottom concentrations of NO_3^- of the order of 0.1-0.3 μM and lesser increases of PO_4^{3-} were consistently observed in the central lagoon indicating some (near-) continuous lateral transport thermocline waters into the lagoon. Regardless of depth, the ratio of summed concentrations of inorganic N species, including likely concentrations of NH_4^+ to PO_4^{3-} were consistently below the canonical Redfield ratio of 16:1, indicating that phytoplankton biomass was strongly constrained by nitrogen availability.

Low DIN:DIP ratios (< 16) are a common feature of non-divergent tropical oceanic waters. Concurrently measured concentrations of silicate were considerably higher, of the order of 1-2 μM . Given the low ambient concentrations of dissolved inorganic N and P and the dominance of cyanobacteria which do not require silica for growth, it is unlikely that phytoplankton in the Scott Reef system were Si-limited at any time.

Comparisons of Scott Reef with other regions

Phytoplankton

Phytoplankton communities at Scott Reef are similar in community composition and abundance to those found in oligotrophic stratified oceanic waters throughout the tropics (Partensky et al., 1999), and in lagoonal systems within these waters (e.g. Charpy and Blanchot, 1998). Tropical oceanic phytoplankton communities are overwhelmingly dominated by unicellular cyanobacteria $< 2 \mu\text{m}$ in size (picoplankton) from the genera *Synechococcus* and *Prochlorococcus*. *Prochlorococcus* (ca. 0.6 μm) is the most abundant form in oceanic waters and is found over a deeper depth range (0 – ca. 200+ m). *Synechococcus* (1 – 2 μm) is largely restricted to the upper 100 m. *Prochlorococcus* is usually present at abundances of 1 – 10 times that of *Synechococcus* (Pro:Syn = 1 – 10) in low-nutrient surface waters. The photosynthetic picoplankton also include a diverse assemblage of very small eukaryotic algal forms, both motile and non-motile, at abundances 1 – 4 orders of magnitude lower than the prokaryotic forms. The sparse community of larger phytoplankton ($> 5 \mu\text{m}$) is largely dominated by small flagellates in the 5 – 20 μm size range with fewer larger diatoms and dinoflagellates. These larger species are globally distributed in tropical and sub-tropical oceanic and continental shelf water masses.

Phytoplankton communities within lagoons of tropical oceanic atolls, including the South Reef lagoon, are characterised by high abundance of *Synechococcus*, high abundance of picoplankton eukaryotes and low abundance of *Prochlorococcus* (Pro:Syn < 1) (Charpy and Blanchot, 1998). This is most likely due to the lower intrinsic growth rate of *Prochlorococcus* ($u_{\max} = 2$ doublings day⁻¹) relative to those of *Synechococcus* ($u_{\max} = 3$ doublings day⁻¹) and picoeukaryotes ($u_{\max} > 2$ doublings day⁻¹) (Furnas and Crosbie, 1999) in the face of intensified microzooplankton grazing pressure.

The relative abundance of *Prochlorococcus* to *Synechococcus* across a range of oceanic and coastal ecosystems has been shown to be inversely related to nutrient availability in ecosystems. Ultra-low nutrient oceanic waters are almost always characterized by picoplankton assemblages with high Pro:Syn ratios (> 10), while more eutrophied, but still low-nutrient tropical coastal waters have very low Pro:Syn ratios (ca. <0.1). French oceanographers working in the atoll lagoons of the Tuamotu Archipelago (French Polynesia) have shown that the abundance of *Prochlorococcus* and *Synechococcus*, and the Pro:Syn ratio varied directly with the degree of lagoon closure and the resulting extent to which the enclosed water body was modified by the enclosure. Semi-open lagoons with a greater degree of exchange with surrounding oceanic waters had the highest relative abundance of *Prochlorococcus* and high Pro:Syn ratios while highly enclosed and eutrophied lagoons had the lowest *Prochlorococcus* abundance and low Pro:Syn ratios. The Pro:Syn ratio therefore acts as an indicator of water quality independent of the ambient nutrient concentrations. Within this context, the South Reef lagoon shows picoplankton community characteristics of being a relatively open system with a low level of eutrophication or water quality modification by enclosure.

Bacteria

The abundance of bacterioplankton in Scott Reef waters ($10^5 - 10^6$ cells ml⁻¹; including both true bacteria and Archaea) is of a similar order to the abundance found in other oligotrophic pelagic systems and associated reef lagoons (e.g. Torreton, 1996). Oceanic bacterial assemblages are hyper-diverse, with individual water samples containing thousands of genetically distinct strains (Venter et al., 2004). The bacterioplankton is the major functional group responsible for the recycling of organic matter in the water column by assimilating dissolved organic matter from a range of sources into biomass, which re-enters the various pelagic food webs operating within the ecosystem. Bacterioplankton, in turn, are prey items for viruses, nano-flagellates and larger specialized filter feeders such as larvaceans which were of higher abundance in lagoon waters.

Within vertical profiles, the abundance of pelagic bacteria generally tracked the distribution of phytoplankton biomass (as chlorophyll) or cellular abundance of *Prochlorococcus*, the dominant primary producer in the waters surrounding Scott Reef as the excretion or loss of dissolved organic carbon (DOC) from primary producers is the major energy supply for bacteria (e.g. Burney et al., 1979, 1981, 1982).

Bacterial production rates within the water column ranged between 34 and 102 mg C m⁻² d⁻¹; this production rate is strongly dependent upon the depth interval integrated. Estimates of bacterial production in atoll lagoons of French Polynesia ranged from 60 to 600 mg C m⁻² d⁻¹ (Ferrier-Pages and Furla, 2001). Individual daily production rates at Scott Reef ranged from 3 to 15% (median = 6%) of concurrent primary production by primary producers. For comparison, estimated bacterial production rates in the Sargasso Sea (BATS) ranged from 1.3 to 128% of concurrent primary production (median = 18%). Pelagic bacterial production in waters of North West Cape averaged approximately 13% of concurrent primary production (Furnas, 2007). Low efficiencies of carbon utilization are not unexpected. Estimates of the carbon growth efficiency (CGE) of bacterial production in pelagic systems range from <10 to 70% (Jones et al., 1996); however, most estimates of GGE are less than 30%. Torreton (1996) found that bacterioplankton in the Great Astrolabe Reef lagoon had a CGE of 5.7%, similar to that for Scott Reef.

Viruses

Viruses are the most abundant 'living' organisms in the Scott Reef lagoon and the surrounding ocean waters ($10^6 - 10^7$ ml⁻¹). Most bacteria in Scott Reef waters succumb to viral infection and eventual lysis. Vertical distributions of viruses in Scott Reef waters closely paralleled the distribution of their primary prey organisms, heterotrophic bacteria and *Prochlorococcus*. Calculated viral lysis rates were 100% or more in December 2008 (Lagoon) and June 2009 (Lagoon, Channel and NE margin). The precision of these high calculated rates is unresolved, but it is clear that viral infection and lysis are the major source of bacterioplankton mortality in Scott Reef waters. In essence, the bacterioplankton community in Scott Reef waters turns over on a daily basis.

Lytic infections appeared to be the dominant mode of bacterial infections at Scott Reef. These high lysis rates and subsequent release of cellular products are likely to be important for supporting microbial food web processes at Scott Reef. However, up to half of the bacterioplankton community in some samples contained inducible lysogenic viruses. Lysogeny commonly occurs during unfavourable conditions, such as during periods of low microbial growth. At present, there is no clear indication when, where, or for what reasons, lysogeny predominantly occurred at Scott Reef.

This was the first time that viral life strategies have been investigated for a coral reef system of the Indian Ocean. Viral production rates at Scott Reef ($0.6 - 12 \times 10^9$ l⁻¹ d⁻¹) were comparable to, and on some occasions higher than, viral production rates from other oligotrophic ocean regions, including the Southern Ocean (Weinbauer et al., 2009; $0.86 - 3.63 \times 10^9$ l⁻¹ d⁻¹), Sargasso Sea (Rowe et al., 2008; $0.24 - 4.8 \times 10^9$ l⁻¹ d⁻¹) and North Atlantic (Rowe et al., 2008; $1.2 - 7.2 \times 10^9$ l⁻¹ d⁻¹).

Primary production

Pelagic primary production (¹⁴C fixation) rates measured in the general vicinity of Scott Reef during this study ranged between 200 and 1,300 mg C m⁻² d⁻¹ with average winter (June – July) and summer (November – December) rates of 572 and 831 mg C m⁻² d⁻¹, respectively. The ¹⁴C method measures something between gross photosynthesis and net community production (see below). For the relatively short (4 hr) incubations used in this study, the rates measured are probably closer to gross photosynthesis. The average community gross primary production measured concurrently by oxygen metabolism was 950 mg C m⁻² d⁻¹, assuming a photosynthetic quotient of 1.4. The two approaches to estimating primary production yield estimates of similar order, being mindful that they measure production in a different manner and use slightly different experimental approaches.

Daily primary production rates measured by ¹⁴C uptake at oceanic sites of similar character (eg. BATS, HOTS; http://www1.who.edu/jgdms_info.html) generally fall between 100 and 1,200 mg C m⁻² d⁻¹ with long-term site averages of the order of 350 – 550 mg C m⁻² d⁻¹ (125 – 200 g C m⁻² year⁻¹). Cruise averages of daily production rates measured on earlier campaigns in the vicinity of Scott Reef were in the 700 – 750 mg C m⁻² d⁻¹ range. For comparison, historical measurements of primary production in oceanic regions of the Coral Sea (Furnas and Mitchell, 1996) and the Great Barrier Reef (Furnas, unpubl.) have averages close to 600 mg C m⁻² d⁻¹ and 780 mg C m⁻² d⁻¹, respectively. Daily production rates in the vicinity of Scott Reef are therefore within, but nearer to the upper end of, the range of modern production rates measured in a number of oligotrophic oceanic environments.

Estimates of primary production in reef lagoon habitats is somewhat more variable, being dependent upon the size, depth of the lagoon, as well as the degree of closure, water replacement times and the presence of alternative nutrient sources from adjacent islands in some cases. Furnas et al. (1990) measured daily primary production rates between 200 and 1,600 mg C m⁻² in shallow reef lagoons of the Great Barrier Reef. The deep atoll lagoons of the South Pacific are a better comparison, with depths, in many cases, of similar order to the South Reef lagoon, but often with much higher degrees of enclosure and reduced exchange with the surrounding ocean. Estimated primary production rates in these larger lagoonal systems range from 10 to 1,600 mg C m⁻² d⁻¹ across a number of studies and

lagoon systems. As at Scott Reef, primary production in these lagoonal systems was dominated by very small ($< 5 \mu\text{m}$) phytoplankton.

In summary, the productivity regime of the South Reef lagoon and the surrounding oceanic waters is similar to that encountered at oceanic reef systems in other regions of the tropical ocean.

Metabolism

Water column metabolism establishes the balance between production and respiration, and determines whether the system consumes CO_2 to form organic material ('autotrophic') or combusts organic carbon to form CO_2 ('heterotrophic'). The consumption of O_2 in water samples incubated in the dark is an index of water column respiration (metabolic activity by all microorganisms including bacteria, phytoplankton, and microzooplankton). O_2 evolution as a result of photosynthesis in water samples incubated in the light is an index of net primary production. Gross primary production (GPP) is the sum of respiration and net primary production. Globally, a threshold of GPP of $1 - 3 \text{ mmol m}^{-3} \text{ d}^{-1}$ is required to achieve metabolic balance (net production = respiration) in open-ocean planktonic communities (Duarte and Regaudie de Gioux, 2009). At Scott Reef, it was determined that this threshold is $1.50 \text{ mmol O}_2 \text{ m}^{-3} \text{ d}^{-1}$, which is similar to oligotrophic systems such as the subtropical Atlantic Ocean. The respiration rate of water column microbes was correlated with temperature, resulting in generally higher rates during the November – December cruises. Consequently, of 19 sets of oxygen flux measurements integrated throughout the water column at four sites around Scott Reef, 11 resulted in net water column heterotrophy, and of these seven were in the summer months. Overall, the Scott Reef metabolic data are similar to other areas of the tropical or subtropical ocean (Banda Sea, Tijssen et al., 1990; Arabian Sea, Dickson et al., 2001; Equatorial Atlantic, Perez et al., 2005) and align with the low end of data from similar experiments conducted in the Timor Sea and the Coral Sea. The frequent occurrence of heterotrophy at Scott Reef is similar to Station ALOHA off Hawaii (Williams et al., 2004), which is consistently heterotrophic; these authors suggest that this may be the case in many areas of the open ocean.

Measurements of primary production on the basis of oxygen flux differ from those made on the basis of ^{14}C incorporation, because of inherent methodological differences. For instance, the mean production rate in the lagoon measured by the ^{14}C method is $\sim 0.80 \text{ g C m}^{-2} \text{ d}^{-1}$, and by the O_2 method respiration corresponded to $1.32 \text{ g C m}^{-2} \text{ d}^{-1}$ and net production only $0.06 \text{ g C m}^{-2} \text{ d}^{-1}$ (summing to a measurement of gross production of $1.38 \text{ g C m}^{-2} \text{ d}^{-1}$), assuming photosynthetic and respiratory quotients of 1.4 and 1.1 respectively (Bender et al., 1999). The incorporation of ^{14}C -labelled bicarbonate into algal tissue is the most widely used method for measurement of primary production. Depending on a number of factors, including the trophic state of the waters of interest (oligotrophic or eutrophic etc.) and the incubation time, this measurement corresponds to a value of production at some point on a continuum between net and gross primary production (Williams and Lefèvre, 1996). In contrast, the measurement of production based on oxygen flux allows an estimate of both gross and net *community* production, but extrapolation to carbon fluxes is confounded by the choice of an appropriate photosynthetic quotient, as well as by the respiration of heterotrophs. It is expected that these ^{14}C -based measurements are closer to gross than net primary production, and therefore given the difference in techniques we consider that the disparity between estimates of gross production is reasonable. The data do suggest, however, that most production is lost to respiration.

Zooplankton

Zooplankton biomass data can be compared directly to that of the earlier North West Cape study as reported by Sampey et al. (2004), though that study was restricted to the summer months. Zooplankton biomass in the lagoon of South Reef during the summer ($31 - 41 \text{ mg dry weight m}^{-3}$) was comparable to that in Exmouth Gulf ($38 \text{ mg dry weight m}^{-3}$), but at the deeper water stations mixed layer biomass was half that of the shelf break at North West Cape ($12 \text{ vs } 25 \text{ mg dry weight m}^{-3}$; Sampey et al., 2004). Similarly, the summer abundance data at North West Cape reported by

McKinnon and Duggan (2003) was similar to that in the lagoon at Scott Reef (10,000 m⁻³ vs 6,000-9,000 m⁻³ respectively) but 2 to 4-fold higher than that in the mixed layer at the deeper water stations (1,800 – 5,300 m⁻³).

The only directly comparable study of zooplankton community composition is that of McKinnon et al. (2008) from North West Cape, which though restricted to summer coastal communities did use plankton nets with similar mesh size to the present study, and applied the same degree of taxonomic resolution. As at Scott Reef, copepods overwhelmingly dominated the mesozooplankton community. The copepod community at North West Cape was very similar to that found in the lagoon of South Reef and in the mixed layer at the deeper water stations, and was dominated by small paracalanid and oithonid copepods, as well as the same epipelagic species of Oncaidae. The Scott Reef samples are more oceanic in character, as well as depth stratified. The only other study of plankton community composition from the Eastern Indian Ocean was that of CSIRO in the early 1960's, which focused on the 110°E meridian between 9° and 32° S. (Tranter, 1977a, b). That study used plankton nets of substantially larger mesh (330 µm), and so targeted larger organisms. Despite this, there was a large overlap in the species of calanoid copepods recorded because of the presence of the same oceanic water masses. However, the present study is the first to study depth-stratified zooplankton communities, and the first to include small species.

Multivariate analysis of the zooplankton data discriminated distinct communities associated both with depth strata and with the site of collection. The lagoon zooplankton community formed part of a larger surface water community, but differed slightly from that taken from a similar depth range at the deeper water sites because of the presence of more reef-associated organisms. Zooplankton from the 50 – 100 m stratum formed a distinct community associated with the location of the deep chlorophyll maximum, and those from intermediate depths (represented by the 100 – 200 and 200 – 300 m strata) formed a third community typical of the SW open-water site. The fourth, and most distinct zooplankton community, was the near-bottom zooplankton community typical of the 300 – 400 m depth stratum at the deep channel and NE margin sites, where the deepest samples collected coincided with the maximum water depth. These samples contained representatives of copepod families known to occur in near-bottom waters, and which are very poorly known in Australian waters.

Six genera of tropical krill (Euphausiid shrimps) have been identified from Scott Reef, as sampled at at our three deep water sites (CH, NE and SW) as well as an additional site at the location of the sediment fan to the east of the deep channel (ER, Fig. 78). Of these genera, two showed no differences in abundance with location or time of day (day/night), but all of the others were more likely to occur at night and had differences according to the site of collection. On the basis of this sample series, it was unable to be demonstrated that the deep channel was a 'hotspot' of krill abundance that might possibly act as a cue for the attraction of megafauna. This result should be taken in the context of the methods used (bongo net samples), which do not necessarily have sufficient resolution to detect localised aggregations of krill associated with complex bathymetry. Consequently, the results do not necessarily discount the hypothesis that the deep channel is a preferred feeding area for megafauna. It is possible that amplification of strong current flow near the bottom enhances the flux of suspended particles used by suspension feeders. If this is the case, food particles from large volumes of water would accumulate in a relatively small area ("trophic focusing"), initiating localised aggregations of macroplankton/micronekton including krill. In addition, the reef structure itself could form refugia for these organisms. If either of these mechanisms occurs, Scott Reef could be attractive to passing plankton feeding megafauna. However, demonstrating this linkage requires a more targeted study than has been possible within the present project.

Strongest gradients in the vertical

The analyses of water column properties, water chemistry and plankton community structure consistently show that the greatest changes are related to depth, with relatively little horizontal difference between samples from the same depth at deeper sites or locations around Scott Reef. Within the lagoon, however, subtle differences between sites were observed. Picoplankton exhibited some spatial pattern (generally high *Synechococcus* and low *Prochlorococcus* in the lagoon), but these patterns were of the same order as those found vertically through the water column, with the greatest abundance found in the deep chlorophyll maximum. In contrast, nano- and microplankton abundances were significantly higher in the surface layer (<30 m depth).

The zooplankton community was very strongly structured according to depth, with mixed layer communities (surface and chlorophyll maximum) having both a higher abundance than, and distinct communities from, mid-water and near-bottom depth strata. The measurements of pelagic processes also showed strong depth structure, and only slight differences between sites. On the basis of these lines of evidence, it is concluded that the strongest gradients of biophysical variables occur in the vertical rather than the horizontal; i.e. that depth effects outweigh the differences between sites. This result means that the general patterns observed during the study can be extrapolated regionally.

Is the lagoon different from the surrounding ocean?

Yes, to a degree. The South Reef lagoon is a very open system in comparison with the highly enclosed atoll lagoon systems of French Polynesia. However, a variety of evidence clearly indicates that the bulk of water within the lagoon environment remains for sufficient time for persistent differences to develop between the lagoon environment and surrounding surface waters. The differences, as described above, include:

- Average temperature and salinity characteristics
- The degree of light attenuation by suspended particulate matter
- The spectral characteristics of reflected light at the surface (Remote Sensing Reflectance)
- Higher average concentrations of dissolved nutrients within the lagoon
- Higher average surface chlorophyll concentrations within the lagoon
- Higher abundances of autotrophic picoplankton, bacterioplankton and viruses
- Different relative abundances of autotrophic picoplankton toward ratios more indicative of eutrophied systems
- Higher zooplankton biomass inside the lagoon
- Differences in zooplankton community structure (more reef associated zooplankton)

Persistent differences in characteristics between the lagoon and surrounding waters show that the water within the lagoon has a sufficient residence time for internal processes to modify its character and for local planktonic biological communities to form and stabilise.

From an environmental management perspective, these differences mean that any wastewater or other discharges released into or reaching the lagoon (whether planned or unplanned) will be retained for some time until flushed out, with the potential to affect local biological communities within the lagoon. The retention time is poorly constrained at this time (but see below), but depends on the tidal range, tidal and residual currents, wind speed and wind direction.

Flushing times and circulation pathways will vary with location in the lagoon, with a general gradient of decreased flushing with distance away from the channel. Our observational evidence suggests

reduced flushing times in the central and southern sections of the lagoon, compared to locations closer to the deep channel. Short term flushing characteristics are controlled by the spring-neap tidal cycle, with increased flushing occurring during the larger tidal range of spring tides. A first order approximation of lagoon flushing times based on tidal flushing alone is of the order of 10 days.

Origin of cool water intrusions

This research has used multiple approaches to determine if the lagoonal waters are significantly different from those of the surrounding ocean. Part of this problem has been to determine the origin of the cool water intrusions into the South Reef lagoon. Observations of instantaneous temperature and temperature range along the margin of the channel, coupled with detailed knowledge of the temperature structure within the channel suggest that the origin of cool water intruded into the lagoon is from within the thermocline from depths of less than 160 m. There is some seasonality to this depth, driven by the density of the surrounding ocean, and the data suggest intruded water from a depth of ~100 – 160 m during winter, with a shallower origin (<100 m) during summer.

The analysis of zooplankton community structure determined that certain species are associated with particular depth strata. One family, the Oncaidae, in which the species are known to be associated with certain depth horizons, was used as an indicator species to detect the presence of upwelled or intruded water within the lagoon. Furthermore, this concept was developed by calculating a numerical index of indicator species for all taxa counted in the plankton samples. The occurrence within the lagoon of species corresponding to the 50 – 100 m stratum at the deeper stations was validated against the instrumental record of intrusive activity and gave moderately good agreement; i.e. that these animals do have some utility as indicators of the presence of water originating at sub-thermocline depths off-reef. There was, however, no indication whatsoever of the presence of deeper water (such as from the 250 – 450 m horizon) within the lagoon.

Carbon Budget

Volumetric exchange between the lagoon and the channel

The lagoon of South Reef has a spatial area, at mean sea level, of ~360 km², with a volume of ~13.5 km³, as estimated from a digital elevation model with 10 m horizontal resolution. Using an average tidal range of 2 m, the tidal prism of the lagoon is ~0.72 km³ or ~5% of the lagoon's volume. Assuming complete flushing of the tidal prism every tidal cycle, a first order approximation of lagoon flushing times based on tidal flushing alone would be of the order of 10 days.

The surface mixed layer around Scott Reef contains extremely low nutrient levels, and thus to determine the biological significance of the cool water intrusions, it is important to resolve the volume of the exchange of water from below the thermocline. Time series data from the two temperature moorings within the deep channel and on the sill of the lagoon were used together with current observations from the northern margin of the lagoon (site PE06) to estimate the volumetric exchanges of sub-thermocline water – taken to be water of a temperature of <26.5 °C (Table 40).

The total volumetric exchange of sub-thermocline water per month at times exceeds the total volume of the lagoon (e.g. September 2009), with an estimated annual exchange of greater than twice the volume of the lagoon. Maximum daily exchange rates are ~0.53 km³ d⁻¹, equivalent to the (semi-diurnal) tidal prism.

Total nitrate introduced through the intrusions of sub-thermocline water (Table 40) was estimated based on the relationships between temperature and nitrate concentrations (Fig. 37, Table 6), integrated for depths below the 26.5°C isotherm, multiplied by the volumetric inflow for a particular temperature range. Maximum daily nitrate input rates were estimated at 0.6 Mm (mol x 10⁶).

Table 40 Total volume and daily input rates for sub-thermocline water and nitrate during intrusion events.

	2009							2010	
	Jun	July	Aug	Sept	Oct	Nov	Dec	Jan	Total
Volume (km ³)	0.00	0.03	10.10	15.94	1.22	0.34	1.67	0.92	30.22
Vol. exchange (km ³ d ⁻¹)	0.000	0.001	0.326	0.531	0.039	0.011	0.054	0.030	
Nitrate (10 ⁶ mol)	0.00	0.13	3.66	18.07	1.54	0.57	4.02	3.04	31.04
Nitrate (10 ⁶ mol d ⁻¹)	0.000	0.004	0.118	0.602	0.050	0.019	0.130	0.098	

Based on pelagic primary production rates of $\sim 800 \text{ mg C m}^{-2} \text{ d}^{-1}$, the total carbon production for the lagoon can be estimated at $\sim 288 \text{ T C d}^{-1}$. Inputs of carbon production due to the sub-thermocline intrusions, based on a conservative estimate of 10% mixing and retention of intruded water and nitrate, are estimated to be of the order of 6 T C d^{-1} . This estimate is based on the assumption that $0.5 \mu\text{m}$ of nitrogen is equivalent to $1.0 \mu\text{g}$ of chlorophyll, and 50g C is equivalent to 1g chl . (Charpy and Charpy-Roubaud, 1990).

Even using the upper limit of nitrate supply via the cool water intrusions, daily pelagic production far exceeds (by two orders of magnitude) the carbon inputs in response to the deep water intrusions. The carbon fixed by photosynthesis within the euphotic zone ($0 - 100 \text{ m}$) each day at Scott Reef is quickly consumed within the upper water column (Fig. 80). Measured community respiration rates, whether on a volumetric or areal basis, usually equalled or exceeded carbon fixation or net oxygen production rates. Measured sedimentation fluxes of organic carbon down out of the euphotic zone (100 m) were generally $< 10\%$ of daily production rates. There is also a small downward mixing flux of dissolved organic carbon (DOC) driven by the ca. $20 \mu\text{M}$ concentration difference between the surface mixed layer and the deeper thermocline.

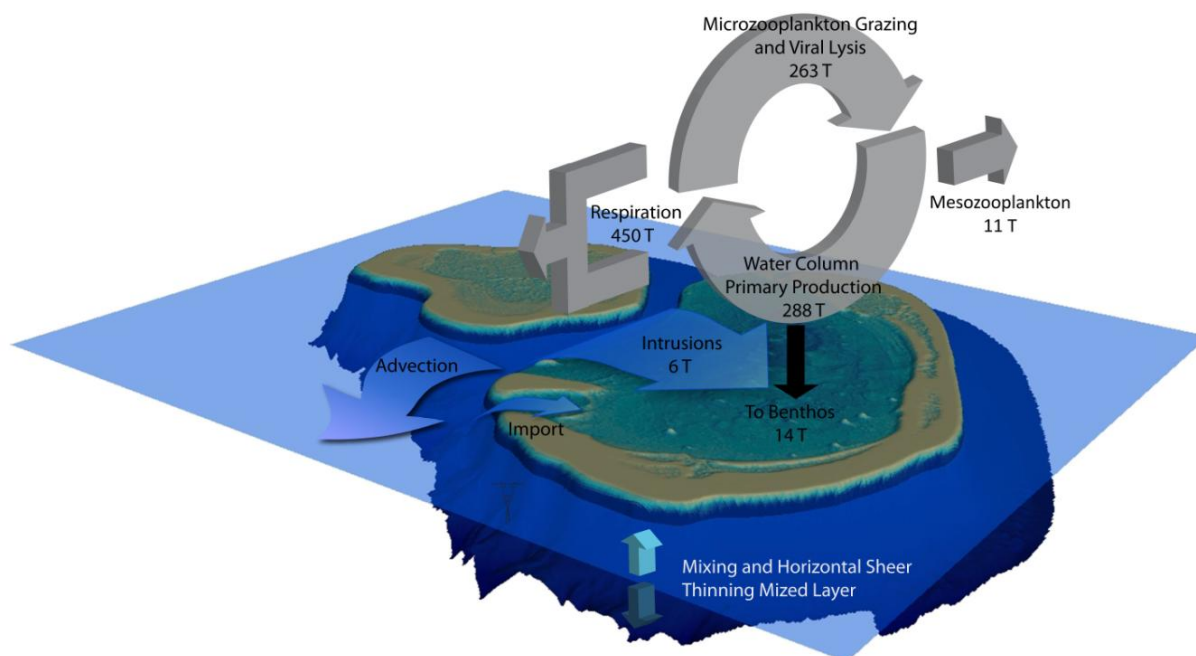


Fig. 80 A conceptual model of carbon cycling and export from the mixed layer at Scott Reef, showing daily rates in tonnes of carbon.

Biological consequences

Grazing by very small micro-zooplankters (flagellates and ciliates) and lysis by viruses results in the small cells responsible for most primary production turning over on a daily basis. Carbon consumed by bacteria is largely produced by direct excretion from phytoplankton cells and from the cellular debris released during the lysis of virus-infected cells. Respiratory losses by micro-organisms within the euphotic zone result in very little of the pelagic organic matter produced in the South Reef lagoon and surrounding waters being transferred to the benthic communities via sedimentation from the water column. The energy and organic matter required by benthic communities in the South Reef lagoon must therefore be largely produced autotrophically through primary production by benthic microflora, attached algae and photosynthetic symbionts (eg. zooxanthellae) in the corals and sponges (Cooper et al., 2009). While it is known that both corals and sponges are capable of feeding on very small particles such as picoplankters (eg. Fabricius et al., 1995), the densities of these organisms within both the lagoon and surrounding waters are too low to provide an adequate food source.

Lagoonal water quality and the dynamics of coral reef communities

The health and resilience of reef associated coral and fish communities are intimately linked to the physical, chemical and biological properties of the waters that surround them. The highly transparent, nutrient poor waters that bathe Scott Reef are highly suited for the development of coral reefs, and this is reflected in the biological diversity of the Scott Reef system which supports approximately 720 species of fish, 300 species of corals (Gilmour et al. 2010). The isolation of Scott Reef insulates the local reef communities from major terrestrial inputs and associated stressors affecting coral reefs closer to the coast. However, a range of natural disturbances such as cyclones, increasing ocean temperatures and changing ocean chemistry still perturb the dynamics of coral and fish communities at Scott Reef. The underlying drivers that determine whether communities recover, and the rate and extent to which the recovery trajectory converges towards a prior state, include the supply of new recruits (numbers and types), the rates of growth and survival of the corals and their competitors, and the prevailing physical and biological conditions at the location (Gilmour et al. 2010). This project has shown that water quality within the lagoon of Scott Reef is persistently high, with high clarity, low nutrients, low sedimentation rates and temperatures which are, in general, well suited to coral reef growth. If high water quality is maintained, then the dynamics of reef associated coral and fish communities at Scott Reef will be driven primarily by cycles of natural disturbance and recovery, with the timescales, rates and variability of recovery as documented in SRRP Project I (Gilmour et al. 2010).

Coral bleaching is a disturbance forecast to increase in frequency with increasing ocean temperatures. Recent research on the trophic response of corals to the combined effects of increased turbulence and reduced temperature associated with internal waves suggests that exposure to internal waves results in higher energy reserves, which may be crucial for coral resilience to stress and survival during periods of reduced or inactive photosynthesis, as is known to occur after coral bleaching (Roder et al., 2010). Therefore, the coral communities most exposed to the cool water intrusion and turbulence associated with internal wave activity around the perimeter and with the deep channel of Scott Reef may show enhanced resilience to temperature induced coral bleaching.

Benthic-Pelagic Coupling

One of the original hypotheses of this study was that the deep-living coral communities of the South Reef lagoon (depth 30 – 60 m) would be significantly light limited (0.4 – 7 ‰ based on a depth-averaged attenuation coefficient of 0 – 0.09 m⁻¹ in the lagoon) and there would be sediment resuspension so that the corals would be relatively more dependent on catching plankton or harvesting sedimenting detritus from the water column to survive and grow. However, measurements of the photosynthesis-irradiance (P vs I) characteristics of deep-living corals (SRRP Project 2) indicate that corals living on the lagoon floor are highly photoadapted to low light intensities and efficiently use the low available light. The corals therefore obtain most of their energy from symbiotic photosynthesis.

Direct measurements of inorganic and organic matter sedimentation fluxes by bottom-mounted and floating (Lagrangian) sediment traps clearly show that fluxes to the benthos are very low within the lagoon and on the deep margins of Scott Reef. Time-averaged daily collections of new and resuspended sediment by bottom-mounted sediment traps were generally less than 5,000 mg DW m⁻² d⁻¹, with all but one average value < 8,000 mg m⁻² d⁻¹. Daily organic matter fluxes measured in the central part of the South Reef lagoon ranged between 2.1 and 5.1 mmol C m⁻² (25 – 61 mg C m⁻²), or between 0.5 and 1 percent of the inorganic sedimentation flux. Concurrent organic nitrogen fluxes ranged between 0.12 and 0.46 mmol C m⁻² (1.7 – 6.2 mg C m⁻²). There are very few direct measurements of sedimentation fluxes from suitably deep reef lagoon habitats for comparison. Charpy and Charpy-Roubaud (1990) measured an average C sedimentation flux of 29 mmol C m⁻² d⁻¹ (350 mg C m⁻² d⁻¹) in the Tikehau Atoll (French Polynesia) lagoon. This site was both shallower and closer to the lagoon margin than the South Reef lagoon sedimentation site.

Zooplankton Biodiversity

This project has included a detailed taxonomic study of the copepod component of the zooplankton, and has identified >220 species of copepods, belonging to 5 of the 9 orders. Most excitingly, 68 (31%) are new records for Australian waters and at least 16 are likely to be new species. The hitherto unappreciated biodiversity within the family Oncaidae alone is remarkable, and appears to comprise >65 species, of which 35 are new records for Australia and 11 are undescribed, one of which represents a new genus

By comparison, 122 species of copepods were identified during the North West Cape study (McKinnon et al., 2008), substantially fewer than found at Scott Reef. The reason for the difference is the greater presence of the deep-water community at Scott Reef, with many species not having been sampled by any studies in Australian tropical waters. Copepod communities of the Great Barrier Reef, as compiled by McKinnon et al. (2007), have a similar number of species (~200) to those of Scott Reef, but do not include the very diverse small copepods included in the present study.

The extent to which Scott Reef represents a unique or special habitat is unknown, since there has been no study conducted with a comparable sampling strategy on similar habitats. Previous studies in open water have used nets with larger mesh sizes, which are now recognized to not sample the most abundant small (<1.0 mm) copepods in the zooplankton, such as those that constituted the bulk of the collections from Scott Reef. However, it is likely that the communities sampled at Scott Reef are typical of the plankton of the Eastern Equatorial Indian Ocean, since only a few of the species collected appear to be necessarily reef-associated, and these are typical of coral reef zooplankton elsewhere such as in the Great Barrier Reef.

Regional Applicability

The absence of appreciable differences in hydrographic structure, vertical nutrient distributions, plankton biomass, community structure and productivity between the three deep-water sites around Scott Reef (Deep Channel, NE Margin, Open Water) strongly indicates that the biological and chemical oceanographic observations made at these sites will be generally applicable to the wider deep water (>100 m) environment of the outer continental shelf overlying the Browse Basin region. This would include the Brecknock and Calliance gas fields. The water column conditions and processes, and pelagic ecosystem attributes observed in the vicinity of Scott Reef will likely apply to inshore shelf waters, with a shoreward boundary existing where significant interactions between deep-water internal waves or tides and the bottom begins, creating significant bottom stress or enhanced vertical mixing due to breaking internal waves and tides. In these regions where internal waves interact with the continental shelf, unpublished observations from an Acoustic Doppler Current Profiler in ~200m water depth in the Browse Basin collected by the University of Western Australia (Dr N Jones, *pers comm.*) show an increase in acoustic echo intensity up to 25m above the seabed during the passage of internal waves, presumably due to the resuspension of bottom sediments and work to confirm the source of the backscatter and better understand these processes is continuing.

Applicability to North Reef

North Reef differs from South Reef in having a much shallower and more enclosed lagoon with only two primary points of exchange with the surrounding ocean, and therefore presumably limited tidal exchange. North Reef is likely to exhibit average temperatures that are higher than the surrounding ocean as the contained water warms due to solar radiation. Salinities will also diverge from the surrounding ocean, being higher during times when evaporation is in excess of rainfall, and visa versa. With limited flushing, tidal currents within the interior of the lagoon will be weak, and the surficial sediments are likely to contain a larger percentage of fine material which will be more susceptible to resuspension during strong wind events. As such light attenuation may be more variable than observed in South Reef lagoon.

References

- Aristegui, J. and W.G. Harrison 2002. Decoupling of primary production and community respiration in the ocean: implications for regional carbon studies. *Aquatic Microbial Ecology* 29: 199–209.
- Behrenfeld, M.J. and P.G. Falkowski 1997. Photosynthetic rates derived from satellite-based chlorophyll concentration. *Limnology and Oceanography* 42 (1): 1–20.
- Behrenfeld, M.J., R.T. O'Malley, and D.A. Siegel 2006. Climate-driven trends in contemporary ocean productivity. *Nature* 444 (7120): 752–755.
- Bender, M., J. Orchardo, M. Dickson, R. Barber, and S. Lindley 1999. In vitro O₂ fluxes compared with ¹⁴C production and other rate terms during the JGOFS Equatorial Pacific experiment. *Deep-Sea Research I* 46: 637–654.
- Bertilsson, S., O. Berglund, D. Karl, and S.W. Chisholm 2003. Elemental composition of marine *Prochlorococcus* and *Synechococcus*: Implications for the ecological stoichiometry of the sea. *Limnology and Oceanography* 48:1721–1731.
- Bird, J., C. Steinberg, R. Brinkman, and F. McAllister 2004. Biological and Physical Environment at Scott Reef: 2003 to 2004, II: Physical Environment. Australian Institute of Marine Science.
- Brinton, E., M.D. Ohman, A.W. Townsend, M.D. Knight, and A.L. Bridgeman 2000. Euphausiids of the World Ocean. Biodiversity Center of ETI, World Biodiversity Database CD-ROM.
- Burney, C.M., K.M. Johnson, D.M. Lavoie, and J. McN. Sieburth 1979. Dissolved carbohydrate and microbial ATP in the North Atlantic: concentrations and interactions. *Deep-Sea Research* 26A: 1267–1290.
- Burney, C.M., P.G. Davis, K.M. Johnson, and J. McN. Sieburth 1981. Dependence of dissolved carbohydrate concentrations upon small scale nanoplankton and bacterioplankton distributions in the western Sargasso Sea. *Marine Biology* 65: 289–296.
- Burney, C.M., P.G. Davis, K.M. Johnson, and J. McN. Sieburth 1982. Diel relationships of microbial trophic groups and in situ dissolved carbohydrate dynamics in the Caribbean Sea. *Marine Biology* 67: 311–322.
- Calbet, A. and M.R. Landry 2004. Phytoplankton growth, microzooplankton grazing, and carbon cycling in marine systems. *Limnology and Oceanography* 49: 51–57.
- Charpy, L. and J. Blanchot 1998. Photosynthetic picoplankton in French Polynesian atoll lagoons: estimation of taxa contribution to biomass and production by flow cytometry. *Marine Ecology – Progress Series* 162: 57–70.
- Charpy, L. and J. Blanchot 1999. Picophytoplankton biomass, community structure and productivity in the Great Astrolabe Lagoon, Fiji. *Coral Reefs* 18:255–262.
- Charpy, L. and C.J. Charpy-Roubaud 1990. Trophic structure and productivity of the lagoonal communities of Tikehau Atoll (Tuamotu Archipelago, French Polynesia). *Hydrobiologia* 207: 43–52.
- Cooper TF, Dandan SS, Heyward A, Kühl M, McKinney DW, Moore C, O'Leary R, Ulstrup KE, Underwood JN, van Oppen MJH, Ziersen B (2009) Characterising the genetic connectivity and photobiology of deep water reef building corals at South Scott Reef, Western Australia. Report to the Browse Joint Venture Partners. Australian Institute of Marine Science, Perth Western Australia. 84pp.
- Crosbie, N.D. and M.J. Furnas 2001. Abundance, distribution and flow-cytometric characterization of picophytoprookaryote populations in central (17°S) and southern (20°S) shelf waters of the Great Barrier Reef. *Journal of Plankton Research* 23:809–828.
- Cresswell, G.R., A. Frische, J. Peterson, and D. Quadfasel 1993. Circulation in the Timor Sea. *Journal of Geophysical Research* 98:14,379–14,389.

- Dickson, M.-L., J. Orchardo, R. Barber, J. Marra, J. McCarthy, and R. Sambrotto 2001. Production and respiration rates in the Arabian Sea during the 1995 Northeast and Southwest Monsoons. *Deep-Sea Research II*, 48 (6–7): 1199–1230.
- Dinsdale, E.A., O. Pantos, S. Smriga, R.A. Edwards, F. Angly, L. Wegley, M. Hatay, D. Hall, E. Brown, M. Haynes, L. Krause, E. Sala, S.A. Sandin, R. Vega-Thurber, B.L. Willis, F. Azam, N. Knowlton, and F. Rohwer 2008. Microbial ecology of four coral atolls in the Northern Line Islands. *PLoS One* 3:e1584.
- Duarte, C. M. and A. Regaudie-de-Gioux 2009. Thresholds of gross primary production for the metabolic balance of marine planktonic communities. *Limnology and Oceanography* 54:1015–1022.
- Dufrêne, M. and P. Legendre 1997. Species assemblages and indicator species: the need for a flexible asymmetrical approach. *Ecological Monographs* 67, 345–366.
- Ducklow, H.W. 1990. The Biomass, Production and Fate of Bacteria in Coral Reefs. In: Dubinsky Z. (ed) *Ecosystems of the World*, Vol. 25. Elsevier Science Publishers, Amsterdam, p 265–289.
- Elliott, D. T. and K.W. Tang 2009. Simple staining method for differentiating live and dead marine zooplankton in field samples. *Limnology and Oceanography: Methods* 7, 585–594.
- Fabricius, K.E., Y. Benayahu, and A. Genin 1995. Herbivory in asymbiotic Soft Corals. *Science* 268:90–92.
- Ferrier-Pages, C. and J.P. Gattuso 1998. Biomass, production and grazing rates of pico- and nanoplankton in coral reef waters (Miyako Island, Japan). *Microbial Ecology* 35:46–57.
- Ferrier-Pages, C. and P. Furla 2001. Pico- and nanoplankton biomass and production in the two largest atoll lagoons of French Polynesia. *Marine Ecology Progress Series* 211: 63–76.
- Fitzwater, S.E., G.A. Knauer, and J.H. Martin 1982. Metal contamination and its effect on primary production measurements. *Limnology and Oceanography* 27: 544–551.
- Fuhrman, J.A. and F. Azam 1980. Bacterioplankton secondary production estimates for coastal waters of British Columbia, Antarctica and California. *Applied and Environmental Microbiology* 39(6): 1085–1095.
- Fuhrman, J.A. and F. Azam 1982. Thymidine incorporation as a measure of heterotrophic bacterioplankton production in marine surface waters. Evaluation and field results. *Marine Biology* 66: 109–120.
- Fuhrman, J.A., T.D. Sleeter, C.A. Carlson, and L.M. Proctor 1989. Dominance of bacterial biomass in the Sargasso Sea and its ecological implications. *Marine Ecology Progress Series* 57:207–217.
- Fukuda, R., H. Ogawa, T. Nagata, and I. Koike 1998. Direct determination of carbon and nitrogen contents of natural bacterial assemblages in marine environments. *Applied and Environmental Microbiology* 64:3352–3358.
- Furnas, M. 2007. Intra-seasonal and inter-annual variations in phytoplankton biomass, primary production and bacterial production at North West Cape, Western Australia; Links to the 1997-98 El Niño event. *Continental Shelf Research* 27: 958–980.
- Furnas, M. and N.D. Crosbie 1999. In situ growth dynamics of photosynthetic prokaryotic picoplankters, *Synechococcus* and *Prochlorococcus*. *Bulletin de l'Institut de Oceanographie de Monaco* 19: 387–414.
- Furnas, M.J. and A.W. Mitchell 1989. Shelf-scale estimates of phytoplankton primary production in the Great Barrier Reef. 6th International Coral Reef Symposium 2: 557–562.
- Furnas, M.J. and A.W. Mitchell 1996. Pelagic primary production in the Coral and southern Solomon Seas. *Marine and Freshwater Research* 47: 695–706.
- Furnas, M.J. and A.W. Mitchell 1999. Winter-time carbon and nitrogen fluxes on Australia's Northwest Shelf. *Estuarine, Coastal and Shelf Science* 49: 165–179.

- Furnas, M.J., A.W. Mitchell, M. Gilmartin, and N. Revelante 1990. Phytoplankton biomass and primary production in semi-enclosed reef lagoons of the central Great Barrier Reef, Australia. *Coral Reefs* 9: 1–10.
- Gasol, J. M., P. A. del Giorgio and C. M Duarte 1997. Biomass distribution in marine planktonic communities. *Limnology and Oceanography* 42:1353–1363.
- Genin, A. 2004. Bio-physical coupling in the formation of zooplankton and fish aggregations over abrupt topographies. *Journal of Marine Systems* 50: 3–20.
- Gilmour et al 2010; Long-term monitoring of coral and fish communities at Scott Reef. AIMS Document No SRRP-RP-RT-045. SRRP Project 1: 2010 Annual Report for Woodside as operator of the Browse LNG Development. Australian Institute of Marine Science, Townsville. 254pp
- Gobler, C.J., D.A. Hutchins, N.S. Fisher, E.M. Cosper, and S.A. Wilhemy-Sanudo 1997. Release and bioavailability of C, N, P, Se and Fe following viral release of a marine chrysophyte. *Limnology and Oceanography* 42(7):1492–1504.
- Gundersen, K., M. Heldal, S. Norland, D.A. Purdie, and A.H. Knap 2002. Elemental C, N and P cell content of individual bacteria collected at the Bermuda Atlantic Time-series Study (BATS) site. *Limnology and Oceanography* 47:1525–1530.
- Heldal, M., D.J. Scanlan, S. Norland, F. Thingstad, and N.H. Mann 2003. Elemental composition of single cells of various strains of marine *Prochlorococcus* and *Synechococcus* using X-ray microanalysis. *Limnology and Oceanography* 48:1723–1743.
- Hessen, D. O. and T. R. Anderson 2008. Excess carbon in aquatic organisms and ecosystems: Physiological, ecological and evolutionary implications. *Limnology and Oceanography* 53:1685–1696.
- Hirst, A. G. and T. Kiørboe 2002. Mortality of marine planktonic copepods: global rates and patterns. *Marine Ecology Progress Series* 230: 195–209.
- Holloway, P.E. 1983. Internal tides on the Australian North West Shelf. A preliminary investigation. *Journal of Physical Oceanography* 13: 1357–1370.
- Holloway, P.E. 1984. On the semidiurnal internal tide at the shelfbreak region on the Australian North West Shelf. *Journal of Physical Oceanography* 14: 1787–1799.
- Holloway, P.E. 1996. A numerical model of internal tides with application to the Australian North West Shelf. *Journal of Physical Oceanography* 26: 21–37.
- Holloway, P.E., S.E. Humphries, M. Atkinson, and J. Imberger 1995. Mechanisms for nitrogen supply to the Australian North West Shelf. *Australian Journal of Marine and Freshwater Research* 36: 753–764.
- Holmes, R.M., A. Minot, R. Kerouel, B.A. Hooker, and B.J. Peterson 1999. A simple and precise method for measuring ammonium in marine and freshwater ecosystems. *Canadian Journal of Fisheries and Aquatic Sciences* 56: 1801–1808.
- Jacquet, S., B. Delesalle, J.-P. Torréton, and J. Blanchot 2006. Response of phytoplankton communities to increased anthropogenic influences (southwestern lagoon, New Caledonia). *Marine Ecology Progress Series* 320:65–78.
- Jaspers, C., T.G. Nielsen, J. Carstensen, R.R. Hopcroft, and E.F. Møller 2009. Metazooplankton distribution across the Southern Indian Ocean with emphasis on the role of Larvaceans. *Journal of Plankton Research*. doi:10.1093/plankt/fbp002.
- Jitts, H.R. 1969. Seasonal variations in the Indian Ocean along 100 E. IV. Primary production. *Australian Journal of Marine and Freshwater Research* 20(1): 65–75.
- Jones, D.R., D.M. Karl and E.A. Laws 1996. Growth rates and production of heterotrophic bacteria and phytoplankton in the North Pacific subtropical gyre. *Deep Sea Research Part I*. 43(10): 1567–1580.
- Karl, D.M., E.A. Laws, P. Morris, P.J. LeB. Williams, and S. Emerson 2003. Metabolic balance of the open sea. *Nature* 426:32.
- Kimmerer, W. J. and A.D. McKinnon 1987. Growth, mortality, and secondary production of the copepod *Acartia tranteri* in Westernport Bay, Australia. *Limnology and Oceanography* 32: 14–28.

- Kirk, J.T.O. 1994. Light and photosynthesis in aquatic ecosystems, 2nd ed. Cambridge.
- Knauer, G.A., J.H. Martin, and K.W. Bruland 1979. Fluxes of particulate carbon, nitrogen and phosphorus in the upper water column of the northeast Pacific. *Deep-Sea Research* 26: 97–108.
- Kunze, E. and S. G. Llewellyn Smith 2004. The role of small-scale topography in turbulent mixing of the global ocean. *Oceanography*: 55–64.
- Laws, E.A., D.G. Redalje, L.W. Haas, P.K. Bienfang, R.W. Eppley, W.G. Harrison, D.M. Karl, and J. Marra 1984. High phytoplankton growth and production rates in oligotrophic Hawaiian coastal waters. *Limnology and Oceanography* 29: 1161–1169.
- Laws, E.A., G.R. Ditullio, and D.G. Redalje 1987. High phytoplankton growth and production rates in the North Pacific subtropical gyre. *Limnology and Oceanography* 32: 905–918.
- Marañón, E., P.M. Holligan, M. Varela, B. Mourino, and A.J. Bale 2000. Basin-scale variability of phytoplankton biomass, production and growth in the Atlantic Ocean. *Deep-Sea Research I* 47: 825–857.
- Martin, T. G., B.A. Wintle, J.R. Rhodes, P.M. Kuhnert, S.A. Field, S.J. Low-Choy, A.J. Tyre, and H.P. Possingham 2005. Zero tolerance ecology: improving ecological inference by modelling the source of zero observations. *Ecology Letters* 8: 1235–1246.
- McKinnon, A.D. and S. Duggan 2003. Summer copepod production in subtropical waters adjacent to Australia's North West Cape. *Marine Biology* 143: 897–907.
- McKinnon, A.D., S. Duggan, J.H. Carleton, and R. Bottger-Schnack 2008. Summer planktonic copepod communities of Australia's North West Cape (Indian Ocean) during the 1997–99 El Niño/La Niña. *Journal of Plankton Research* 30 (7): 839–855.
- McKinnon, A.D., A.J. Richardson, M.A. Burford, and M.J. Furnas 2007. Chapter 6: Vulnerability of Great Barrier Reef plankton to climate change. Pp. 121–152 in Marshall, P. & Johnson, J. (Eds.) *Assessing Climate Change Vulnerability of the Great Barrier Reef*. Great Barrier Reef Marine Park Authority, Townsville.
- Mobley, C.D. 1999. Estimation of the remote sensing reflectance from above-surface measurements. *Applied Optics* 38: 7442–7455.
- Parada, V., G. J. Herndl and M.G. Weinbauer 2006. Viral burst size of heterotrophic prokaryotes in aquatic systems. *Journal of the Marine Biological Association of the United Kingdom* 86:613–621.
- Parsons, T.R., Y. Maita, and C.M. Lalli 1984. *A Manual of Chemical and Biological Methods for Seawater Analysis*, Elsevier, New York.
- Partensky, F., W.R. Hess, and D. Vaultot 1999. Prochlorococcus, a marine photosynthetic prokaryote of global significance. *Microbiology and Molecular Biology Reviews* 63: 106–127.
- Perez, V., E. Fernandez, E. Marañón, P. Serret, R. Varela, A. Bode, M. Varela, M.M. Varela, X.A.G. Moran, E.M.S. Woodward, V. Kitidis, and C. Garcia-Soto 2005. Latitudinal Distribution of Microbial Plankton Abundance, Production, and Respiration in the Equatorial Atlantic in Autumn 2000. *Deep-Sea Research Part I-Oceanographic Research Papers* 52: 861–880.
- Preisendorfer, R.W. 1986. Secchi disk science: visual optics of natural waters. *Limnology and Oceanography* 31: 909–926.
- Robinson, C. and P.J.leB. Williams 1999. Plankton net community production and dark respiration in the Arabian Sea during September 1994. *Deep Sea Research II*, 46:745–765.
- Robinson, C. and P.J.leB. Williams 2005. Respiration and its measurement in surface marine waters. pp. 147–180 in: *Respiration in Aquatic Systems*, del Giorgio, P & Williams, P.J.leB (eds), Oxford University Press.
- Roder, C., L. Fillinger, C. Jantzen, M. Schmidt, S. Khokiattiwong, and C. Richter 2010. Trophic response of corals to large amplitude internal waves. *Marine Ecology Progress Series* 412:113–128.

- Rogers, C.S. 1990. Responses of coral reefs and reef organisms to sedimentation. *Marine Ecology Progress Series* 62: 185–202.
- Rowe, J.M., M.A. Saxton, M.T. Cottrell, J.M. DeBruyn, G. Mine Berg, D.L. Kirchman, D.A. Hutchins and S.W. Wilhelm 2008. Constraints on viral production in the Sargasso Sea and North Atlantic. *Aquatic Microbial Ecology* 52:233–244.
- Runge, J. A. and J.C. Roff 2000. The measurement of growth and reproductive rates. in: Harris, R. P.; Wiebe, P. H.; Lenz, J.; Skjoldal, H. R., and Huntley, M. Eds. *Zooplankton Methodology Manual*. London: Academic Press.
- Ryle, V.D., H.R. Mueller and P. Gentian 1981. Automated analysis of nutrients in tropical seawaters. *Australian Institute of Marine Science Technical Bulletin, Oceanography Series, No. 3*, AIMS, Townsville.
- Ryther, J.H. 1969. Photosynthesis and Fish Production in the Sea. *Science* 166 (3901): 72–76.
- Sampey, A., M.G. Meekan, J.H. Carleton, A.D. McKinnon, and M.I. McCormick 2004. Temporal patterns in distributions of tropical fish larvae on the North West Shelf of Australia. *Marine and Freshwater Research* 55: 473–487.
- Serret, P., E. Fernandez, C. Robinson, E.M.S. Woodward, and V. Perez 2006. Local Production Does Not Control the Balance Between Plankton Photosynthesis and Respiration in the Open Atlantic Ocean. *Deep-Sea Research Part II-Topical Studies in Oceanography* 53: 1611–1628.
- Sileshi, G. 2008. The excess-zero problem in soil animal count data and choice of appropriate models for statistical inference. *Pedobiologia* 52: 1–17.
- Sneath, P. H. A. and R. R. Sokal 1973. *Numerical Taxonomy*. San Francisco: Freeman.
- Sprintall, J. and M. Tomczak 1992. Evidence of the barrier layer in the surface layer of the Tropics. *Journal of Geophysical Research* 97: 7305–7316.
- Sprintall, J., S.E. Wijffels, R. Molcard, and I. Jaya. 2009. Direct estimates of the Indonesian throughflow entering the Indian Ocean: 2004–2006. *Journal of Geophysical Research—Oceans* vol. 114, C07001, doi: 10.1029/2008JC00527.
- Steehan Nielsen, E. 1952. The use of radioactive carbon (¹⁴C) for measuring organic production in the sea. *Journal of Cons. perm. International Exploration Mer.* 18: 117–140.
- Steinberg, C.R., R.M. Brinkman, J.C. Bird, and C. McLean 2003. *Biological and Physical Environment at Scott Reef: 1994;2003. III: The Physical Environment. A report produced for the Joint Venture Partners of WA 33-P (Woodside Energy Operator)*. Australian Institute of Marine Science. 38 p.
- Strickland, J.D.H. and T. R. Parsons 1972. *A practical handbook of seawater analysis*, 2nd Edition. *Bulletin of the Fisheries Research Board of Canada*, 311 pp.
- Tijssen, S.B., M. Mulder, and F.J. Wetsteyn 1990. Production and consumption rates of oxygen, and vertical oxygen structure in the upper 300 m in the eastern Banda Sea during and after the upwelling season, August 1984 and February/March 1985. *Netherlands Journal of Sea Research* 25: 485–499.
- Tomczak, M. and D.G.B. Large 1989. Optimum multiparameter analysis of mixing in the thermocline of the eastern Indian Ocean. *Journal of Geophysical Research* 94: 16141–16149.
- Torreton, J.-P. 1996. Biomass, production and heterotrophic activity of bacterioplankton in the Great Astrolabe Reef lagoon (Fiji). *Notes et Doc. Oceanogr.* 46: 78–90.
- Tranter, D. 1977a. Further studies of plankton ecosystems in the eastern Indian Ocean. I. Introduction - the study and the study area. *Australian Journal of Marine and Freshwater Research* 28: 529–540.
- Tranter, D. 1977b. Further studies of plankton ecosystems in the eastern Indian Ocean. V. Ecology of the Copepoda. *Australian Journal of Marine and Freshwater Research* 28: 593–625.
- Vaulot, D. and D. Marie 1999. Diel variability of photosynthetic picoplankton in the equatorial Pacific. *Journal of Geophysical Research* 104:3297–3310.

- Venter, J. C., K. Remington, J.F. Heidelberg, A.L. Halpern, D. Rusch, J.A. Eisen, D. Wu, I. Paulsen, K.E. Nelson, W. Nelson, D.E. Fouts, S. Levy, A.H. Knap, M.W. Lomas, K. Nealson, O. White, J. Peterson, J. Hoffman, R. Parsons, H. Baden-Tillson, C. Pfannkoch, Y.-H. Rogers and H.O. Smith 2004. Environmental genome shotgun sequencing of the Sargasso Sea. *Science* 304: 66–74.
- Verity, P.G., C.Y. Robertson, C.R. Tronzo, M.G. Andrews, J.R. Nelson, and M.E. Sieracki 1992. Relationship between cell volume and the carbon and nitrogen content of marine photosynthetic nanoplankton. *Limnology and Oceanography* 37:1434–1446.
- Wainwright, L., G. Meyers, S. Wijffels, and L. Pigot 2008. Change in the Indonesian throughflow with the climatic shift of 1976/77. *Geophysical Research Letters*, vol. 35, L03604, doi: 10.1029/2007GL031911.
- Weinbauer, M.G., I. Brettar, and M.G. Hofle 2003. Lysogeny and virus-induced mortality of bacterioplankton in surface, deep, and anoxic marine waters. *Limnology and Oceanography* 48:1457–1465.
- Weinbauer, M.G., J.-M. Arrieta, C. Griebler, and G.J. Herndl 2009. Enhanced viral production and infection of bacterioplankton during an iron-induced phytoplankton bloom in the Southern Ocean. *Limnology and Oceanography* 54:774–784.
- Wijffels, S.E., G. Meyers, and J.S. Godfrey 2008. A 20-yr average of the Indonesian throughflow: regional currents and the interbasin exchange, *Journal of Physical Oceanography*, vol. 38, no. 9, pp. 1965–78.
- Wilhelm, S.W., S.M. Brigden, and C.A. Suttle 2002. A dilution technique for the direct measurement of viral production: A comparison in stratified and tidally mixed coastal waters. *Microbial Ecology* 43:168–173.
- Williams, P.J. le B. 1998. The balance of plankton respiration and photosynthesis in the open oceans. *Nature* 394:55–57
- Williams, P. J. I. B. and D. Lefèvre 1996. Algal ¹⁴C and total carbon metabolisms. I. Models to account for respiration and recycling. *Journal of Plankton Research* 18: 1941–1959.
- Williams, P.J.I.B., P.J. Morris, and D.M. Karl 2004. Net community production and metabolic balance at the oligotrophic ocean site, station ALOHA. *Deep Sea Research I* 51: 1563–1578.
- Wolanski, E. and E. Deleersnijder 1998. Island-generated internal waves at Scott Reef, Western Australia. *Continental Shelf Research* 18(13): 1649–1666.
- Worden, A.Z. and B.J. Binder 2003. Application of dilution experiments for measuring growth and mortality rates among *Prochlorococcus* and *Synechococcus* populations in oligotrophic environments. *Aquatic Microbial Ecology* 30:159–174.

Previous reports submitted to Woodside with information related to internal wave activity at Scott Reef

- Furnas, M. and C. Steinberg 1995. Environmental and oceanographic measurements at Scott Reef, Western Australia, Report to Woodside Energy Limited, January 1995.
- Furnas, M. and C. Steinberg 1996. Environmental and oceanographic measurements at Scott Reef, Mermaid Reef and Broome, Western Australia: September 1994 to October 1995, Report to Woodside Energy Limited, February 1996.
- Furnas, M. and C. Steinberg 1997. Environmental and oceanographic measurements at Scott Reef, Mermaid Reef and Broome, Western Australia: August 1995 to November 1996, Report to Woodside Energy Limited, April 1997.
- Furnas, M. and C. Steinberg 1997. Environmental and oceanographic measurements at Scott Reef, Mermaid Reef and Broome, Western Australia: November 1996 to November, 1997, Report to Woodside Energy Limited, May 1998.
- Furnas, M. and C. Steinberg 1999. Environmental and oceanographic measurements at Scott Reef, Mermaid Reef and Broome, Western Australia: October 1997 to January, 1999, and Final project review of observations August 1993 to January 1999, Report to Woodside Energy Limited, October 1999.

Glossary

- Archaea:** are a group of single-celled microorganisms. They have no cell nucleus or any other membrane-bound organelles within their cells.
- Autotroph (ic):** organisms that produces complex organic compounds from simple inorganic molecules using energy from light or inorganic chemical reactions.
- Bacterioplankton:** single-celled microorganism with no nucleus of membrane bound organelles. In aquatic waters, bacterioplankton are composed of phylogenetically and metabolically diverse members. In marine waters in the euphotic zone, the majority of bacterioplankton are heterotrophic; that is they obtain their energy requirements from organic substrates.
- BATS (Bermuda Atlantic Time Series):** a long-term time-series study examining biogeochemical cycles in the Sargasso Sea near Bermuda. The BATS team is involved in making monthly measurements of important hydrographic, biological and chemical parameters throughout the water column at sites within the Sargasso Sea.
- Biogeochemistry:** the scientific study of the chemical, physical, geological, and biological processes and reactions that govern the composition of the natural environment (including the biosphere, the hydrosphere, the pedosphere, the atmosphere, and the lithosphere), and the cycles of matter and energy that transport the Earth's chemical components in time and space.
- Chlorophyll:** a green pigment found in most plants, algae, and cyanobacteria. Its name is derived from Greek: χλωρός (chloros "green") and φύλλον (phyllon "leaf"). Chlorophyll absorbs light most strongly in the blue and red but poorly in the green portions of the electromagnetic spectrum, hence the green colour of chlorophyll-containing tissues. Chlorophyll is vital for photosynthesis, which allows plants to obtain energy from light.
- Conductivity:** a measure of a material's ability to conduct an electric current.
- Copepods:** are a group of small crustaceans found in the sea and freshwater habitats.
- CTD (Conductivity/Temperature/Depth):** main instrument for measuring water characteristics such as salinity, temperature, pressure, depth and density.
- Cyanobacteria:** blue-green algae, blue-green bacteria or Cyanophyta, is a phylum of aerobic bacteria that obtain their energy through photosynthesis. They are a significant component of the marine nitrogen cycle and an important primary producer in many areas of the ocean.
- Diatom:** a major group of eukaryotic algae, and are one of the most common types of phytoplankton. Most diatoms are unicellular, although they can exist as colonies in the shape of filaments or ribbons (e.g. *Fragillaria*), fans (*Meridion*), zigzags (*Tabellaria*), or stellate colonies (*Asterionella*). Diatoms are primary producers. A characteristic feature of diatom cells is that they produce a cell wall made of silica (hydrated silicon dioxide) called a frustule.
- Diel:** pertaining to a 24-hour period
- Dinoflagellate:** a large group of flagellate protists. About half of all dinoflagellates are photosynthetic.
- DIN (Dissolved Inorganic Nitrogen):** is the sum of the concentrations of nitrate, nitrite and ammonia.
- DIP (Dissolved Inorganic Phosphorus):** the amount of dissolved inorganic phosphorus available for plant growth. Phosphorus is a major plant nutrient, and is often considered the most limiting nutrient in freshwater systems. DIP dynamics is complicated by the absorption of phosphate onto particles, making it temporarily unavailable for plant growth.
- DOC (Dissolved Organic Carbon):** organic carbon remaining in a sample after filtering the sample, typically using a 0.45 μm filter.
- DON (Dissolved Organic Nitrogen):** nitrogen incorporated into dissolved organic molecules. Most DON-N is not immediately bioavailable to phytoplankton and bacteria as it is part of large and stable molecules. Some small organic molecules (urea, amino acids) can be taken up, but their concentrations are very low in tropical oceanic waters (10^{-8} – 10^{-9} moles L^{-1}).
- DOP (Dissolved Organic Phosphorus):** phosphorus incorporated into dissolved organic molecules. DOP-P is bioavailable to some phytoplankton and bacteria which excrete enzymes that break down the DOP to release PO_4^{3-} . Concentrations are very low in tropical oceanic waters (typically, 10^{-8} – 10^{-9} moles L^{-1}).
- Downwelling:** the process of accumulation and sinking of higher density material beneath lower density material, such as cold or saline water beneath warmer or fresher water or cold air

beneath warm air. It is the sinking limb of a convection cell. Upwelling is the opposite process and together these two forces are responsible in the oceans for the thermohaline circulation.

Eukaryotes: organisms whose cells are organized into complex structures enclosed within membranes. The defining membrane-bound structure that differentiates eukaryotic cells from prokaryotic cells is the nucleus. The presence of a nucleus gives these organisms their name.

Euphotic zone: the near-surface layer of water receiving sufficient sunlight for photosynthesis to occur. The depth of the euphotic zone can be greatly affected by turbidity. In general practice, the euphotic zone is taken to extend from the surface to a depth where in situ light intensity falls to 1% of that at the surface, so its thickness depends on the extent of light attenuation in the water column. In clear tropical waters, dark-adapted phytoplankton at depth may still have limited photosynthesis to the 0.1% light depth. Since the euphotic zone is the only zone of water where primary productivity occurs, an exception being the productivity connected with abyssal hydrothermal vents along mid-oceanic ridges, the depth of the photic zone is generally proportional to the level of primary productivity that occurs in that area of the ocean. About 90% of all marine life lives in this region.

Femtoplankton: the size fraction of plankton organisms smaller than 0.2 μm . This primary organisms in this size fraction are viruses, but a few types of free-living bacteria are also this small.

Flagellates: cells with one or more whip-like organelles called flagella. Some flagellates are autotrophic (with chlorophyll) and are members of the phytoplankton, while others are wholly or partly heterotrophic and feed on bacteria, detritus and other small phytoplankton.

FlowCam: uses flow-cytometry principles to count cells in a larger size fraction than the flow-cytometer and also takes photographic images of each particle to facilitate their identification.

Flow cytometry: is a technique for counting and examining microscopic particles by suspending them in a stream of fluid and passing them by an electronic detection apparatus.

Fluorescence: light emission that is mostly found as an optical phenomenon in cold bodies, in which the molecular absorption of a photon triggers the emission of another photon with a longer wavelength.

Gross production: see primary production.

Heterotroph (ic): organisms that require organic substrates to obtain energy for growth and development. This contrasts with autotrophs such as plants which are able to directly use sources of energy such as light to produce organic substrates from inorganic carbon dioxide.

HOTS (Hawaii Ocean Time Series): long-term oceanographic study based at the University of Hawaii at Manoa. Scientists working on this program have been making repeated observations of the hydrography, chemistry and biology of the water column at a station north of Oahu, Hawaii since October 1988.

Hydrography: the measurement of physical characteristics of waters and marginal land. In the generalised usage, "hydrography" pertains to measurement and description of any waters. With that usage oceanography and limnology are subsets of hydrography.

Internal waves: gravity waves that oscillate within, rather than on the surface of, a fluid medium. They arise from perturbations to hydrostatic equilibrium, where balance is maintained between the force of gravity and the buoyant restoring force. A simple example is a wave propagating on the interface between two fluids of different densities, such as oil and water. Internal waves typically have much lower frequencies and higher amplitudes than surface gravity waves because the density differences (and therefore the restoring forces) within a fluid are usually much smaller than the density of the fluid itself. Internal wave motions are ubiquitous in both the ocean and atmosphere. Internal waves at a tidal frequency are known as internal tides. Nonlinear solitary internal waves are called solitons.

Irradiance: the radiant power (rate of flow of electromagnetic energy) incident per unit area upon a surface.

Lysis: refers to the breaking down of a cell, often by viral, enzymic, or osmotic mechanisms that compromise its integrity.

Metabolism: the set of chemical reactions that occur in living organisms in order to maintain life.

Metazoa(n): eukaryotic multicellular animals.

Microalgae: microscopic, usually uni-cellular algae typically found in freshwater and marine systems. They are unicellular species which exist individually, or in chains or groups. Depending on the species, their sizes can range from a few micrometers (μm) to a few hundreds of micrometers.

Microzooplankton: zooplankton between 20 and 200 micrometres in size.

Net production: see primary production.

NH₄⁺ (Ammonium): the principal N form excreted by zooplankton and the preferred form of inorganic N as it is readily assimilated into amino acids and other biomolecules. Concentrations are typically very low (10^{-8} – 10^{-9} moles L⁻¹) in surface seawater due to rapid uptake by phytoplankton and bacteria.

NO₂⁻ (Nitrite): a transitional oxidational form between ammonium and nitrate produced by phytoplankton and bacteria. Usually only detectable at very low concentrations (10^{-8} – 10^{-9} moles L⁻¹) in a layer at the top of the thermocline.

NO₃⁻ (Nitrate): the most stable and predominant form of inorganic N in deep oceanic waters. Concentrations range from 10^{-9} moles L⁻¹ at the surface to 10^{-5} moles L⁻¹ at depths > 1,000 m. Nitrate is energetically expensive to reduce to ammonium which can be assimilated into biomolecules.

Nutrient: chemical that an organism needs to live and grow that must be taken in from its environment.

Oceanography: the branch of Earth science that studies the ocean. It covers a wide range of topics, including marine organisms and ecosystem dynamics; ocean currents, waves, and geophysical fluid dynamics; plate tectonics and the geology of the sea floor; and fluxes of various chemical substances and physical properties within the ocean and across its boundaries. These diverse topics reflect multiple disciplines that oceanographers blend to further knowledge of the world ocean and understanding of processes within it: biology, chemistry, geology, meteorology, and physics.

Oligotrophic: an ecosystem or environment that offers little to sustain life. The term is commonly utilised to describe bodies of water with very low nutrient levels.

PAR (Photosynthetically Active Radiation): the spectral range of solar light from 400 to 700 nanometers that is useful to plants in the process of photosynthesis. PAR is measured as $\mu\text{mol Q m}^{-2} \text{sec}^{-1}$, where Q = photons.

Pelagic: water in the sea that is not close to the bottom is in the pelagic zone. The word pelagic comes from the Greek πέλαγος or pélagos, which means open sea.

Photosynthetic quotient: in photosynthesis, the moles of oxygen produced, divided by the moles of carbon dioxide assimilated.

Phytoplankton: the autotrophic component of the plankton community. Most phytoplankton are too small to be individually seen with the unaided eye.

Picoplankton: the size fraction of plankton composed by cells between 0.2 and 2 micrometers. Important members of the picoplankton size fraction include: heterotrophic and autotrophic bacteria, cyanobacteria, very small eukaryotic cells (autotrophic and heterotrophic).

PO₄³⁻ (Phosphate): the predominant form of inorganic P in seawater and the most common form of P excreted by zooplankton. Concentrations typically range from 10^{-8} moles L⁻¹ at the surface to 10^{-6} moles L⁻¹ at depth.

Primary production: the production of organic compounds from atmospheric or aquatic carbon dioxide, principally through the process of photosynthesis, with chemosynthesis being much less important. All life on earth is directly or indirectly reliant on primary production. The organisms responsible for primary production are known as primary producers or autotrophs, and form the base of the food chain. In aquatic ecoregions algae are primarily responsible. Primary production is distinguished as either net or gross, the former accounting for losses to processes such as cellular respiration, the latter not.

Protists: a diverse group of eukaryotic microorganisms. Historically, protists were treated as the kingdom Protista but this group is no longer recognized in modern taxonomy. The protists do not have much in common besides a relatively simple organisation -- either they are unicellular, or they are multicellular without specialized tissues.

Quantum (plural: quanta): is the minimum amount of any physical entity involved in an interaction.

Redfield Ratio: the molecular ratio of carbon, nitrogen and phosphorus in phytoplankton. The optimal ratio is C:N:P = 106:16:1.

Respiration: the set of the metabolic reactions and processes that take place in organisms' cells to convert biochemical energy from nutrients into adenosine triphosphate (ATP), and then release waste products.

Secchi disk: a circular disk used to measure water transparency.

Si (OH)₄ (Silicate): silicic acid is required by diatoms to synthesise their hydrated silicate (opal) cell walls. Concentrations in tropical oceanic waters range from 10^{-6} moles L⁻¹ at the surface to 10^{-4} moles L⁻¹ at depths > 1,000 m.

- Stratification (thermal):** temperature layering effect that occurs in water. Stratification is due to differences in water density: warm water is less dense than cool water and therefore tends to float on top of the cooler, heavier water.
- Thermocline:** a thin but distinct layer in a large body of water, such as an ocean or lake, in which temperature changes more rapidly with depth than it does in the layers above or below. In the ocean, the thermocline may be thought of as an invisible blanket which separates the upper mixed layer from the calm deep water below. Depending largely on season, latitude and turbulent mixing by wind, thermoclines may be a semi-permanent feature of the body of water in which they occur, or they may form temporarily in response to phenomena such as the radiative heating/cooling of surface water during the day/night. Factors that affect the depth and thickness of a thermocline include seasonal weather variations, latitude, and local environmental conditions, such as tides and currents.
- Topography:** relief or terrain of the ocean bottom, the three-dimensional quality of the surface.
- T-S plots:** plots of salinity as a function of temperature, called T-S plots, are used to delineate water masses and their geographical distribution, to describe mixing among water masses, and to infer motion of water in the deep ocean. Water properties, such as temperature and salinity, are formed only when the water is at the surface or in the mixed layer. Heating, cooling, rain, and evaporation all contribute. Once the water sinks below the mixed layer, temperature and salinity can change only by mixing with adjacent water masses.
- Turbidity:** the cloudiness or haziness of a fluid caused by individual particles (suspended solids) that are generally invisible to the naked eye, similar to smoke in air. The measurement of turbidity is a key test of water quality.
- Upwelling:** wind-driven motion of dense, cooler, and usually nutrient-rich water towards the ocean surface, replacing the warmer, usually nutrient-depleted surface water. There are at least five types of upwelling: coastal upwelling, large-scale wind-driven upwelling in the ocean interior, upwelling associated with eddies, topographically-associated upwelling, and broad-diffusive upwelling in the ocean interior.
- Virus:** infectious micro-organisms that cannot reproduce outside host cells. In aquatic waters, native viruses predominantly infect bacterioplankton and picoplankton. Through cell lysis, viral activity promotes nutrient cycling through the microbial food web.
- Zooplankton:** the heterotrophic (sometimes detritivorous) type of plankton. Plankton are organisms drifting in the water column of oceans, seas, and bodies of fresh water. Many zooplankton are too small to be seen individually with the naked eye.

Appendices

Appendix I: Methods used on Biological Oceanography Cruises.

SAMPLING

Vertical Profiling (T°C, S‰, Chlorophyll fluorescence, Beam transmittance, PAR)

Vertical profiles of temperature (T°C), salinity (S‰), chlorophyll fluorescence (Wetlabs Wetstar), photosynthetically available radiation (PAR: 400 – 700 nm Biospherical QSP-200), and beam transmittance (Seatech 25 cm path length) were determined at all sampling stations with a Seabird SBE19+ CTD profiler. The instrument was operated according to the manufacturer's directions. The SBE19+ samples at 4 Hz, and was lowered/raised at ca. 1 m sec⁻¹ during profiles. After casts, the raw data was downloaded to disk and converted to engineering values using manufacturer's software (DATCNV) and supplied instrument coefficients, filtered to remove bad scans (FILTER, WILDEDIT and binned (BINAvg)) at 1m intervals for further analysis and plotting.

Temperature and salinity profile data was checked against discrete temperature and salinity values measured in parallel water bottle casts. Temperatures were measured with RTM digital reversing thermometers and discrete salinity samples were collected from Niskin bottles. The salinity samples were analysed with a Guildline AutoSal laboratory salinometer calibrated against IAPSO standard seawater.

Chlorophyll fluorescence values were initially calculated with the software provided by Seabird (DATCNV). Profile fluorescence values were compared to chlorophyll concentrations in discrete samples collected in parallel Niskin bottle casts.

Discrete Water Samples

Discrete water samples were collected by hydrocasts using Niskin bottles closed at depth. Two of the bottles were fitted with reversing thermometers for CTD profile validation. The number of bottles in a cast was determined by the sampling requirements and water column depth. In deep waters, up to six depths were sampled and as few as two depths in the shallowest part of the South Reef lagoon.

Sub-samples of water were drawn from the Niskin bottles in order of priority: dissolved oxygen (when run), dissolved nutrients, chlorophyll, picoplankton abundance, total suspended solids (TSS), particulate nutrients (PN, PP, POC) and salinity.

Water Clarity (Secchi Disk)

At some stations occupied between approximately 09:00 and 15:00, estimates of water clarity were determined using a Secchi disk (Preisendorfer, 1986). The Secchi disk is a 30 cm weighted white disk with a line marked at 1 m intervals that was lowered through the water until it just disappeared from view and the depth was then recorded. Deployment of the Secchi disk depended upon sea and light conditions at the station being suitable for making reliable measurements. In rough seas, the hard chine of the R.V. Solander created significant surface spray and bubbles that made it difficult to make accurate Secchi disk disappearance measurements. When done properly, this measure gives a general index of the depth of the

euphotic zone (ca. 1% of surface irradiance – I_0) and the diffuse attenuation coefficient ($K_d \approx 1.7/\text{depth}_{\text{Secchi}}$).

Zooplankton sampling (Multinet)

Vertically stratified tows were taken four times over a day at each process site with a multinet (Midi model, 50 cm mouth size, Hydro-Bios, Kiel) equipped with five 100 μm -mesh nets. Each of the five nets was equipped with a calibrated Hydro-Bios flowmeter, to allow for individual estimates of filtered volume for each sample. Depth strata sampled by each net was selected to span three layers of sub-thermocline water, mixed layer water and the surface layer.

Each net sample was split into equal portions, one of which was preserved in formaldehyde for analysis of community composition, and the other filtered onto a pre-weighed disk of 73 μm mesh and frozen.

Zooplankton sampling (Bongo net)

Oblique bottom to surface tows were taken four times over a day at the lagoon site with a bongo net equipped with 2 WP-2 100 μm -mesh nets. Each of the nets was equipped with a calibrated Hydro-Bios flowmeter, to allow for individual estimates of filtered volume for each sample. For sampling larger plankton, such as krill, the nets were replaced with 500 μm -mesh nets.

Each net sample was split into equal portions, one of which was preserved in formaldehyde for analysis of community composition, and the other filtered onto a pre-weighed disk of 73 μm mesh and frozen.

Organic sedimentation (Lagrangian Sediment Traps)

Downward fluxes of particulate matter from the euphotic zone were measured using Lagrangian surface-tethered particle interceptor trap arrays (Knauer et al., 1979). The trap arrays consist of twelve (12) 75 x 600 mm polycarbonate tubes standing vertically in a fixed submerged array that acts as a drogue. The individual traps were fitted with a baffle at the top end to prevent intrusion of turbulence into the trap during retrieval or from current shear, and a near-bottom drain to allow removal of most water within, without disturbing the sedimented material resting at the bottom of the trap tubes.

Lagrangian surface-tethered traps were deployed to drift freely with the current to “tag” a particular water mass and minimise cross-trap current shear. During deployments, the trap array was suspended from a linear string of surface floats that served to dampen vertical array movements due to surface wave motion. A dan buoy with radar reflector and flashing light was used to track the movement of the array. The depth of trap deployment depended upon the sampling site. In open ocean waters, traps were generally deployed at the base of the euphotic zone (ca. 100 m). In shallow reef waters, shorter tethers were used so that the trap floated approximately 5m above the bottom. Trap deployments were ~12 hours (shelf waters with reefs) (Furnas and Mitchell, 1999). Because of the short duration of the deployments, no preservatives were used in the traps, making all available for chemical analysis.

Upon recovery, the traps were visually inspected to determine which were affected by undue in-trap turbulence and mixing. The trap contents were then allowed to settle for ca. 1 hr. Relatively little suspended matter was usually seen in individual traps. After settlement, overlying water in the individual trap tubes was carefully drained away to reduce trap contents to the sedimented material in the bottom water (ca. 350 ml) of the tubes. After the traps

were drained, the contents were swirled to mix them up and the remaining water in individual tubes filtered onto a pre-weighed and pre-combusted glass fibre filter (Whatman GF/F, 47 mm). The filtered material from individual traps was then frozen for later analysis.

CTD and water bottle casts were undertaken immediately next to the deployed trap array at the time of deployment and recovery to establish water column concentrations and distributions of materials collected in the traps.

Primary Production (¹⁴C uptake)

Estimates of primary production in intact and size fractionated water samples were made using the uptake of radioactive ¹⁴C-bicarbonate into particulate matter (Steeman Nielsen, 1952). This method has been in general use within biological oceanography groups over the last 25 years (Furnas, 2007; Furnas and Mitchell, 1996, 1999).

Water samples for primary production measurements were collected between 08:00 and 09:00 local time from multiple depths in the water column using Niskin bottles with well-aged rubber closures. The sampling depths (between four and eight at a given station depending on water depth) were selected to have nominal mid-day in situ irradiance levels (100, 50, 30, 20, 8, 4, 1.6 and 0.6 percent of surface irradiance) close to those simulated in an on-deck incubator. Nominal isolume depths were estimated from mid-day underwater light profiles made at or near the production measurement site with an underwater irradiance sensor. Where a pre-experiment light profile could not be made, isolumes depths were estimated from previous light casts made in waters of similar optical characteristics.

In most cases, primary production was measured using the total population and two size classes: > 10 µm and > 2 µm. In these experiments, aliquots to be size fractionated were filtered after the incubations onto polycarbonate membrane filters. Photosynthesis rates in size fractions not directly measured (e.g. 2 to 10 µm, <2 µm) were calculated by difference.

Production incubations were carried out in 250 ml clear polycarbonate bottles (Nalgene). The bottles were acid-soaked (10% trace metal grade HCl), deionised water soaked, deionised water rinsed and dried between cruises. Nine sub-samples were taken from the Niskin bottle at each sampling depth. Care was taken throughout to minimise contamination by metals or organic materials (Fitzwater et al., 1982). Filled sample bottles were stored in closed deck boxes between filling and the start of incubations and between the end of incubations and filtration.

Water samples were spiked under dim light conditions with 5 µCi (0.9 MBq) of ¹⁴C-bicarbonate (GE Life Sciences). Isotope stocks were stored refrigerated in Teflon bottles. All plasticware used for isotope handling and spikes was cleaned, soaked in trace-metal grade HCl and rinsed with deionised water (MilliQ). After spiking, three incubation bottles from each sampling depth and size fraction were wrapped in aluminium foil to serve as dark bottles. The incubation bottles were then transferred to a multi-tank deck incubator filled with running surface seawater. Surface-to-bottom temperature gradients in shelf waters were <5°C. Individual tanks were screened with one or more layers of black plastic shade cloth to simulate in-situ light levels. The spiked samples were incubated for 4 hours, nominally 10:00 to 14:00 local time.

Following incubation, sample bottles were retrieved from the incubator tanks and stored in a dark deck box. The contents of each bottle were filtered under low vacuum (0.5 atm) and dim light onto either a Whatman GF/F glass fibre filter (25 mm – whole population) or polycarbonate membrane filters (2 or 10 µm pores – 25 mm diameter). After filtration, the

filters were placed in a scintillation vial and blotted with 100 μl of 10% HCl to remove residual inorganic carbon.

Radioactivity remaining on the filters was counted by liquid scintillation spectrometry. After appropriate quench and blank corrections, hourly carbon uptake (photosynthesis) rates ($\text{mg C m}^{-3} \text{ hr}^{-1}$) were calculated according to Strickland and Parsons (1972).

Estimates of areal primary production ($\text{mg C m}^{-2} \text{ hr}^{-1}$) were calculated by trapezoidal integration of measured rates over the depth profile. Daily primary production ($\text{g C m}^{-2} \text{ day}^{-1}$) was estimated by dividing the calculated production during the incubation period (nominally 4 hours) by the proportion of daily surface irradiance (nominally about half) during that period. During experiments, surface irradiance was measured at 1 minute intervals from pre-dawn to after dark with a logging quantum sensor (Biospherical QSR-240) located in the ship's superstructure.

Bacterial Production (^3H -thymidine uptake)

Bacterial secondary production in the water column was estimated from the assimilation of radio-labelled thymidine (methyl- ^3H -thymidine) into trichloroacetic acid (TCA) insoluble macro-molecules, nominally DNA (Fuhrman and Azam, 1980, 1982).

Triplicate sub-samples (10 ml) of water from each production sampling depth were dispensed into clean plastic screw-cap test tubes (12ml). The tubes were spiked with 10 μCi (1.8 MBq) of methyl- ^3H -thymidine (GE Life Sciences) and incubated at ambient water temperature for 1 hour. At the end of the incubation period, the samples were killed by the addition of 2 ml of 10% (w/w) TCA. After a short period, the samples were filtered onto polycarbonate membrane filters (0.2 μm pore size). Thymidine not incorporated into TCA-insoluble macro-molecules was rinsed from the filters with 3 x 2 ml washes with ice-cold 3% TCA. The filters were then stored in scintillation vials until the particulate phase radioisotopes were counted by liquid scintillation spectrometry. A parallel set of formalin-killed water samples were run in parallel with each sample batch to blank for abiotic absorption of thymidine.

Bacterial secondary production was calculated from the assimilated thymidine assuming that 1.7×10^9 bacterial cells were produced from 1 nmol of thymidine free-living bacterial cells have an average carbon content of 2.0×10^{-14} gm C per cell (Fuhrman and Azam, 1980, 1982).

Pelagic metabolism

Production and respiration experiments were conducted on water samples taken from the same station as the ^{14}C production measurements. Immediately after retrieval on board, seawater from the Niskin bottles was used to fill calibrated acid-washed iodine flasks with a nominal volume of 125 ml. Nine flasks were filled from each depth at every station; three were fixed for Winkler titrations immediately (zero-time samples), three were placed in a lightproof deck incubator (dark respiration), and three were placed in deck incubators with appropriate neutral density mesh to simulate the light climate at the depth of collection. Incubations were conducted for 24 hr, after which the incubated flasks were fixed. The entire set of flasks from each experiment was then titrated as a single batch as soon as possible after completion of the experiment.

Dissolved oxygen concentration was determined with an automated precision Winkler titration system developed at the Oceanographic Data Facility, Scripps Institution of Oceanography, University of California, San Diego, and which uses the absorption of 365 nm UV light for endpoint detection. Net community production (NCP) and community

respiration (CR) were estimated as the change in oxygen concentration during a 24 hr period in iodine flasks incubated in the light and dark respectively.

Gross primary production (GPP) is calculated as the sum of NCP and CR, and the P:R ratio calculated as the ratio GPP:CR. Area-specific community rates are computed by trapezoidal integration of volumetric data to the sea bottom or to the 1% isolume, whichever comes first.

Picophytoplankton, bacteria and virus enumeration (Flow cytometry)

Picophytoplankton

Small ($\leq 2\mu\text{m}$), auto-fluorescent phytoplankton were counted live using a Becton Dickinson FACScan flow cytometer aboard the research vessel. Unfiltered, raw seawater sub-samples were collected from the Niskin bottles in clean plastic test tubes and stored at 4°C until they were processed (within 1hr). The water samples were aspirated into the instrument and counted using the BD software (CellQuest). Instrument flow rates were determined by measuring the time taken to aspirate a known volume of water.

Duplicate or triplicate fresh seawater samples were run for 1 – 2 minutes at a flow rate of 50 μl^{-1} minute, with green-fluorescent beads used as an internal reference (1 μm , Polyscience Inc.). Discrimination of living autotrophic phytoplankton cells was based upon their respective side scatter, orange (560 nm) and red (>680 nm) fluorescence after excitation with blue (488 nm) laser light (15 mW in a 40 x 60 μm spot). The algal pigments chlorophyll *a* and phycoerythrin (PE) were fluorescent in the red and orange, respectively.

Three types of small phytoplankters, the prochlorophyte *Prochlorococcus* (small side scatter, red fluorescence only), the cyanobacterium *Synechococcus* (larger size, red and orange fluorescence) and small autotrophic eukaryotes (larger size still, red fluorescence only) could be distinguished.

Bacteria and viruses

Duplicate 1 ml samples for bacteria and viruses were fixed in glutaraldehyde (0.5% final concentration) for 10 minutes in the dark, quick frozen in liquid nitrogen and stored in liquid nitrogen until analysis. Samples were thawed at 37°C, diluted five-fold in 0.02 μm filtered TE-buffer (pH 8, Sigma-Adrich) and stained with SYBR I Green (0.5 X 10⁻⁴ final concentration) in the dark at 80° and then 0.75 μm fluorescent beads (Molecular Probes) added as an internal standard. Bacteria and viruses were analysed using a FACSCANTO II flow cytometer (Becton Dickinson) on high throughput mode at a flow rate of 30 $\mu\text{l min}^{-1}$ for 2 minutes. Virus counts were corrected against a blank consisting of 0.02 μm filtered TE buffer with 0.02 μm filtered (5:1) seawater. Bacteria and viruses were discriminated based on side scatter and green (SYBR I) fluorescence.

Viral production

Viral (lytic) production (VP), the fraction of infected cells (FIC) and the fraction of lysogenic cells (FLC) were estimated using a dilution approach (Wilhelm et al., 2002) in December 2008 and June and November 2009 at the Lagoon, Channel, NE margin and Open water sites. Surface seawater (5 m depth) was collected and 250 ml filtered over a 47 mm 0.22 μm polycarbonate filter (Osmonics, Poretics) at vacuum pressure < 5 KPa. During filtration the volume was maintained to ~250 ml by gradually adding 500 ml virus-free seawater (30 KDa filter, PALL Ultrasette Suspended Screen). To prevent bacteria settling, the sample was mixed

during filtration by drawing water into and injecting it from a transfer pipette. The diluted sample was filtered down to 50 ml and further diluted with 250 ml virus-free seawater. This procedure resulted in the concentration of viruses in the diluted sample ~ 60 – 80% lower than in the initial seawater sample. The filter paper was rinsed gently in the virus-reduced sample in an attempt to remove any attached bacteria. Sub-samples (25 ml) of this virus-reduced sample were gently poured into 6 x 30 ml polycarbonate bottles. The first three bottles served to determine (lytic) viral production, with 1 ml samples were taken at the start of incubations (time = 0) and thereafter, every 3 to 4 hours up to 9 to 12 hours except in December 2008 where samples were taken at 0, 4 and 12 hours. In December 2008, samples were also taken at 24 hours, however high bacterial growth commonly occurred within bottles at this time point and so data from 24 hours was not used for subsequent analyses. Viruses and bacteria were enumerated with flow cytometry (see Flow cytometry methods).

Viral production was calculated as: $VP = (V_2 - V_1)/(t_2 - t_1)$ and corrected for loss of bacterioplankton in diluted sample (i.e. $VP \times b/B$), where V_2 and V_1 represented the maximum and minimum viral concentration in the incubation respectively and t_2 and t_1 are the times during the incubations and b and B bacterial abundance in the diluted samples at time 0 and B is the abundance of bacteria in the undiluted natural sample (Weinbauer et al., 2009). FIC was then calculated as: $FIC = 100 \times (V_2 - v_1)/(BS \times b)$ where BS represents the burst size. We used a BS of 20, as this value represented a mean BS value for range of oligotrophic marine waters (Parada et al., 2006). This first set of bottles further served as controls for the lysogeny assays (below).

To induce lysogenic bacteria, Mitomycin C (Sigma) was added to the second lot of triplicate bottles at a final concentration of $1 \mu\text{g ml}^{-1}$ (Weinbauer et al., 2003) and 1 ml sub-samples taken at time intervals as above. The difference between the concentration of viruses in the Mitomycin C treated and control samples represented the number of induced viruses. FLC was then calculated as: $FLC = 100 ((VMC - VC)/(BS \times b))$, where VMC and VC represent the maximum difference in virus concentrations between the Mitomycin C treated and control samples respectively at corresponding time points. The percent of bacterioplankton abundance lysed daily through viral infections (viral mediated mortality) (%VMM) was calculated as: $\%VMM = VP/v$, where v = ambient virus abundance.

ANALYTICAL PROCEDURES (LABORATORY)

Chlorophyll (Fluorometry)

Replicate subsamples of water from Niskin bottles or surface buckets were filtered through Whatman GF/F (nominal pore size – 0.7 mm: total community) or polycarbonate membrane filters (2 mm pore, 10 mm pore - > 2 and > 10 mm size fractions). After filtration under subdued light, the samples were folded, stored in pre-combusted foil packet envelopes and frozen (<-10°C) until analysis.

In the laboratory, the filtered samples were ground in a tissue grinder with a 90% acetone: water mixture and extracted in the dark for ca. 1hr. After centrifugation to remove suspended matter, chlorophyll fluorescence in the supernatant extract was determined using a Turner Designs Model 10 fluorometer with a red-sensitive photomultiplier. Following the initial reading, the sample was acidified with 1 drop of 10% HCl and the fluorescence re-measured.

Chlorophyll and phaeophytin concentrations were calculated according to Parsons et al. (1984). Chlorophyll concentrations in size fractions not directly measured (2 – 10 mm, <2 mm) were calculated by difference between measured size fraction.

Dissolved inorganic nutrients (NO_2^- , NO_3^- , PO_4^{3-} , $Si(OH)_4$)

Duplicate water sub-samples (10 ml) were syringe filtered (0.45 mm) into acid-washed screw-capped plastic test tubes (12 ml) and stored frozen (ca. -20°C) until analysis ashore.

Dissolved inorganic nutrient concentrations in the filtered samples were determined by standard colorimetric methods (Parsons et al., 1984) implemented on a Braune and Lubbe segmented flow analyser (SFA: Ryle et al., 1981).

Duplicate water sub-samples (10 ml) for dissolved silicate analyses were stored at room temperature prior to analysis to prevent polymerisation of the silicic acid monomers during frozen storage.

Dissolved organic nutrients (DON, DOP)

Dissolved organic nutrient concentrations were estimated as the difference between measured total dissolved nutrient (TDN, TDP) concentrations in oxidised water samples and summed inorganic nitrogen ($DIN = NH_4^+ + NO_2^- + NO_3^-$) and phosphorus (PO_4^{3-}) concentrations in parallel sets of un-oxidised samples.

The organic matter in 10 ml filtered water samples were oxidised by alkaline persulfate digestion under high temperature (110°C) and pressure in an autoclave. After oxidation, the total inorganic nutrient (TDN, TDP) concentrations were determined by segmented flow analysis as above.

Dissolved organic carbon (DOC)

Water sub-samples (10 ml) for DOC analysis were syringe filtered ($0.45\mu\text{m}$) into duplicate, acid-washed screw-cap plastic test tubes. The tube contents were acidified with 100 ml of AR-grade HCl and stored at 4°C until analysis ashore.

In the laboratory, DOC in the sample water was determined by high temperature (1000°C) combustion (HTC) using a Shimadzu TC-5000 carbon analyser. Prior to analysis, CO_2 remaining in the sample water is removed by sparging with O_2 carrier gas.

Particulate carbon (PC)

The particulate carbon content of material collected on filters was determined by high temperature combustion (HTC) using a Shimadzu TC-5000 carbon analyser fitted with a solid sample inlet.

Filters containing sampled material were placed in pre-combusted (450°C) ceramic sample boats. After the sample inlet was purged of atmospheric CO_2 , inorganic C on the filters (e.g. $CaCO_3$) was removed by addition of concentrated phosphoric acid and quantified by non-dispersive infra-red gas analysis (IRGA). After this quantification is completed, the filter was introduced into the sample oven (1000°C) where the remaining organic carbon was combusted in an oxygen stream and again quantified by IRGA. The analyses were standardised using certified reference materials (e.g. MESS-1).

Particulate nitrogen (PN)

Total particulate carbon (PC) and nitrogen (PN) measurements was made by filtering 250 ml sub-samples through pre-combusted Whatman GF/F glass fibre filters, which were

subsequently analysed for C and N content on an Antek chemi-luminescent nitrogen analyser with a Beckman 880 NDIR carbon analyser mounted in series. The instrument was standardised with acetanilide.

Particulate phosphorus (PP)

Particulate phosphorus (PP) was determined by filtering 250 ml sub-samples through pre-combusted Whatman GF/F glass fibre filters and then refluxing these filters and their associated organic matter to dryness with acid persulfate (5%), redissolving the digest in deionised water and colorimetrically determining the PO_4^{3-} content of the supernatant (Parsons et al., 1984). The analysis was standardised with potassium phosphate and an organic sugar phosphate (e.g. fructose-6-phosphate).

Zooplankton analysis

In the laboratory, the frozen mesh was dried (65°) and re-weighed to estimate zooplankton community biomass. The preserved zooplankton sample was washed to remove formaldehyde and diluted to a known volume with water. A Stempel pipette was used to provide a subsample containing approximately 500 organisms that were then enumerated in a Bogorov tray under a Wild stereomicroscope. All taxa were counted to convenient taxonomic categories, and all nauplii and copepodites of calanoid and cyclopoid copepods counted. Adult copepods were identified to species and sex.

Organic sedimentation (Lagrangian Sediment Traps)

In the laboratory, 10 of the 12 filters from each deployment were dried to constant weight and weighed to establish the mass of material collected. After the weighing, pairs of dried filters were haphazardly assigned for analysis: PC, PN, PP, protein, carbohydrate. The pair of filters not dried and weighed was kept frozen until analysed for phytoplankton pigments.

Vertical fluxes were estimated as the mass of material or constituent sedimenting per m^2 over a 24 hr period.

Phytoplankton counts (Flow cytometry)

Small ($< 10 \mu\text{m}$), auto-fluorescent phytoplankton were counted live using a Becton Dickinson FACScan flow cytometer aboard the research vessel. Seawater sub-samples were collected directly from the Niskin bottles into clean plastic centrifuge tubes and processed immediately or stored at 4°C until they were processed (within 2 hr). Duplicate or triplicate seawater samples were run for 1 – 2 minutes at a flow rate of $45 \mu\text{l minute}^{-1}$, with yellow-green fluorescent beads added as an internal reference ($1 \mu\text{m}$, Polyscience Inc.) and the threshold set to red fluorescence. Data for individual sub-samples were collected in list-mode files and data analysed using CYTOWIN (freely downloadable). Discrimination of living autotrophic phytoplankton cells was based upon their respective side scatter, orange (560 nm) and red ($>680 \text{ nm}$) fluorescence after excitation with blue (488 nm) laser light (15mW in a $40 \times 60 \mu\text{m}$ spot). The algal pigments chlorophyll *a* and phycoerythrin (PE) were fluorescent in the red and orange, respectively. Three types of small phytoplankters, the prochlorophyte *Prochlorococcus* (low side scatter, red fluorescence only), the cyanobacterium *Synechococcus* (larger size/higher side scatter, red and orange fluorescence) and small autotrophic eukaryotes (larger size/higher side scatter still, red fluorescence only) could be distinguished.

Seawater samples for enumeration of bacteria and viruses were also taken in Nov/Dec 2008 and May/June 2009. Seawater was collected from niskin bottles as above and 1 ml sub-samples were fixed in electron microscope grade glutaraldehyde (0.5% final concentration) for 15 minutes in the dark and frozen in liquid nitrogen until analysis. Samples were analysed within 2 – 4 months of collection. Samples were diluted 1:5 in 0.02 µm filtered Tris EDTA buffer (Sigma, pH = 8), stained with SYBR I Green (5×10^{-5} dilution) and incubated at 80°C for 10 minutes in the dark. Flow cytometric analysis was conducted on a Becton Dickinson FACSCanto II flow cytometer with the discriminator set to green fluorescence.. Duplicate sub-samples were run for 2 minutes at a flow rate of 30 µl second⁻¹, with yellow green fluorescent beads (0.75 or 1µm diameter) added as an internal reference. Data for individual sub-samples were collected in list-mode files and data analysed using CYTOWIN. Two virus populations (V1 and V2) and 3 bacterial populations (low DNA, high DNA 1 and HDNA 2) could be distinguished according to their different side scatter (indicative of cell size/complexity) and Green (SYBR) fluorescence (indicative of nucleic acid content) signals. Virus populations (V1 and V2) exhibit lower side scatter and green fluorescence intensity than all bacterial populations. Low DNA and high DNA bacterial populations show similar side scatter signals but high DNA1 population exhibited higher green fluorescence. High DNA2 population exhibited highest side scatter and green fluoresce signals.

Appendix II: Units of Measurement

- fg:** femtogram, a measure of weight, represents a factor of 10^{-15} , so 1 femtogram (fg) = 10^{-15} grams.
- Hz:** hertz, the SI unit of frequency defined as the number of cycles per second of a periodic phenomenon.
- kHz:** kilohertz, is a unit of alternating current (AC) or electromagnetic (EM) wave frequency equal to one thousand hertz (1,000 Hz).
- m:** metre, is the base unit of length in the International System of Units (SI).
- mg C m⁻³ hr⁻¹:** milligrams of carbon per metre cubed per hour.
- mg cm⁻² d⁻¹:** milligrams per centimetre squared per day.
- mg dry weight m⁻³:** milligrams of dry weight per metre cubed.
- mg m⁻²:** milligrams per metre squared.
- MHz:** megahertz, one MHz denotes one million hertz or one million cycles per second.
- ml:** millilitre, equals a thousandth of a litre.
- mm:** millimetre, equals a thousandth of a metre.
- mmol O₂ m⁻² d⁻¹:** millimole of oxygen per metre squared per day.
- nm:** nanometres, is a unit of length in the metric system, equal to one billionth of a metre.
- no. m⁻³:** number per metre cubed.
- no. 100m⁻³:** number per 100 metre cubed.
- NTU (Nephelometric Turbidity Units):** these are the units of turbidity from a calibrated nephelometer.
- PSU (Practical Salinity Units):** salinity is expressed as PSU that are based on water temperature and conductivity measurements.
- S.D.:** standard deviation, is a widely used measurement of variability or diversity that shows how much variation there is from the average.
- sigma-t:** a unit used in oceanography to measure the density of seawater at a given temperature.
- µg/L:** microgram per litre.
- µL⁻¹:** microlitre, a measure of volume, there are a thousand microlitres for every 1 millilitre.
- µM:** micromolar, one millionth of a mole per litre.
- µm:** micrometre, one millionth of a metre.
- µmol Q m⁻² sec⁻¹:** unit of measurement of PAR (Photosynthetically Active Radiation) where Q = photons.

Appendix III: Logger time series statistics

Table A.1 Monthly aggregated daily statistics for water temperature time series collected by in-situ loggers. Unless otherwise indicated, all units are in °C. Days of data indicates temporal data coverage, Min = minimum of all data for that month, Max = maximum of all data for month, Std Dev = standard deviation of all data for month, Median = median of all data for month, Mean Daily Max = arithmetic mean of the daily maximum temperatures, Mean Daily Min = arithmetic mean of the daily minimum temperatures, Mean Daily Range = arithmetic mean of the daily temperature ranges (daily max – daily min),

Site	Jan (62 days)										Feb (56 days)										Mar (62 days)									
	Days of data	Min	Mean	Max	Std Dev	Median	Mean Daily Max	Mean Daily Min	Mean Daily Range		Days of data	Min	Mean	Max	Std Dev	Median	Mean Daily Max	Mean Daily Min	Mean Daily Range		Days of data	Min	Mean	Max	Std Dev	Median	Mean Daily Max	Mean Daily Min	Mean Daily Range	
PE01	31	28.89	29.47	29.86	0.20	29.44	29.62	29.31	0.31		26	28.45	28.89	29.51	0.26	28.88	29.01	28.78	0.24		40	28.73	29.44	30.29	0.31	29.44	29.74	29.08	0.59	
PE02	31	28.88	29.19	29.59	0.17	29.16	29.27	29.12	0.15		26	28.43	28.76	29.15	0.18	28.79	28.82	28.68	0.14		41	28.65	29.16	29.80	0.23	29.20	29.28	29.02	0.22	
PE03	31	28.35	29.42	30.12	0.24	29.44	29.72	28.98	0.74		26	27.73	28.67	29.34	0.30	28.66	28.94	28.24	0.70		41	27.13	29.35	30.58	0.45	29.38	29.89	28.53	1.24	
PE04	31	26.37	29.15	30.17	0.64	29.32	29.78	27.37	2.40		26	26.02	28.43	29.55	0.60	28.56	28.98	26.88	2.11		39	25.34	29.06	30.79	0.70	29.13	29.92	27.12	2.61	
PE05	62	24.44	27.76	29.63	0.99	27.83	29.30	25.96	2.77		45	23.60	27.29	29.69	1.10	27.42	28.93	25.20	3.05		41	24.74	27.97	29.94	1.00	28.14	29.30	26.21	2.95	
PE06	62	25.57	28.27	29.48	0.63	28.41	29.15	26.81	1.73		44	24.71	27.89	29.77	0.71	28.00	28.93	26.39	1.98		39	25.35	28.43	29.60	0.57	28.51	29.04	27.25	1.67	
PE07	62	24.26	28.07	29.61	0.82	28.21	29.29	26.25	2.35		45	24.19	27.94	29.82	0.84	27.96	28.93	26.15	2.01		39	25.41	28.11	29.65	0.73	28.26	28.89	26.64	2.04	
PE08	62	25.40	28.44	29.72	0.66	28.49	29.33	27.22	1.47		45	24.76	28.00	30.23	0.96	28.09	29.02	26.55	1.52		40	25.97	28.19	29.55	0.63	28.22	28.91	27.21	1.48	
PE09	62	28.10	28.85	29.36	0.29	28.89	29.04	28.63	0.10		47	28.11	28.49	29.03	0.26	28.42	28.71	28.28	0.08		41	28.51	28.92	29.31	0.22	28.92	28.92	28.80	0.08	
PE10																					8	28.15	28.89	29.21	0.31	29.04	29.00	28.72	0.27	
PE11																					9	28.37	28.93	29.53	0.25	28.94	29.22	28.58	0.64	
PE12																					9	29.56	29.99	30.22	0.13	30.03	30.11	29.85	0.26	
PE13	62	27.87	28.75	29.49	0.31	28.80	29.07	28.42	0.28		45	27.93	28.42	29.20	0.37	28.31	28.72	28.09	0.17		40	28.22	28.74	29.26	0.25	28.68	28.84	28.54	0.20	
PE14	62	27.58	28.58	29.21	0.41	28.65	28.93	28.20	0.17		47	27.67	28.34	29.12	0.41	28.25	28.70	27.97	0.15		31	27.81	28.57	29.33	0.31	28.56	28.66	28.47	0.19	
PE15	62	26.68	28.29	29.18	0.55	28.38	28.82	27.54	0.57		30	26.80	28.33	29.65	0.70	28.39	28.89	27.94	0.47											
PE16	62	24.62	27.87	29.67	0.85	28.04	29.12	25.80	2.76		45	23.81	27.63	29.80	0.97	27.75	28.87	25.37	2.85		31	24.60	27.88	29.48	0.80	27.99	28.85	26.04	2.81	

Table A. I (cont'd)

Site	Apr (60 days)							May (62 days)							Jun (60 days)												
	Days of data	Min	Mean	Max	Std Dev	Median	Mean Daily Max	Mean Daily Min	Mean Daily Range	Days of data	Min	Mean	Max	Std Dev	Median	Mean Daily Max	Mean Daily Min	Mean Daily Range	Days of data	Min	Mean	Max	Std Dev	Median	Mean Daily Max	Mean Daily Min	Mean Daily Range
PE01	60	29.02	29.90	30.81	0.41	29.86	30.42	29.35	0.43	48	27.19	28.88	30.43	0.62	28.94	28.98	28.27	0.53	30	26.35	27.20	27.70	0.31	27.35	27.34	26.95	0.39
PE02	60	28.83	29.72	30.40	0.36	29.70	30.07	29.32	0.20	46	26.56	28.84	30.25	0.69	28.90	28.96	28.20	0.49	30	25.74	27.03	27.41	0.34	27.21	27.13	26.79	0.34
PE03	60	28.04	29.82	30.86	0.40	29.76	30.44	29.01	0.79	45	27.19	28.94	30.48	0.64	28.97	29.02	28.16	0.61	30	26.42	27.27	27.69	0.29	27.39	27.43	27.02	0.41
PE04	60	24.86	29.46	30.72	0.66	29.48	30.44	26.89	2.52	48	25.48	28.82	30.39	0.70	28.87	29.07	27.24	1.29	25	25.98	27.20	27.71	0.35	27.32	27.41	26.74	0.67
PE05	60	24.86	28.58	30.59	1.00	28.73	30.03	26.35	2.82	58	25.79	28.48	30.06	0.68	28.57	29.20	27.10	1.47	60	26.36	27.71	28.81	0.59	27.57	28.45	26.86	0.61
PE06	60	25.73	28.90	30.29	0.67	29.08	29.87	27.15	1.78	59	27.02	28.72	30.20	0.49	28.74	29.21	27.97	0.71	60	26.72	27.85	28.96	0.64	27.65	28.53	27.21	0.23
PE07	60	24.48	28.61	30.28	0.77	28.72	29.81	26.76	2.06	60	25.02	28.44	29.95	0.75	28.63	29.15	26.94	1.42	60	25.71	27.82	28.94	0.66	27.58	28.52	27.12	0.40
PE08	60	25.91	28.80	30.19	0.80	29.01	29.77	27.32	1.21	60	26.29	28.69	29.81	0.51	28.74	29.11	27.87	0.64	60	26.73	27.86	28.96	0.65	27.74	28.50	27.24	0.16
PE09	60	28.83	29.53	30.38	0.33	29.45	29.79	29.25	0.09	51	27.08	28.86	29.99	0.57	28.80	29.09	28.61	0.13	60	26.54	27.77	28.89	0.69	27.43	28.42	27.11	0.07
PE10	30	27.62	28.82	29.39	0.41	28.90	28.93	28.68	0.25	31	27.49	28.55	29.42	0.46	28.51	28.62	28.46	0.16	30	26.65	27.21	27.61	0.25	27.30	27.23	27.18	0.05
PE11	30	27.92	28.98	29.70	0.32	29.02	29.22	28.74	0.48	31	27.64	28.65	29.42	0.45	28.69	28.75	28.53	0.22	30	26.61	27.22	27.72	0.26	27.31	27.27	27.18	0.09
PE12	30	29.16	29.77	30.32	0.32	29.84	29.84	29.68	0.17	31	27.19	28.55	29.39	0.68	28.81	28.63	28.45	0.19	30	26.41	27.12	27.55	0.34	27.22	27.20	27.02	0.18
PE13	60	28.16	29.26	30.03	0.40	29.31	29.65	28.86	0.17	60	27.38	28.81	29.78	0.49	28.85	29.13	28.47	0.15	60	26.59	27.75	28.95	0.68	27.48	28.39	27.12	0.08
PE14	30	29.22	29.56	30.10	0.20	29.55	29.63	29.50	0.13	29	28.60	29.07	29.68	0.28	29.01	29.13	28.99	0.13	30	27.88	28.41	28.94	0.37	28.61	28.44	28.37	0.07
PE15	30	25.06	28.59	30.18	0.83	28.78	29.70	26.45	3.25	11	28.63	28.84	28.93	0.07	28.85	28.87	28.79	0.08	30	27.89	28.44	28.93	0.34	28.63	28.49	28.40	0.09
PE16	30	25.06	28.59	30.18	0.83	28.78	29.70	26.45	3.25	28	25.34	28.57	29.88	0.71	28.72	29.16	26.75	2.41	30	24.92	28.27	28.92	0.51	28.42	28.49	27.24	1.26

Table A. I (cont'd)

Site	Jul (62 days)							Aug (62 days)							Sep (60 days)												
	Days of data	Min	Mean	Max	Std Dev	Median	Mean Daily Max	Mean Daily Min	Mean Daily Range	Days of data	Min	Mean	Max	Std Dev	Median	Mean Daily Max	Mean Daily Min	Mean Daily Range	Days of data	Min	Mean	Max	Std Dev	Median	Mean Daily Max	Mean Daily Min	Mean Daily Range
PE01	29	25.53	26.34	27.02	0.32	26.28	26.46	26.02	0.45	31	25.18	25.99	26.34	0.20	26.00	26.09	25.81	0.28	29	25.93	26.45	27.11	0.23	26.43	26.69	26.28	0.41
PE02	28	25.30	26.19	26.84	0.33	26.16	26.30	25.95	0.36	31	25.41	25.90	26.27	0.16	25.93	25.98	25.78	0.20	29	26.01	26.30	26.56	0.11	26.33	26.32	26.27	0.06
PE03	30	25.27	26.40	27.00	0.29	26.37	26.56	26.06	0.50	31	25.27	26.04	26.46	0.18	26.05	26.17	25.78	0.40	29	25.19	26.31	27.48	0.28	26.25	26.76	25.96	0.80
PE04	30	25.31	26.38	27.05	0.34	26.38	26.55	25.84	0.70	31	25.35	26.01	26.41	0.20	26.02	26.15	25.74	0.41	28	25.18	26.15	27.80	0.35	26.10	26.73	25.65	1.08
PE05	61	25.03	26.76	28.04	0.61	26.70	27.56	25.91	0.79	62	24.57	26.15	26.97	0.41	26.12	26.82	25.38	0.88	59	23.53	25.98	27.40	0.64	25.99	27.10	24.77	1.63
PE06	61	25.77	26.89	28.03	0.62	26.79	27.55	26.24	0.29	62	25.39	26.32	27.05	0.36	26.28	26.77	25.89	0.29	59	24.68	26.22	27.43	0.46	26.09	27.06	25.49	0.89
PE07	61	24.95	26.88	27.99	0.63	26.84	27.56	26.23	0.36	62	25.40	26.32	27.02	0.36	26.30	26.81	25.89	0.36	59	24.62	26.26	27.67	0.44	26.16	27.10	25.38	1.05
PE08	61	25.61	26.92	27.99	0.61	26.92	27.55	26.26	0.27	62	25.15	26.31	27.08	0.38	26.27	26.84	25.85	0.38	59	24.31	26.15	27.33	0.49	26.09	26.98	25.24	1.04
PE09	61	25.79	26.85	28.06	0.71	26.98	27.51	26.17	0.09	62	25.71	26.37	27.02	0.44	26.27	26.82	25.92	0.07	59	25.88	26.58	27.12	0.42	26.62	27.02	26.14	0.07
PE10	30	25.83	26.26	26.78	0.31	26.17	26.27	26.21	0.06	31	25.62	25.92	26.17	0.15	25.95	25.94	25.89	0.05	25	25.88	26.06	26.20	0.07	26.07	26.10	26.03	0.08
PE11	23	25.86	26.32	26.87	0.35	26.26	26.39	26.25	0.13	31	25.65	25.96	26.23	0.14	25.99	26.02	25.91	0.11	24	25.40	26.09	26.45	0.17	26.15	26.23	25.90	0.34
PE12	30	25.62	26.20	26.91	0.36	26.14	26.27	26.08	0.19	31	25.32	26.00	26.78	0.33	25.91	26.09	25.87	0.22	24	26.35	26.91	27.40	0.22	26.92	27.03	26.79	0.25
PE13	61	25.83	26.89	28.01	0.71	26.91	27.54	26.20	0.08	62	25.58	26.33	26.97	0.45	26.15	26.80	25.87	0.07	58	25.93	26.54	27.16	0.43	26.74	26.99	26.11	0.08
PE14	31	27.04	27.54	28.10	0.32	27.41	27.56	27.50	0.06	31	26.55	26.78	27.05	0.10	26.77	26.80	26.75	0.06	31	26.33	26.93	27.21	0.16	26.96	26.99	26.87	0.10
PE15	31	27.02	27.52	28.02	0.28	27.41	27.56	27.46	0.10	31	26.39	26.74	27.05	0.11	26.74	26.79	26.69	0.10	31	26.21	26.81	27.18	0.21	26.84	26.96	26.60	0.34
PE16	31	24.39	27.34	28.01	0.38	27.31	27.54	26.76	0.78	31	24.58	26.53	26.93	0.25	26.57	26.76	25.81	0.94	31	23.84	26.36	27.41	0.51	26.45	26.99	25.13	1.84

Table A. 1 (cont'd)

Site	Oct (62 days)										Nov (60 days)										Dec (62 days)									
	Days of data	Min	Mean	Max	Std Dev	Median	Mean Daily Max	Mean Daily Min	Mean Daily Range		Days of data	Min	Mean	Max	Std Dev	Median	Mean Daily Max	Mean Daily Min	Mean Daily Range		Days of data	Min	Mean	Max	Std Dev	Median	Mean Daily Max	Mean Daily Min	Mean Daily Range	
PE01	31	26.64	27.72	29.63	0.59	27.68	28.31	27.30	1.01		28	28.20	29.01	30.41	0.43	28.92	29.69	28.51	1.18		31	28.12	29.06	30.02	0.38	29.12	29.41	28.71	0.70	
PE02	31	26.51	27.20	28.02	0.41	27.14	27.28	27.13	0.14		28	27.87	28.39	28.69	0.18	28.44	28.50	28.32	0.18		31	28.15	28.56	29.06	0.22	28.49	28.67	28.49	0.18	
PE03	31	25.42	27.38	29.52	0.66	27.42	28.47	26.58	1.89		28	26.95	28.90	30.77	0.71	28.81	29.89	27.80	2.09		31	27.62	29.20	30.33	0.42	29.23	29.73	28.47	1.27	
PE04	31	24.68	27.70	29.79	0.86	27.72	28.75	26.13	2.62		28	26.25	28.86	30.61	0.81	28.93	30.04	27.20	2.84		31	26.04	28.87	30.22	0.71	28.99	29.71	27.12	2.59	
PE05	62	24.63	26.69	28.66	0.76	26.73	27.89	25.30	1.93		57	25.42	27.37	29.35	0.76	27.40	28.73	26.03	2.20		62	25.06	27.16	29.21	0.84	27.15	28.68	25.68	2.39	
PE06	62	25.23	26.99	28.72	0.59	27.07	27.91	25.93	1.30		55	25.77	27.81	28.99	0.44	27.85	28.67	26.79	1.46		62	24.91	27.64	29.16	0.71	27.67	28.73	26.34	1.84	
PE07	62	24.45	26.95	28.65	0.65	27.00	27.76	25.67	1.38		51	25.15	27.46	29.31	0.59	27.50	28.41	26.29	1.67		62	24.16	27.54	29.59	0.85	27.59	28.69	25.91	2.03	
PE08	62	24.40	26.94	28.41	0.69	26.98	27.74	25.84	1.09		55	26.20	27.85	29.24	0.50	27.89	28.59	26.95	1.11		62	25.90	27.86	29.35	0.67	27.90	28.65	26.78	1.21	
PE09	62	26.40	27.33	28.03	0.44	27.32	27.65	27.01	0.06		57	27.72	28.25	28.60	0.21	28.26	28.43	28.08	0.07		62	27.31	28.10	28.80	0.32	28.13	28.36	27.83	0.12	
PE10																														
PE11																														
PE12																														
PE13	62	26.35	27.25	28.01	0.40	27.27	27.59	26.93	0.12		56	27.59	28.05	28.62	0.22	28.03	28.36	27.79	0.22		62	26.88	27.96	29.18	0.42	27.92	28.34	27.62	0.27	
PE14	62	26.41	27.27	28.03	0.39	27.27	27.58	26.96	0.11		54	27.64	28.01	28.45	0.18	27.95	28.17	27.80	0.13		62	26.89	27.79	28.95	0.41	27.77	28.09	27.49	0.19	
PE15	62	26.04	27.15	28.02	0.43	27.20	27.52	26.67	0.30		58	26.97	27.75	28.61	0.29	27.71	28.10	27.38	0.37		62	26.38	27.60	29.01	0.56	27.56	28.07	27.02	0.49	
PE16	62	24.63	26.82	28.29	0.62	26.86	27.77	25.47	1.67		55	24.66	27.37	29.21	0.60	27.40	28.58	26.04	2.09		62	24.75	27.36	29.18	0.83	27.36	28.59	25.69	2.42	

Table A. 1 Monthly aggregated daily statistics for salinity time series collected by in-situ loggers. Unless indicated otherwise, all units are in PSU. Days of data indicates temporal data coverage, Min = minimum of all data for that month, Max = maximum of all data for month, Std Dev = standard deviation of all data for month, Median = median of all data for month, Mean Daily Max = arithmetic mean of the daily maximum salinities, Mean Daily Min = arithmetic mean of the daily minimum salinities, Mean Daily Range = arithmetic mean of the daily salinity ranges (daily max – daily min),

Site	Jan (62 days)										Feb (56 days)										Mar (62 days)									
	Days of data	Min	Mean	Max	Std Dev	Median	Mean Daily Max	Mean Daily Min	Mean Daily Range	Days of data	Min	Mean	Max	Std Dev	Median	Mean Daily Max	Mean Daily Min	Mean Daily Range	Days of data	Min	Mean	Max	Std Dev	Median	Mean Daily Max	Mean Daily Min	Mean Daily Range			
PE01	31	34.46	34.58	34.66	0.03	34.58	34.60	34.56	0.04	26	34.38	34.49	34.63	0.05	34.46	34.50	34.47	0.03	40	34.31	34.41	34.47	0.04	34.43	34.45	34.40	0.03			
PE02	31	34.54	34.58	34.64	0.02	34.57	34.59	34.56	0.03	26	34.44	34.54	34.64	0.04	34.54	34.55	34.52	0.03	41	34.38	34.46	34.53	0.03	34.47	34.49	34.44	0.02			
PE03	31	34.46	34.60	34.71	0.04	34.60	34.64	34.55	0.09	26	34.26	34.45	34.60	0.08	34.42	34.49	34.40	0.09	41	34.26	34.37	34.56	0.03	34.38	34.43	34.33	0.09			
PE04	31	34.28	34.55	34.70	0.06	34.56	34.63	34.42	0.22	26	34.28	34.46	34.80	0.06	34.44	34.53	34.38	0.14	39	34.20	34.41	34.60	0.04	34.42	34.49	34.34	0.14			
PE05	62	34.26	34.48	34.78	0.09	34.46	34.62	34.36	0.16	45	34.33	34.57	34.91	0.15	34.50	34.73	34.40	0.13	41	34.25	34.41	34.53	0.05	34.42	34.47	34.36	0.08			
PE06	62	34.34	34.47	34.77	0.07	34.45	34.56	34.38	0.11	44	34.32	34.59	34.97	0.17	34.47	34.75	34.42	0.11	39	34.27	34.41	34.53	0.04	34.43	34.47	34.37	0.08			
PE07	62	34.33	34.49	34.75	0.06	34.48	34.61	34.39	0.14	45	34.36	34.59	34.92	0.15	34.54	34.70	34.43	0.10	39	34.28	34.40	34.49	0.04	34.41	34.45	34.35	0.08			
PE08	62	34.35	34.50	34.67	0.06	34.49	34.58	34.40	0.10	45	34.37	34.59	34.93	0.14	34.56	34.70	34.47	0.08	40	34.28	34.42	34.49	0.05	34.44	34.46	34.38	0.05			
PE09	62	34.33	34.50	34.63	0.07	34.53	34.56	34.43	0.02	47	34.48	34.58	34.71	0.07	34.56	34.62	34.52	0.01	41	34.33	34.46	34.49	0.04	34.47	34.48	34.45	0.01			
PE10																			8	34.33	34.37	34.39	0.02	34.37	34.38	34.35	0.03			
PE11																			9	34.30	34.34	34.39	0.02	34.35	34.36	34.32	0.04			
PE12																			9	34.31	34.34	34.36	0.01	34.34	34.35	34.33	0.02			
PE13	62	34.28	34.50	34.65	0.08	34.53	34.58	34.40	0.03	45	34.45	34.57	34.75	0.08	34.57	34.61	34.51	0.02	40	34.33	34.44	34.47	0.04	34.45	34.46	34.43	0.01			
PE14	62	34.36	34.51	34.69	0.07	34.53	34.58	34.44	0.02	47	34.42	34.58	34.80	0.12	34.57	34.66	34.49	0.01	31	34.41	34.43	34.44	0.01	34.43	34.43	34.42	0.01			
PE15	62	34.43	34.53	34.77	0.06	34.52	34.58	34.48	0.04	30	34.49	34.73	34.97	0.14	34.75	34.84	34.70	0.04												
PE16	53	34.31	34.50	34.88	0.10	34.49	34.63	34.42	0.14	36	34.37	34.67	35.07	0.20	34.76	34.80	34.54	0.12	31	34.34	34.43	34.65	0.02	34.44	34.49	34.39	0.11			

Table A. 2 (cont'd)

Site	Apr (60 days)										May (62 days)										Jun (60 days)									
	Days of data	Min	Mean	Max	Std Dev	Median	Mean Daily Max	Mean Daily Min	Mean Daily Range		Days of data	Min	Mean	Max	Std Dev	Median	Mean Daily Max	Mean Daily Min	Mean Daily Range		Days of data	Min	Mean	Max	Std Dev	Median	Mean Daily Max	Mean Daily Min	Mean Daily Range	
PE01	60	34.31	34.44	34.59	0.05	34.43	34.49	34.39	0.05		48	34.35	34.50	34.69	0.09	34.46	34.56	34.41	0.06		30	34.23	34.38	34.52	0.06	34.37	34.43	34.35	0.08	
PE02	60	34.35	34.45	34.61	0.06	34.46	34.51	34.39	0.03		46	34.26	34.47	34.74	0.14	34.42	34.56	34.35	0.06		30	34.24	34.36	34.49	0.06	34.34	34.38	34.33	0.05	
PE03	60	34.23	34.39	34.51	0.05	34.40	34.45	34.33	0.07		45	34.22	34.41	34.61	0.08	34.44	34.47	34.34	0.06		30	34.16	34.33	34.48	0.07	34.34	34.39	34.28	0.11	
PE04	60	34.23	34.42	34.73	0.05	34.41	34.53	34.31	0.16		48	34.19	34.46	34.76	0.12	34.44	34.57	34.31	0.15		25	34.18	34.31	34.45	0.07	34.32	34.41	34.26	0.15	
PE05	60	34.26	34.41	34.58	0.04	34.41	34.49	34.35	0.10		58	34.26	34.46	34.68	0.11	34.46	34.59	34.34	0.09		60	34.13	34.38	34.52	0.08	34.38	34.47	34.26	0.10	
PE06	60	34.28	34.41	34.57	0.04	34.41	34.48	34.35	0.08		59	34.26	34.47	34.70	0.11	34.43	34.59	34.35	0.06		60	34.19	34.40	34.56	0.07	34.38	34.46	34.31	0.07	
PE07	60	34.27	34.41	34.57	0.04	34.41	34.47	34.34	0.09		60	34.25	34.46	34.66	0.10	34.45	34.58	34.33	0.09		60	34.15	34.39	34.54	0.08	34.40	34.45	34.31	0.07	
PE08	60	34.33	34.42	34.56	0.05	34.41	34.48	34.37	0.05		60	34.28	34.48	34.68	0.10	34.46	34.59	34.37	0.06		59	34.12	34.39	34.54	0.08	34.40	34.45	34.31	0.07	
PE09	60	34.33	34.43	34.57	0.05	34.45	34.48	34.39	0.01		51	34.32	34.47	34.64	0.09	34.46	34.52	34.39	0.04		60	34.09	34.35	34.50	0.11	34.39	34.43	34.27	0.03	
PE10	30	34.35	34.39	34.45	0.03	34.39	34.40	34.39	0.02		31	34.34	34.43	34.48	0.03	34.44	34.44	34.42	0.03		30	34.35	34.44	34.48	0.03	34.44	34.44	34.43	0.01	
PE11	30	34.33	34.39	34.44	0.02	34.38	34.40	34.38	0.03		31	34.35	34.42	34.48	0.03	34.43	34.44	34.41	0.04		30	34.31	34.42	34.47	0.04	34.43	34.43	34.40	0.03	
PE12	30	34.27	34.44	34.54	0.06	34.43	34.46	34.43	0.03		31	34.39	34.45	34.52	0.03	34.45	34.46	34.44	0.03		30	34.30	34.41	34.50	0.05	34.42	34.42	34.39	0.03	
PE13	60	34.34	34.43	34.55	0.04	34.43	34.47	34.39	0.01		60	34.39	34.54	34.71	0.10	34.50	34.64	34.44	0.03		60	34.16	34.41	34.64	0.11	34.44	34.48	34.34	0.03	
PE14	30	34.40	34.45	34.54	0.04	34.43	34.45	34.44	0.01		29	34.52	34.60	34.69	0.05	34.61	34.62	34.60	0.02		30	34.13	34.34	34.55	0.14	34.40	34.36	34.33	0.03	
PE15											11	34.54	34.61	34.67	0.04	34.61	34.62	34.60	0.02		30	34.16	34.37	34.54	0.11	34.40	34.39	34.35	0.04	
PE16	30	34.33	34.44	34.62	0.04	34.44	34.50	34.39	0.11		28	34.41	34.56	34.69	0.05	34.57	34.61	34.49	0.12		30	34.19	34.40	34.55	0.09	34.42	34.47	34.36	0.11	

Table A. 2 (cont'd)

Site	Jul (62 days)										Aug (62 days)										Sep (60 days)									
	Days of data	Min	Mean	Max	Std Dev	Median	Mean Daily Max	Mean Daily Min	Mean Daily Range	Days of data	Min	Mean	Max	Std Dev	Median	Mean Daily Max	Mean Daily Min	Mean Daily Range	Days of data	Min	Mean	Max	Std Dev	Median	Mean Daily Max	Mean Daily Min	Mean Daily Range			
PE01	29	34.21	34.31	34.52	0.06	34.31	34.36	34.29	0.07	31	34.29	34.38	34.47	0.03	34.39	34.40	34.37	0.04	29	34.32	34.38	34.45	0.01	34.38	34.40	34.36	0.04			
PE02	28	34.17	34.33	34.48	0.07	34.34	34.37	34.31	0.06	31	34.33	34.39	34.46	0.03	34.41	34.41	34.39	0.02	29	34.36	34.39	34.41	0.01	34.40	34.40	34.39	0.01			
PE03	30	34.12	34.30	34.40	0.05	34.31	34.34	34.25	0.09	31	34.28	34.37	34.44	0.04	34.39	34.40	34.35	0.06	28	33.92	34.36	34.51	0.05	34.36	34.40	34.31	0.09			
PE04	30	34.14	34.29	34.42	0.06	34.30	34.37	34.25	0.12	31	34.26	34.38	34.48	0.04	34.39	34.43	34.35	0.07	28	34.21	34.37	34.53	0.04	34.37	34.43	34.33	0.10			
PE05	61	34.18	34.40	34.57	0.09	34.40	34.52	34.28	0.08	62	34.25	34.44	34.64	0.10	34.42	34.58	34.31	0.07	59	34.24	34.45	34.67	0.12	34.45	34.61	34.29	0.12			
PE06	61	34.23	34.40	34.56	0.08	34.38	34.50	34.30	0.05	62	34.29	34.46	34.60	0.07	34.45	34.55	34.37	0.04	59	34.23	34.46	34.74	0.10	34.46	34.60	34.35	0.08			
PE07	61	34.20	34.39	34.53	0.08	34.39	34.48	34.31	0.04	62	34.29	34.44	34.58	0.07	34.42	34.53	34.36	0.05	59	34.26	34.46	34.66	0.09	34.47	34.59	34.34	0.08			
PE08	61	34.21	34.39	34.52	0.09	34.38	34.47	34.29	0.05	62	34.32	34.44	34.60	0.07	34.43	34.53	34.36	0.04	59	34.24	34.47	34.66	0.10	34.48	34.60	34.34	0.08			
PE09	61	34.24	34.36	34.45	0.05	34.37	34.39	34.33	0.02	62	34.30	34.39	34.45	0.04	34.37	34.44	34.34	0.01	59	34.30	34.38	34.45	0.04	34.37	34.42	34.34	0.01			
PE10	30	34.26	34.36	34.43	0.05	34.36	34.37	34.35	0.02	31	34.35	34.40	34.44	0.01	34.40	34.40	34.39	0.02	25	34.32	34.38	34.42	0.02	34.39	34.39	34.37	0.01			
PE11	23	34.22	34.34	34.42	0.05	34.34	34.36	34.31	0.05	31	34.35	34.40	34.44	0.01	34.40	34.41	34.39	0.02	24	34.33	34.39	34.45	0.02	34.38	34.41	34.37	0.04			
PE12	30	34.24	34.36	34.47	0.07	34.38	34.37	34.34	0.03	31	34.37	34.41	34.48	0.03	34.40	34.42	34.40	0.02	24	34.37	34.41	34.48	0.03	34.40	34.42	34.40	0.02			
PE13	61	34.26	34.43	34.59	0.08	34.42	34.49	34.36	0.03	62	34.38	34.49	34.60	0.08	34.45	34.58	34.40	0.01	58	34.36	34.48	34.58	0.08	34.52	34.56	34.39	0.01			
PE14	31	34.29	34.42	34.50	0.06	34.45	34.44	34.41	0.02	31	34.46	34.51	34.53	0.01	34.51	34.51	34.50	0.01	31	34.36	34.48	34.56	0.03	34.48	34.50	34.47	0.02			
PE15	31	34.30	34.44	34.52	0.05	34.44	34.45	34.42	0.03	31	34.46	34.51	34.54	0.02	34.52	34.52	34.50	0.02	31	34.28	34.51	34.63	0.06	34.51	34.54	34.49	0.04			
PE16	31	34.32	34.46	34.56	0.05	34.47	34.50	34.44	0.06	31	34.46	34.53	34.60	0.02	34.53	34.56	34.51	0.05	31	34.33	34.54	34.70	0.05	34.54	34.62	34.48	0.13			

Table A. 2 (cont'd)

Site	Oct (62 days)										Nov (60 days)										Dec (62 days)									
	Days of data	Min	Mean	Max	Std Dev	Median	Mean Daily Max	Mean Daily Min	Mean Daily Range		Days of data	Min	Mean	Max	Std Dev	Median	Mean Daily Max	Mean Daily Min	Mean Daily Range		Days of data	Min	Mean	Max	Std Dev	Median	Mean Daily Max	Mean Daily Min	Mean Daily Range	
PE01	31	34.35	34.42	34.53	0.03	34.42	34.47	34.39	0.08		28	34.38	34.47	34.58	0.04	34.46	34.52	34.43	0.09		31	34.38	34.47	34.61	0.06	34.45	34.50	34.45	0.04	
PE02	31	34.36	34.38	34.41	0.01	34.38	34.39	34.38	0.01		28	34.39	34.41	34.43	0.01	34.41	34.42	34.41	0.02		31	34.35	34.44	34.62	0.08	34.39	34.46	34.43	0.03	
PE03	31	34.31	34.42	34.55	0.04	34.43	34.48	34.38	0.11		28	34.25	34.47	34.65	0.05	34.47	34.56	34.38	0.18		31	34.35	34.52	34.64	0.05	34.52	34.58	34.46	0.12	
PE04	31	34.20	34.39	34.63	0.05	34.39	34.51	34.27	0.24		28	34.22	34.43	34.65	0.07	34.42	34.55	34.29	0.26		31	34.29	34.48	34.71	0.07	34.50	34.57	34.37	0.21	
PE05	62	34.23	34.46	34.66	0.08	34.44	34.58	34.36	0.12		57	34.18	34.37	34.59	0.07	34.36	34.48	34.29	0.12		62	34.28	34.44	34.64	0.06	34.43	34.55	34.35	0.13	
PE06	62	34.15	34.44	34.64	0.08	34.43	34.56	34.32	0.13		55	34.19	34.37	34.61	0.07	34.37	34.47	34.28	0.11		62	34.23	34.43	34.69	0.08	34.42	34.54	34.32	0.12	
PE07	62	34.23	34.44	34.63	0.06	34.43	34.54	34.36	0.10		51	34.17	34.37	34.55	0.05	34.37	34.45	34.30	0.10		62	34.31	34.45	34.60	0.06	34.46	34.53	34.37	0.11	
PE08	62	34.26	34.42	34.60	0.06	34.41	34.50	34.34	0.07		55	34.19	34.36	34.52	0.04	34.35	34.42	34.31	0.07		62	34.31	34.45	34.63	0.06	34.45	34.50	34.39	0.06	
PE09	62	34.33	34.38	34.43	0.02	34.38	34.40	34.36	0.01		57	34.30	34.37	34.43	0.04	34.38	34.41	34.33	0.01		62	34.33	34.41	34.53	0.05	34.41	34.45	34.38	0.01	
PE10																														
PE11																														
PE12																														
PE13	62	34.37	34.46	34.58	0.06	34.43	34.52	34.40	0.01		56	34.26	34.40	34.50	0.06	34.42	34.44	34.36	0.02		62	34.32	34.42	34.56	0.06	34.41	34.45	34.38	0.02	
PE14	62	34.33	34.43	34.54	0.04	34.42	34.46	34.39	0.02		54	34.26	34.39	34.44	0.04	34.39	34.41	34.36	0.02		62	34.34	34.44	34.57	0.06	34.45	34.47	34.41	0.02	
PE15	62	34.28	34.44	34.58	0.05	34.43	34.50	34.38	0.03		58	34.22	34.38	34.49	0.05	34.39	34.43	34.33	0.04		62	34.34	34.47	34.59	0.07	34.46	34.52	34.42	0.03	
PE16	62	34.20	34.45	34.66	0.06	34.44	34.57	34.36	0.12		55	34.15	34.38	34.62	0.08	34.39	34.52	34.27	0.14		62	34.12	34.45	34.70	0.10	34.44	34.60	34.31	0.12	

Table A. 2 Monthly aggregated daily statistics for Turbidity time series collected by in-situ loggers. Unless indicated otherwise, all units are in NTU
 Days of data indicates temporal data coverage, Min = minimum of all data for that month, Max = maximum of all data for month, Std Dev = standard deviation of all data for month,
 Median = median of all data for month,

Site	Jan (62 days)						Feb (56 days)						Mar (62 days)					
	Days of data	Min	Mean	Max	Std Dev	Median	Days of data	Min	Mean	Max	Std Dev	Median	Days of data	Min	Mean	Max	Std Dev	Median
PE01	31	0.05	0.17	0.75	0.07	0.15	26	0.07	0.20	1.36	0.10	0.18	40	0.06	0.19	1.20	0.08	0.17
PE02	31	0.04	0.98	10.95	0.63	0.89	26	0.06	0.65	5.86	0.58	0.49	41	0.07	0.63	6.12	0.46	0.55
PE03	31	0.04	0.09	0.98	0.04	0.08	9	0.04	0.29	1.36	0.30	0.16	10	0.04	0.08	0.48	0.03	0.08
PE04	31	0.05	0.10	0.53	0.04	0.09	26	0.03	0.11	0.90	0.08	0.09	39	0.04	0.08	0.79	0.04	0.08
PE05	62	0.03	0.07	2.06	0.06	0.06	41	0.03	0.09	2.34	0.08	0.08	41	0.04	0.10	2.01	0.09	0.07
PE06	31	0.04	0.07	0.28	0.02	0.07	35	0.04	0.08	0.31	0.03	0.08	39	0.04	0.08	0.29	0.02	0.08
PE07	62	0.06	0.17	2.00	0.10	0.19	45	0.05	0.18	1.05	0.08	0.19	39	0.05	0.19	0.72	0.07	0.20
PE08	54	0.05	0.13	3.38	0.17	0.11	35	0.04	0.12	1.72	0.08	0.11	40	0.04	0.07	0.53	0.03	0.07
PE09	62	0.05	0.25	4.69	0.18	0.26	37	0.04	0.27	11.72	0.37	0.18	39	0.00	0.12	5.37	0.12	0.10
PE10													8	0.05	0.08	0.41	0.03	0.08
PE11													9	0.03	0.10	1.58	0.08	0.09
PE12													9	0.11	0.31	1.22	0.12	0.28
PE13	62	0.05	0.14	1.73	0.09	0.17	45	0.03	0.17	1.21	0.09	0.13	40	0.05	0.11	0.48	0.03	0.11
PE14	62	0.03	0.30	1.08	0.24	0.49	47	0.00	0.18	0.94	0.18	0.08	31	0.00	0.04	4.47	0.10	0.03
PE15	62	0.03	0.11	0.52	0.04	0.12	46	0.05	0.12	1.23	0.08	0.10	31	0.06	0.10	1.10	0.05	0.10
PE16	55	0.05	0.09	1.09	0.04	0.08	36	0.05	0.10	1.24	0.05	0.08	31	0.05	0.09	1.85	0.05	0.08

Table A. 3 (cont'd)

Site	Apr (60 days)						May (62 days)						Jun (60 days)					
	Days of data	Min	Mean	Max	Std Dev	Median	Days of data	Min	Mean	Max	Std Dev	Median	Days of data	Min	Mean	Max	Std Dev	Median
PE01	60	0.08	0.19	2.45	0.09	0.17	48	0.07	0.23	2.03	0.12	0.20	30	0.06	0.23	2.00	0.13	0.20
PE02	59	0.06	0.52	5.85	0.36	0.46	46	0.06	0.32	5.22	0.24	0.28	30	0.06	0.26	2.81	0.16	0.24
PE03	30	0.04	0.09	2.75	0.08	0.08	30	0.04	0.11	2.80	0.13	0.08	30	0.03	0.10	1.97	0.09	0.08
PE04	60	0.02	0.08	1.34	0.05	0.07	48	0.03	0.10	1.15	0.05	0.08	22	0.04	0.10	1.04	0.08	0.07
PE05	60	0.04	0.13	2.89	0.11	0.13	57	0.04	0.20	5.87	0.58	0.13	59	0.04	1.15	5.90	1.19	0.16
PE06	60	0.02	0.06	0.31	0.02	0.06	59	0.01	0.05	0.31	0.02	0.05	60	0.02	0.05	0.32	0.02	0.05
PE07	60	0.05	0.15	0.80	0.07	0.16	60	0.05	0.15	1.57	0.08	0.16	60	0.05	0.15	3.21	0.11	0.17
PE08	60	0.04	0.08	1.10	0.04	0.08	60	0.04	0.10	2.12	0.07	0.09	60	0.03	0.08	1.98	0.05	0.08
PE09	30	0.05	0.18	1.40	0.08	0.18	44	0.05	0.31	1.41	0.14	0.35	60	0.04	0.25	1.37	0.17	0.26
PE10	30	0.03	0.06	0.95	0.04	0.06	31	0.03	0.07	2.69	0.09	0.06	30	0.04	0.09	2.77	0.13	0.08
PE11	30	0.00	0.09	0.73	0.05	0.08	31	0.00	0.07	2.00	0.12	0.05	30	0.00	0.08	1.76	0.07	0.07
PE12	30	0.09	0.30	1.27	0.12	0.28	31	0.10	0.30	1.23	0.13	0.28	30	0.14	0.39	1.32	0.16	0.36
PE13	60	0.04	0.10	0.53	0.04	0.10	60	0.03	0.11	0.53	0.06	0.09	60	0.04	0.08	0.55	0.04	0.07
PE14	26	0.00	0.19	9.63	0.96	0.03	26	0.00	0.12	9.78	0.62	0.07	30	0.04	0.07	0.58	0.02	0.07
PE15	30	0.06	0.12	0.93	0.04	0.11	28	0.06	0.13	0.72	0.04	0.13	30	0.10	0.13	0.58	0.03	0.13
PE16	30	0.05	0.08	1.81	0.06	0.07	28	0.04	0.08	1.30	0.03	0.07	30	0.04	0.07	1.70	0.08	0.06

Table A. 3 (cont'd)

Site	Jul (62 days)						Aug (62 days)						Sep (60 days)					
	Days of data	Min	Mean	Max	Std Dev	Median	Days of data	Min	Mean	Max	Std Dev	Median	Days of data	Min	Mean	Max	Std Dev	Median
PE01	29	0.07	0.23	1.98	0.12	0.20	31	0.07	0.22	0.84	0.09	0.20	29	0.07	0.21	0.78	0.08	0.20
PE02	28	0.06	0.29	2.24	0.17	0.26	31	0.15	0.41	2.00	0.14	0.41	29	0.36	0.72	7.03	0.37	0.62
PE03	30	0.04	0.13	3.37	0.19	0.09	31	0.05	0.11	0.99	0.06	0.10	29	0.05	0.12	3.54	0.19	0.09
PE04	4	0.04	0.11	0.72	0.07	0.09	31	0.05	0.10	1.98	0.07	0.08	28	0.04	0.09	1.99	0.08	0.07
PE05	61	0.04	1.06	5.15	1.19	0.10	62	0.04	0.11	3.16	0.13	0.07	59	0.04	0.08	3.81	0.12	0.07
PE06	61	0.03	0.07	0.30	0.02	0.06	62	0.05	0.09	0.27	0.03	0.10	59	0.04	0.09	0.28	0.03	0.08
PE07	61	0.05	0.17	3.20	0.13	0.18	62	0.05	0.15	0.92	0.07	0.16	59	0.04	0.15	1.12	0.07	0.16
PE08	61	0.04	0.10	1.67	0.05	0.09	62	0.05	0.09	2.02	0.05	0.08	59	0.05	0.09	1.51	0.04	0.09
PE09	61	0.05	0.14	1.31	0.07	0.13	62	0.04	0.09	0.97	0.04	0.08	59	0.05	0.09	0.73	0.04	0.08
PE10	30	0.03	0.10	2.05	0.12	0.08	31	0.02	0.08	1.94	0.07	0.07	25	0.03	0.11	1.16	0.06	0.10
PE11	23	0.00	0.14	1.82	0.12	0.10	31	0.17	0.27	2.69	0.09	0.25	24	0.21	0.29	1.72	0.07	0.28
PE12	30	0.13	0.39	1.29	0.15	0.36	31	0.15	0.36	1.02	0.14	0.34	24	0.14	0.30	1.02	0.10	0.28
PE13	61	0.04	0.10	0.55	0.04	0.09	62	0.04	0.08	0.55	0.03	0.07	58	0.03	0.08	1.09	0.04	0.07
PE14	31	0.05	0.09	0.75	0.04	0.08	31	0.06	0.09	0.51	0.03	0.08	31	0.05	0.09	1.06	0.03	0.08
PE15	31	0.10	0.14	1.04	0.04	0.14	31	0.10	0.15	0.74	0.03	0.15	31	0.06	0.17	1.05	0.04	0.17
PE16	31	0.04	0.07	0.42	0.02	0.06	31	0.04	0.07	0.77	0.03	0.07	31	0.04	0.07	0.62	0.03	0.07

Table A. 3 (cont'd)

Site	Oct (62 days)						Nov (60 days)						Dec (62 days)					
	Days of data	Min	Mean	Max	Std Dev	Median	Days of data	Min	Mean	Max	Std Dev	Median	Days of data	Min	Mean	Max	Std Dev	Median
PE01	31	0.05	0.16	0.49	0.05	0.15	28	0.04	0.17	0.63	0.06	0.15	31	0.05	0.18	0.74	0.09	0.16
PE02	31	0.40	1.30	12.06	0.66	1.18	28	0.14	1.50	16.22	1.74	0.96	31	0.12	1.48	16.28	1.79	1.03
PE03	31	0.04	0.10	1.12	0.05	0.08	28	0.04	0.12	4.29	0.19	0.09	31	0.04	0.11	1.01	0.06	0.09
PE04	31	0.06	0.11	1.75	0.05	0.10	28	0.05	0.11	2.93	0.12	0.09	31	0.06	0.11	0.57	0.05	0.09
PE05	62	0.03	0.18	2.97	0.23	0.09	57	0.03	0.16	3.19	0.20	0.07	62	0.03	0.07	2.30	0.07	0.06
PE06	62	0.03	0.07	0.37	0.02	0.07	45	0.04	0.07	0.59	0.02	0.07	31	0.04	0.07	0.26	0.02	0.06
PE07	52	0.01	0.23	3.09	0.08	0.23	44	0.06	0.22	4.11	0.15	0.24	62	0.06	0.18	1.43	0.09	0.19
PE08	62	0.01	0.09	1.35	0.04	0.09	55	0.05	0.11	2.96	0.06	0.10	62	0.04	0.11	3.29	0.10	0.10
PE09	62	0.05	0.13	1.66	0.07	0.12	57	0.05	0.16	1.22	0.09	0.13	62	0.06	0.16	4.29	0.11	0.14
PE10																		
PE11																		
PE12																		
PE13	62	0.04	0.09	0.42	0.05	0.07	55	0.04	0.09	1.41	0.04	0.08	62	0.04	0.13	1.44	0.07	0.13
PE14	62	0.05	0.09	0.67	0.02	0.08	54	0.04	0.12	0.98	0.07	0.09	62	0.04	0.31	1.11	0.27	0.24
PE15	62	0.04	0.21	1.15	0.13	0.20	57	0.05	0.16	1.51	0.12	0.11	62	0.04	0.11	0.75	0.04	0.12
PE16	62	0.05	0.10	1.20	0.05	0.10	55	0.04	0.10	1.29	0.04	0.08	62	0.00	0.08	1.23	0.04	0.07

Table A. 3 Monthly aggregated daily statistics for Chlorophyll fluorescence time series collected by in-situ loggers. Unless indicated otherwise, all units are notionally in mg m⁻³. Days of data indicates temporal data coverage, Min = minimum of all data for that month, Max = maximum of all data for month, Std Dev = standard deviation of all data for month,

Site	Jan (62 days)					Feb (56 days)					Mar (62 days)				
	Days of data	Min	Mean	Max	Std Dev	Days of data	Min	Mean	Max	Std Dev	Days of data	Min	Mean	Max	Std Dev
PE01	31	0.05	0.29	0.86	0.13	26	0.12	0.45	1.71	0.20	40	0.05	0.46	1.18	0.18
PE02	31	0.04	1.01	5.89	0.51	25	0.03	2.66	13.77	3.11	41	0.27	2.37	13.60	1.67
PE03	31	0.01	0.19	0.92	0.14	10	0.02	0.24	0.77	0.14	10	0.08	0.37	0.94	0.18
PE04	31	0.07	0.22	0.64	0.10	26	0.02	0.27	0.76	0.14	39	0.04	0.28	0.97	0.13
PE05	62	0.10	0.47	2.17	0.20	40	0.11	0.51	3.36	0.28	41	0.09	0.47	1.20	0.17
PE06	31	0.07	0.31	1.01	0.13	35	0.01	0.41	1.25	0.21	39	0.10	0.49	1.28	0.17
PE07	62	0.06	0.32	1.45	0.17	45	0.05	0.38	1.37	0.17	39	0.17	0.48	1.28	0.16
PE08	54	0.03	0.33	15.63	0.41	35	0.00	0.36	4.89	0.22	40	0.13	0.42	1.76	0.17
PE09	62	0.07	0.55	3.13	0.35	37	0.01	0.75	10.38	0.82	39	0.34	1.41	8.81	0.83
PE10											8	0.16	0.69	1.38	0.27
PE11											9	0.18	0.43	0.96	0.16
PE12											9	0.04	0.26	0.74	0.12
PE13	62	0.06	0.45	2.65	0.25	45	0.10	0.43	3.04	0.23	40	0.19	0.61	1.73	0.19
PE14	62	0.04	0.32	2.05	0.23	47	0.07	0.36	8.16	0.36	31	0.24	0.66	7.35	0.29
PE15	61	0.09	0.43	2.12	0.33	46	0.08	0.55	2.36	0.30	31	0.19	0.61	2.08	0.22
PE16	55	0.07	0.46	1.70	0.21	36	0.06	0.56	1.83	0.36	31	0.10	0.45	1.04	0.13

Table A. 4 (cont'd)

Site	Apr (60 days)					May (62 days)					Jun (60 days)				
	Days of data	Min	Mean	Max	Std Dev	Days of data	Min	Mean	Max	Std Dev	Days of data	Min	Mean	Max	Std Dev
PE01	60	0.02	0.42	1.69	0.24	48	0.03	0.41	1.71	0.31	30	0.03	0.23	0.96	0.12
PE02	60	0.04	1.54	13.68	1.35	46	0.01	0.43	2.85	0.35	30	0.04	0.29	3.13	0.17
PE03	30	0.09	0.44	1.36	0.22	30	0.07	0.40	2.66	0.24	30	0.11	0.45	1.61	0.21
PE04	60	0.02	0.28	1.22	0.14	48	0.03	0.25	1.67	0.16	22	0.07	0.32	1.69	0.13
PE05	60	0.13	0.53	7.49	0.26	57	0.12	0.48	3.33	0.19	60	0.07	0.28	6.16	0.17
PE06	59	0.05	0.41	1.30	0.18	59	0.06	0.43	1.26	0.18	60	0.15	0.46	1.22	0.15
PE07	60	0.12	0.49	1.65	0.21	60	0.13	0.49	1.58	0.22	60	0.17	0.51	1.76	0.18
PE08	60	0.06	0.45	1.32	0.19	60	0.09	0.53	1.79	0.28	60	0.15	0.47	1.65	0.20
PE09	30	0.18	0.61	1.56	0.26	44	0.13	0.45	1.54	0.20	60	0.12	0.36	1.52	0.12
PE10	30	0.22	0.60	3.28	0.20	31	0.19	0.53	6.13	0.27	30	0.25	0.63	11.12	0.55
PE11	30	0.16	0.51	1.36	0.19	31	0.10	0.44	1.50	0.17	30	0.14	0.44	1.29	0.15
PE12	30	0.02	0.25	0.88	0.13	31	0.07	0.35	0.95	0.15	30	0.09	0.37	0.97	0.16
PE13	60	0.15	0.74	1.66	0.26	60	0.13	0.48	1.76	0.17	60	0.11	0.52	1.65	0.19
PE14	26	0.18	0.98	11.13	1.19	26	0.11	0.73	11.64	1.23	30	0.09	0.33	0.89	0.11
PE15	30	0.14	0.58	2.68	0.29	28	0.14	0.44	1.83	0.15	30	0.12	0.41	1.92	0.17
PE16	30	0.08	0.37	1.04	0.17	28	0.12	0.37	1.29	0.15	30	0.14	0.41	1.34	0.14

Table A. 4 (cont'd)

Site	Jul (62 days)					Aug (62 days)					Sep (60 days)				
	Days of data	Min	Mean	Max	Std Dev	Days of data	Min	Mean	Max	Std Dev	Days of data	Min	Mean	Max	Std Dev
PE01	29	0.06	0.32	1.17	0.17	31	0.02	0.36	1.00	0.20	29	0.16	0.51	1.17	0.17
PE02	28	0.06	0.34	2.90	0.22	31	0.03	0.38	1.22	0.26	29	0.19	0.81	9.40	0.84
PE03	30	0.11	0.51	7.73	0.41	31	0.10	0.51	1.48	0.20	29	0.03	0.46	1.88	0.23
PE04	4	0.16	0.46	1.06	0.17	31	0.13	0.53	1.20	0.18	28	0.05	0.44	1.13	0.17
PE05	61	0.06	0.29	3.20	0.14	62	0.02	0.33	2.23	0.14	59	0.07	0.43	1.42	0.13
PE06	61	0.12	0.44	1.23	0.14	62	0.09	0.46	1.25	0.15	59	0.06	0.46	1.22	0.18
PE07	61	0.16	0.45	2.29	0.15	62	0.08	0.51	1.32	0.16	59	0.11	0.49	1.06	0.15
PE08	61	0.15	0.51	1.64	0.17	62	0.10	0.52	1.60	0.15	59	0.12	0.53	1.63	0.16
PE09	61	0.11	0.37	1.38	0.15	62	0.13	0.42	1.19	0.15	59	0.20	0.64	1.56	0.19
PE10	30	0.13	0.57	6.79	0.29	31	0.18	0.56	1.40	0.18	25	0.23	0.74	1.43	0.17
PE11	23	0.20	0.50	1.53	0.14	31	0.17	0.60	1.38	0.20	24	0.22	0.71	1.41	0.19
PE12	30	0.15	0.45	1.15	0.19	31	0.12	0.44	1.19	0.17	24	0.11	0.37	0.96	0.13
PE13	61	0.22	0.63	2.13	0.23	62	0.17	0.56	1.56	0.20	58	0.20	0.75	2.10	0.24
PE14	31	0.11	0.42	0.90	0.14	31	0.11	0.32	0.88	0.09	31	0.15	0.38	0.83	0.11
PE15	31	0.12	0.42	2.04	0.20	31	0.11	0.41	1.00	0.13	31	0.16	0.44	1.22	0.12
PE16	31	0.08	0.39	1.21	0.11	31	0.08	0.39	1.40	0.12	31	0.05	0.41	1.18	0.13

Table A. 4 (cont'd)

Site	Oct (62 days)					Nov (60 days)					Dec (62 days)				
	Days of data	Min	Mean	Max	Std Dev	Days of data	Min	Mean	Max	Std Dev	Days of data	Min	Mean	Max	Std Dev
PE01	31	0.07	0.42	1.23	0.18	28	0.04	0.53	1.35	0.24	31	0.05	0.42	1.21	0.24
PE02	31	0.51	1.37	7.02	0.55	27	0.49	4.14	23.24	3.58	30	0.01	4.19	23.37	3.98
PE03	31	0.03	0.36	1.34	0.20	28	0.01	0.35	1.36	0.21	31	0.01	0.27	1.20	0.22
PE04	31	0.04	0.24	0.68	0.11	28	0.03	0.18	0.69	0.07	31	0.05	0.18	0.64	0.09
PE05	62	0.11	0.47	2.18	0.17	57	0.14	0.57	1.78	0.26	62	0.08	0.47	4.74	0.24
PE06	62	0.04	0.42	1.27	0.22	45	0.04	0.44	1.91	0.24	31	0.00	0.24	0.84	0.14
PE07	52	0.05	0.44	1.32	0.15	44	0.06	0.37	4.97	0.26	62	0.05	0.33	1.52	0.21
PE08	62	0.01	0.39	1.16	0.17	55	0.01	0.34	3.68	0.18	62	0.01	0.33	4.12	0.23
PE09	61	0.21	0.68	1.55	0.21	57	0.20	0.61	2.49	0.18	59	0.18	0.84	3.12	0.60
PE10															
PE11															
PE12															
PE13	59	0.20	0.79	2.18	0.29	55	0.12	0.68	2.51	0.31	61	0.12	0.82	3.21	0.58
PE14	62	0.11	0.39	0.89	0.12	54	0.16	0.46	1.43	0.14	61	0.07	0.52	2.30	0.40
PE15	62	0.17	0.70	2.69	0.26	57	0.06	0.68	2.27	0.39	62	0.04	0.42	2.08	0.26
PE16	62	0.06	0.36	1.02	0.14	55	0.09	0.42	1.72	0.18	62	0.08	0.44	2.11	0.21

Table A. 4 Monthly aggregated daily statistics for PAR time series collected by in-situ loggers.

Unless indicated otherwise, all units are notionally in mmol/ ph/m²/s

Days of data indicates temporal data coverage, Max = maximum of all data for month, Mean Daily Range = arithmetic mean of the daily temperature ranges (daily max – daily min),

Site	Jan (62 days)		Feb (56 days)		Mar (62 days)		Apr (60 days)		May (62 days)		Jun (60 days)	
	Days of data	Max	Days of data	Max	Days of data	Max	Days of data	Max	Days of data	Max	Days of data	Max
PE01	31	207.92	11	164.85	9	245.70	30	251.90	31	212.19	30	244.39
PE02	31	124.54	8	94.25	10	69.33	30	73.49	31	73.98	30	58.05
PE03	31	714.10	26	610.12	41	444.52	60	430.19	45	418.64	30	222.22
PE04	31	239.61	26	263.41	39	264.22	60	264.83	48	263.61	25	227.09
PE05	62	218.72	45	201.49	41	169.37	60	169.30	58	144.40	60	150.39
PE06	31	207.61	9	152.45	8	114.44	30	118.01	44	116.77	60	97.03
PE07	62	183.92	45	197.10	39	149.67	59	167.14	60	100.05	59	80.31
PE08	31	136.93	35	168.72	40	192.61	59	193.76	60	149.07	60	99.77
PE09	62	106.18	29	86.59	10	75.40	29	82.57	43	57.19	57	45.40
PE10					8	70.12	30	70.18	31	58.30	30	50.22
PE11					9	115.21	30	115.28	31	95.12	30	88.76
PE12					9	291.91	30	286.15	31	209.28	30	239.93
PE13	31	86.91	37	86.40	39	84.65	60	80.93	50	80.09	30	43.93
PE14	31	44.94	21	43.65					11	37.07	30	42.59
PE15	62	125.91	30	125.64					11	36.82	30	63.06
PE16	31	81.23	35	117.02	31	118.39	8	119.30		30.10	30	43.86

Table A. 5 (cont'd)

Site	Jul (62 days)			Aug (62 days)			Sep (60 days)			Oct (62 days)			Nov (60 days)			Dec (62 days)			
	Days of data	Max	Mean Daily Max	Days of data	Max	Mean Daily Max	Days of data	Max	Mean Daily Max	Days of data	Max	Mean Daily Max	Days of data	Max	Mean Daily Max	Days of data	Max	Mean Daily Max	
PE01	29	224.36	157.96	31	260.70	155.01	29	258.21	171.13	31	277.56	185.25	28	287.14	194.65	31	208.68	158.54	
PE02	28	106.92	54.98	31	101.41	75.91	29	98.49	60.84	31	134.00	94.13	28	137.22	77.21	31	126.27	73.89	
PE03	30	262.90	172.73	31	311.15	236.60	29	418.96	299.75	31	351.56	261.87	28	629.24	364.95	31	724.86	505.08	
PE04	30	194.54	137.41	31	102.19	74.73	28	219.01	106.11	31	375.09	269.16	28	389.60	269.12	31	249.45	185.53	
PE05	61	178.50	105.44	62	192.21	121.45	59	187.01	121.25	62	213.42	174.10	57	220.44	148.11	62	218.72	159.63	
PE06	61	111.33	76.44	62	165.31	97.28	55	163.97	133.54	30	165.11	139.23	22	185.83	132.36	31	208.24	154.24	
PE07	60	106.32	71.02	38	130.70	95.16	29	170.48	124.87	31	157.23	121.97	44	193.13	136.68	62	197.25	155.47	
PE08	61	109.66	69.58	62	133.08	90.17	59	158.62	118.37	62	194.47	130.15	46	167.69	123.50	31	139.97	92.12	
PE09	32	58.69	41.10	31	67.70	38.39	29	70.16	46.97	31	98.47	72.40	45	108.01	66.72	62	107.26	67.25	
PE10	30	66.29	42.29	31	61.77	36.45	25	66.27	46.75										
PE11	23	81.35	48.33	31	45.37	31.48	24	52.66	37.66										
PE12	30	252.48	165.14	31	220.40	157.94	24	319.49	229.80										
PE13	30	54.31	37.59	31	60.55	42.79	28	70.81	47.05	31	83.61	66.26	38	99.63	80.17	31	94.73	53.29	
PE14	31	36.10	21.50	31	54.75	37.98	31	59.98	44.79	62	64.73	52.04	44	57.44	43.19	31	44.22	31.43	
PE15	31	70.22	40.10	31	69.79	41.11	31	83.06	61.28	61	118.51	82.61	57	120.85	86.76	62	125.86	103.37	
PE16							1	99.79	99.79	31	168.49	125.09	35	184.17	97.06	31	85.49	56.92	